NASA/CR—2012-217270

Calibration of the NASA Glenn 8- by 6-Foot Supersonic Wind Tunnel (1996 and 1997 Tests)

E. Allen Arrington
Sierra Lobo, Inc., Fremont, Ohio

January 2012

NASA STI Program . . . in Profile

Since its founding, NASA has been dedicated to the advancement of aeronautics and space science. The NASA Scientific and Technical Information (STI) program plays a key part in helping NASA maintain this important role.

The NASA STI Program operates under the auspices of the Agency Chief Information Officer. It collects, organizes, provides for archiving, and disseminates NASA's STI. The NASA STI program provides access to the NASA Aeronautics and Space Database and its public interface, the NASA Technical Reports Server, thus providing one of the largest collections of aeronautical and space science STI in the world. Results are published in both non-NASA channels and by NASA in the NASA STI Report Series, which includes the following report types:

- TECHNICAL PUBLICATION. Reports of completed research or a major significant phase of research that present the results of NASA programs and include extensive data or theoretical analysis. Includes compilations of significant scientific and technical data and information deemed to be of continuing reference value. NASA counterpart of peer-reviewed formal professional papers but has less stringent limitations on manuscript length and extent of graphic presentations.

- TECHNICAL MEMORANDUM. Scientific and technical findings that are preliminary or of specialized interest, e.g., quick release reports, working papers, and bibliographies that contain minimal annotation. Does not contain extensive analysis.

- CONTRACTOR REPORT. Scientific and technical findings by NASA-sponsored contractors and grantees.

- CONFERENCE PUBLICATION. Collected papers from scientific and technical conferences, symposia, seminars, or other meetings sponsored or cosponsored by NASA.

- SPECIAL PUBLICATION. Scientific, technical, or historical information from NASA programs, projects, and missions, often concerned with subjects having substantial public interest.

- TECHNICAL TRANSLATION. English-language translations of foreign scientific and technical material pertinent to NASA's mission.

Specialized services also include creating custom thesauri, building customized databases, organizing and publishing research results.

For more information about the NASA STI program, see the following:

- Access the NASA STI program home page at *http://www.sti.nasa.gov*

- E-mail your question via the Internet to *help@sti.nasa.gov*

- Fax your question to the NASA STI Help Desk at 443–757–5803

- Telephone the NASA STI Help Desk at 443–757–5802

- Write to:
  NASA Center for AeroSpace Information (CASI)
  7115 Standard Drive
  Hanover, MD 21076–1320

NASA/CR—2012-217270

Calibration of the NASA Glenn 8- by 6-Foot Supersonic Wind Tunnel (1996 and 1997 Tests)

E. Allen Arrington
Sierra Lobo, Inc., Fremont, Ohio

Prepared under Contract NNC05CA95C

National Aeronautics and
Space Administration

Glenn Research Center
Cleveland, Ohio 44135

January 2012

Level of Review: This material has been technically reviewed by expert reviewer(s).

Available from

NASA Center for Aerospace Information
7115 Standard Drive
Hanover, MD 21076–1320

National Technical Information Service
5301 Shawnee Road
Alexandria, VA 22312

Available electronically at http://www.sti.nasa.gov

Calibration of the NASA Glenn 8- by 6-Foot Supersonic Wind Tunnel (1996 and 1997 Tests)

E. Allen Arrington
Sierra Lobo, Inc.
Fremont, Ohio 43420

Summary

There were several physical and operational changes made to the NASA Glenn[1] Research Center 8- by 6-Foot Supersonic Wind Tunnel during the period of 1992 through 1996. Following each of these changes, a facility calibration was conducted to provide the required information to support the research test programs. Due to several factors (facility research test schedule, facility downtime and continued facility upgrades), a full test section calibration was not conducted until 1996. This calibration test incorporated all test section configurations and covered the existing operating range of the facility. However, near the end of that test entry, two of the vortex generators mounted on the compressor exit tailcone failed causing minor damage to the honeycomb flow straightener. The vortex generators were removed from the facility and calibration testing was terminated. A follow-up test entry was conducted in 1997 in order to fully calibrate the facility without the effects of the vortex generators and to provide a complete calibration of the newly expanded low speed operating range. During the 1997 tunnel entry, all planned test points required for a complete test section calibration were obtained. This data set included detailed in-plane and axial flow field distributions for use in quantifying the test section flow quality.

Introduction

During the late 1980s and through the mid-1990s, the NASA Glenn Research Center has continued to improve the capabilities of its aeropropulsion test facilities, including the large wind tunnels. The 8-by 6-Foot Supersonic Wind Tunnel (SWT) had major modifications to enhance the test section flow quality, upgrades to the data systems and facility controls, and changes to its operational procedures to expand its Mach number range. After each major facility change, some manner of test section calibration was conducted to ensure the test section flow conditions were always accurately known. However, there had not been a full test section calibration that covered all facility configurations and the entire Mach number range during this period of facility enhancement. The first comprehensive test section calibration was conducted in 1996 following the completion of all planned facility improvements. Due to the failure and subsequent removal of a recently installed flow quality improvements device, a second calibration entry was conducted in 1997[2]. Details of these calibration tests including descriptions of the test hardware and procedures, data reduction and calibration data, as well as background information, are described in this report.

Background

As a matter of record and to give the reader with a better understanding of the calibration activities being conducted in the 8- by 6-ft SWT, the following history of the calibration tests is provided:

[1]At the time these tests were conducted, the center name was Lewis Research Center. The name was changed in 1999 to the John H. Glenn Research Center at Lewis Field, NASA Glenn for short. The center is referred to as NASA Glenn throughout this report.

[2]The 1996 test entry was conducted from January through April, 1996. This was the fifth tunnel calibration test entry in the 8x6 SWT since the project was started in 1990. The 1997 test spanned from November 1996 through April 1997 and was the sixth test entry.

Baseline Calibration

Two baseline calibration test entries were conducted (1991 and 1992). The transonic array and 4-in. diameter cone cylinder were used to determine the existing flow field characteristics in the test section prior to planned facility flow quality improvements. The data from these calibration tests was used to construct a database for the tunnel flow quality prior to the planned facility enhancements and will be compared to data collected following the enhancements in order to gage the improvement to the facility flow quality. Reference 1 describes the details of these baseline tests.

Facility Flow Quality Improvements

During 1992, the following flow quality improvements were made to the 8- by 6-ft SWT:

1. Replacement of the tunnel shell downstream of the drive compressor with and acoustically treated section.
2. Replacement of the compressor exit tailcone fairing with a new aerodynamically contoured and acoustically treated fairing. Provisions were made for the mounting of vortex generators (VGs) on the tailcone, but due to delays in fabrication, the VGs were not installed.
3. Replacement of the single turbulence reduction screen. While provisions were made for the installation of up to five new screens, there are currently three 10-mesh screens installed.
4. Replacement of the existing flow straightening honeycomb with a new honeycomb (3/8-in. square cell with an L/D of 16).

Reference 2 is a description of the tunnel loop flow quality tests that were used in designing the above tunnel improvements.

Initial Flow Field Surveys

Due to scheduling constraints, there was not enough time to perform a full test section calibration following the installation of the facility flow quality improvements prior to the first research test. A test specific calibration was conducted to obtain calibration and flow quality data to address the requirements of that particular research test program. The details of these flow field surveys are listed in Reference 3.

Low-Speed Calibration

In order to support a request for low-speed testing in the 8- by 6-ft SWT, the operating procedures for the facility drive system were modified to achieve lower compressor rotational speeds and therefore lower mass flow and test section airspeeds (Ref. 4). Very low speed conditions were achieved by using the air dryer air circulation fans to push air through the facility. A test entry was conducted in 1995 to calibrate the facility over the newly expanded low speed operating range (Ref. 5).

First Full Calibration Test

The first full tunnel calibration since the installation of the flow quality improvements was attempted in 1996. The compressor exit tailcone vortex generators were installed in the facility for this test. Testing covered the entire operating range of the facility as well as all test section porosity configurations. Near the end of the test, two of the vortex generators failed, causing minor damage to the flow straightening honeycomb. The VGs were removed and calibration testing was halted at that point.

Second Full Calibration Test

After the damage from the VG failure was repaired, a second calibration entry was planned. Initial review of the 1996 calibration data indicated that the VGs had only a small effect on the test section flow field and that was restricted to the higher supersonic Mach numbers. Because of this, it was felt that it was not necessary to repeat the entire calibration test matrix. However, the facility electronically scanned pressure (ESP) data acquisition system (DAS) was being upgraded, and would provide smaller measurement uncertainties to the calibration data. For this reason, it was decided to repeat most of the test matrix from the 1996 test. The first (1996) and second (1997) full calibration tests are described in this report.

Test Objectives

The objective of the test was to provide a full calibration of the 8- by 6-ft SWT following the installation of the facility flow quality improvements, expansion of the operational range and upgrades to the ESP system. Specific test operations are listed below:

1. Provide an empty test section calibration over the entire Mach number range of the 8- by 6-ft SWT for each test section porosity configuration.
2. Provide detailed flow quality surveys in terms of total and static pressure, total temperature, and flow angularity within a plane at selected stations in the test section.
3. Begin collection of model blockage effects data using various diameter cone cylinder models.
4. Quantify the effects of dew point (humidity) on the freestream test section conditions.
5. Determine the boundary layer thickness through the test section.
6. Evaluate effectiveness of bellmouth total pressure measurement system.
7. Determine the effects of the supersonic strut on the test section flow field and calibration.

Data were collected to support each of these objectives. The results of all of the test objectives are discussed in this report, with the exception of item number 3, which has been deferred to a follow on report that will focus on blockage effects testing.

Description of Facility

The 8- by 6-Ft Supersonic/9- by 15-Ft Low-Speed Wind Tunnel complex is an atmospheric-pressure, continuous-flow propulsion wind tunnel (Fig. 1). It is NASA's only transonic propulsion wind tunnel facility. For standard operation, the airflow is driven through the facility by a 7-stage axial compressor (18-ft inlet diameter) that is powered by three 29 000-hp electric motors. The 8- by 6-ft test section walls, floor and ceiling have no divergence over the 23 ft, 6 in length of the test section. The test section consists of a solid wall supersonic flow region (9 ft, 1 in. length) followed by a porous wall transonic region (14 ft, 5 in). The Mach number range in the transonic test section is 0.36 to 2.0 for standard operation. There are six configurations for the transonic test section based on the length of the porous area used and the open area of the test section surfaces:

1. 14-ft, 5.8-percent-porosity
2. 8-ft, 6.2-percent-porosity
3. 8-ft, 3.1-percent-porosity
4. 8-ft, 6.2-percent-porosity modified
5. 8-ft, 3.1-percent-porosity modified
6. 14-ft, schlieren windows installed

The 14-ft test section used the entire length of the porous area; the 8-ft test section is the aft 8 ft of the porous test section (Fig. 2). The tunnel can be operated in either an aerodynamic (closed loop) or propulsion (open loop) cycle (for propulsion cycle, flow control doors 1 and 2 are open so that the airflow is exhausted from the tunnel).

The conditions in the 8- by 6-ft test section were set by controlling compressor speed, flexible wall position, balance chamber pressure (test section bleed) and shock door (second throat) position. For standard operation of the drive system, the test section Mach number range is 0.36 to 2.0. In order to reduce the test section Mach number below 0.36, it was necessary to slow the compressor speed. This was done by powering the compressor using only one of the three electric drive motors. By operating in this mode, it was possible to expand the operational envelop of the facility by reducing the low-end Mach number to 0.25. Typical operating conditions in the test section for drive motor operation are provided in Table I. Very low speed conditions (below Mach 0.1) were achieved in the 8- by 6-ft test section by using only the air dryer building air circulation fans (the 8 fans are used to pull air through the air dryer building to cool the desiccant beds; by properly configuring the tunnel and air dryer flow control doors, the fans will push air through the 8- by 6-ft test section).

Flow quality improvements were installed in the facility in 1992. The improvements that affect the 8- by 6-ft test section are a flow straightening honeycomb and three 10-mesh turbulence reduction screens in the settling chamber upstream of the test section and an aerodynamically contoured compressor exit tailcone fairing. Two sets of vortex generators that mount on the tailcone were designed to further enhance the flow quality over the supersonic operating range of the facility, but were not installed until just prior to the 1996 calibration test entry. A more complete description of the 8- by 6-ft supersonic wind tunnel is found in Reference 6.

Instrumentation and Test Hardware

Existing calibration hardware and instrumentation was used for the calibration testing. A variety of flow sensing probes, including total pressure, pitot-static, flow angularity, and thermocouple probes, were used during the calibration; cone cylinder models were also used to provide axial static pressure distributions and model blockage effects. Descriptions of the hardware and instrumentation are presented below.

Transonic Array

The transonic array was used to survey the test section flow field to provide information on the total and static pressure, total temperature, flow angle and turbulence characteristics within a plane. The array layout is shown in Figure 3. The standard array instrumentation is comprised of 5 flow angularity probes, 6 pitot-static pressure probes, 11 thermocouples and two hot film anemometry probes. The array is sting mounted in the transonic strut and is further supported by wall plates attached to both ends of the array body and by a vertical support downstream of the array body. All the surfaces of the array have a 10° taper to minimize aerodynamic interference. The array body is made of 304 stainless steel, the sting of 4340 steel, and the wall plates of 6061-T6 aluminum. For the low speed tests, the array was positioned axially at the test plane of the 14-ft test section (the tips of the flow angle probes were at approximately the centerline of the schlieren window blanks; test section station 137.75; the static pressure orifices on the flow angle probes were at station 143.2). The array was tested at five vertical positions at this station (tunnel centerline and 12 and 24 in. above and below tunnel centerline). A 20-in. strut spacer block was used to position the array at the 12- and 24-in. positions above centerline due to limited vertical travel of the transonic strut. Figure 4 shows a typical installation of the array in the test section. The wall plates (which are not shown in Fig. 4) are attached to the tunnel walls using T-nuts which pass through the test section porosity holes. The floor plate for the vertical support is also attached to the tunnel using T-nuts through the porosity holes (same as the wall plates). There is a set of five vertical supports (one for each vertical position). The vertical support is bolted to the floor plate and to a collar that clamps around the

sting just aft of the array body. The sting, through which the instrumentation lines pass, is supported in the transonic strut cradle. One of the sting joints is also an expansion joint to compensate for thermal growth. Figure 5 shows the measurement locations for the transonic array within the test section.

The flow angle probes are five-hole, hemispherical-head design which allow resolution of two flow angle components (pitch and yaw). The flow angle probes were calibrated for a Mach number range of 0.5 to 2.0 (the Mach number range of the 8- by 6-ft SWT is 0.36 to 2.0 for three motor operation; the Mach number range of the probe calibration facility located at Sandia Labs was 0.5 to 4.0 so that probe calibration data was not obtained corresponding to the low end of the 8- by 6-ft SWT Mach number range; at these low Mach number conditions, probe calibration parameters were extrapolated from the calibration data). These probes extend 21.125 in. from the leading edge of the array. The pitot-static probes also extend 21.125 in. from the array leading edge. The thermocouples are mounted to the bottom of the array body, with the heads of the thermocouples about even with the array leading edge.

Cone Cylinders

The cone cylinders were used to measure the axial static pressure and Mach number distributions and to determine the best operating condition in the test section for each Mach number setting. This is done by matching the static pressure distribution on the body of the cylinder as closely as possible to freestream static pressure. Four cone cylinder models were used during the course of the two full calibration test entries:

- 4-in. diameter by 86-in. long (0.18 percent blockage)
- 8-in. diameter by 120-in. long (0.73 percent blockage)
- 12-in. diameter by 120-in. long (1.64 percent blockage)
- 16-in. diameter by 120-in. long (2.91 percent blockage)

The cone cylinder models were selected instead of a static pressure pipe as the primary static pressure calibration hardware. There are advantages and disadvantages to each. The cone cylinders are easier to maintain, install and test, but they only provide a portion of the static pressure distribution through the test section length.

Each cone cylinder model consists of a 10° half angle cone with base diameter as listed above which extends into a constant diameter cylinder. Each model is instrumented with static taps arranged in four axial rows spaced 90° apart. Figure 6 shows the instrumentation layout for 4-in. diameter model. Figure 7 shows a typical installation of the 4-in. diameter cone cylinder. The 4-in. diameter model is used to provide empty test section calibration data; the larger diameter models provided blockage effect data. The cone cylinder models are sting mounted into the tunnel transonic strut. Axial position changes of the model in the tunnel are accomplished by means of a split sting section which can be added to or removed from the model assembly without disconnecting the instrumentation lines. The split sting section allows for an axial position change of 34 in. The tip of the cone cylinders can be positioned at either the inlet of the 8-ft test section or at the centerline of the schlieren window blanks in the 14-ft test section.

Boundary Layer Rakes

The boundary layer rakes were used to measure the boundary layer thickness at three stations in the test section and to document the effect of the test section bleed on the boundary layer. A typical rake used for these measurements is shown in Figure 8. Each rake is comprised of 25 total pressure probes arranged to provide a tight pressure distribution near the test section surface. The rakes were mounted in the test section using fasteners through the porosity holes. Four rakes were used for these measurements and the position of the rakes on the test section surfaces depended on the station and available mounting holes. A typical installation is shown in Figure 9.

8-ft Survey Rake

The 8-ft survey rake was used to provide additional data on the bellmouth total pressure in order to better determine how well the facility bellmouth rakes were operating and to provide additional data for the determination of the total pressure loss through the test section. The 8-ft rake (Fig. 10) is a vertically oriented rake with eleven evenly spaced pitot-static probes (8-in. spacing between probes). The rake was mounted at the bellmouth (contraction section) exit along the tunnel centerline, with the probes stationed even with the bellmouth rake total pressure probes.

Facility Instrumentation

The following permanent facility instrumentation was used during the low-speed calibration testing:

Bellmouth rakes.—Two wall mounted rakes near the exit of the bellmouth upstream of the test section. One rake is mounted to the north tunnel wall and the other to the south tunnel wall at approximately the tunnel centerline (the rakes are designated north and south). The instrumentation mounted on each rake consists of four total pressure and two total temperature probes (Fig. 11).

Test section static taps.—Figure 12 shows the location of all of the static pressure taps located in the 8- by 6-ft test section and the high speed diffuser section. The majority of the test section ceiling and wall static pressures were recorded during the low-speed calibration tests.

Data Systems

The standard tunnel data system was used for the low-speed calibration test. Steady-state pressure data was acquired with an Electronically Scanned Pressure (ESP) System. The ESP system uses plug-in modules, each containing 32 individual transducers, which can be addressed and scanned at a rate of 10,000 ports per second. On-line calibration of all ESP transducers can be performed automatically every 20 min or at the discretion of the test engineer. Calibration is carried out by the operation of a pneumatic valve in each module which allows three pressures measured with precision digital quartz transducers, to be applied. Throughout this calibration program, the ESP transducers were calibrated at each Mach number setting. For these tests, ±15 psid modules were used.

Real-time data acquisition and display was provided by Escort D+, the standard data system used in the large test facilities at the NASA Glenn Research Center. This system accommodates the ESP inputs, plus all steady-state analog and digital signals used including survey rake and tunnel facility thermocouples and pertinent tunnel control parameters such as compressor speed, shock door positions and positions of flow control doors 1 and 2. The Escort D+ facility microcomputer acquires these data, converts them to engineering units, executes performance calculations, checks limits on selected channels and displays the information in alpha-numeric and graphical form with 1 second update rate. For this test, each collected data reading was the average of 20 scans (20 sec) of data.

Operational Considerations

Descriptions of test setup, operational procedures and test matrices used during the 1996 and 1997 test entries are contained in this section. In general, the procedures, etc. are identical for the two test entries; differences are noted where they occurred.

Test Setup and Procedures

The test procedures specific to each piece of calibration hardware are described in the following sections. These procedures were used during both the 1996 and 1997 test entries.

Cone Cylinder

Following installation of a cone cylinder model in the test section, end-to-end checks of all instrumentation lines were conducted to insure data quality; any problems were resolved prior the start of testing and noted in the test log. Prior to each test run, the cone cylinder was positioned so that the cone tip was at the test section centerline and leveled in pitch with respect to the centerline. During a typical tunnel run, the highest Mach number condition was set first in order to conserve air dryer capacity, and then the Mach number was reduced incrementally to cover the entire operating range of the facility. The model pitch angle was monitored during the run using both an electrolytic inclinometer mounted in the forward portion of the cylinder and visually using a scale marked on a video monitor. The pitch angle was adjusted back to 0° as required during the test using the transonic pitch attitude.

Transonic Array

Following the initial installation of the array in the test section, the flow angle probe pitch and yaw alignment offsets were measured using an optical transit and the baseline rake pitch and yaw angles were measured using a digital inclinometer and tape measure. For each rake height change, the rake pitch and yaw angles were measured and compared to the baseline values. The differences from the baseline values were used to correct the measured flow angles for rake misalignment. End-to-end instrumentation checks were also made following the array installation. The same Mach number schedule described for the cone cylinder procedures was used for the array surveys. Vertical and axial position changes for the array were made manually, so there was no translation of the hardware while the tunnel was running.

Boundary Layer Rakes

Four boundary layer rakes were used during the 1997 calibration test entry. Surveys were made at three stations is the test section: forward (inlet of the 14-ft test section, station 108), mid (inlet of the 8-ft test section, station 170), and aft (near the exit of the 8-ft test section, station 240). The position of the rakes in the test section was dependent on the location of porosity holes for use as mounting points. Figure 9 shows the three configurations used during the testing. Configuration A (one rake mounted at the centerline of each test section surface) was used at both the mid and aft stations. Configuration B (rakes at off-centerline locations) was also used at the middle station. At the forward station a different rake configuration was needed since the rakes could not be mounted to the tunnel walls (the porous wall blanks used at the schlieren window location were thicker than the test section walls causing and interference with the angle of the fasteners, so it was not possible to mount the rakes on the blanks). At the forward station, two rakes were mounted on the floor and ceiling, one at centerline and one-quarter or three-quarter point (configuration C). As was the case with all calibration hardware, the instrumentation lines were thoroughly checked following the initial installation and after each rake position change.

8-ft Survey Rake

The 8-ft survey rake was only used during the 1996 calibration entry. The rake was mounted along the tunnel centerline at the exit of the tunnel contraction (bellmouth) section at the measurement plan of the facility bellmouth total pressure rakes. The only alignment check was the station to insure that the 8-ft rake probes and the bellmouth rake probes were in the same plane. Instrumentation checks were also completed following installation.

Test Matrices

The test matrices for the 1996 and 1997 test entries are listed in tables II and III, respectively. All testing in support of the tunnel calibration was conducted in open loop (propulsion cycle). In this mode of

operation, air is brought into the tunnel circuit through doors 4 and 5 and exhausted through doors 1 and 2 (Fig. 1). By operating in this mode, there is no airflow through the 9- by 15-ft test section and work can continue in that facility while tests are conducted in the 8- by 6- ft test section. Operating the facility in open versus closed (aerodynamic) loop does not have any effect on the test section conditions in terms of flow quality or calibration, but there is the potential for reduced operating time on dry air (low dew point) when operating in the open loop mode. The calibration tests were conducted during the winter to take advantage of the cold dry atmospheric conditions in order to maximize available supersonic test time.

The original plan was to complete calibration of three of the six test section porosity during each of the two test entries. However, since the first entry was not completed due to the vortex generator failure, and because the facility data system was upgraded prior to the second entry, it was decided to calibrate all six configurations during the 1997 entry. During the 1996 entry, the bellmouth total pressure rake checkout (using the 8-ft survey rake), all planned transonic array tests and testing with the 4- and 8-in. diameter cone cylinders were completed before the test entry was ended (boundary layer surveys and tests using the 12- and 16-in. cones were not completed). For the 1997 entry, the boundary layer surveys were completed first, prior to the facility data system upgrade. After the data system upgrade, all of the planned transonic array tests and the 4-in. diameter cone cylinder tests were completed. Only a portion of the 16-in. diameter cone cylinder tests were completed before the hardware was damaged and testing was halted[3].

At each test condition, three data readings were recorded. During the 1996 test entry, the data system was calibrated at each Mach number setting; however, following the data system upgrade, DAS calibration was only required about every hour during the 1997 test entry. The typical Mach number schedule for drive motor operation is listed below:

- Mach 2.0 to 1.0 in decrements of 0.1 (three drive motor operation)
- Mach 1.0 to 0.4 in decrements of 0.05 (three drive motor operation)
- Mach 0.5 to 0.25 in decrements of 0.05 (one drive motor operation)

For the air dryer fan tests, all eight fans were initially brought on-line and were then dropped off one-by-one to set very low-speed conditions; testing was suspended following four fan operation[4] since the test section airspeed was below 10 ft/sec. Each time the number of air blowers was changed, 10 minutes were required to allow the compressor speed to stabilize (the compressor was wind-milling during the air blower runs).

In addition to the six standard empty test section configurations, a non-empty test section configuration using the facility supersonic strut was also calibrated. This configuration was added to the test matrix following a research test that used the supersonic strut to support the test article in the 14-ft test section (the transonic strut would normally be used, but for this test it was used to support auxiliary equipment). During that research test, it was necessary to set the flexible wall 0.1 Mach higher than the desired test condition (i.e. to achieve a Mach number of 1.5, it was necessary to set the flexible wall at the Mach 1.6 position); it was thought that the additional blockage of the supersonic strut was responsible for this operational anomaly and therefore should be investigate. For array surveys, the supersonic strut was used in place of the secondary vertical support. During the cone cylinder tests, the supersonic strut (without the cradle used to accept a support sting) was simply extended into the test section to within 4-in. of the model.

[3] Although some testing using the large diameter cone cylinders was completed during the 1996 and 1997 test entries, discussion of these data will not be included in this report. The results of the testing using the larger diameter cone cylinder models will be covered in a separate report.

[4] During the initial data sweep, only the 0 percent open shock door position was set for 7 and 5 air blower operation due to limited available test time. Since no data was collected for 3, 2 or 1 air blower operation, there was enough time available to repeat the 5 and 7 air blower conditions and collect data for the three shock door positions.

For all testing, a detailed log was maintained to track test points, collected data reading numbers, hardware and instrumentation problems, etc. On-line data monitoring was used to ensure data quality.

Data Reduction

The data analysis methodology used for each part of the calibration tests was described in the following sections. The information presented here applies to the general treatment of the data; for some specific applications, details of the data reduction are included in the discussion section. The majority of the data review was done on-line using the facility Escort data system.

The first step of the data reduction and analysis was a thorough review of the data to insure data quality. While most instrumentation and data problems were detected and resolved either prior to or during the testing there were instances where bad or questionable data was collected and editing of the data was required (i.e. bad data points were flagged and therefore not used in subsequent steps of the analysis). Also corrections to data files were made at this point (these corrections were generally to the test configuration descriptions, such as hardware positions or number designations, and not to measured pressure or temperatures). Notes taken during the testing as part of the test engineers log proved invaluable in troubleshooting problems with data channels and test configurations.

At the completion of the test entry, the data were reprocessed using a program that mimicked the on-line data reduction. This step corrected any errors in the data from instrumentation problems or test setup errors[5]. Data files were then created and downloaded to a PC based spreadsheet program for final analysis.

Cone Cylinder Data

A detailed description of the development of the cone cylinder data analysis methodology is contained in Reference 1. The average static pressure on the cone portion of the model was used to determine the local freestream static pressure for supersonic conditions. The average static pressure over the aft portion of the cylinder provided a direct measurement of the freestream static pressure for all Mach number settings.

Flow Field Surveys—Transonic Array Data

The local Mach number at each probe was determined based on the ratio of static to total pressure sensed by each probe. The isentropic flow equation was used to calculate the Mach number in the subsonic regime (Eq. 44 from Ref. 7, with $\gamma = 1.4$):

$$M = \sqrt{5\left[\left(\frac{P_S}{P_T}\right)^{-0.2857} - 1\right]}$$

where P_S is the static pressure and P_T is the total pressure. For supersonic conditions, the results of Rayleigh pitot formula as tabulated in Reference 7 were used to compute the Mach number. This formula relates the ratio of static pressure upstream of a normal shock to the total pressure downstream of the normal shock ($P_{S,1}/P_{T,2}$) to freestream Mach number. In supersonic flows, a normal shock forms upstream of each of the pressure probes. The total pressure sensed by each probe is then the total pressure downstream of the normal shock. The static pressure ports on the flow angle probes are located far enough downstream of the probe tip (14.7 probe diameters) so that static pressure has recovered to freestream conditions ($P_{S,1}$). During the course of testing the static pressures measured by the array probes

[5] Following the 1996 test entry, the post-processing capabilities were migrated from the VAX based system to a UNIX platform.

were used to determine Mach number on-line. However, the average static pressure from the aft cylinder portion of the 4-in. diameter cone cylinder was used during the final post-test data analysis to determine actual test section conditions. It is believed that the cone cylinder data provides a more accurate measurement of the freestream static pressure, particularly at supersonic conditions.

Two components of flow angle were also measured by the five-hole hemispherical head flow angularity probes on the survey rake. As the name implies, the head of each probe has five pressure orifices as shown in Figure 13. The center port (P_5) senses the total pressure, P_T. Ports P_1 and P_3 are used in determining the pitch flow angle and P_2 and P_4 are used for the yaw flow angle. The difference in pressure measured by a pair of opposing ports is related to the flow angle through an extensive probe calibration. The probe calibration is based on the relationship between the probe attitude (flow angle) and two pressure ratios, P_α and P_β. The pressure ratios are defined as

$$P_\alpha = \frac{P_3 - P_1}{P_5 - P_{av}} \qquad \text{and} \qquad P_\beta = \frac{P_4 - P_2}{P_5 - P_{av}}$$

where $P_{av} = 0.25(P_1+P_2+P_3+P_4)$. The measured flow angles are related to these pressure ratios through calibration equations. The equations for the pitch angle, α_m, and yaw angle, β_m, are respectively

$$\alpha_m = \alpha_p + \frac{P_\alpha}{A_1} \qquad \text{and} \qquad \beta_m = \beta_p + \frac{P_\beta}{B_1}$$

Positive pitch angle ($P_3>P_1$) is defined as an upflow in the test section. Positive yaw flow ($P_4>P_2$) is from left to right when looking downstream (or flow moving from the inside test section wall toward the outside wall).

As mentioned, the flow angle probes were calibrated at the Sandia National Laboratory Trisonic Wind Tunnel. Details of the probe calibration are not included in this report, but are found in References 8 and 9. Details on correcting the flow angle data for rake and probe misalignment are described in Reference 1.

8-ft Survey Rake

The 8-ft survey rake was only used in subsonic flow conditions since it was mounted upstream of the facility flexible wall. The total pressure data from the 8-ft survey rake was used to check the pressure data from the facility rakes, so simple deltas were computed, as described in the Discussion of Results section.

Boundary Layer Data

Boundary layer data reduction was restricted to generating velocity ratio profiles and computing boundary layer thickness. As previously mentioned, boundary layer surveys were conducted using four rakes fitted with twenty-five total pressure probes each (Figures 8 and 9). The equations used in the data reduction are the standard isentropic compressible flow equations with ratio of specific heats, γ, equal to 1.4.

The data reduction procedure first required calculation of the freestream test section Mach number, M_{ts}, freestream test section static temperature, $T_{S,ts}$, and freestream test section speed of sound, a_{ts}. These parameters were calculated using bellmouth total pressure, $P_{T,bm}$, and bellmouth total temperature, $T_{T,bm}$, measured by the two bellmouth rakes and static pressure measured with the test section ceiling/wall static pressure ports, $P_{S,ts}$.

$$M_{ts} = \sqrt{5\left[\left(\frac{P_{S,ts}}{P_{T,bm}}\right)^{-0.2857} - 1\right]} \qquad T_{S,ts} = \frac{T_{T,ts}}{1 + 0.2 \cdot M_{ts}^{\,2}} \qquad a_{ts} = \sqrt{\gamma R T_{S,ts}}$$

It was assumed that the static pressure and speed of sound values would remain constant throughout the four measured boundary layers. This permitted calculation of the Mach number and velocity profiles at each rake location using the compressible flow and the previously calculated freestream parameters. For subsonic conditions, the Mach number and airspeed at each probe location were determined using the following equations:

$$M_{bl}(i,j) = \sqrt{5\left[\left(\frac{P_{s,ts}}{P_{T,bl}(i,j)}\right)^{-0.2857} - 1\right]} \qquad U_{bl}(i,j) = M_{bl}(i,j) \cdot a_{ts}$$

where the index *i* indicates the specific boundary layer rake (rake 1 to 4) and the index *j* indicates the particular total pressure probe on each rake (probe 1 to 25, where probe 1 is nearest to the base of the rake.

For supersonic conditions, the boundary layer rakes are sensing the total pressure downstream of a normal shock, $P_{T,2}$. The Mach number at each probe location can be calculated from the ratio of the total pressure measured by the boundary layer rake and the test section static pressure, $P_{T,2}/P_{S,ts} = P_{T,2}/P_{S,1}$, using the Rayleigh pitot formula (Eq. 100 in Ref. 7).

$$\frac{P_{T,2}}{P_{S,ts}} = \left(\frac{6 \cdot M_1^2}{5}\right)^{7/2} \cdot \left(\frac{6}{7 \cdot M_1^2 - 1}\right)^{5/2}$$

To solve for Mach number, the tabulated corresponding values for M_1 and $P_{T,2}/P_{S,ts}$ from Reference 7 were plotted and curve fit to provide an equation for M_1 as a function of $P_{T,2}/P_{S,ts}$. Using this curve fit equation allowed for the calculation of Mach number and subsequently airspeed at each probe location for the supersonic conditions.

The velocity profile data were normalized using the velocity calculated for the twenty-fifth total pressure probe (a probe known to be in the tunnel core flow) on each individual boundary layer rake. This insured that all boundary layer velocity profiles would approach 1.0 as the distance from the tunnel wall increased. Computation of the velocity ratios is illustrated with the following equation:

$$UR = \left(\frac{U_{bl}}{U_{ts}}\right)(i,25) = \frac{U_{bl}(i,j)}{U_{bl}(1,25)}$$

Once the velocity ratio profiles were plotted from the experimental data, the boundary layer thickness was estimated from the data plots. The boundary layer thickness, δ, was defined as the point where the velocity ratio of 0.99 occurred. In mathematical terms, δ can be defined as follows:

$$\delta = Z\big|_{UR-0.99}$$

The boundary layer thickness was estimated by linearly interpolating between the measured data that bracketed the *UR* = 0.99 point.

Measurement Uncertainty

The accuracy of the pressure measuring system used was ±0.0097 psi for absolute pressure levels. An error analysis was performed to determine the accuracy of the Mach number and flow angularity data. This analysis is very similar to that described in Reference 5. The analysis showed that the Mach number measurement accuracy improved from ±0.004 at Mach 0.5 to ±0.001 at Mach 2.0. The measurement

uncertainty for the flow angularity data is ±0.1°. The accuracy in the total temperature measurements is ±2.39 °F for absolute readings and ±0.39 °F for temperature gradients (probe to probe variation).

Discussion of Results

As this calibration included all six test section configurations available in the 8x6 SWT, there was a very large data set collected during the testing. To make the report less cumbersome for the reader, most of the data figures are contained in the appendices, with one set of data plots used as the primary example and provided in the figures. In general, the 14-ft, 5.8 percent porosity test section (configuration 1) will be used as the example in the figures, although some other specific examples may also be used.

Flow Quality Goals

Flow quality goals for the NASA Glenn wind tunnels have been defined and are listed in Table IV. These flow quality goals are based on information and recommendations from the Wind Tunnel Calibration Workshop held at NASA Langley (Ref. 10) and modified for the specific missions of the propulsion wind tunnel facilities at NASA Glenn.

Bellmouth Total Pressure Measurement Evaluation

The bellmouth total pressure measurement is one of the key parameters used in setting the test section operating conditions and is used as a key measurement in the test section calibration equations. It is therefore very important that there is a high degree of confidence in and understanding of the measurement being made. Leaks in the pressure lines were very common, often requiring the one or more of the eight measurements were “coded-out” (not used in further calculations to determine operating conditions). Determining “good” and “bad” measurements was further complicated since there appears to be a pressure gradient across the tunnel as the south rake generally read higher than the north rake.

To provide a better understanding of the bellmouth total pressure measurement, an 8-ft pressure survey rake was installed along the tunnel centerline at the bellmouth exit such that the tips of the probes were at the same station as the facility bellmouth total pressure rakes. Three pressure differences were used to compare the measurements from the facility rakes to the 8-ft rake data:

$$\Delta P_{T,bm,\text{north}} = P_{T,\text{8-ft},avg} - P_{T,bm,\text{north},avg}$$

$$\Delta P_{T,bm,\text{south}} = P_{T,\text{8-ft},avg} - P_{T,bm,\text{south},avg}$$

$$\Delta P_{T,bm,avg} = P_{T,\text{8-ft},avg} - P_{T,bm,avg}$$

It should be noted that during the data review, one of the total pressure measurements on the south rake was in error due to a leak in the line so this data was subsequently not used in the analysis. Also, the two probes at either end of the 8-ft rake were not used in computing the average total pressure from the rake; this was done to insure that boundary layer effects were not included in the average.

Figure 14 shows the total pressure difference data over the Mach number range of the tunnel. The data indicate that the south rake measurement is always slightly greater than the centerline value (from the 8-ft rake) while the north rake measurement is always slightly less than the centerline value. This could indicate a pressure gradient across the tunnel. It is unlikely that this difference between the north and south rakes is related to boundary layer as previous studies showed the boundary layer in this area is on the order of 2 in. or less (Ref. 2). The average total pressure measured by the two facility rakes matches the centerline total pressure very closely. Looking at the average across the entire data set, the measured total pressure from the north rake is 0.004 psia less than the centerline value, the average from the south rake is 0.005 greater than the centerline value and the overall average of the two rakes generally matches the centerline value from the 8-ft rake within ±0.002 psia.

This simple study showed that even though the average pressure measured by the south bellmouth rake was consistently higher that that measured by the north bellmouth rake, the average total pressure sensed by both rakes provided a accurate representation of the total pressure along the centerline of the tunnel at the bellmouth exit. The difference between the measurements from the two bellmouth rakes is the result of an undefined local flow non-uniformity. In general, the difference between the south and north rakes is about 0.010 psia and can be as high as 0.015 psia. However, this difference should not be a concern to research customer, as this effect is accounted for in the calibration curves used to set the operating conditions. The important item to note is that four individual measurements on each rake agree within approximately ±0.003 psia from the average for that rake. Measurements that deviate from the average more than this amount should be reviewed and possibly "coded-out" for that tunnel run.

Axial Static Pressure Distribution

The static pressure distributions over the 4-in.-diameter cone cylinder for the 14-ft, 5.8 percent porosity test section configuration (configuration 1) are shown in Figure 15 (similar data for selected other test section configurations are found the data appendix). These data were collected during the 1997 calibration entry. Each data set is the average of thee data readings collected at a given test condition. Each data point in the data set is the average of the two or four static taps around the circumference of the cone cylinder model at each station (i.e. the data point at station 2.972 in. downstream of the cone tip is the average of the four static taps at that station, one from each row of taps; the next point, at station 4.94 in. downstream of the cone tip is the average of the two taps at that station, and so on). For simplicity, the static pressure ratio data are plotted with respect to the distance downstream cone tip rather than the test section station. Note that when the cone cylinder model is placed in the forward position, the cone tip is nominally at test section station 144 which corresponds to the centerline of the window blank in the porosity section (testing in test section configurations 1 and 6). For test section configurations 2 through 5, the cone tip was placed at the entrance of the 8-ft test section (nominally test section station 178).

Also shown in Figure 15 and the appendix is the average static pressure ratios from the cone surface (for supersonic operation) and aft portion of the cylinder as well as the theoretical pressure distribution over the model for supersonic settings (details on the theoretical data are found in Ref. 1). The average static pressure over the aft portion of the cylinder is based on all measurements from model station 40 and aft, since the theoretical data indicates that the pressure should be constant along the cylinder starting at station 40.

Figure 16 shows the Mach number distribution over the length of the 4-in.-diameter cone cylinder model for the 14-ft, 5.8 percent porosity test section configuration (configuration 1); similar data for the other test section configurations are provided in the appendix. The Mach number at each station is based on the ratio of the static pressure measured at that station to the measured bellmouth total pressure. At supersonic conditions, the Mach number values over the cone portion of the model represent the freestream conditions (the ratio of cone static pressure to bellmouth total pressure, $P_{S,\text{cone}}/P_{T,bm}$, is used to calculate the cone surface Mach number, M_{cone}; M_{cone} is then used to determine the freestream Mach number, $M_{fs,\text{cone}}$, based on the data provided in Ref. 1). The average freestream Mach number based on cone conditions and the Mach number based on average conditions over the aft portion of the cylinder are also shown on these figures for each test point. In order to gage the Mach number gradient through the test section, a linear best fit of the Mach number data over the aft portion of the cylinder was added to each data set (static taps starting at model station 40). Table V lists the Mach number gradient over the operating range of the tunnel for each test section configuration.

For each test section configuration, the subsonic static pressure and Mach number distributions over the cone cylinder model indicate very well behaved and uniform flow. There was nominally no Mach number gradient over the aft portion of the cylinder at subsonic conditions. The 14-ft, 5.8 percent porosity, the 8-ft, 3.1 percent modified porosity and the 14-ft schlieren window test section configurations showed no gradient at all over the subsonic operating range. The other configurations showed only very

small gradients on the order of 0.001/ft or less. The only other point to note was at a Mach number setting of 0.25 where the gradient was 0.001 to 0.002/ft.

At supersonic conditions, each test section configuration demonstrated different trends and characteristics in terms of static pressure and Mach number distributions. There is no clear best test section configuration in terms of static pressure or Mach number distribution through the test section. The 8-ft, 3.1 percent modified, 8-ft, 6.2 percent and 8-ft, 6.2 percent modified test section configurations have the least gradient at the high supersonic conditions ($M > 1.7$). The 14-ft test section configurations have the highest gradients in the high supersonic regime. In the mid-range supersonic regime ($1.3 \leq M \leq 1.7$), the 14-ft, schlieren window configuration provides the least gradient over the cylinder. The best of the 8-ft test section configurations is the 3.1 percent modified porosity test section. For this test section configuration, the Mach number gradient ranged from 0 to ±0.006/ft over the supersonic operating range.

The data collected in 1997 compares very favorably with historical data collected in the 1960s, as described by Mitchell (Ref. 11). While the hardware used in the 1960s and 1997 tests are not the same, the later hardware was based on the original 1960 vintage test articles. The disturbances in the pressure profiles due to nonporous areas of the test section walls, reflected shocks and terminal shocks that were noted in Reference 11 are also seen in the 1997 data.

Since the cone cylinder model only provides part of freestream static pressure distribution through the test section (the data along the aft portion of the cylinder), a study was conducted to piece together the overall freestream static pressure distribution by running the 4-in.-diameter cone cylinder at two axial positions for a given test section configuration. Combining the data from the two model positions should provide a better overall representation of the static pressure or Mach number distribution axially through the test section. The results of this study would also help to confirm if using the average cylinder static pressure provides a representative measurement of the freestream static pressure in the forward portion of the test section.

Figure 17 shows the results of this study. The testing was conducted in the 8-ft, 3.1 percent modified test section. The 4-in. diameter cone cylinder was first positioned such that the cone tip was at the inlet of the 8-ft test section (station 178) as is the normal procedure for testing this hardware in the 8-ft test section, then the model was moved forward so that the tip of the cone was at the centerline of the schlieren window blank (station 144) as is the case for calibration in the 14-ft test section. The data collected from these two configurations provided enough information to construct a freestream static pressure distribution through the length of the 8-ft test section. Figure 17 also shows the average values of freestream Mach number based on the cone and cylinder average conditions (data from the cone is used for supersonic conditions only).

The combined data sets shown in Figure 17 indicate that for the 8-ft, 3.1 percent modified test section the axial static pressure distribution is fairly uniform throughout the test section. For subsonic operation, the combined data set shows that the Mach number gradient through the 8-ft test section is 0.001/ft or less. The distribution shows no gradient in the forward portion of the 8-ft test section with a slight acceleration over the aft few feet of the test section length.

The supersonic data results, while not as uniform as the subsonic, also show good axial trends, although each Mach number condition exhibits slightly different characteristics. A very important and encouraging trend is that the shape of the distributions is repeatable where the combined data sets overlap. This is most evident for nominal Mach number settings from 1.5 to 2.0. For the cylinder data, the comparison area[6] is from test section station 210 to 230. Over this range, the data from the upstream and downstream model locations match nearly exactly, which provides a good indication of the repeatability of the flow field. At the lower supersonic settings (nominal Mach numbers of 1.4 and lower), the comparison between the data sets is not as close, primarily due to shock impingement and difference in the location of the terminal shock on the model. It was also possible to compare the calculated freestream

[6]Over this range of test section station, the cylinder data from the upstream model location is in the constant pressure region (according to theoretical data), while the constant pressure range does not start until about station 220 for the downstream model location.

Mach number from the cone data at the downstream location to cylinder data from the upstream location. Here again, the Mach number profiles were very repeatable and the average Mach number values matched very well. This again demonstrates the highly repeatable nature of setting operating conditions in the test section.

Flow Field Surveys Results

The transonic array was used to collect several flow field parameters, including total and static pressure, Mach number, total temperature and pitch and yaw flow angles. Each of these flow field parameters are discussed in this section. As the flow quality results are similar for each test section configuration, the 14-ft, 5.8 percent porosity is used for the discussion of results and the data for the other configurations are contained in the appendices. The data plots for each parameter include the data from five vertical survey positions (five array vertical heights) within the survey plane. For the 14-ft test section, the survey plane is the centerline of the porous schlieren window blank, which is a typical test article location. Surveys were also made at the inlet of the 8-ft test section (downstream of the schlieren windows). The surveys locations are shown in Figure 5. The pressure, temperature and Mach number data are normalized to account for run-to-run variations in conditions. The specific operating conditions from the centerline run are listed with each data plot for reference.

Figure 18 shows the total pressure distributions measured in the 14-ft, 5.8 percent test section. With the exception of the highest Mach number settings (M_{nom} = 2.0 and 1.9), the measured total pressure distributions show very uniform flow field in the supersonic, transonic and subsonic regimes. At M_{nom} = 2.0 and 1.9, there is a total pressure deficit in the center of the test section, most likely due to a flow separation from the compressor exit tailcone (Ref. 2). In the deficit region the total pressure is 0.3 to 0.4 psi less than the pressure levels measured nearer to the test section boundaries.

Figure 19 shows the Mach number distributions at the same station in the test section. The Mach numbers at each probe locations were calculated from the total pressure measured by the array and the calibrated static pressure (based on cone cylinder results). This was done as that static pressure data measured by the array was adversely affected by probe-to-probe interference at several test settings. The trends shown in the Mach number data are therefore very similar to those of the total pressure data. The total pressure deficit region recorded at the higher Mach numbers resulted in a 0.014 Mach number spanwise variation at the test section centerline for the M_{nom} = 2.0 setting and a variation was 0.024 at M_{nom} = 1.9 in the core of the test section. At M_{nom} = 1.8 the variation has dropped to less than 0.010 and the variation continues to drop with decreasing Mach number. In the subsonic regime the variation is 0.001.

Total temperature distributions are provided in Figure 20. Overall, the total temperature distributions are uniform across the test section, with only minor variations. At the high supersonic Mach number settings, there is a slight gradient across the test section, with higher temperatures recorded nearest the inside test section wall. At M_{nom} = 2.0, the gradient is about 2 °R and at M_{nom} = 1.8 the gradient is 3.5 to 4 °R, depending on the vertical position of the array. As the Mach number decreases, the trend changes from a gradient to a profile with the higher temperatures near the core of the test section and lower temperatures nearer the walls. This profile is evident at M_{nom} = 1.3 and lower, including subsonic conditions, although the profiles become much flatter at the low speed settings and one-motor operation. There is also some vertical spread between the horizontal surveys. At M_{nom} = 2.0, there is about a 3 °R spread between the horizontal surveys indicating a vertical temperature gradient in the test section.

Pitch and yaw flow angularity data are presented in Figure 21. The flow angularity in the 8x6 test section has a maximum variation of about ±1°, however, for most Mach number settings, the flow angularity in pitch and yaw varies between ±0.6°. In general, the yaw angle is larger than the pitch angle. The flow angularity in the 8x6 SWT is caused in large part due to the location of the facility compressor directly upstream of the test section. The rotational flow from the compressor is fed directly into the test section. Improvements to the flow conditioners in the settling chamber upstream of the test section (3

turbulence reduction screens and a flow straightening honeycomb) have improved the overall flow quality, but the flow angularity is still greater than the stated flow quality goals. Reference 4 provides a comparison of the 8x6 test section flow quality before and after the flow conditioner upgrades. The general trend over the Mach number range is that there is a downflow (negative pitch angle) in the center of the test section, and a left to right crossflow (positive yaw angle) across the span of the test section.

Calibration Curves for Determining Test Section Operating Conditions

One of the primary goals of the calibration testing was to develop a set of relationships, or calibration curves, that relate test section flow parameters to parameters outside the test section sensed by the facility instrumentation. In the case of the 8x6 SWT, four calibration curves were developed for each test section configuration, two related to total pressure (on each for subsonic and supersonic operation) and one each for static pressure and total temperature (covering the entire Mach number range). From these curves, all other test section operating conditions are calculated. Six sets of curves were developed, one for each test section configuration, to account for subtle differences in axial station (between the 14- and 8-ft test sections) and in wall porosity. Each set of calibration curves covers the 8x6 SWT over its operating range for 1- and 3-drive motor operation (Mach 0.25 to 2.0). The calibration curves were constructed from data collected during the 1997 calibration test entry. This section lists the needed inputs, calibration outputs and calculated test section conditions based on the calibrated values. The information contained in this section was used to develop the subroutine used in all data collection programs to calculate the test section conditions[7].

The inputs for the calibration relationships are listed below:

- Bellmouth total pressure (psia), $P_{T,bm}$: average of eight bellmouth total pressure measurements, $P_{T,bm}(i)$, i=1 to 8, four pressures each on two rakes located at the bellmouth exit (north and south rakes)
- Balance chamber static pressure (psia), $P_{S,bal}$: average of 4 balance chamber static ports, $P_{S,bal}(i)$, i = 1 to 4
- Bellmouth total temperature (°F), $T_{T,bm}$: average of 4 bellmouth total temperature measurements, $T_{T,bm}(i)$, i=1 to 4. Note that the bellmouth total temperature is measured in °R, and must be converted to °F; this was done to simplify the construction of the total temperature calibration curve. In subsequent calculations, the units are converted back to °R.

$$T_{T,bm}\ (°\mathrm{F}) = T_{T,bm}\ (°\mathrm{R}) - 459.6$$

- Test section configuration, TSCFG

  TSCFG = 1 for the 14-ft, 5.8 percent porosity test section
  TSCFG = 2 for the 8-ft, 6.2 percent porosity test section
  TSCFG = 3 for the 8-ft, 3.1 percent porosity test section
  TSCFG = 4 for the 8-ft, 6.2 percent modified porosity test section
  TSCFG = 5 for the 8-ft, 3.1 percent modified porosity test section
  TSCFG = 6 for the 14-ft schlieren window configuration

The calibration relationships were based on data collected using the transonic array and the 4-in. diameter cone cylinder. All calibration conditions are based on measurements made at the test section

[7]In addition to the final set of calibration curves described in this report, there were four preliminary sets of calibration curves that were developed for specific customer tests that occurred prior to the final curves being completed. These preliminary calibration curves were similar in form and function to the final curves but were test specific in that they covered only one test section configuration, and general only a portion of the operating range.

centerline and at defined axial stations, depending on the test section configuration (centerline of the schlieren window blank for the 14-ft test section configurations, or inlet of the 8-ft test section for all other configurations). The calibration coefficients listed in each equation depend on the test section configuration (TSCFG) and are listed in Table VI. The calibration curves for each test section configuration are very similar, so only the curves for the 14-ft, 5.8 percent porosity test section are included for reference (Figs. 22 through 25).

A key parameter used in the operation of the facility is the ratio of the balance chamber static to bellmouth total pressure; this parameter was also used in the calibration relationships for the test section total and static pressure:

$$PR_{bal/bm} = \frac{P_{S,bal,avg}}{P_{T,bm}}$$

There were three test section static pressure measurements available from the calibration data, the average value measured by the array, the average pressure over the aft portion of the cone cylinder and a calculated value based on the conditions measured on the cone portion of the cone cylinder. All three values agree within reason; however the static pressure over the aft portion of the cone cylinder seems to provide the best representation of the static pressure over the entire operating range of the facility. The data from the cone portion of the cone cylinder is useful for supersonic conditions. At transonic conditions, there is some scatter in the array data, plus the mounting of the array to the test section walls has a small localized effect on the static pressure. As a result, the calibrated test section static pressure, $P_{S,ts}$ (psia), is based on the average static pressure measured over the aft portion of the 4-in. diameter cone cylinder. Figure 22 shows the calibration curve for determining the test section static pressure. The equation for the calibrated test section static pressure is:

$$P_{S,ts} = P_{T,bm} \cdot \left(B_0 + B_1 \cdot x + B_2 \cdot x^2 + B_3 \cdot x^3 + B_4 \cdot x^4 + B_5 \cdot x^5 + B_6 \cdot x^6\right), \text{ where: } x = PR_{bal/bm}$$

The test section total temperature is determined from the calibration curve built from measurements made from the array. The calibrated test section total temperature is related to the bellmouth total temperature through this calibration curve. Note that the data in Figure 23 are in °F, so the calibrated value must be converted to °R, as shown below:

$$T_{T,ts} = \left(C_0 + C_1 \cdot T_{T,bm} + C_2 \cdot {T_{T,bm}}^2 + C_3 \cdot {T_{T,bm}}^3 + C_4 \cdot {T_{T,bm}}^4\right) + 459.6$$

Total pressure calibration is based on measurements made in the test section by the array and in the bellmouth by the facility rakes. For subsonic operation ($PR_{bal/bm} > 0.5330$), the calibrated test section total pressure is determined from a simple relationship to the bellmouth total pressure (Figure 24):

$$P_{T,ts} = A_0 + A_1 \cdot P_{T,bm} + A_2 \cdot {P_{T,bm}}^2$$

The test section Mach number, $M_{ts,}$ is then calculated based on the calibrated values of test section total and static pressure

$$M_{ts} = \sqrt{5\left[\left(\frac{P_{S,ts}}{P_{T,ts}}\right)^{-0.2857} - 1\right]}$$

For supersonic operation ($PR_{bal/bm} \leq 0.5330$), the test section total pressure is not calculated directly from a calibration curve. In the supersonic regime, the calibration is based on the total pressure

downstream of a normal shock (psia), $P_{T,2}$, which is sensed directly by the array pressure probes. The resulting calibration curve is shown in Figure 25:

$$P_{T2} = P_{T,bm} \cdot \left(AS_0 + AS_1 \cdot x + AS_2 \cdot x^2 + AS_3 \cdot x^3 + AS_4 \cdot x^4 + AS_5 \cdot x^5 + AS_6 \cdot x^6\right), \text{ where } x = PR_{bal/bm}$$

Test section Mach number for supersonic operation is based on the ratio of calibrated test section static pressure to the total pressure downstream of a normal shock ($P_{S,ts}/P_{T,2}$) and is calculated using the Rayleigh pitot formula (Eq. 100 from Ref. 7), which is solved iteratively for Mach number[8]

$$\frac{P_{T,2}}{P_{S,ts}} = \frac{P_{T,2}}{P_{S,1}} = \left[\frac{(\gamma+1)M_1^2}{2}\right]^{\frac{\gamma}{\gamma-1}} \left[\frac{\gamma+1}{2\gamma M_1^2 - (\gamma-1)}\right]^{\frac{1}{\gamma-1}}$$

For the analysis, $M_1 = M_{ts}$.

The test section total pressure, $P_{T,ts}$, is then calculated using Equation 99 from Reference 7.

$$\frac{P_{T,2}}{P_{T,1}} = \left[\frac{(\gamma+1)M_1^2}{(\gamma-1)M_1^2+2}\right]^{\frac{\gamma}{\gamma-1}} \left[\frac{\gamma+1}{2\gamma M_1^2 - (\gamma-1)}\right]^{\frac{1}{\gamma-1}}$$

As $P_{T,2}$ and M_1 are known, $P_{T,1}$ is easily calculated. $P_{T,1}$ is the test section total pressure, $P_{T,ts}$.

The following set of equations is used to compute the test section flow conditions based on the calibrated test section conditions.

Test section static temperature (°R): $$T_{S,ts} = \frac{T_{T,ts}}{1 + 0.2 \cdot M_{ts}^2}$$

Test section airspeed (ft/sec): $$U_{ts} = M_{ts} \cdot a_{ts} = M_{ts}\sqrt{\gamma \cdot R \cdot T_{S,ts}}$$

Test section air density (slugs/ft^3): $$\rho_{ts} = \frac{P_{S,ts}}{R \cdot T_{s,ts}} \cdot 144$$

Test section air viscosity (slugs/(ft·sec)): $$\mu_{ts} = 2.270 \frac{T_{S,ts}^{1.5}}{T_{S,ts} + 198.6} \cdot 10^{-8}$$

Test section Reynolds number (·10^6/ft): $$\mathrm{Re}_{ts} = \frac{\rho_{ts} U_{ts} l}{\mu_{ts}}$$ where l = 1 ft

Test section dynamic pressure (psia): $$q_{ts} = P_{T,ts} \cdot \frac{\gamma}{2} M_{ts}^2 \left(1 + \frac{\gamma-1}{2} M_{ts}^2\right)^{-\frac{\gamma}{\gamma-1}}$$

A summary of the inputs and outputs from the computing requirements is provided in Table VII.

[8] An iterative method is used in the facility data acquisition systems. For local data analysis using Excel, the data from Reference 7 were plotted and a best-fit curve was fit to the data. The equation for this curve is used in the spreadsheet analysis tools.

Boundary Layer Thickness Data

Boundary layer thickness measurements were made along each test section surface at three stations in the test section. Typical boundary layer profiles at selected Mach number settings are shown in Figure 26. The objective of these measurements was to determine the overall thickness of the boundary layer in the test section over the Mach number range in order to know the effective usable area of the test section. Figure 27 shows the boundary layer thickness for each test configuration as a function of Mach number. Note that the data from rake three was not used due to an instrumentation problem for most of the testing. This issue was corrected for the final three boundary layer test configurations and the rake three data is included on those charts.

The boundary layer thickness is greater at subsonic conditions. At the inlet of the porous portion of the test section, the boundary layer is 5.5 to 6 in. thick at subsonic conditions, but only 3.5 to 4 in. thick for supersonic settings. Similar trends were noticed at the downstream stations, although the difference in boundary layer thickness was not as pronounced. For example, at the aft most station, the boundary layer thickness at subsonic conditions was 5.5 to 7 in. and 4.5 to 5.5 in. at supersonic Mach numbers.

In the region of the test section where the test articles are generally positioned (in or immediately downstream of the downstream schlieren windows), the boundary layer is 5.5 to 6 in. thick at subsonic conditions and about 4.5 in. thick at supersonic conditions. Using 6 in. at the thickness at subsonic conditions gives an effective test section area of 5- by 7-ft. At supersonic conditions a slightly larger effective area can be used due to the slightly smaller boundary layer thickness.

Other Investigations

In addition to the primary studies already discussed, there were other objectives that were addressed during the 1996 and 1997 test entries, although not all of these were successfully completed. A summary of each is provided here.

Model Blockage Effects

This report has focused on the empty test section calibration and flow quality of the 8x6 SWT. However, testing was also completed to look at the affects of test article (model) blockage on the test section conditions. These studies used the larger diameter cone cylinders. During the 1996 and 1997 tests, data were collected using the 4-, 8-, 12- and 16-in. diameter cone cylinders; additional testing was conducted in a subsequent test entry using a 20-in. diameter cone cylinder. The data and results from these larger diameter cone tests will be documented in a separate report.

Supersonic Strut Effects

During a customer research test, the test article was mounted on the supersonic (forward) strut and the transonic (aft) strut was used to support auxiliary equipment. This was the first time this particular configuration has been used for testing. During this test entry, it was not possible to set desired supersonic Mach numbers using the standard operating procedures. At supersonic conditions, the flexible wall was set at the next higher Mach number position in order to achieve the desired condition in the test section (for example, to get a nominal test section Mach number of 1.7, the flexible wall was set to the Mach 1.8 position). It was thought that the additional blockage of the supersonic strut may have contributed to this situation. While not the ideal way to operate the facility, this method did allow for the successful completion of the test project. However, it was felt that an understanding of why this occurred was needed.

To simulate the condition seen during the customer test, the supersonic strut was extended into the test section and position just below the 16-in. cone cylinder. The cone cylinder model was supported by

the transonic strut. However, the tunnel operated normally during this test. Basically, it was not possible to replicate the condition encountered during the subject customer test.

Since the initial issue, the basic configuration has been used several time (test article mounted on the supersonic strut with the transonic strut used for auxiliary support), but the mismatch between the flexible wall setting and the actual Mach number has not reoccurred.

Effects of Humidity on Freestream Conditions

Standard operating procedures recommend that testing at supersonic conditions should take place at low humidity or dew point conditions. The general practice is that the dew point should be -15° F or lower for supersonic conditions when testing in the 8x6 SWT. During the calibration testing, the test section dew point was allowed to slowly increased while the air dryer beds saturated in order to quantify the affects of humidity on the flow field. This was a time consuming process and ultimately showed little effect on the test section flow field data. Additional investigation is needed.

Summary of Results

The following is a summary of the primary results from the test section calibration and flow quality surveys conducted in the 8- by 6-ft SWT during 1996 and 1997. Relative to the specific test objectives stated is this report:

1. Data collected during the test were used to construct calibration curves that cover the entire operating range of the facility for each test section configuration. A subroutine based on the calibration curves was developed for use in all data collection programs used in testing at the 8- by 6-ft SWT.
2. Detailed flow quality mapping of the test section was completed. The transonic array was used to map the flow field within a place and the 4-in. diameter cone cylinder provided axial static pressure and Mach number distribution data.
    a. Cone cylinder data show that the axial static pressure and Mach number gradient through the test section is generally small. For subsonic conditions, the Mach number gradient is about 0.001/ft or less. The gradient at low supersonic conditions was difficult to determine due to the affects of model generated disturbances reflecting back onto the cone cylinder. At higher supersonic conditions, the Mach number gradient was on the order of 0.010/ft.
    b. The flow quality within a plane of the test section was also found to be good over the entire Mach number range, although the flow quality is superior at subsonic conditions.
        (1) The Mach number variation within the core of the test section is about 0.001 at subsonic conditions, varies from 0.001 to 0.010 at transonic settings, and increases to 0.015 to 0.040 at high supersonic conditions. The highest variations are at the Mach 1.9 and 2.0 settings were flow separation from the compressor exit tailcone causes a deficit region at the center of the test section.
        (2) Total temperature variations in the test section are on the order of 2° to 4°R. At the high supersonic conditions, the temperature is slightly higher near the inside (south) test section wall then decreases across the test section. For all other conditions, the total temperature is highest at the center of the test section and decreases toward each tunnel sidewall.
        (3) The pitch and yaw flow angles in the test section are higher than desired, ranging generally ±0.5°. The flow angularity is attributed to the flow swirl exiting the compressor, which is directly upstream of the test section. The screens and honeycomb flow straightener that were added to the facility in the early 1990s greatly improved the flow angularity in the test section, but did not complete solve the issue.
3. Based on the axial Mach number distributions, the 14-ft, 5.8 percent porosity, the 8-ft, 3.1 percent modified porosity and the 14-ft schlieren window configuration have the best characteristics for subsonic operation. At supersonic conditions, the 8-ft test section has the better characteristics, with

the 3.1percent modified porosity having the smallest axial Mach number gradient. Overall, the 8-ft, 3.1 percent modified porosity configuration has the lowest axial Mach number gradient over the entire operating range of the 8x6 SWT.

4. A portion of the testing using the larger diameter cone cylinders was completed; however, the results of those tests were not included in the current report. That data will be combined with results from other planned cone cylinder testing and will be detailed in a separate document.
5. We were not able to quantify the dew point effects during the 1996 or 1997 test entries. Investigation into dew point affects will be addressed during future calibration testing.
6. Boundary layer data were collected over the operating range of the 8- by 6-ft SWT at three stations in the test section. In general, the boundary layer is 5.5 to 6 in. thick for subsonic conditions and 3.5 to 4.5 in. thick at supersonic settings. The effective test section area is approximately 5- by 7 ft
7. Testing was conducted to investigate the affects of the supersonic strut on the test section flow field and calibration. However, it was not possible to reproduce the conditions documented during earlier testing. Additional discussion on this objective is deferred and will be discussed with the blockage data.
8. A simple study was conducted to check the effectiveness of the bellmouth total pressure measurements. The results showed that even though the average pressure measured by the south bellmouth rake was consistently higher that that measured by the north bellmouth rake, the average total pressure sensed by both rakes provided an accurate representation of the total pressure along the centerline of the tunnel at the bellmouth exit.

Concluding Remarks

A full aero-thermal calibration of the NASA Glenn Research Center 8- by 6-ft supersonic wind tunnel was completed over the course of two test entries during 1996 and 1997. This test program was the first comprehensive calibration in the 8- by 6-ft SWT since major flow quality improvements and data system upgrades had been installed in the facility in 1992. In the intervening time, calibration testing had covered limited areas of the facility operational range to meet customer requirements.

The calibration testing conducted during 1996 and 1997 provided data used to create calibration curves for the facility operation and provided detailed flow quality maps of the test section flow field. The calibration curves and the flow quality maps were the two primary objectives of the test program.

One objective that was not completed was to quantify the effects of humidity on the test section conditions. It is recommended that this objective should be readdressed during the next calibration of the 8- by 6-ft SWT.

Additional recommendations are:

1. No turbulence data were collected during the 1996 or 1997 calibration testing, in large part due to issues with the thermal anemometry data acquisition system. Quantifying the turbulence levels in the test section should be a priority for the next series of calibration and flow quality testing in the 8x6 SWT.
2. While the effects on Mach number setting that were attributed to the test configuration that used both the supersonic and transonic struts could not be repeated during the calibration testing and have not been observed in similar testing, additional review of the data collected and should be done to see if the root cause of this anomaly can be determined.
3. The current version of the test section calibration curves has a unique set of calibration relationships for each test section configuration. The possibility of collapsing this set of curves to a single set of calibration curves should be investigated.
4. Most importantly, the aero-thermal calibration testing in the 8x6 SWT should be set up as a recurring activity to ensure that the facility is operating as expected.
5. Test customers should have a briefing on the tunnel operation and test section flow quality and operation so that they are aware of the operational settings and flow quality attributes of the 8x6

SWT. For example, most customers assume that the flexwall Mach number setting of 2.0 will produce a test section Mach number of 2.0 plus-or-minus a few thousandths. The reality is that at supersonic settings the actual test section Mach number is 0.02 to 0.03 less than the wall setting.

TABLE I.—TYPICAL OPERATING CONDITIONS IN THE 8- BY 6-ft SUPERSONIC WIND TUNNEL, FOR THE 14-ft, 5.8 PERCENT POROSITY TEST SECTION CONFIGURATION. PRESSURE DATA HAS UNITS OF psia; TEMPERATURE DATA IS IN DEGREES RANKIN

Nominal Mach number (wall setting)	Test section Mach number M_{ts}	Test section total pressure, $P_{T,ts}$	Test section static pressure, $P_{S,ts}$	Test section dynamic pressure, q_{ts}	Test section total temperature, $T_{T,ts}$	Test section static temperature, $T_{S,ts}$	Reynolds number per unit length, Re/ft
2.00	1.982	25.182	3.309	9.101	649.2	363.6	5.05×10^6
1.90	1.886	24.747	3.776	9.399	644.5	376.6	5.23×10^6
1.80	1.779	23.164	4.163	9.222	633.6	388.0	5.23×10^6
1.70	1.664	21.535	4.609	8.927	622.5	400.7	5.18×10^6
1.60	1.555	20.067	5.044	8.539	612.4	412.7	5.10×10^6
1.50	1.452	18.958	5.535	8.167	603.6	424.6	5.03×10^6
1.40	1.352	17.955	6.031	7.720	596.7	436.9	4.92×10^6
1.30	1.253	17.248	6.634	7.288	590.5	449.4	4.83×10^6
1.20	1.184	17.015	7.168	7.029	589.0	460.1	4.78×10^6
1.10	1.077	16.647	8.017	6.514	586.9	476.3	4.66×10^6
1.00	1.037	16.753	8.473	6.376	571.8	470.7	4.81×10^6
0.95	0.974	16.811	9.149	6.079	572.0	480.7	4.75×10^6
0.90	0.906	16.751	9.842	5.653	570.6	490.2	4.63×10^6
0.85	0.857	16.744	10.364	5.328	569.6	496.6	4.54×10^6
0.80	0.804	17.031	11.126	5.037	570.9	505.5	4.47×10^6
0.75	0.757	17.188	11.753	4.718	572.0	513.1	4.36×10^6
0.70	0.703	17.413	12.525	4.327	572.8	521.3	4.22×10^6
0.65	0.654	17.502	13.129	3.933	572.1	527.0	4.07×10^6
0.60	0.603	17.347	13.563	3.458	569.0	530.4	3.84×10^6
0.55	0.554	17.021	13.817	2.969	564.1	531.4	3.59×10^6
0.50	0.505	15.573	13.088	2.332	547.9	521.4	3.17×10^6
0.45	0.462	15.369	13.277	1.984	543.2	521.0	2.95×10^6
0.40	0.411	15.154	13.487	1.598	540.0	522.4	2.66×10^6
0.35	0.356	14.856	13.611	1.206	534.5	521.3	2.32×10^6
0.30	0.294	14.945	14.074	0.853	534.0	524.9	1.97×10^6
0.25	0.248	14.977	14.347	0.620	533.0	526.5	1.69×10^6

TABLE II.—FINAL TEST MATRIX FOR THE 1996 (FIFTH CALIBRATION TEST ENTRY)
CALIBRATION OF THE 8-BY 6-ft SUPERSONIC WIND TUNNEL
[See Table III for the key defining test condition and configurations.]

Test section configuration	8-ft rake	Cone cylinders (diam.)			Array		
		4	8	12	14-ft test section	Inlet 8-ft test section	Aft station
14-ft, 5.8% porosity	X	L	L	----------	A	--	--
8-ft, 6.2% modified	--	S	S	----------	--	A	C
8-ft, 3.1% modified	--	S	S	Check out	--	A	C

TABLE III.—FINAL TEST MATRIX FOR THE 1997 (SIXTH CALIBRATION TEST ENTRY)
CALIBRATION OF THE 8-BY 6-ft SUPERSONIC WIND TUNNEL.

Test Section Configuration	Cone Cylinders (diam.)		Array			Boundary Layer Rakes		
	4	16	14-ft test section	Inlet 8-ft test section	Aft station	Forward station	Middle station	Aft station
14-ft, 5.8% porosity	L	L	A	--	--	C	A	A
14-ft, Schlieren	L	--	B	--	--	--	----	--
14-ft, with strut	L	L	B	--	--	--	----	--
8-ft, 6.2% porosity	S	--	--	C	C	--	----	--
8-ft, 3/1% porosity	S	--	--	C	C	--	----	--
8-ft, 6.2% modified	S	S	--	A	C	--	A,B	--
8-ft, 3.1% modified	L,S	S	--	A	C	--	A,B	A

Key:
Cone cylinder testing:
L: Long model (tip of the cone at the centerline of the Schlieren window blank).
S: Short model (tip of the cone at the inlet of the 8-ft test section).
Array:
A: Surveys made at 5 vertical positions (±2 ft, ±1 ft and centerline).
B: Surveys made at 3 vertical positions (±1 ft and centerline).
C: Surveys made at centerline position.
Boundary layer rakes (see Figure 9 for details):
A: Rakes mounted along the centerline of each test section surface
B: Rakes mounted off-centerline.
C: Forward station configuration.
Mach number settings for each test configuration:

- 0 – 0.09 using the air dryer air blowers.
- 0.25 – 0.5 in 0.05 increments using one drive motor
- 0.05 – 0.95 in 0.05 increments using three drive motors
- 1.0 – 2.0 in 0.1 increments using three drive motors.

TABLE IV.—SUMMARY OF THE TEST SECTION FLOW QUALITY
GOALS FOR THE NASA GLENN WIND TUNNELS

Flow quality parameter	Aeropropulsion Tunnels*	Icing Research Tunnel
Mach number variation	0.005	0.005
Flow angularity	±0.25°	±0.25°
Turbulence intensity	0.25%	0.50%
Total temperature variation	4 °F	2° F

*The Aeropropulsion Tunnels at NASA Glenn are the 9- by 15-ft Low Speed, the 8- by 6-ft Supersonic and the 10- by 10-Ft Supersonic Wind Tunnels.

TABLE V.—SUMMARY OF THE MACH NUMBER GRADIENT IN THE 8- BY 6-ft SUPERSONIC WIND TUNNEL OVER THE AFT PORTION OF THE 4-in. DIAMETER CONE CYLINDER MODEL. THE GRADIENT DATA IS PRESENT AS THE CHANGE IN MACH NUMBER PER FOOT AXIAL DISTANCE. A NEGATIVE GRADIENT INDICATES A DECREASE IN MACH NUMBER MOVING DOWNSTREAM.

Nominal Mach number	Test section configuration; cone cylinder position						
	1; forward	2; aft	3; aft	4; aft	5; forward	5; aft	6; forward
2.0	–0.0120	–0.0048	0.0036	0.0012	0.0024	0.0012	0.0072
1.9	–0.0120	–0.0108	0.0000	–0.0048	–0.0036	0.0060	0.0084
1.8	–0.0132	–0.0072	–0.0048	–0.0048	–0.0060	0.0024	0.0000
1.7	–0.0108	–0.0036	0.0000	–0.0012	–0.0012	–0.0036	–0.0048
1.6	–0.0072	–0.0096	–0.0072	–0.0084	–0.0072	–0.0048	–0.0024
1.5	–0.0060	–0.0048	–0.0060	–0.0060	–0.0060	–0.0036	–0.0024
1.4	0.0000	–0.0036	–0.0024	–0.0036	–0.0024	–0.0036	–0.0012
1.3	0.0080	0.0024	0.0036	0.0000	0.0000	0.0048	0.0000
1.2	–0.0064	–0.0072	0.0012	–0.0084	0.0000	0.0060	–0.0060
1.1	–0.0116	0.0096	–0.0024	0.0000	–0.0036	–0.0132	–0.0036
1.0	–0.0001	0.0008	0.0000	0.0010	0.0000	0.0000	–0.0012
0.95	0.0000	0.0011	0.0000	0.0007	0.0007	0.0000	0.0000
0.90	0.0000	0.0011	0.0010	0.0008	0.0011	0.0000	0.0000
0.85	0.0000	0.0012	0.0013	0.0010	0.0014	0.0000	0.0000
0.80	0.0000	0.0011	0.0010	0.0011	0.0013	0.0000	0.0000
0.75	0.0000	0.0012	0.0008	0.0013	0.0012	0.0000	0.0000
0.70	0.0000	0.0012	0.0008	0.0013	0.0012	0.0000	0.0000
0.65	0.0000	0.0011	0.0007	0.0010	0.0011	0.0000	0.0000
0.60	0.0000	0.0008	0.0011	0.0008	0.0012	0.0000	0.0000
0.55	0.0000	0.0007	0.0010	0.0007	0.0010	0.0000	0.0000
0.50	0.0000	0.0000	0.0000	0.0000	0.0007	0.0000	0.0000
0.45	0.0000	0.0000	0.0008	0.0000	0.0007	0.0000	0.0000
0.40	0.0000	0.0000	0.0000	0.0000	0.0000	0.0000	0.0000
0.35	0.0000	0.0000	0.0000	0.0000	0.0000	0.0000	0.0000
0.30	0.0000	0.0000	0.0000	0.0000	0.0000	0.0000	0.0000
0.25	0.0000	0.0007	–0.0023	–0.0017	–0.0023	–0.0007	0.0000
0.10	0.0000	0.0000	0.0000	0.0007	0.0000	0.0000	0.0000
0.05	0.0000	0.0000	0.0000	0.0000	0.0000	0.0000	0.0000

TABLE VI.–COEFFICIENTS FOR THE 8X6 SWT TEST SECTION CALIBRATION RELATIONSHIPS. THESE COEFFICIENTS ARE RELATED TO REVISION 11 OF THE CALIBRATION EQUATION PACKAGE AND COMPUTING SUBROUTINE (CAL8X6), DATED FEBRUARY 5, 2010

Coefficient	TSCFG = 1	TSCFG = 2	TSCFG = 3	TSCFG = 4	TSCFG = 5	TSCFG = 6
A0	–0.02114569	0.04830570	0.04810914	0.05584568	0.02642966	–0.06650522
A1	1.00450372	0.99591085	0.99561935	0.99511181	0.99839724	1.01010764
A2	–0.00020799	0.00005304	0.00007125	0.00007337	–0.00001841	–0.00037751
AS0	0.15884720	0.43583507	0.12071332	0.15506468	0.26402747	0.09637798
AS1	6.49237073	1.69227910	7.25798586	7.33949112	4.51612947	7.95668590
AS2	–23.40551285	8.17242011	–28.17490110	–34.93249601	–6.88038885	–37.33087104
AS3	47.19719057	–49.20304038	63.52764002	114.19147391	–24.60125170	116.14172911
AS4	–37.47021480	90.46670681	–77.89644589	–236.56756794	129.79404954	–223.45244093
AS5	–26.66932254	–58.60286108	39.10303801	268.90911165	–225.51330751	231.07855092
AS6	46.11300981	0.0	0.0	–127.14221644	141.32382941	–97.03010364
B0	0.05128924	–0.00114561	0.00597619	0.02185152	–0.01171580	0.04617664
B1	–0.00648346	0.87933383	0.79605022	0.50153397	1.08638290	0.18378462
B2	5.89854255	0.66961431	1.15972248	2.79796139	–0.68623582	4.25716993
B3	–16.19624065	–1.66947742	–3.27852537	–7.26803748	2.47869255	–10.62352959
B4	22.56109136	1.77787430	4.82086545	9.32197942	–4.49947664	13.60324308
B5	–15.48663996	–0.65627453	–3.58231661	–5.71574217	3.90847670	–8.61939454
B6	4.17879353	0.0	1.08326941	1.34054077	–1.27525960	2.15259269
C0	–26.81177495	–12.20583241	–17.33850761	–9.41273368	–10.56842273	–11.66755464
C1	1.74987278	1.4999034	1.64556762	1.40902588	1.42280591	1.42591556
C2	–0.00535707	–0.00426684	–0.00560190	–0.00344605	–0.00340432	–0.00321519
C3	0.00001140	0.00001025	0.00001409	0.00000825	0.00000778	0.00000664
C4	0.0	0.0	0.0	0.0	0.0	0.0

TABLE VII.—SUMMARY OF PARAMETERS USED TO DETERMINE THE TEST SECTION AERO-THERMAL CONDITIONS IN THE 8X6 SWT

Parameter	Program name	Description	Units	Source
Average Bellmouth and Balance Chamber Conditions				
$P_{T,bm}$	PTBM	Bellmouth total pressure	psia	Input
$P_{S,bal}$	PSBAL	Balance chamber static pressure	psia	Input
$T_{T,bm}$	TTBMA	Bellmouth total temperature	°R	Input
$T_{T,bm(F)}$	TTBMF	Bellmouth total temperature	°F	Calculated
TSCFG	TSCFG	Test Section Configuration	N/A	Input
Test Section Conditions—Calibrated Parameters (all operating conditions)				
$PR_{bal/bm}$	RPBHBM	Ratio of balance chamber static to bellmouth total pressure	Dimensionless	Calculation
$P_{S,ts}$	PSTS	Test section static pressure	psia	Calibration
$T_{T,ts}$	TOTS	Test section total temperature	°R	Calibration
Test Section Conditions—Calibrated Parameters (subsonic operating conditions)				
$P_{T,ts}$	PTTS	Test section total pressure	psia	Calibration
M_{ts}	MTS	Test section Mach number	Dimensionless	Calculated
Test Section Conditions—Calibrated Parameters (supersonic operating conditions)				
$P_{T,2}$	PT2	Test section total pressure downstream of a normal shock	psia	Calibration
M_{ts}	MTS	Test section Mach number	Dimensionless	Calculated
$P_{T,ts}$	PTTS	Test section total pressure	psia	Calculated
Test Section Conditions—Calculated Parameters				
$T_{S,ts}$	TSTS	Test section static temperature	°R	Calculated
U_{ts}	UTS	Airspeed	ft/sec	Calculated
$U(knt)_{ts}$	UTSK		knots	Calculated
ρ_{ts}	RHOTS	Air density	slugs/ft^3	Calculated
μ_{ts}	MUTS	Air viscosity	slugs/(ft sec)	Calculated
Re_{ts}	REFT	Reynolds number	10^6/ft	Calculated
Test Section Conditions—Calculated Parameters				
$q_{s,ts}$	QTS	Test section dynamic pressure	psia	Calculated
Constants and coefficients				
γ	GAMMA	Ratio of specific heats = 1.4	none	Constant
R	R	Gas constant = 1716	lbf-ft/(slug°R)	Constant
	A0 - A4	P_T calibration (subsonic)		Table VI
	AS0 - AS6	P_T calibration (supersonic)		
	B0 - B6	P_S calibration		
	C0 - C4	T_T calibration		

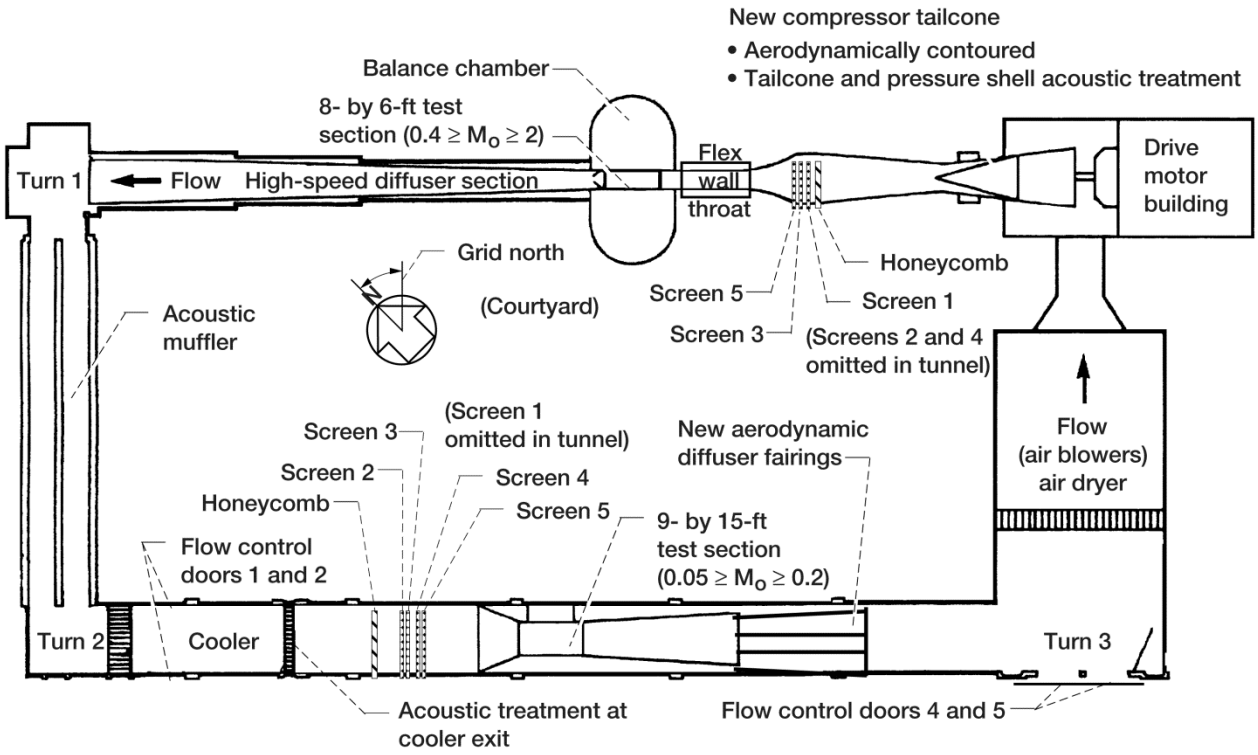

Figure 1.—Planview of the 8- by 6-Ft Supersonic/9- by 15-Ft Low-Speed Wind Tunnel Complex showing locations of flow quality improvements.

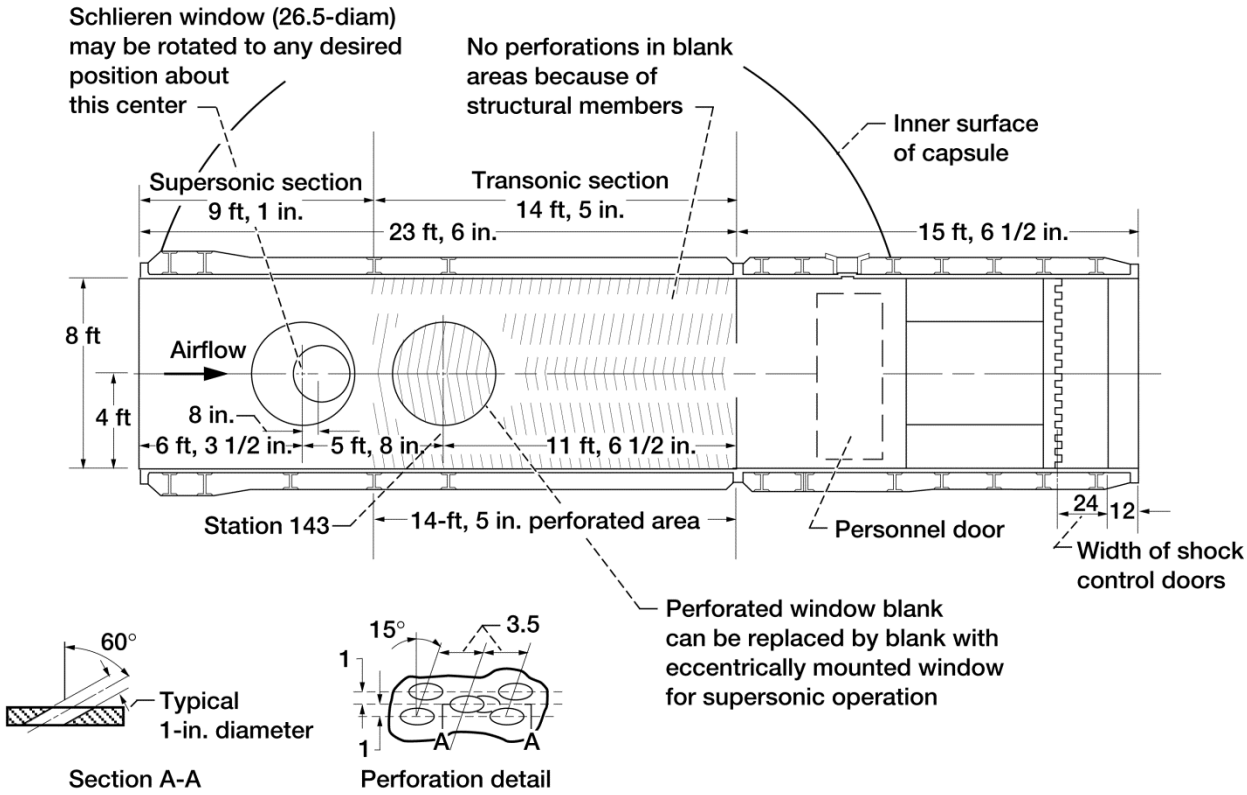

Figure 2.—8- by 6-ft test section elevation view. Dimensions are in inches unless otherwise noted.

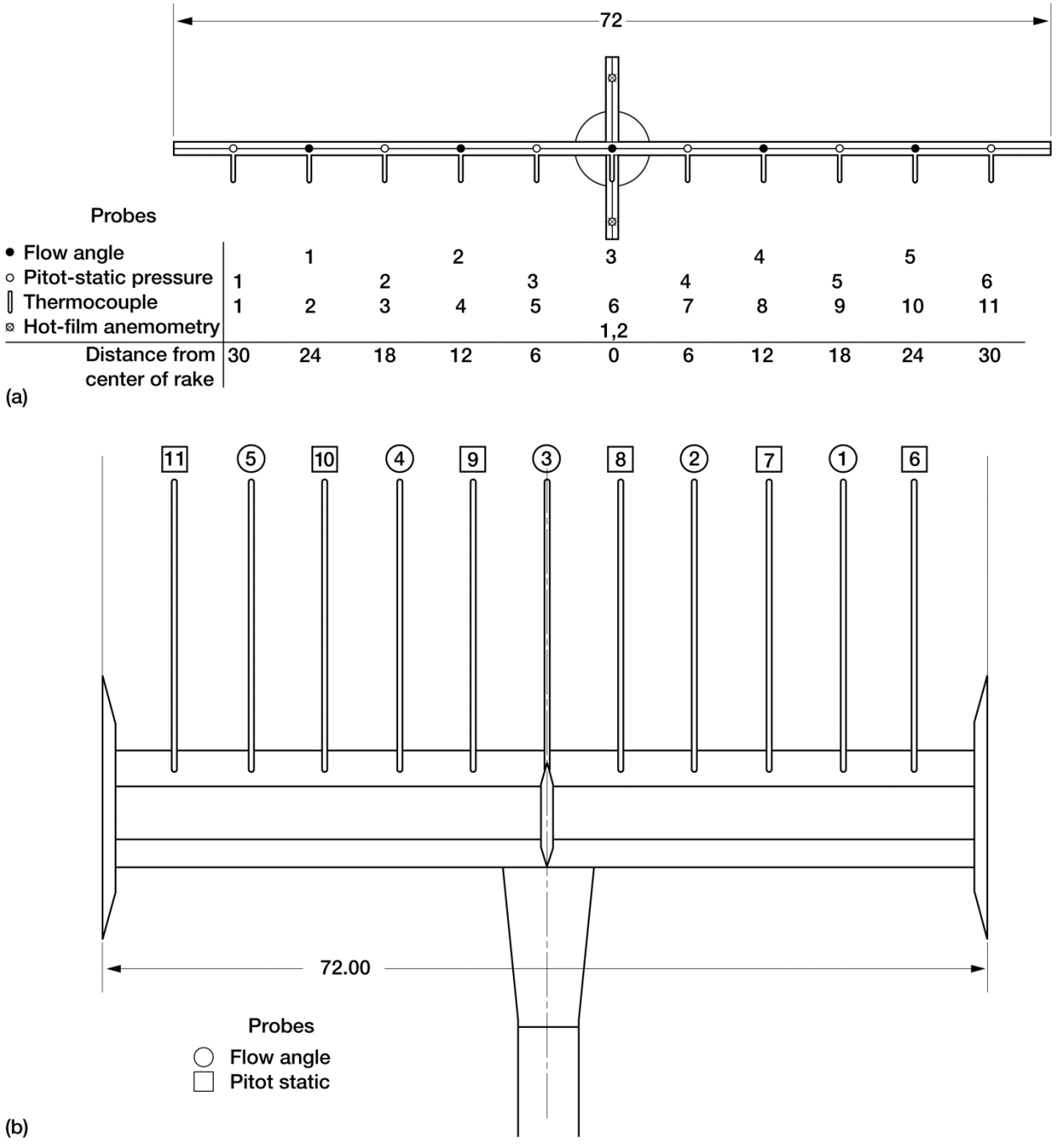

Figure 3.—Instrumentation layout of transonic array. (a) Downstream view. (b) Plan view. All dimensions are in inches.

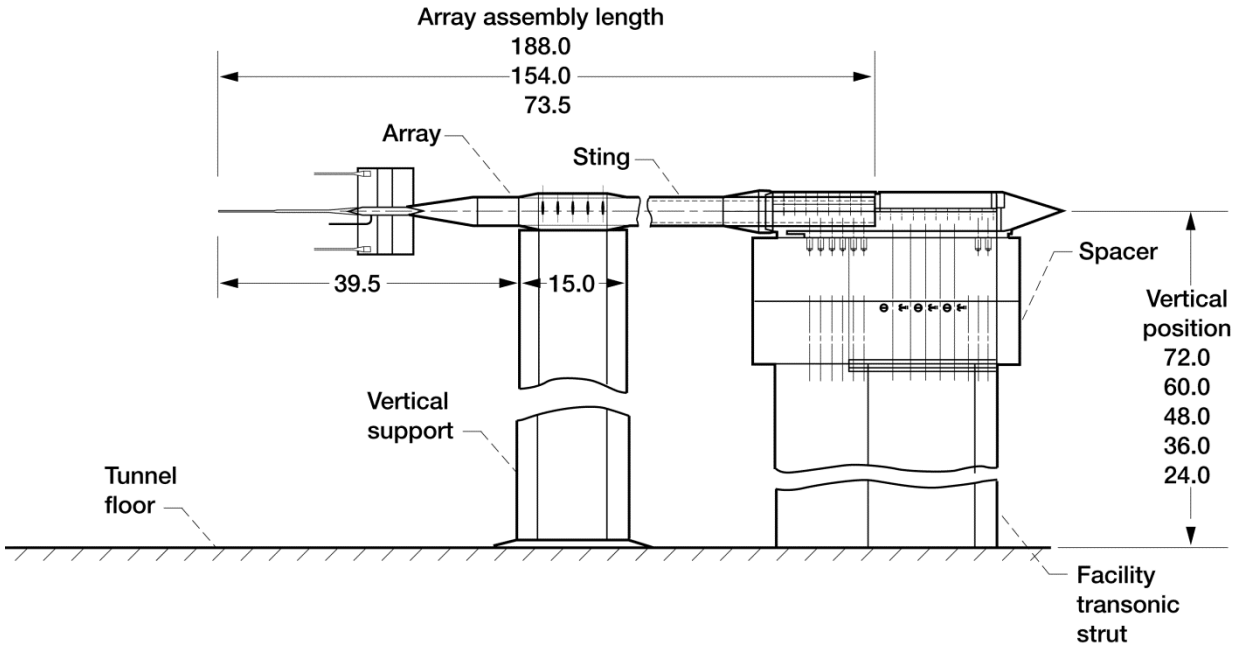

Figure 4.—Installation of transonic array in the 8- by 6-ft test section (elevation view). The array can be stationed axially in three positions. At each axial station, the array can be positioned at five vertical heights. All dimensions are in inches.

Nominal axial station (x) location of measurement planes in 8×6 SWT		
Model	14-ft TS	8-ft TS
Array	138.4 in.	171.4 in.
Cone cylinders	144.2 in.	178.4 in.

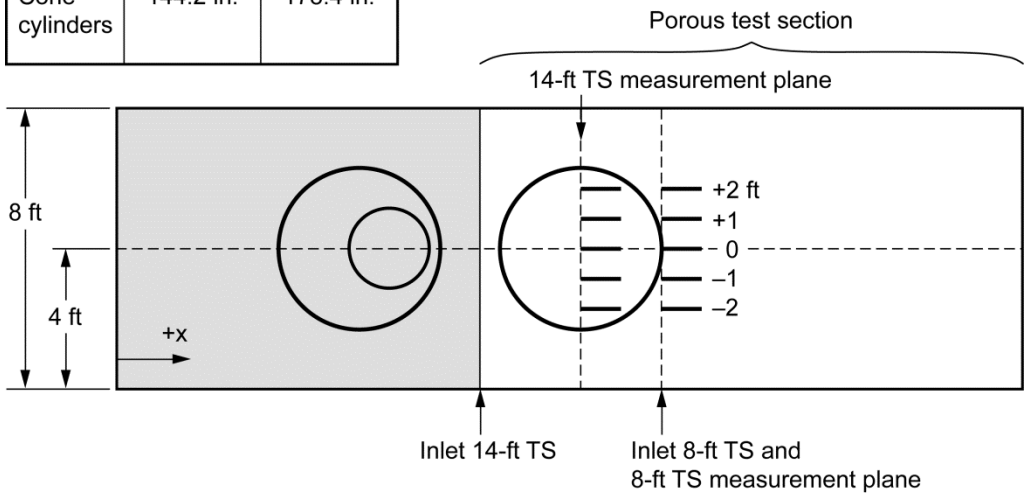

Figure 5.—Measurement locations for the transonic array in the 8- by 6-ft test section. Air flow is from left to right.

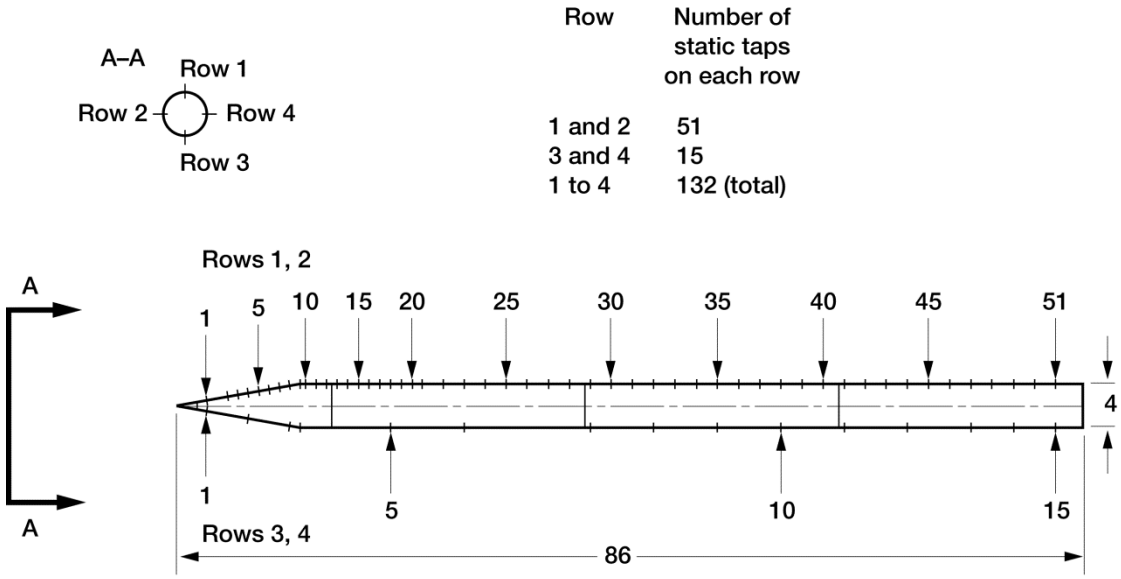

Figure 6.—Instrumentation layout of the 4-in. diameter cone cylinder. All dimensions are in inches.

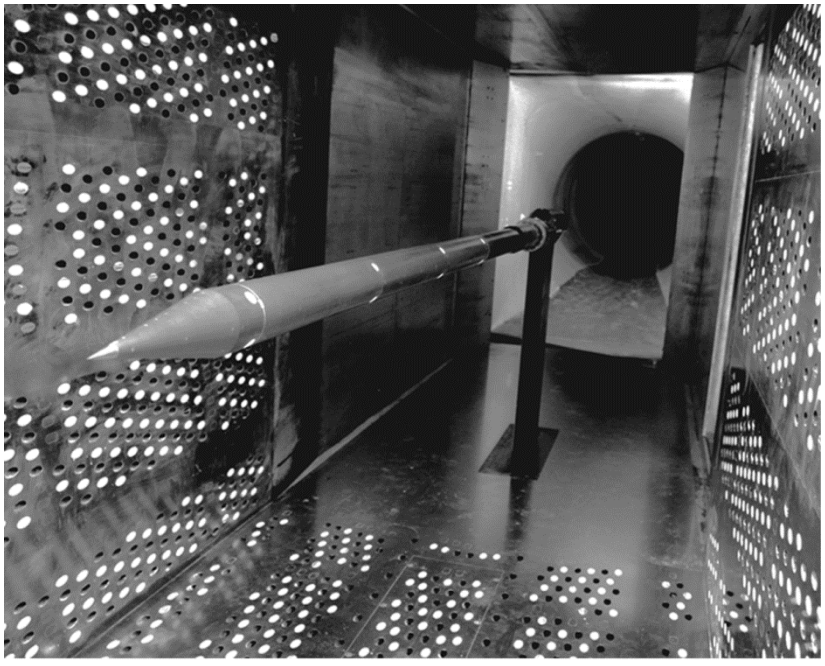

Figure 7.—Typical installation of the 4-in. diameter cone cylinder in the 8- by 6-ft test section. Model is shown with the tip of the cone at station 178 (inlet of the 8-ft test section).

Probe number	Distance from tunnel surface, Z, in.	Probe number	Distance from tunnel surface, Z, in.
1 base	0.250	14	6.500
2	0.500	15	7.500
3	0.750	16	8.500
4	1.000	17	9.500
5	1.250	18	10.500
6	1.500	19	11.500
7	2.000	20	12.500
8	2.250	21	13.500
9	3.000	22	14.500
10	3.500	23	15.500
11	4.000	24	16.500
12	4.500	25 tip	17.500
13	5.500		

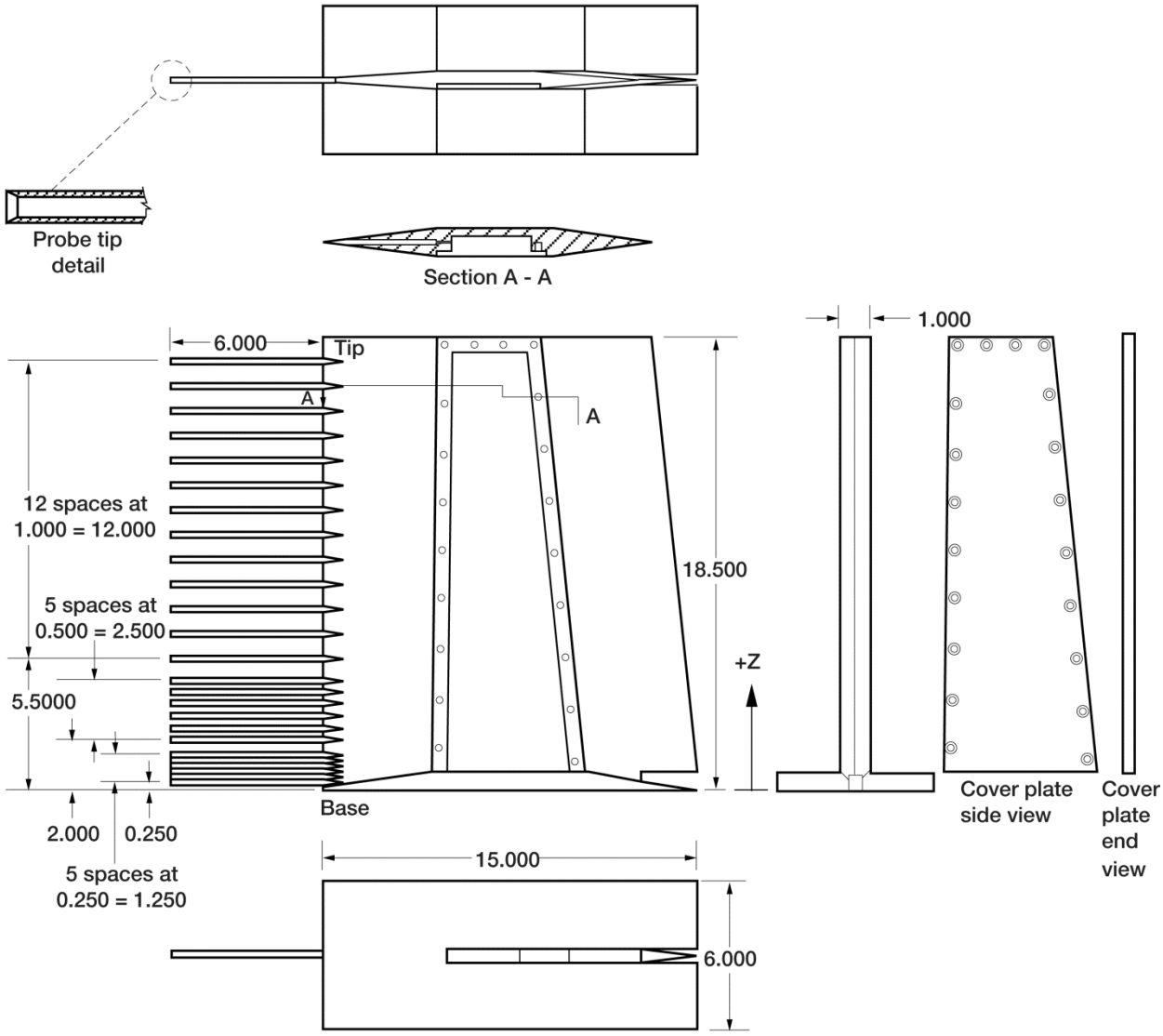

Figure 8.—Boundary layer rake details, layout and dimensions. All dimensions in inches.

Rake	X, axial		Y_i
1	171.4	241.5	36.0
2	175.0	231.0	47.8
3	164.4	241.5	36.0
4	175.0	238.3	48.1

Rake	X, axial	Y_i
1	171.4	55.4
2	175.0	72.5
3	164.4	16.3
4	175.0	25.4

Rake	X, axial	Y_i
1	108.8	35.9
2	107.1	57.6
3	108.1	36.0
4	106.9	14.6

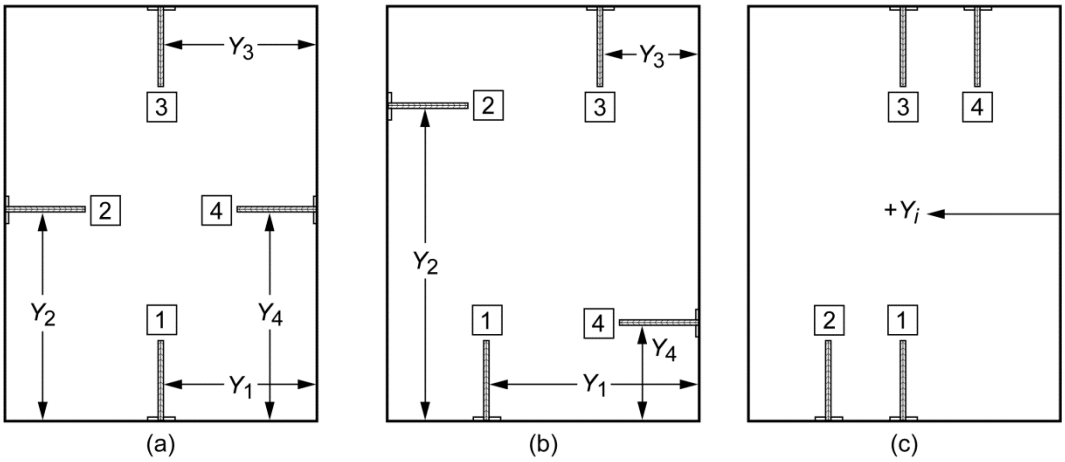

Figure 9.—Boundary layer rake installation in the 8- by 6-ft test section. (a) Configuration used at the inlet of the 8-ft test section and at the aft most station. (b) Off-centerline configuration used at the inlet of the 8-ft test section (middle station). (c) Configuration used at the inlet of the 14-ft test section. Axial station measured from test station 0 to the tips of the pressure probes. View looking downstream. All dimensions are in inches.

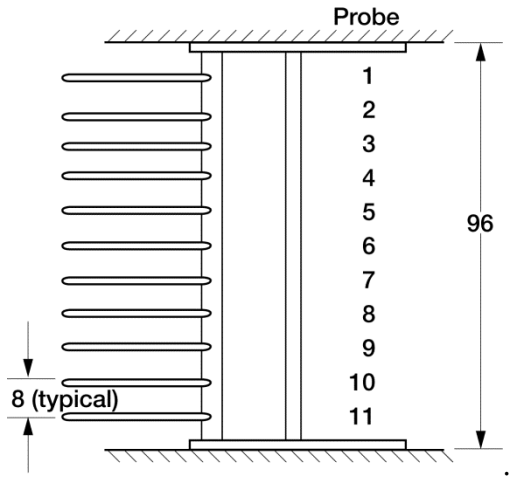

Figure 10.—Instrumentation layout for the 8-ft survey rake. All dimensions are in inches.

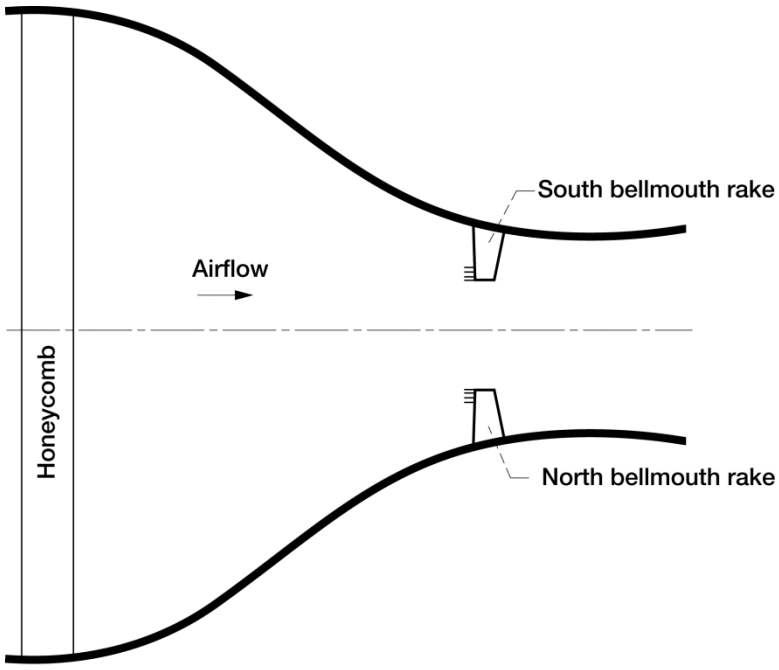

Figure 11.—Installation of the bellmouth total pressure rakes

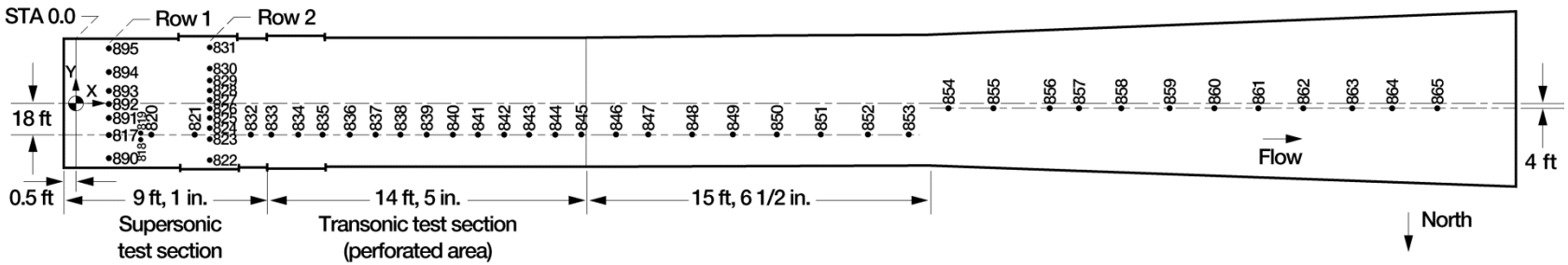

Static tap location	Axial station, X, in.	Distance from centerline, Y, in.	Static tap location	Axial station, X, in.	Distance from centerline, Y, in.
817	17.00	–18.00	838	169.25	–18.00
890	17.00	–30.63	839	183.25	–18.00
891	17.00	–7.50	840	197.50	–18.00
892	17.00	0.00	841	211.50	–18.00
893	17.00	7.56	842	225.50	–18.00
894	17.00	18.06	843	239.50	–18.00
895	17.00	25.78	844	253.38	–18.00
818	32.88	–19.56	845	267.63	–18.00
819	32.88	– 16.56	846	286.50	–18.00
820	39.31	–18.00	847	303.75	–18.00
821	63.31	–18.00	848	327.50	–18.00
822	72.25	–31.50	849	350.50	–18.00
823	72.25	–19.50	850	374.06	–18.00
824	72.25	–13.50	851	398.75	–18.00
825	72.25	–7.50	852	422.63	–18.00
826	72.25	–2.50	853	446.00	–18.00
827	72.25	2.50	854	473.38	–4.00
828	72.25	7.50	855	497.44	–4.00
829	72.25	13.50	856	528.19	–4.00
830	72.25	19.50	857	543.31	–4.00
831	72.25	31.50	858	567.19	–4.00
832	87.50	–18.00	859	593.25	–4.00
833	99.25	–18.00	860	617.31	–4.00
834	113.25	–18.00	861	641.25	–4.00
835	127.25	–18.00	862	665.25	–4.00
836	141.38	–18.00	863	692.31	–4.00
837	155.75	–18.00	864	713.25	–4.00
			865	736.94	–4.00

Figure 12.—Static tap locations in the 8- by 6-ft testing section ceiling.

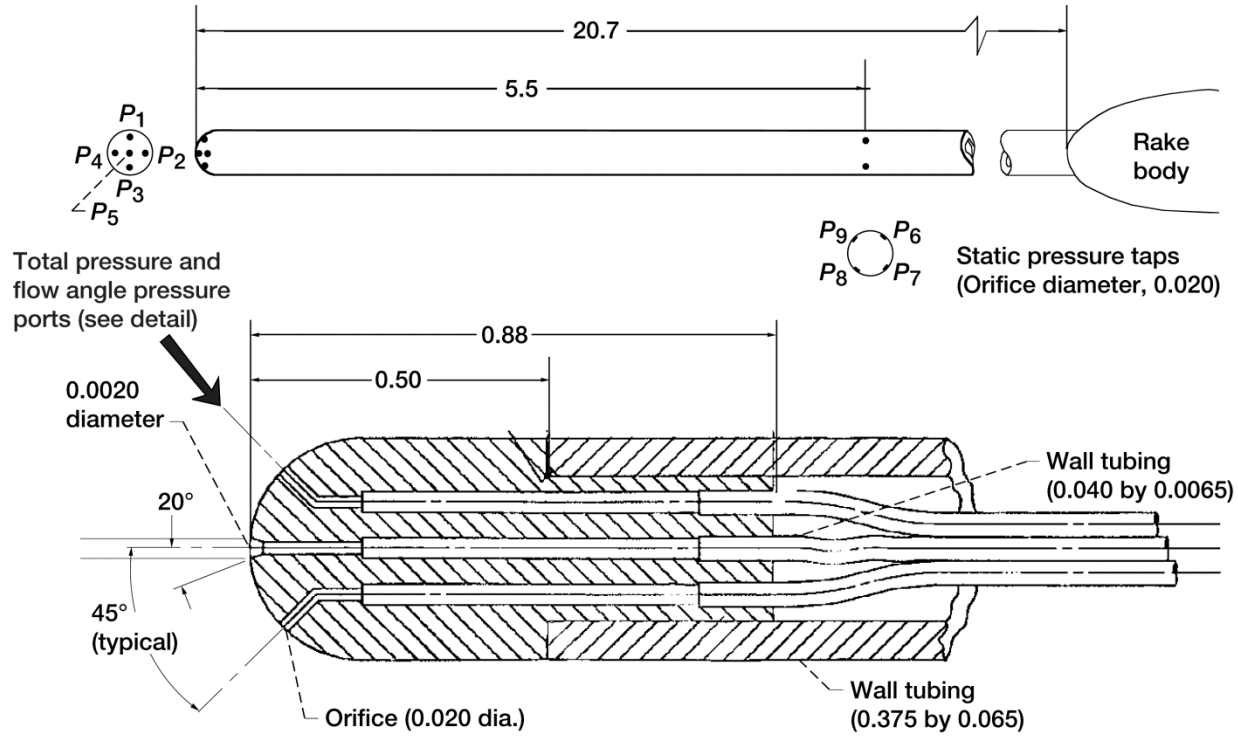

Figure 13.—Typical five-hole hemispherical head Flow-angularity probe layout. Dimensions in inches.

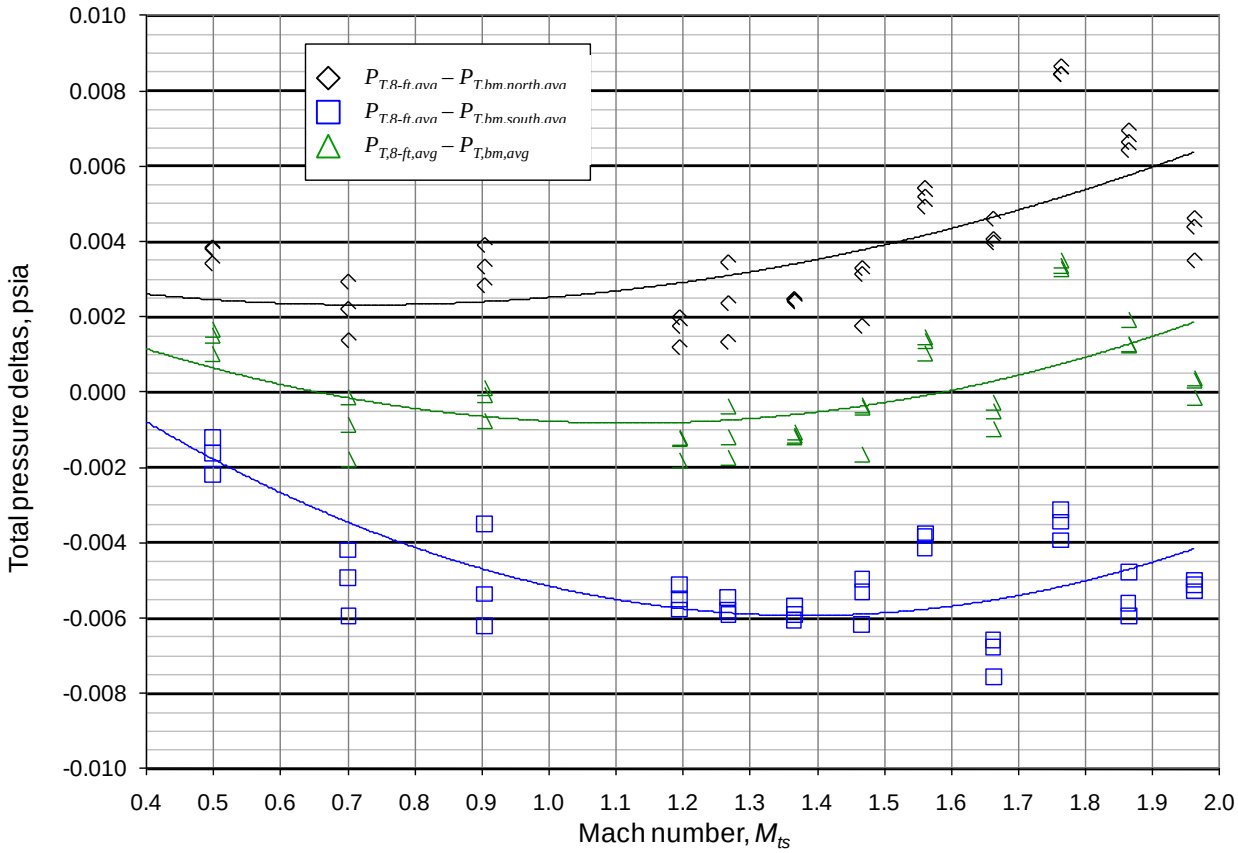

Figure 14.—Results of the bellmouth total pressure rake checkout testing in the 8x6 SWT. The trend lines were added to show the general trend of the deltas of each rake over the Mach number range of the facility.

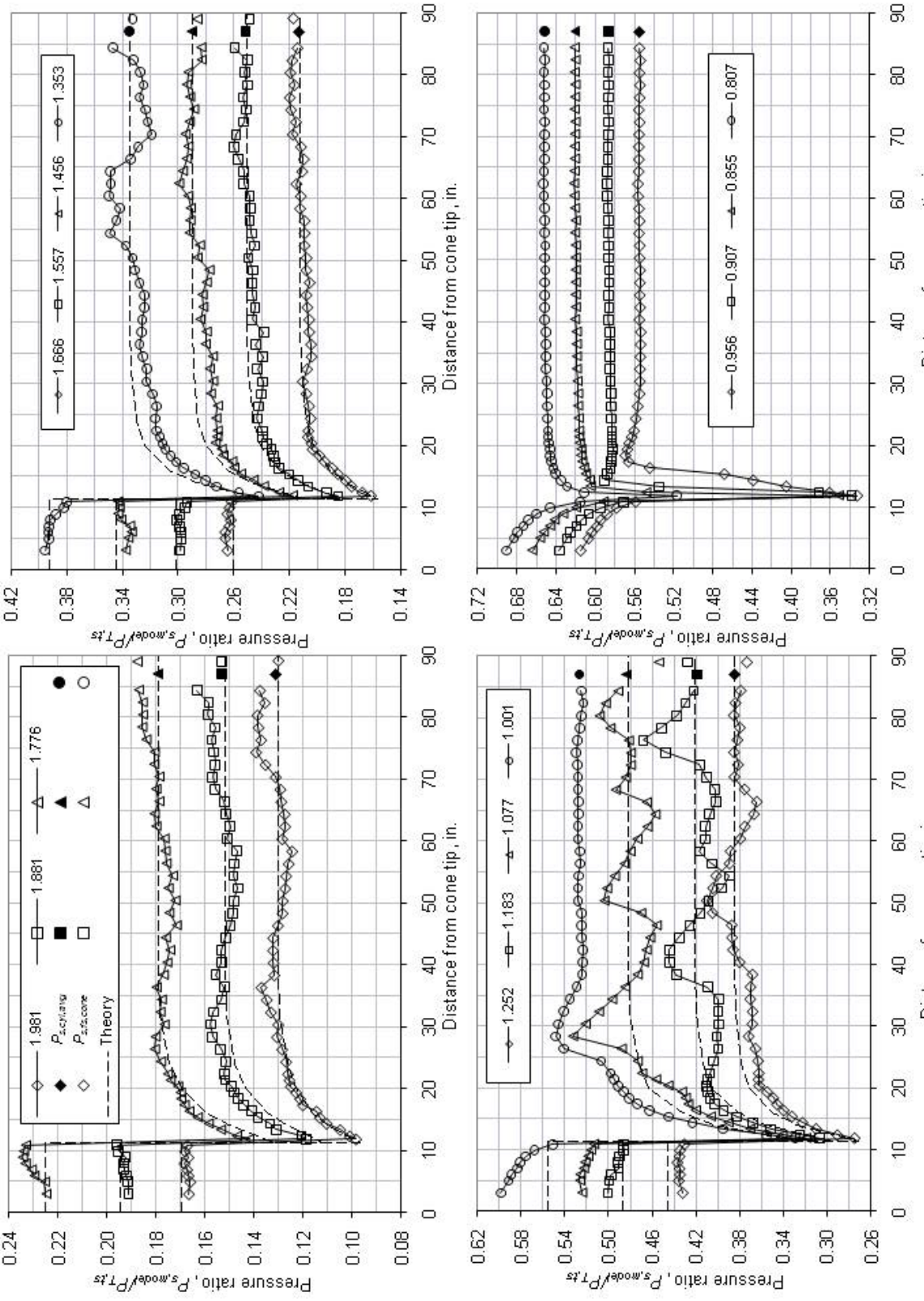

Figure 15.—Axial pressure profiles along the 4-in. diameter cone cylinder. Test section is set to the 14-ft, 5.8 percent porosity configuration. The tip of the cone is positioned at the centerline of the schlieren window (test section station 144).

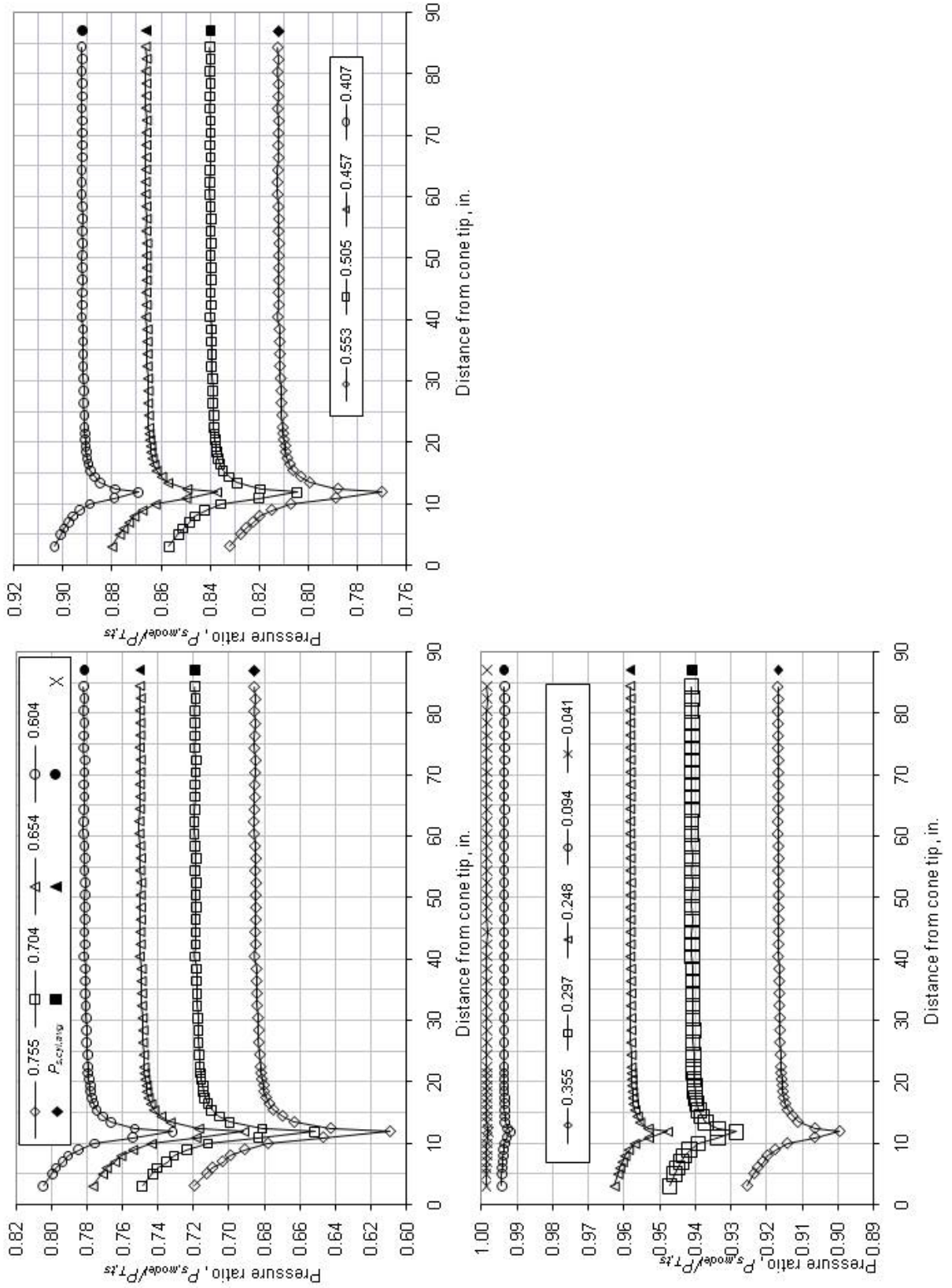

Figure 15.—Concluded.

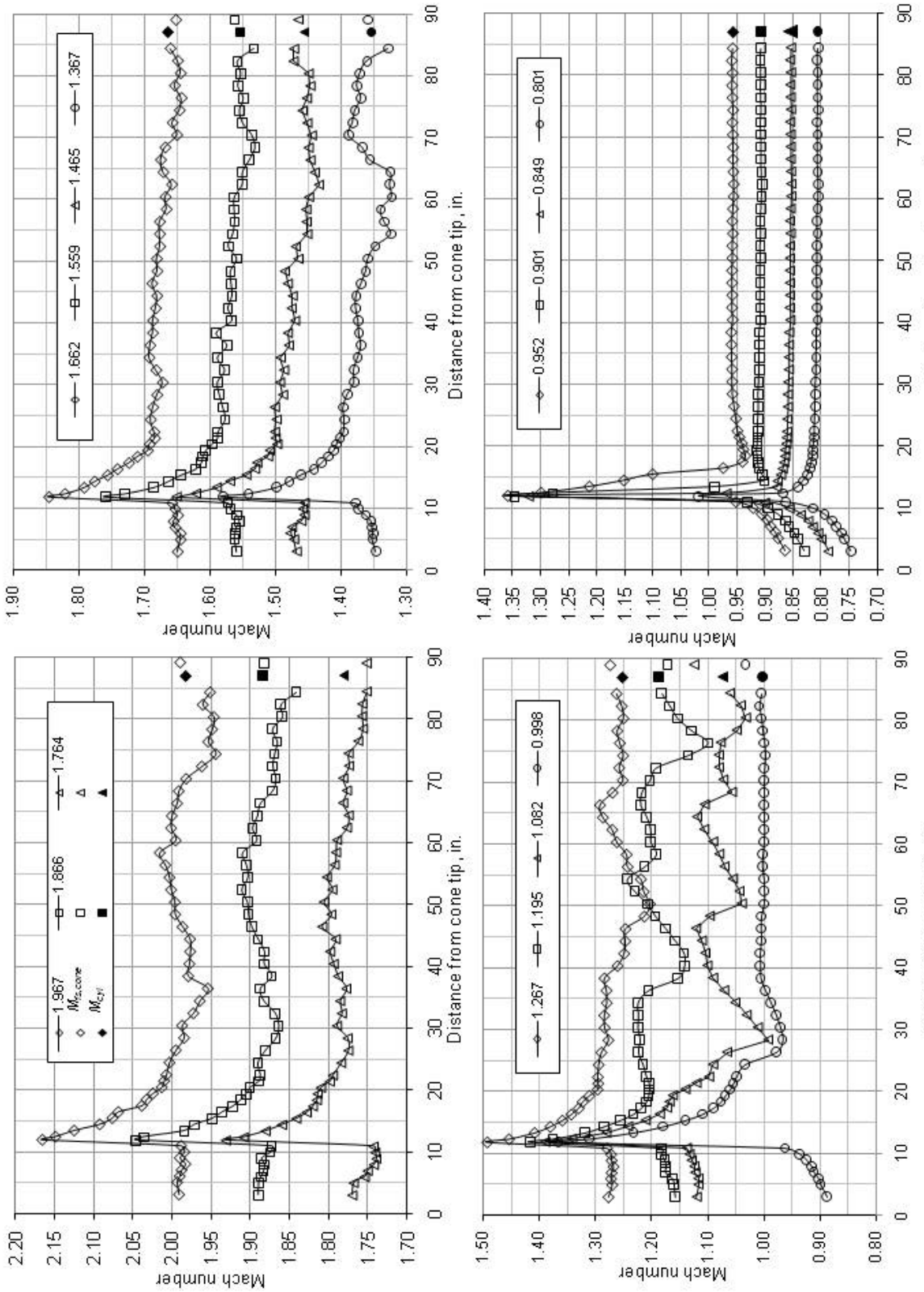

Figure 16.—Axial Mach number distribution from the 4-in. diameter cone cylinder. Test section is set to the 14-ft, 5.8 percent porosity configuration. The tip of the cone is positioned at the centerline of the schlieren window (test section station 144).

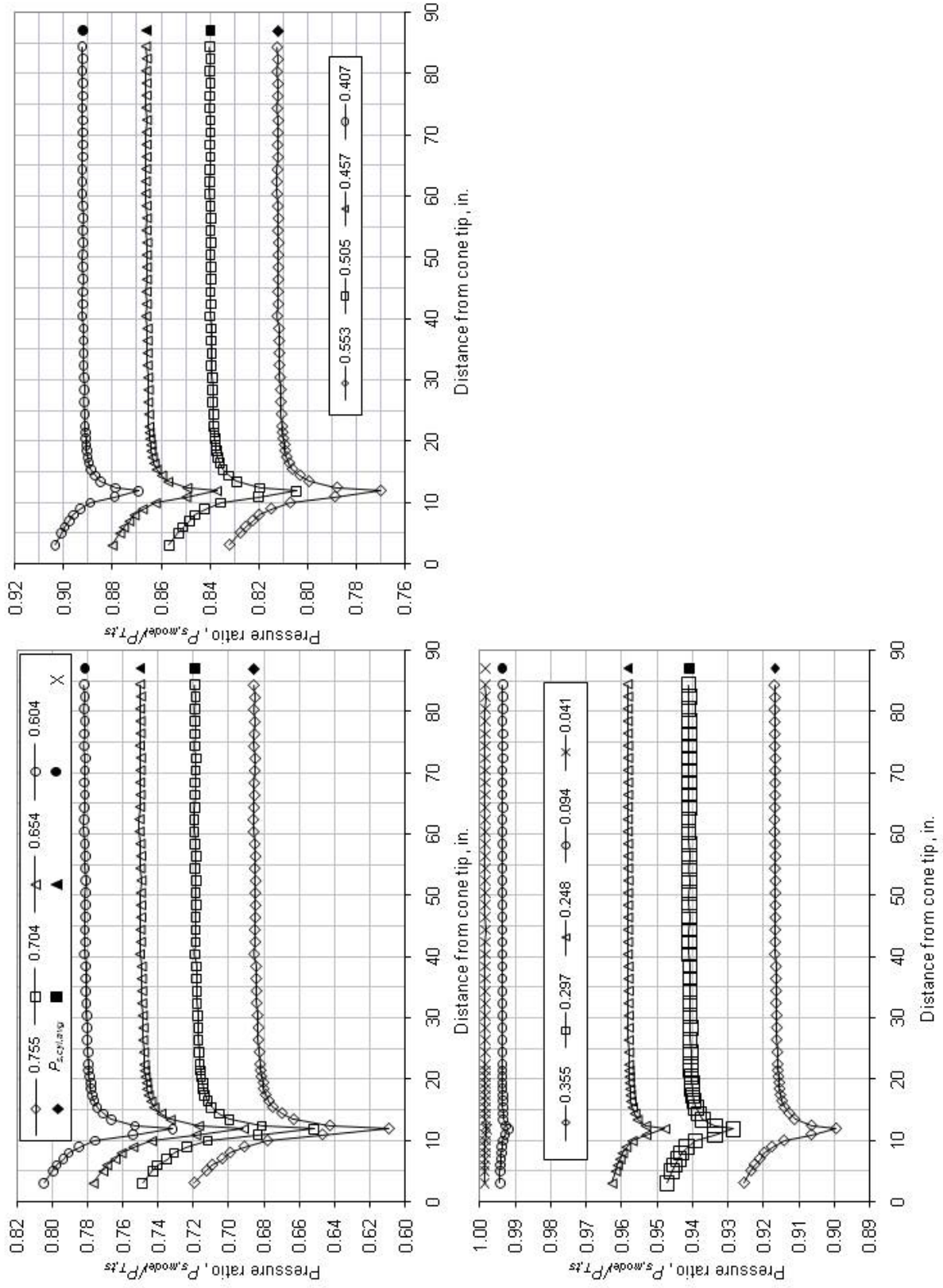

Figure 16.—Concluded.

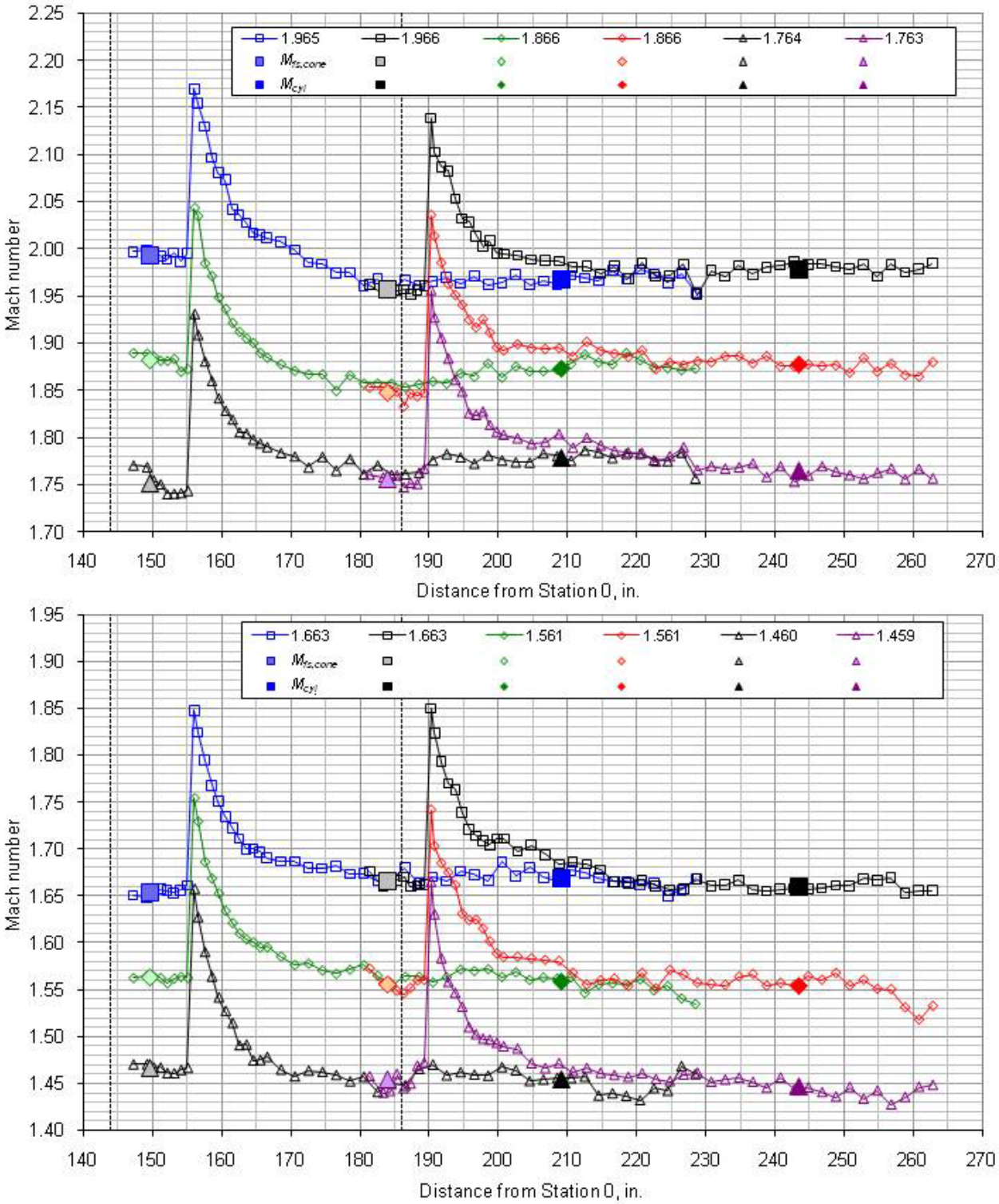

Figure 17.—Combined axial Mach number distributions along the 4-in. diameter cone cylinder with the model positioned at both the forward (long model) and aft (short model) stations. Test section configuration was the 8-ft, 3.1 percent modified porosity. The dashed line at approximately station 144 represents the beginning of the porous region o f the test section (inlet of the 14-ft test section); the dashed line at station 186 is the start of the 8-ft test section.

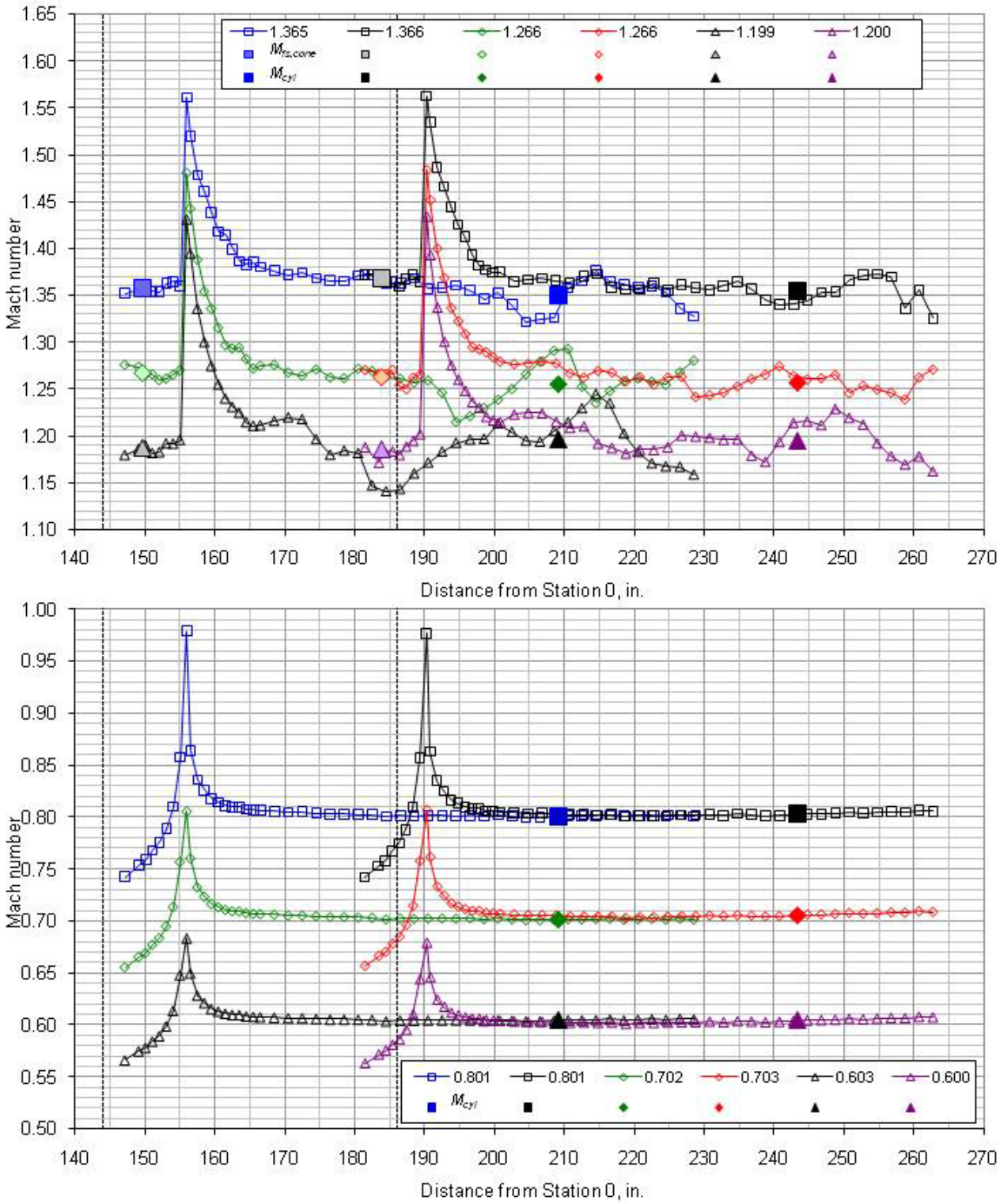

Figure 17.—Concluded.

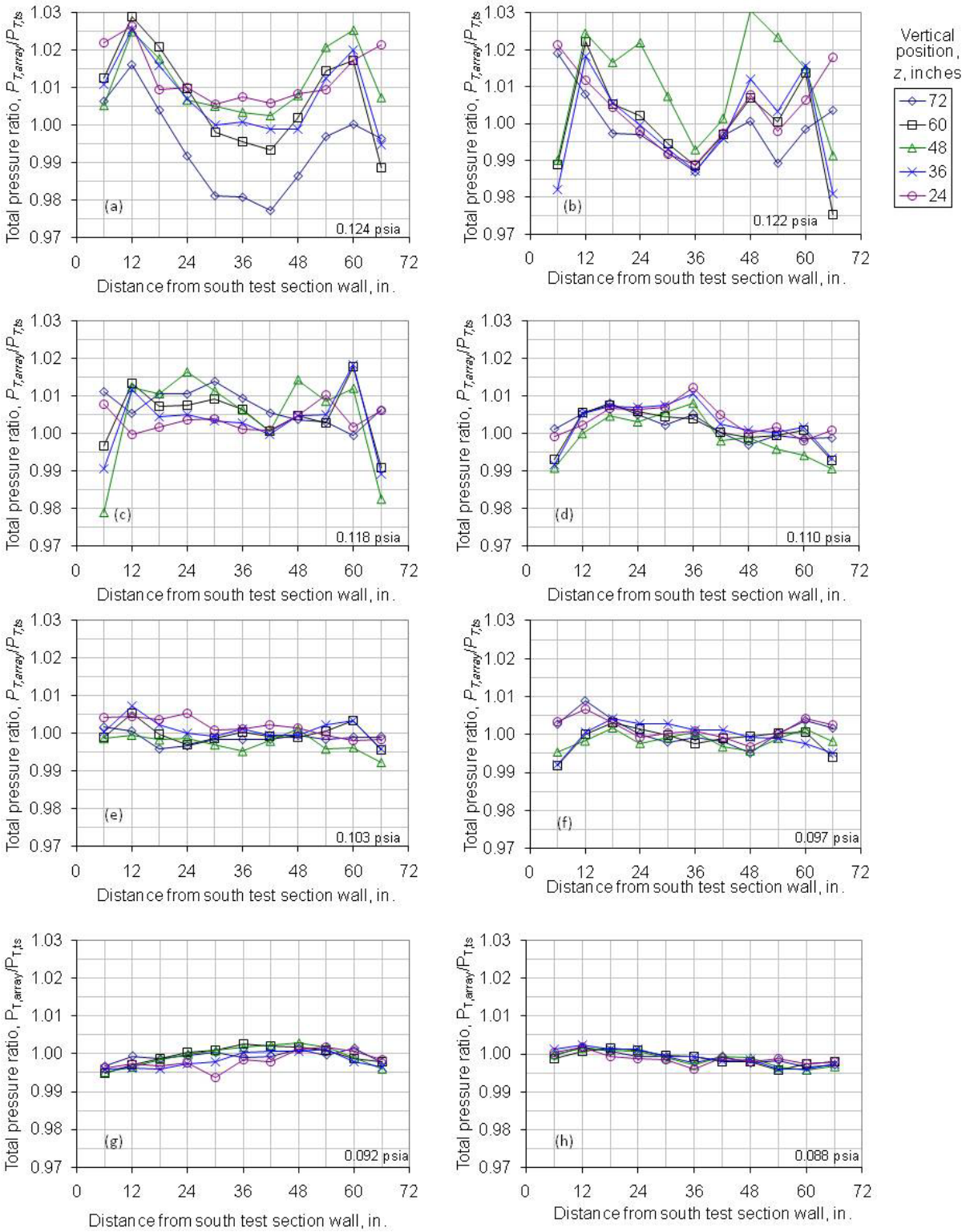

Figure 18.—Total pressure ratio distributions for the 14 ft, 5.8 percent porosity configuration; measurement station is 144. The number in the lower right-hand corner is the approximate delta pressure represented by the minor y-axis division . (a) M_{ts}=1.977; $P_{T,ts}$=24.741 psia. (b) M_{ts}=1.882; $P_{T,ts}$=24.330 psia. (c) M_{ts}=1.777; $P_{T,ts}$=23.532 psia. (d) M_{ts}=1.664; $P_{T,ts}$=21.925 psia. (e) M_{ts} =1.555; $P_{T,ts}$ =20.500 psia. (f) M_{ts} =1.454 $P_{T,ts}$ =19.310 psia. (g) M_{ts} =1.351 $P_{T,ts}$ =18.347 psia. (h) M_{ts} =1.255; $P_{T,ts}$ =17.573 psia.

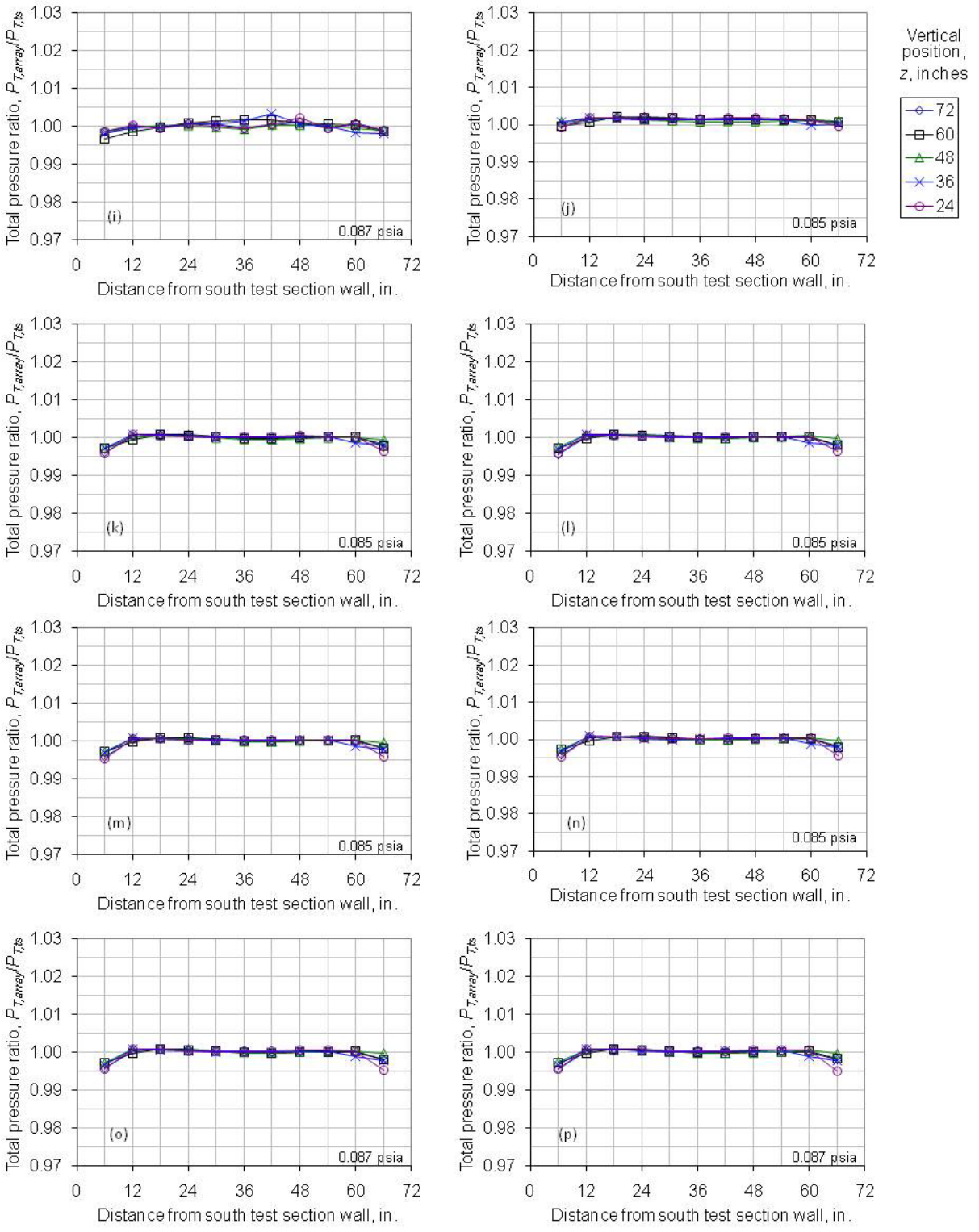

Figure 18.—Continued. (i) M_{ts}=1.186; $P_{T,ts}$=17.338 psia. (j) M_{ts}=1.076; $P_{T,ts}$=16.965 psia. (k) M_{ts}=1.009; $P_{T,ts}$=16.981 psia. (l) M_{ts}=0.958; $P_{T,ts}$=16.951 psia. (m) M_{ts}=0.903; $P_{T,ts}$=17.040 psia. (n) M_{ts}=0.856; $P_{T,ts}$=17.073 psia. (o) M_{ts}=0.807; $P_{T,ts}$=17.307 psia. (p) M_{ts}=0.756; $P_{T,ts}$=17.488 psia.

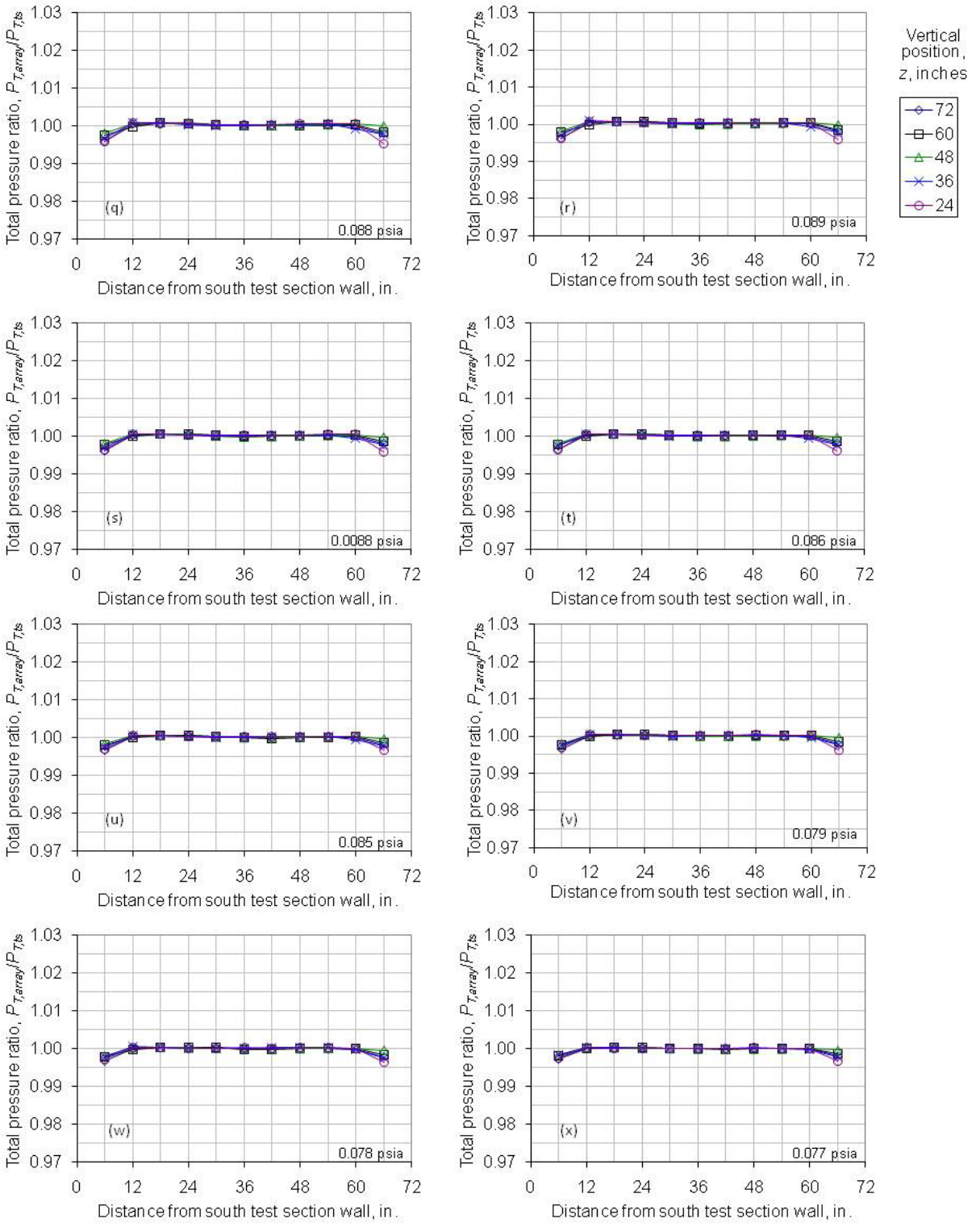

Figure 18.—Continued. (q) M_{ts}=0.706; $P_{T,ts}$=17.682 psia. (r) M_{ts}=0.656; $P_{T,ts}$=17.765 psia. (s) M_{ts}=0.607; $P_{T,ts}$=17.575 psia. (t) M_{ts}=0.556; $P_{T,ts}$=17.254 psia. (u) M_{ts}=0.510; $P_{T,ts}$=16.914 psia. (v) M_{ts}=0.505; $P_{T,ts}$=15.873 psia (1-motor operation). (w) M_{ts}=0.462; $P_{T,ts}$=15.600 psia. (x) M_{ts}=0.414; $P_{T,ts}$=15.347 psia.

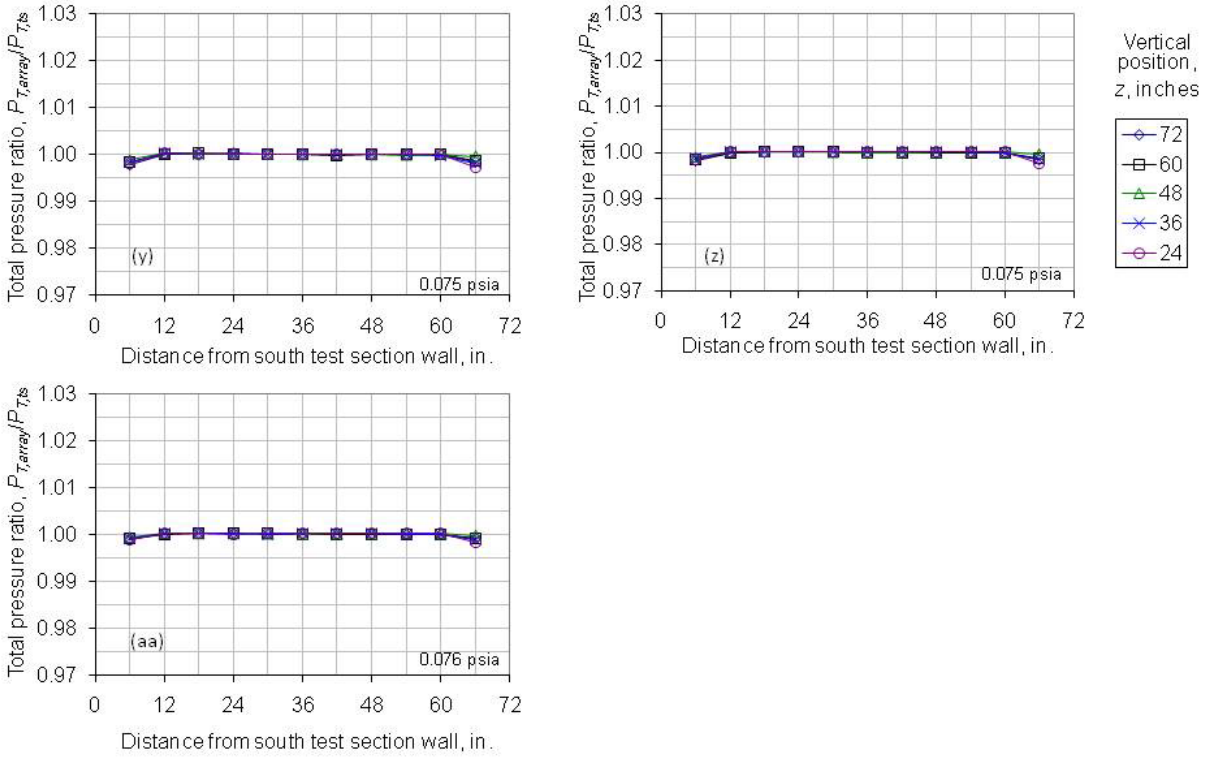

Figure 18.—Concluded. (y) M_{ts}=0.356; $P_{T,ts}$=15.095 psia. (z) M_{ts}=0.304; $P_{T,ts}$=14.960 psia. (aa) M_{ts}=0.255; $P_{T,ts}$=15.253 psia.

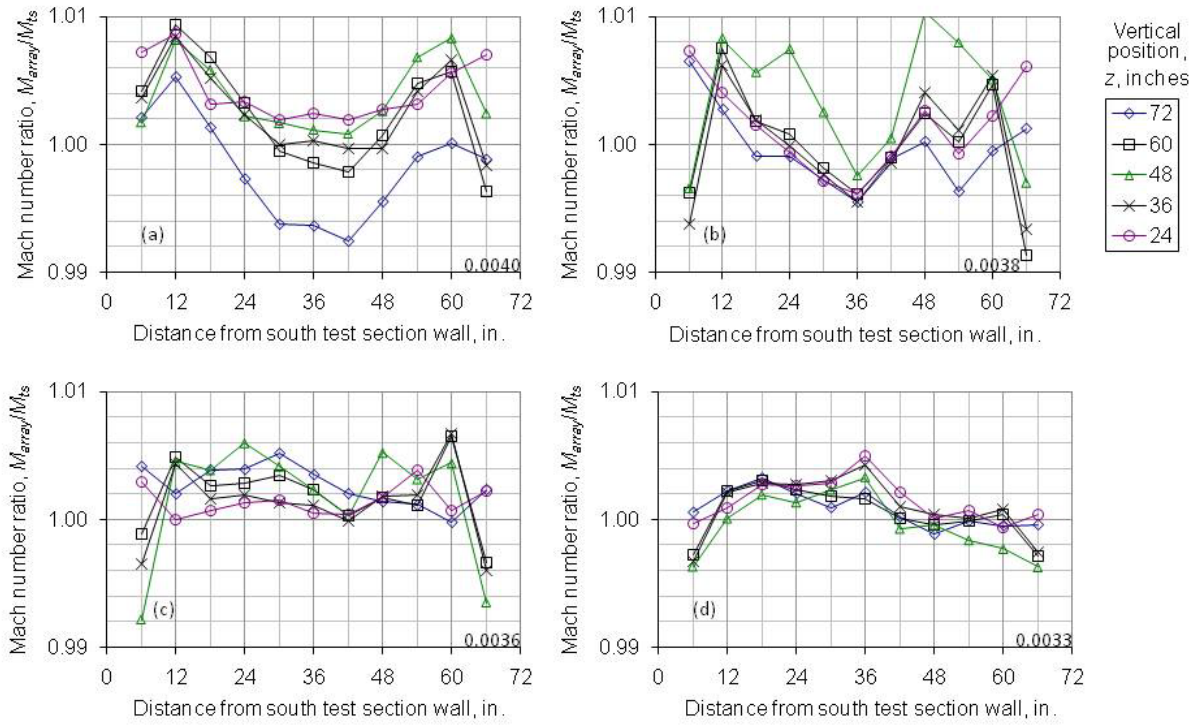

Figure 19.—Mach number ratio distributions at each array height for each Mach number setting in the 8x6 SWT test section. Test section configuration is the 14-ft, 5.8 percent porosity; measurement plane is at station 144. The number in the lower right-hand corner is the approximate delta Mach number represented by the minor y-axis division. (a) M_{ts} = 1.977. (b) M_{ts} = 1.882. (c) M_{ts} = 1.777. (d) M_{ts} = 1.664.

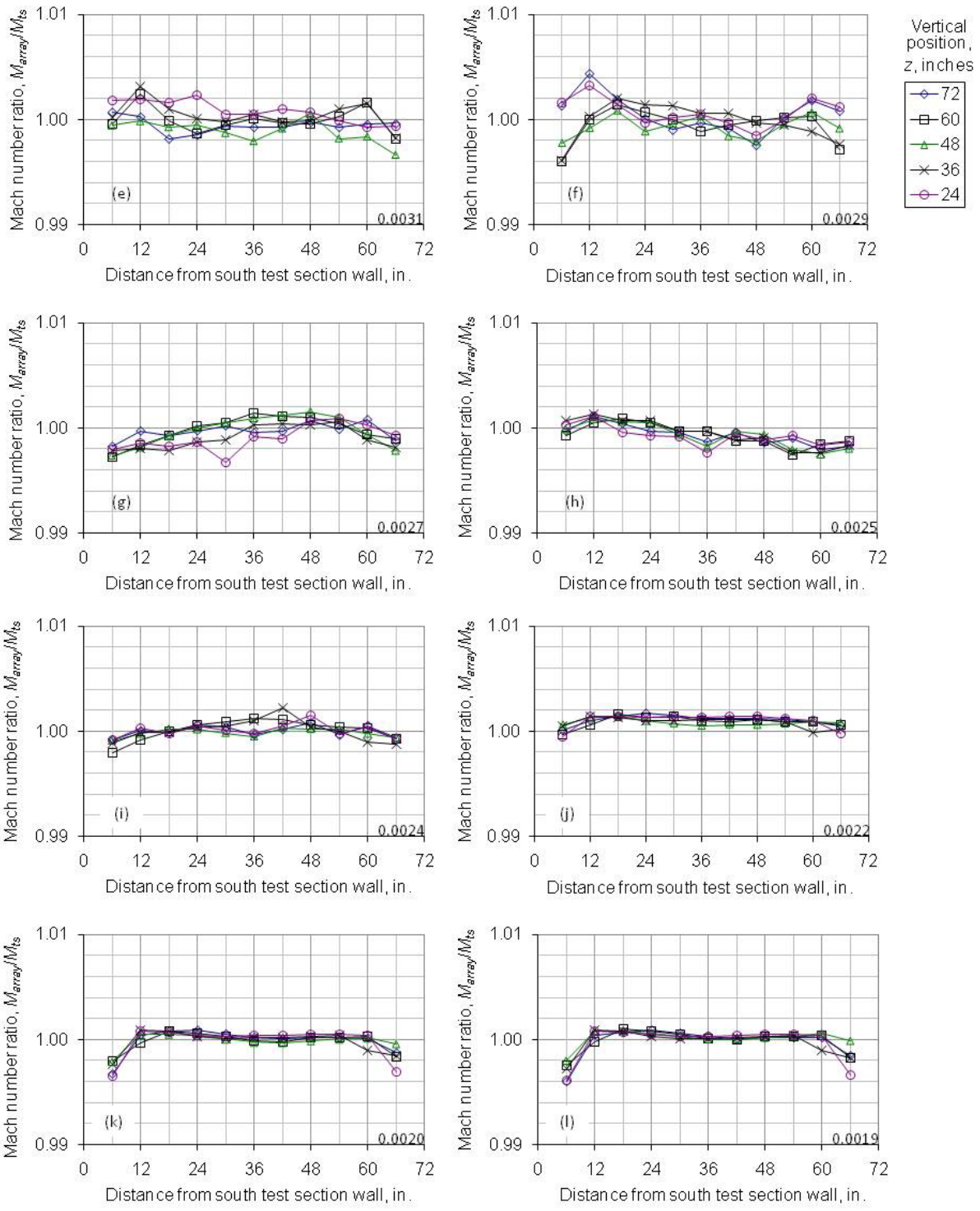

Figure 19.—Continued. (e) M_{ts} = 1.555. (f) M_{ts} = 1.454. (g) M_{ts} = 1.351 (h) M_{ts} = 1.255. (i) M_{ts} = 1.186. (j) M_{ts} = 1.076. (k) M_{ts} = 1.009. (l) M_{ts} = 0.958.

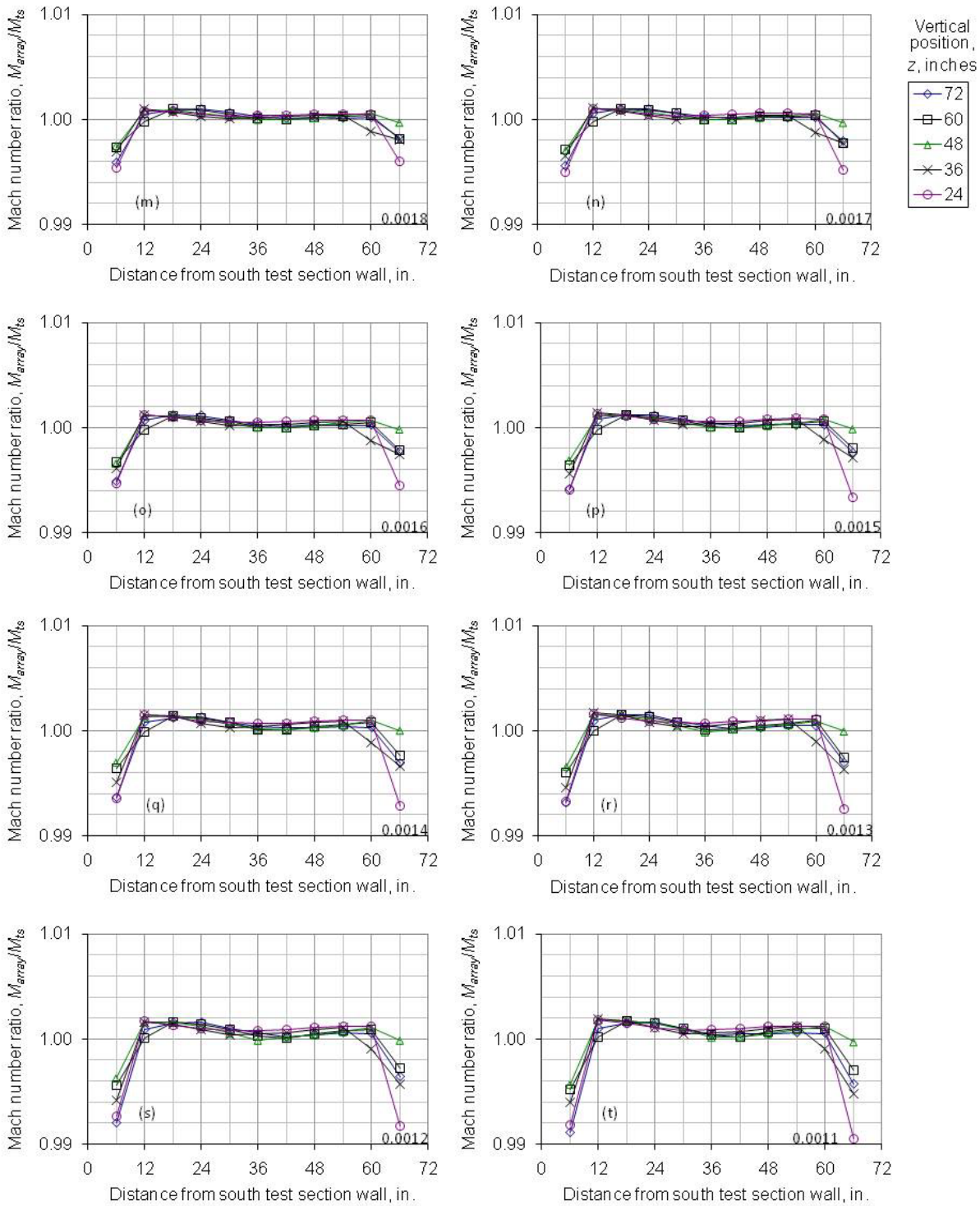

Figure 19.—Continued. (m) M_{ts} = 0.903. (n) M_{ts} = 0.856. (o) M_{ts} = 0.807. (p) M_{ts} = 0.756. (q) M_{ts} = 0.706. (r) M_{ts} = 0.656. (s) M_{ts} = 0.607. (t) M_{ts} = 0.556.

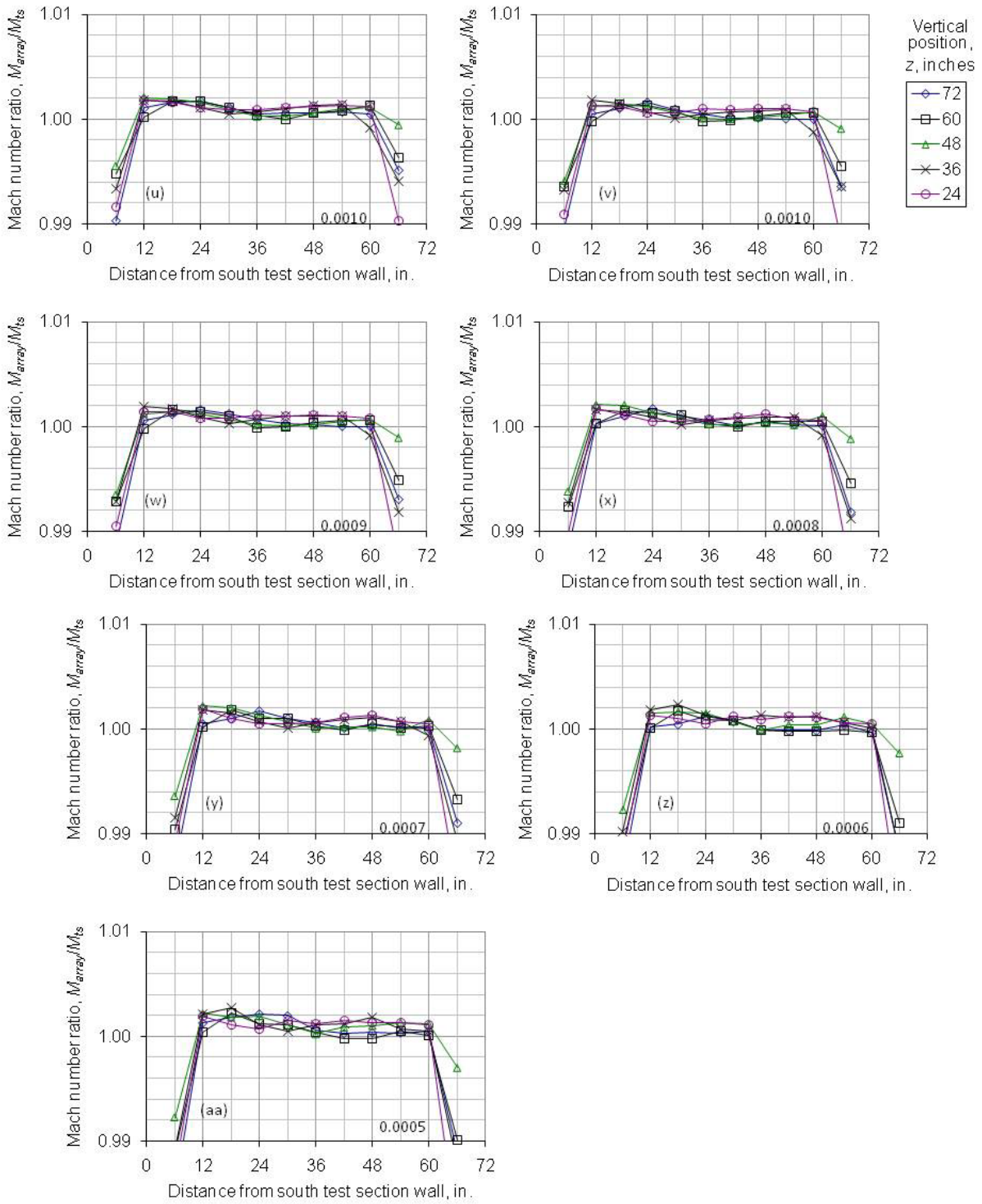

Figure 19.—Concluded. (u) M_{ts} = 0.510. (v) M_{ts} = 0.505 (1-motor). (w) M_{ts} = 0.462. (x) M_{ts} = 0.414. (y) M_{ts} = 0.356. (z) M_{ts} = 0.304. (aa) M_{ts} = 0.255.

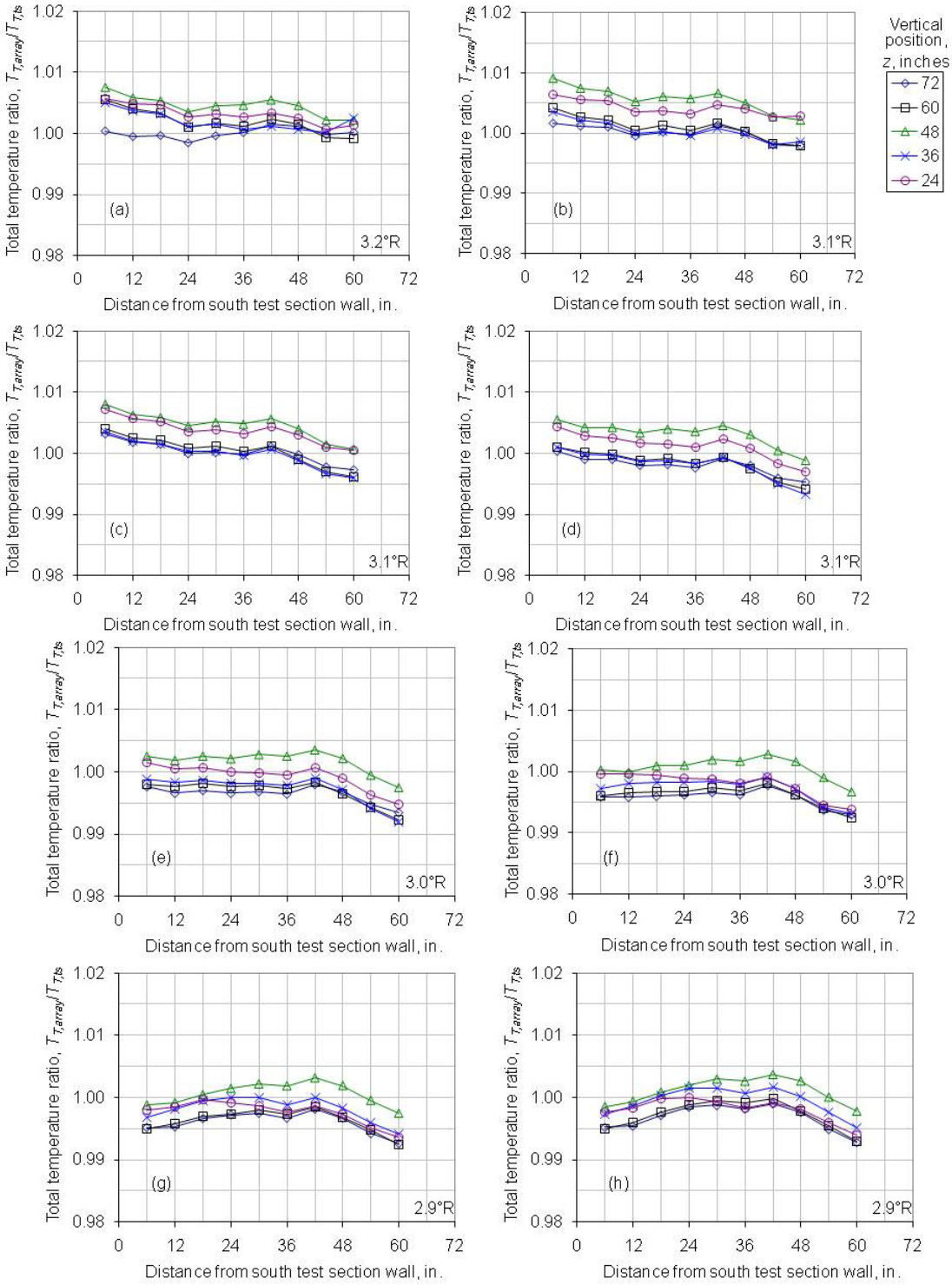

Figure 20.—Total temperature ratio distributions at each array height for each Mach number setting in the 14-ft, 5.8 percent porosity test section. The number in the lower right-hand corner is the approximate delta temperature represented by the minor y-axis division. (a) M_{ts}=1.977; $T_{T,ts}$=638.2 R. (b) M_{ts}=1.882; $T_{T,ts}$=628.0 R. (c) M_{ts}=1.777; $T_{T,ts}$=621.3 R. (d) M_{ts}=1.664; $T_{T,ts}$=610.7 R. (e) M_{ts}=1.555; $T_{T,ts}$=600.8 R. (f) M_{ts}=1.454; $T_{T,ts}$=592.0 R. (g) M_{ts}=1.351; $T_{T,ts}$=584.4 R. (h) M_{ts}=1.255; $T_{T,ts}$=578.1 R.

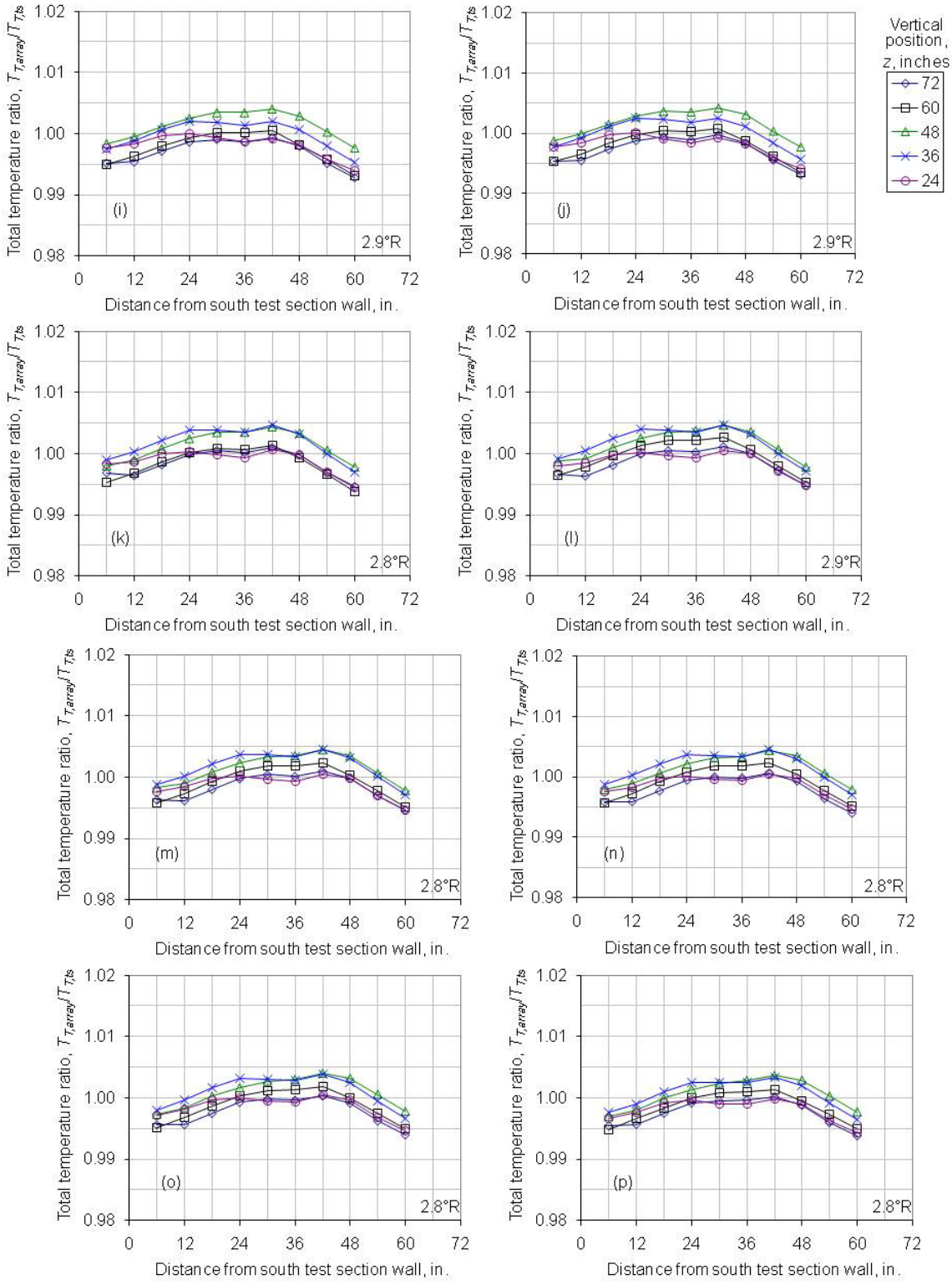

Figure 20.—Continued.(i) M_{ts}=1.186; $T_{T,ts}$=576.2 R. (j) M_{ts}=1.076; $T_{T,ts}$=573.5 R. (k) M_{ts}=1.009; $T_{T,ts}$=562.6 R. (l) M_{ts}=0.958; $T_{T,ts}$=558.9 R. (m) M_{ts}=0.903; $T_{T,ts}$=559.1 R. (n) M_{ts}=0.856; $T_{T,ts}$=558.6 R. (o) M_{ts}=0.807; $T_{T,ts}$=560.0 R. (p) M_{ts}=0.756; $T_{T,ts}$=560.7 R.

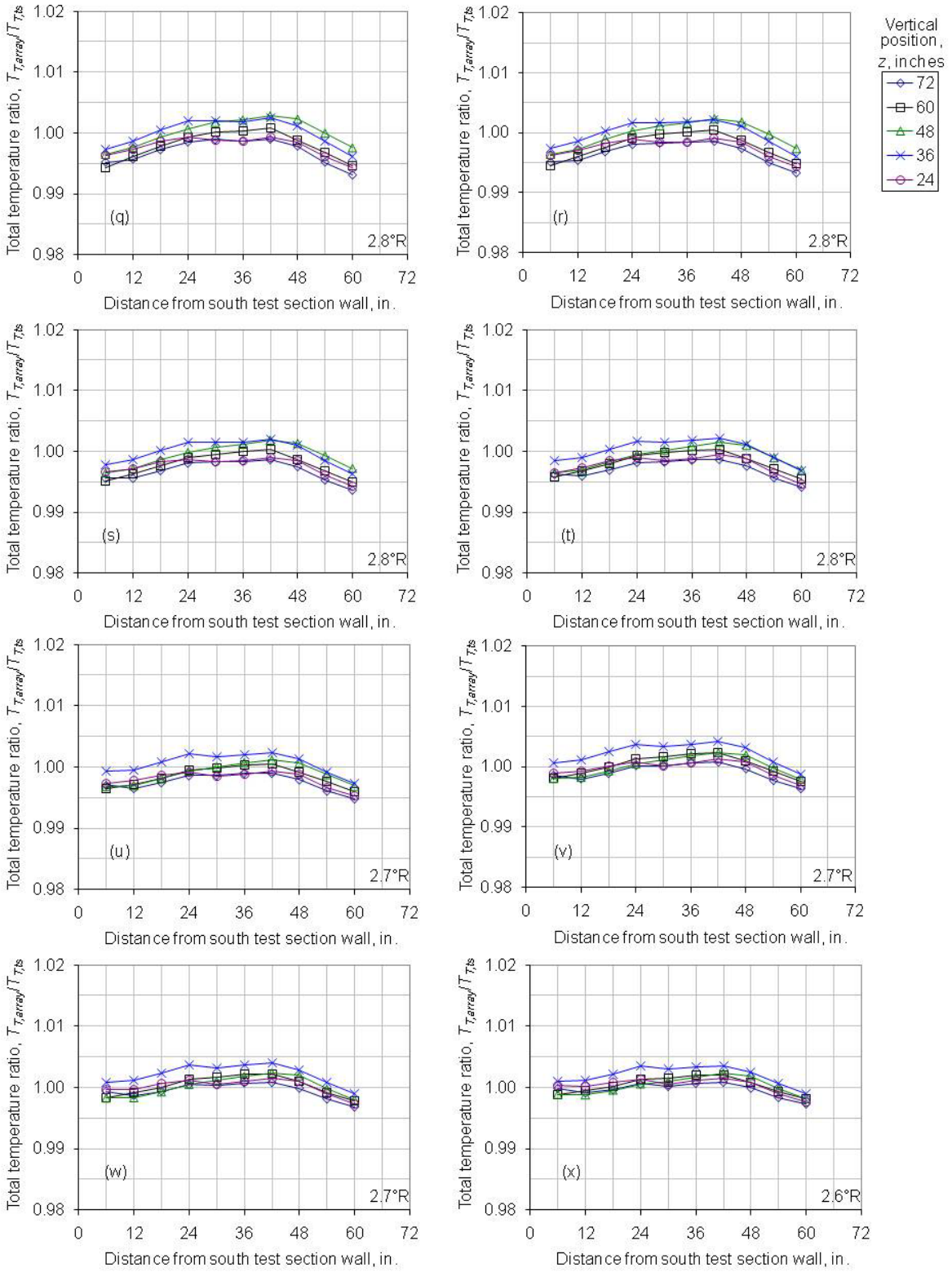

Figure 20.—Continued. (q) M_{ts}= 0.706; $T_{T,ts}$= 561.5 R. (r) M_{ts}= 0.656; $T_{T,ts}$= 560.6 R. (s) M_{ts}= 0.607; $T_{T,ts}$= 557.1 R. (t) M_{ts}= 0.556; $T_{T,ts}$= 551.8 R. (u) M_{ts}= 0.510; $T_{T,ts}$= 546.7 R. (v) M_{ts}= 0.505; $T_{T,ts}$= 535.1 R (1-motor). (w) M_{ts}= 0.462; $T_{T,ts}$= 530.9 R (1-motor). (x) M_{ts}= 0.414; $T_{T,ts}$= 526.7 R (1-motor).

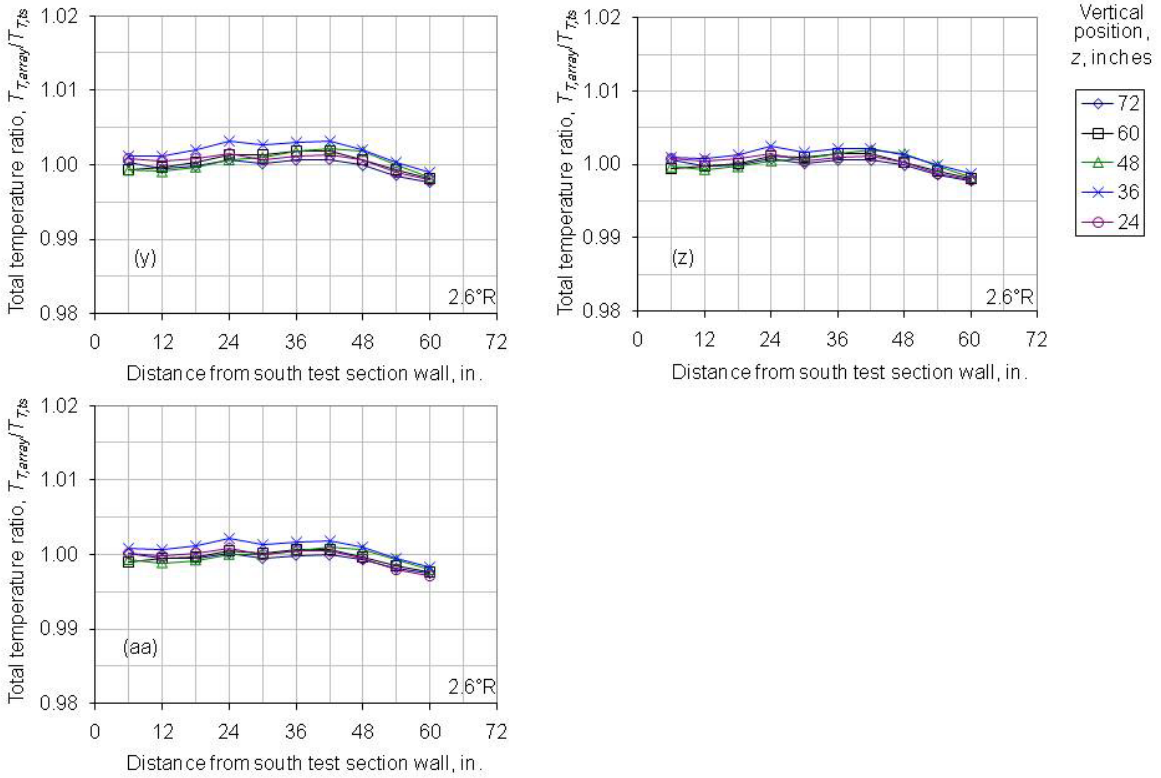

Figure 20.—Concluded. (y) M_{ts}= 0.356; $T_{T,ts}$= 522.6 R (1-motor). (z) M_{ts}= 0.304; $T_{T,ts}$= 519.7 R (1-motor). (aa) M_{ts}= 0.255; $T_{T,ts}$= 521.3 R (1-motor).

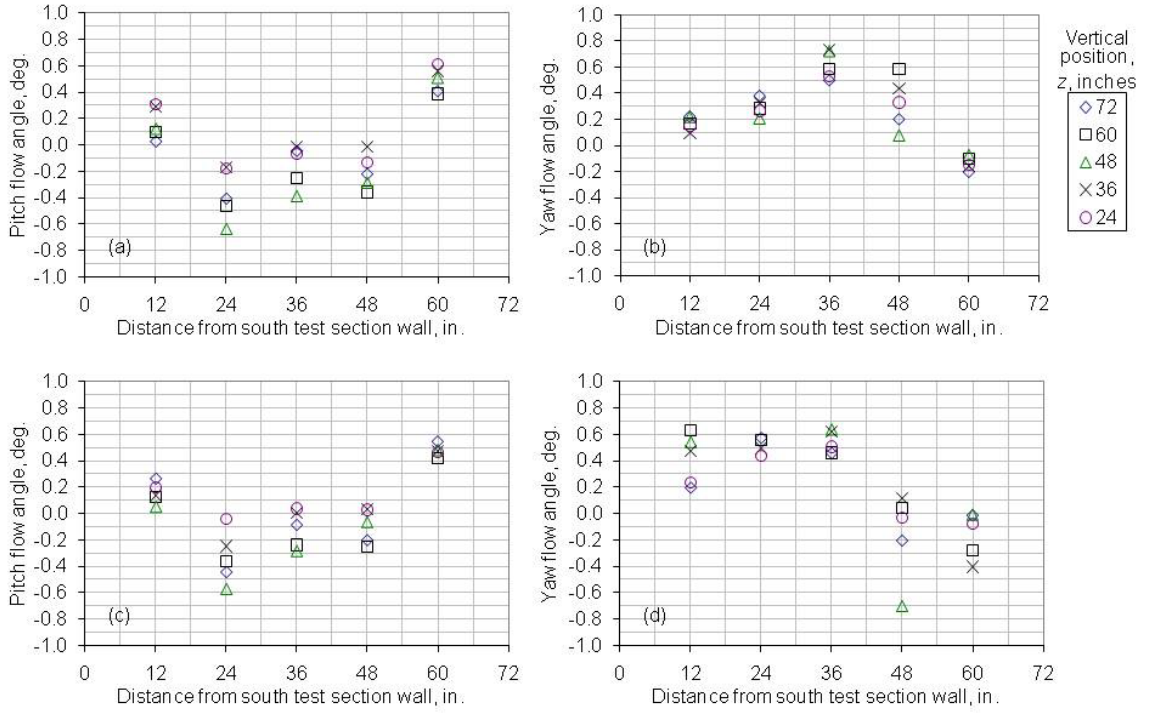

Figure 21.—Pitch and Yaw flow angle data at each array height and Mach number setting in the 8x6 SWT test section. Test section configuration is the 14-ft, 5.8 percent porosity. (a) M_{ts}=1.977. (b) M_{ts}=1.977. (c) M_{ts}=1.882. (d) M_{ts}=1.882.

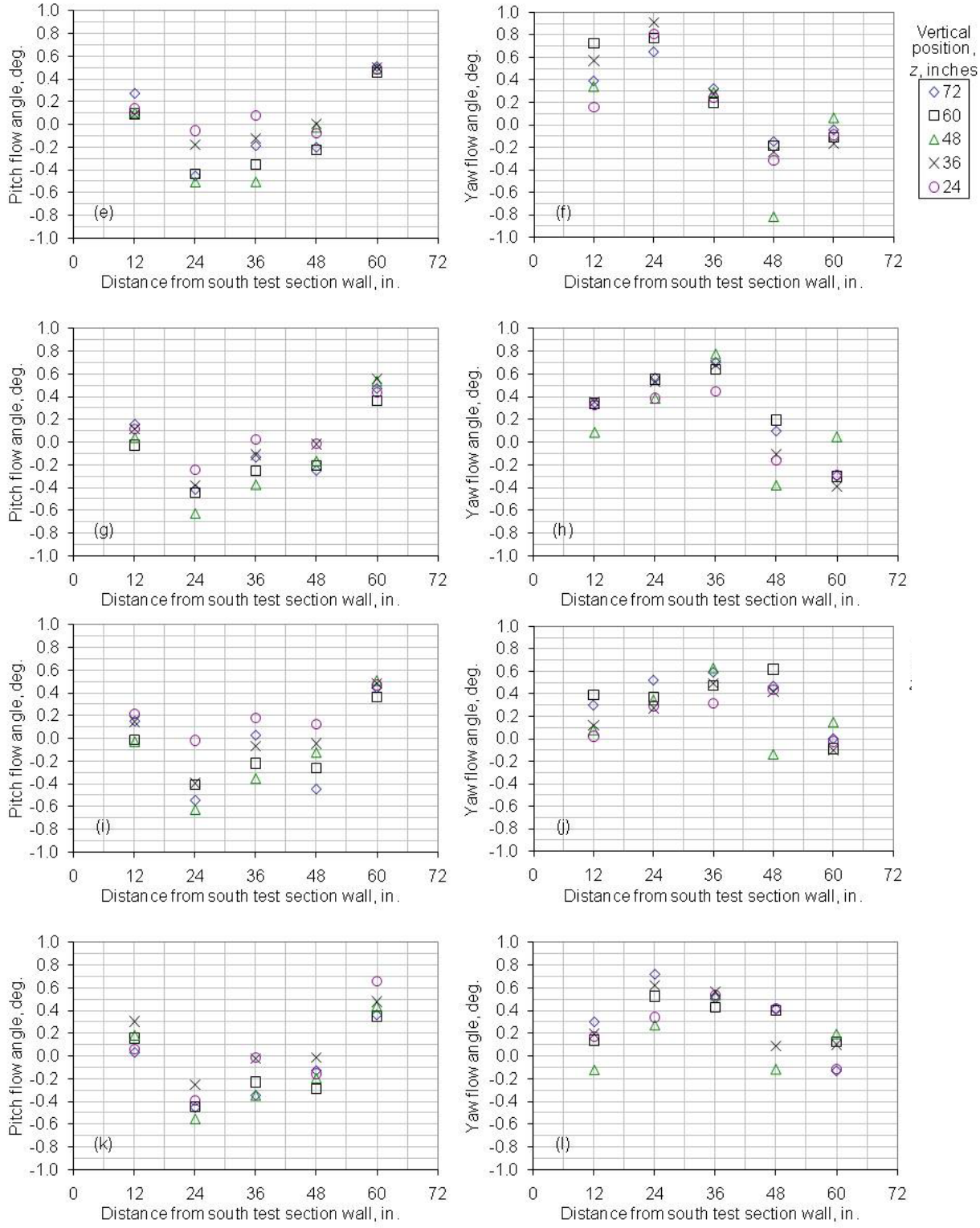

Figure 21.—Continued. (e) M_{ts}=1.777. (f) M_{ts}=1.777. (g) M_{ts}=1.664. (h) M_{ts}=1.664. (i) M_{ts}=1.555. (j) M_{ts}=1.555. (k) M_{ts}=1.454. (l) M_{ts}=1.454.

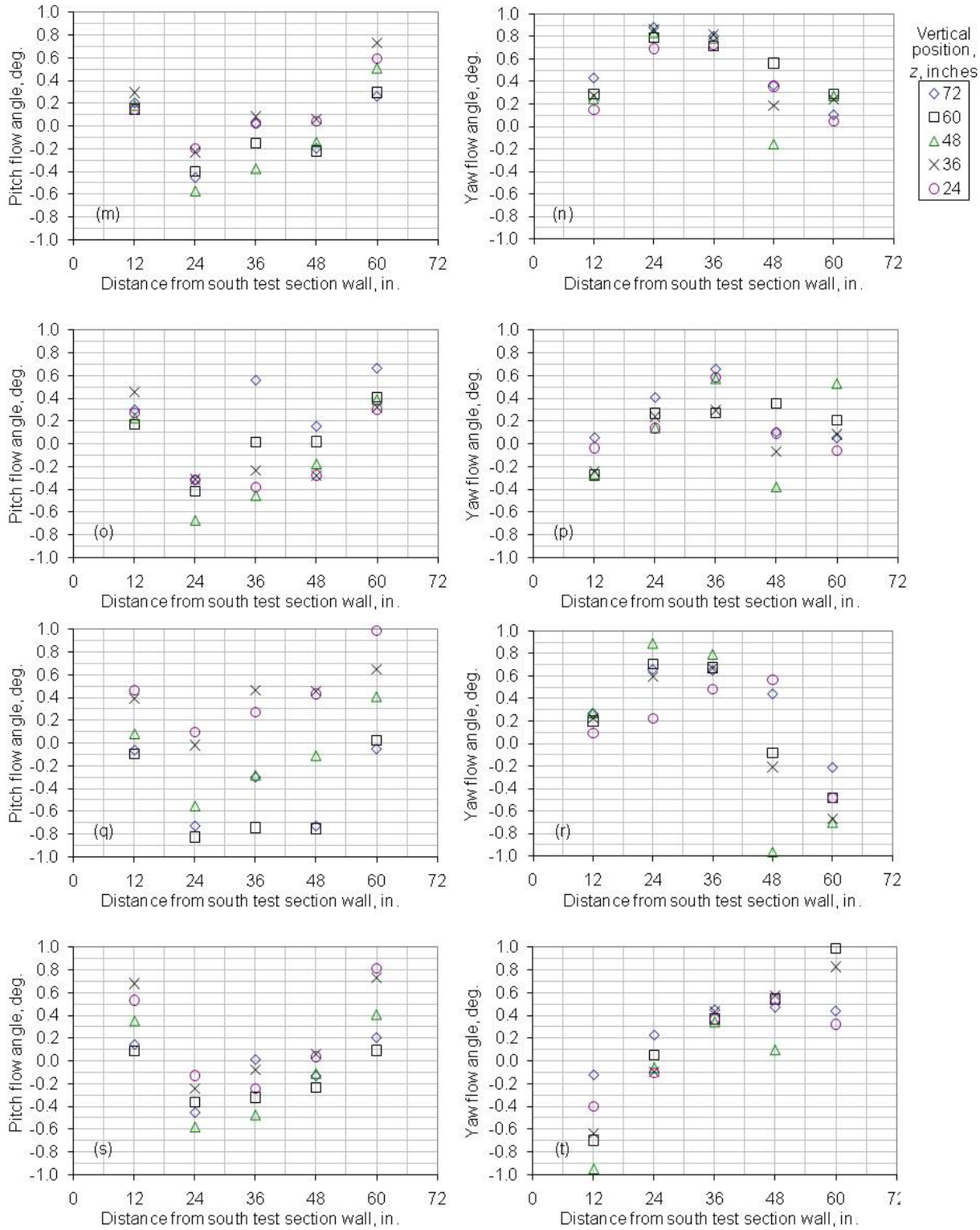

Figure 21.—Continued. (m) M_{ts}=1.351. (n) M_{ts}=1.351. (o) M_{ts}=1.255. (p) M_{ts}=1.255. (q) M_{ts}=1.186. (r) M_{ts}=1.186. (s) M_{ts}=1.076 (t) M_{ts}=1.076.

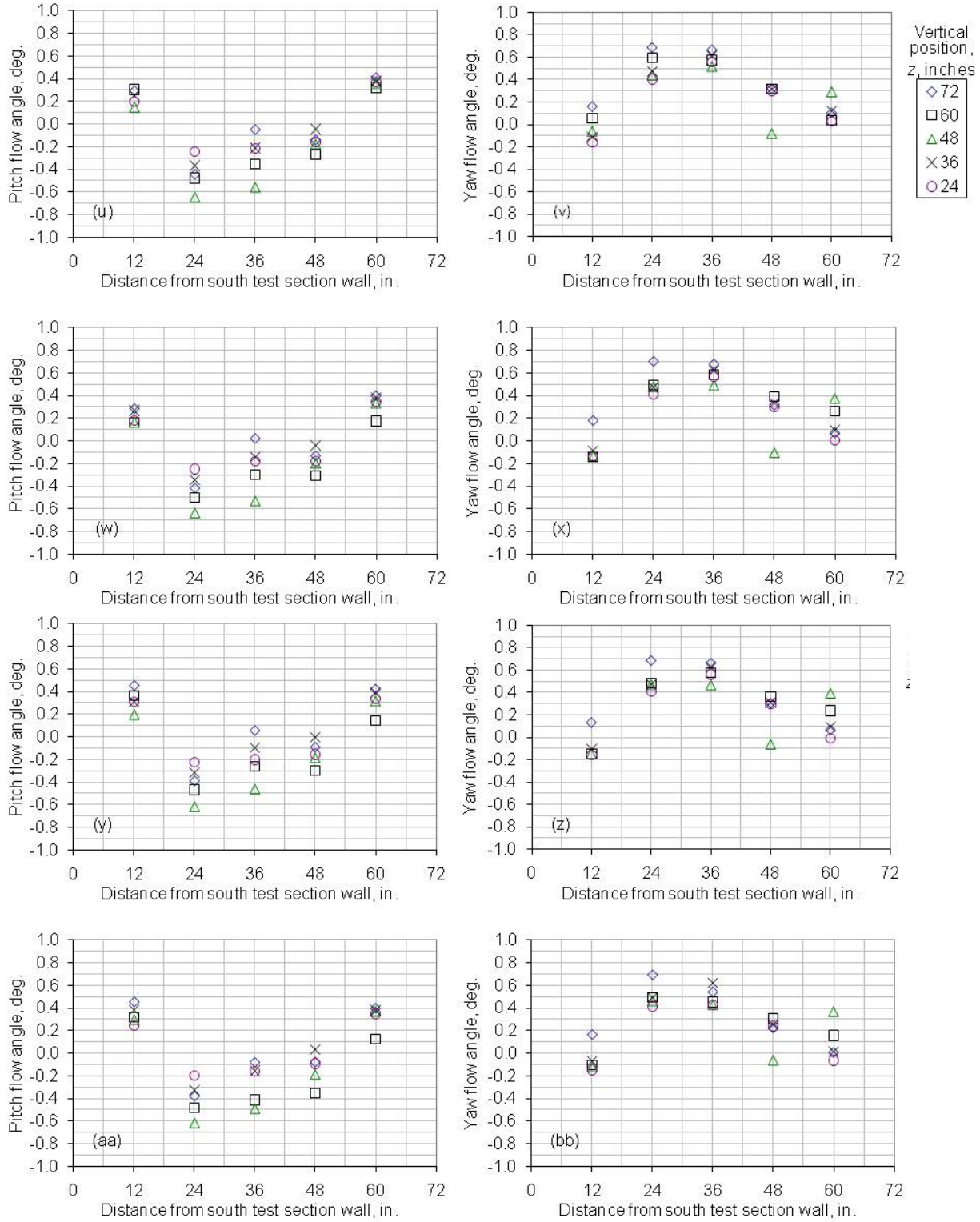

Figure 21.—Continued. (u) M_{ts}=1.009. (v) M_{ts}=1.009. (w) M_{ts}=0.958. (x) M_{ts}=0.958. (y) M_{ts}=0.903. (z) M_{ts}=0.903. (aa) M_{ts}=0.856. (bb) M_{ts}=0.856.

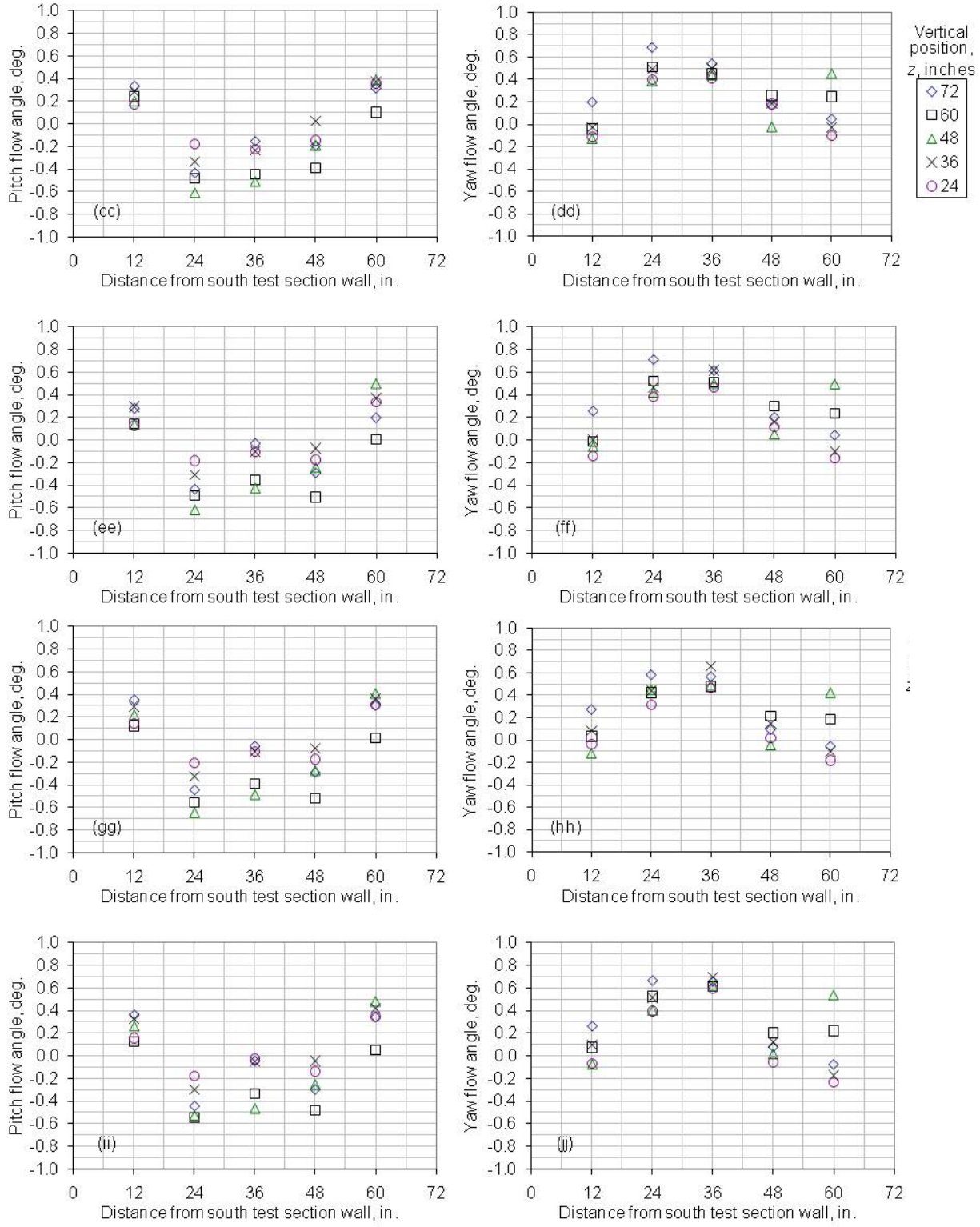

Figure 21.—Continued. (cc) M_{ts}=0.807. (dd) M_{ts}=0.807. (ee) M_{ts}=0.756. (ff) M_{ts}=0.756. (gg) M_{ts}=0.706. (hh) M_{ts}=0.706. (ii) M_{ts}=0.656. (jj) M_{ts}=0.656.

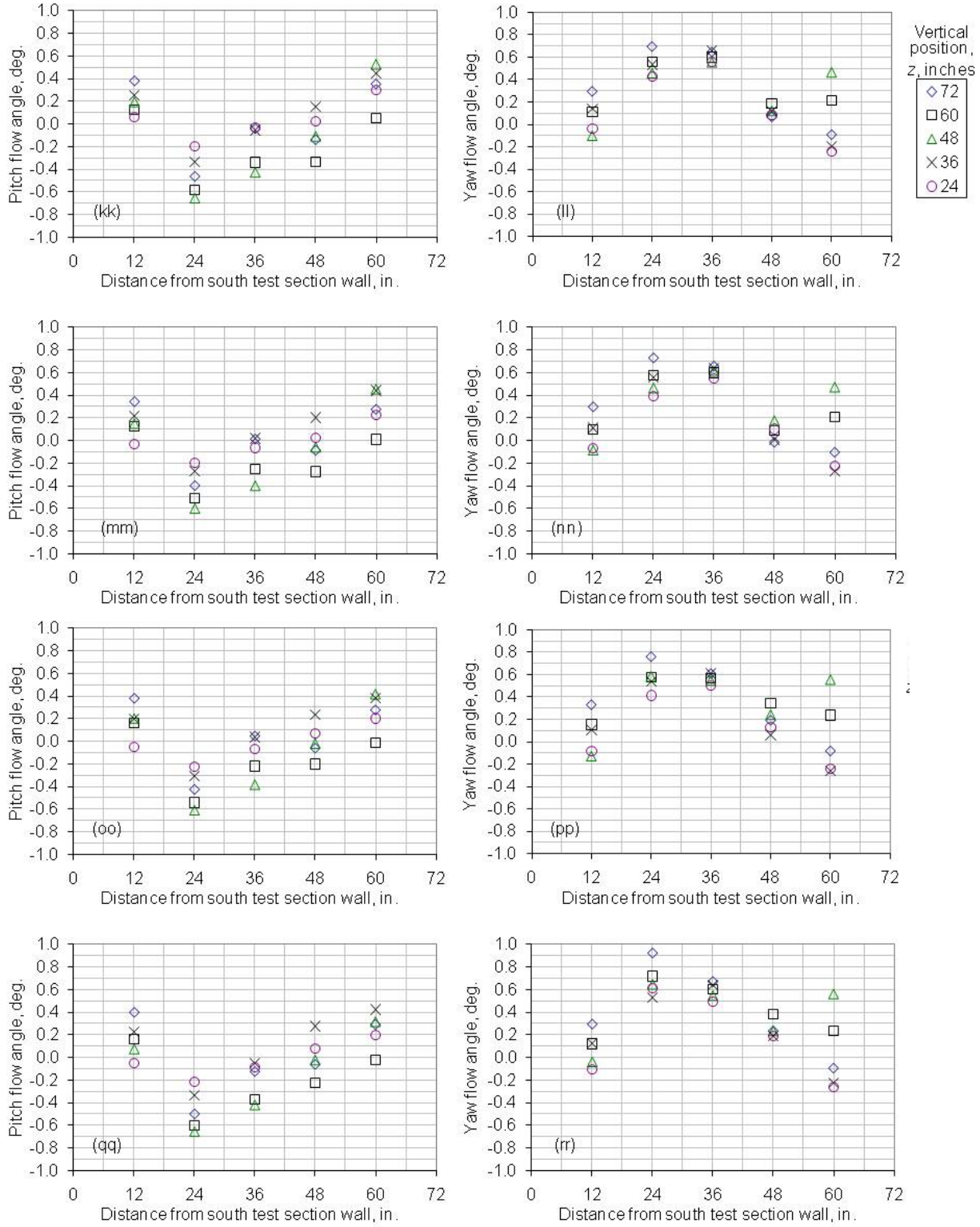

Figure 21.—Continued. (kk) M_{ts}=0.607. (ll) M_{ts}=0.607. (mm) M_{ts}=0.556. (nn) M_{ts}=0.556. (oo) M_{ts}=0.510. (pp) M_{ts}=0.510. (qq) M_{ts}=0.505 (1-motor). (rr) M_{ts}=0.505 (1-motor).

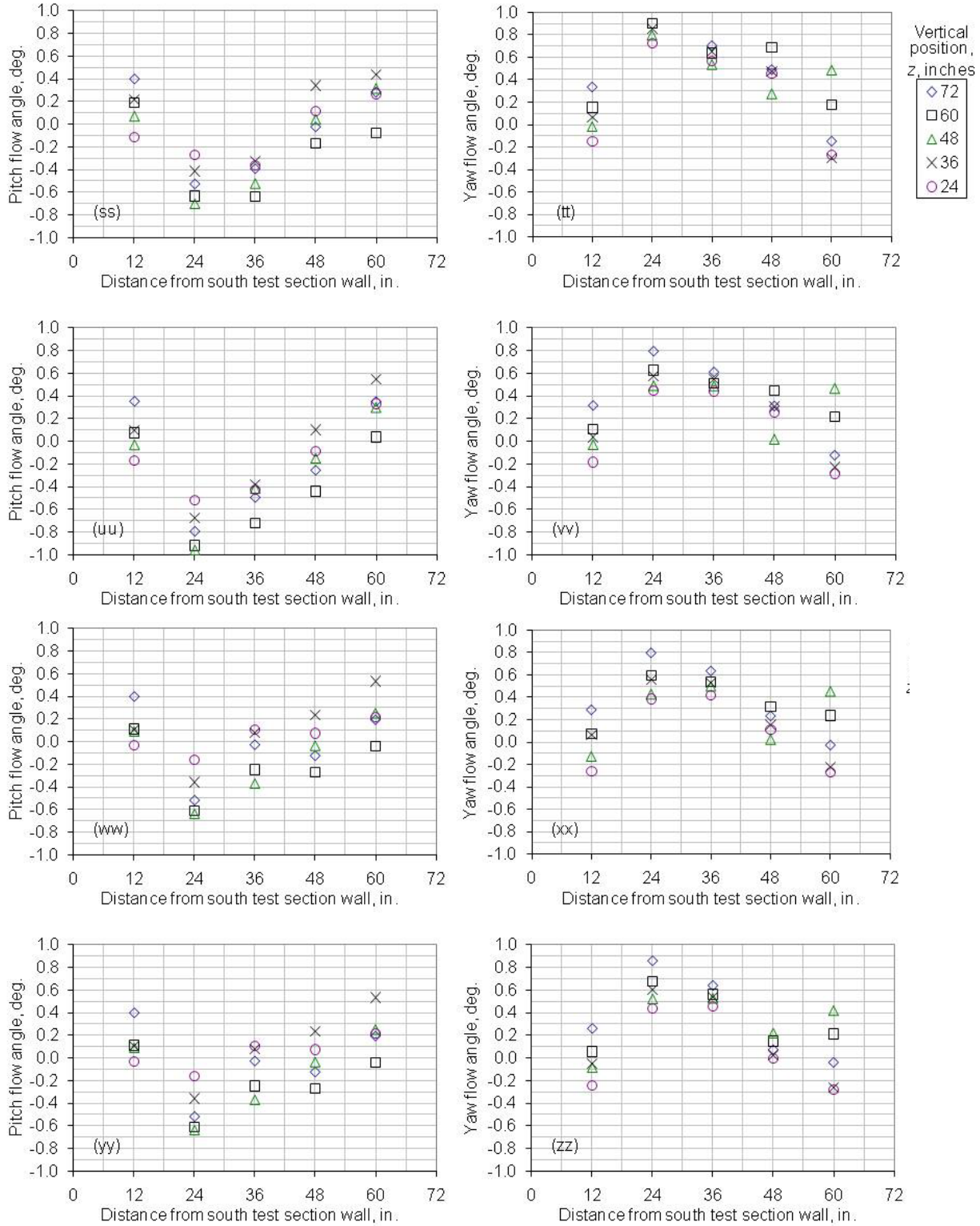

Figure 21.—Continued. (ss) M_{ts}=0.462 (1-motor). (tt) M_{ts}=0.462 (1-motor). (uu) M_{ts}=0.414 (1-motor). (vv) M_{ts}=0.414 (1-motor). (ww) M_{ts}=0.356 (1-motor). (xx) M_{ts}=0.356(1-motor). (yy) M_{ts}=0.304 (1-motor). (zz) M_{ts}=0.304 (1-motor).

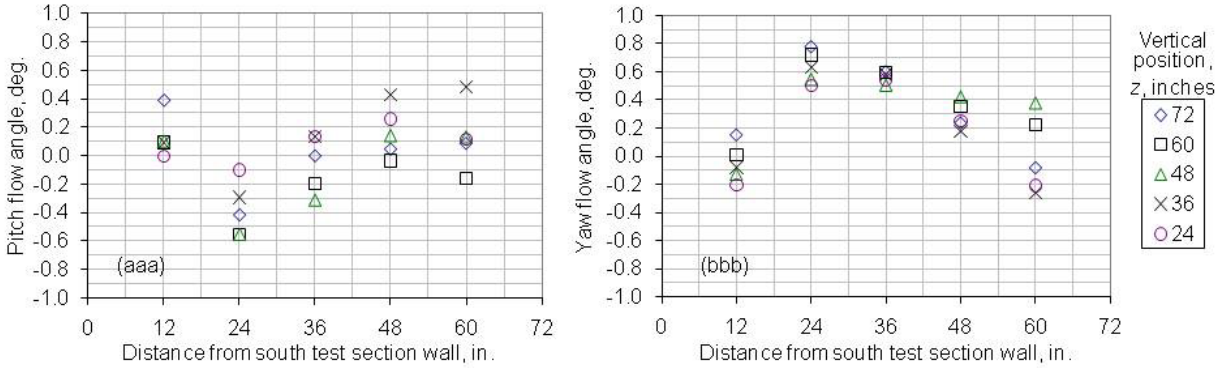

Figure 21.—Concluded. (aaa) M_{ts}=0.255 (1-motor). (bbb) M_{ts}=0.255 (1-motor).

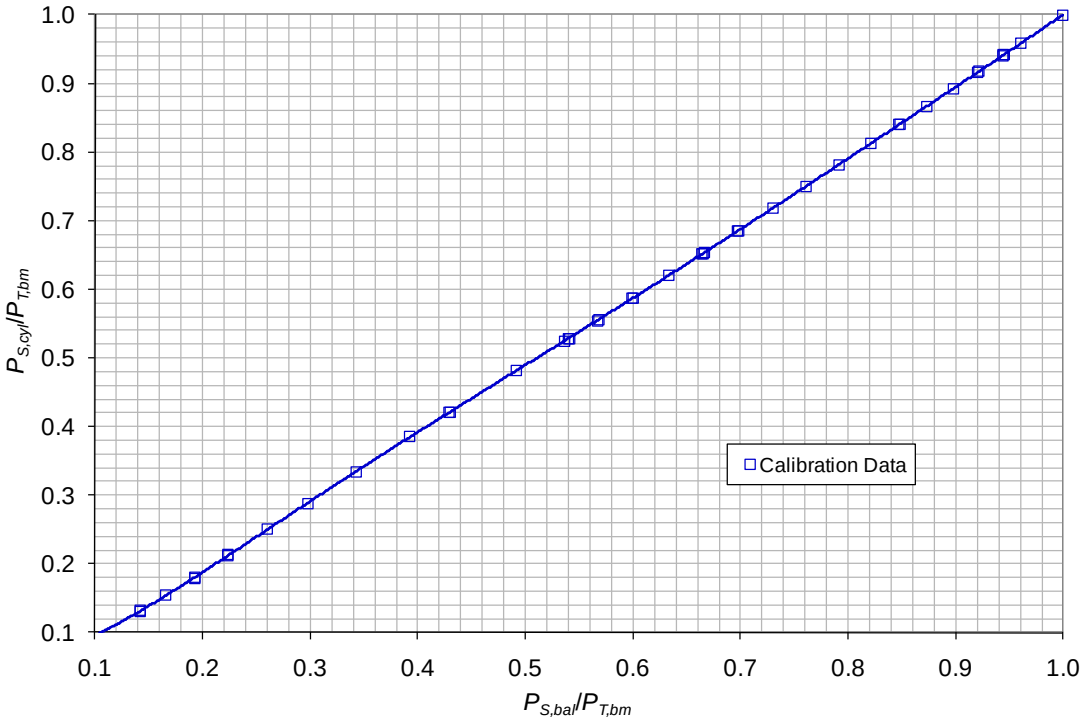

Figure 22.—Static pressure calibration for the 8x6 SWT test section over the entire operating range of the facility. Data collected from the aft portion of the cylinder from the 4-in. diameter cone cylinder were used to represent the test section static pressure. The curve shown is for the 14-ft, 5.8 percent porosity configuration.

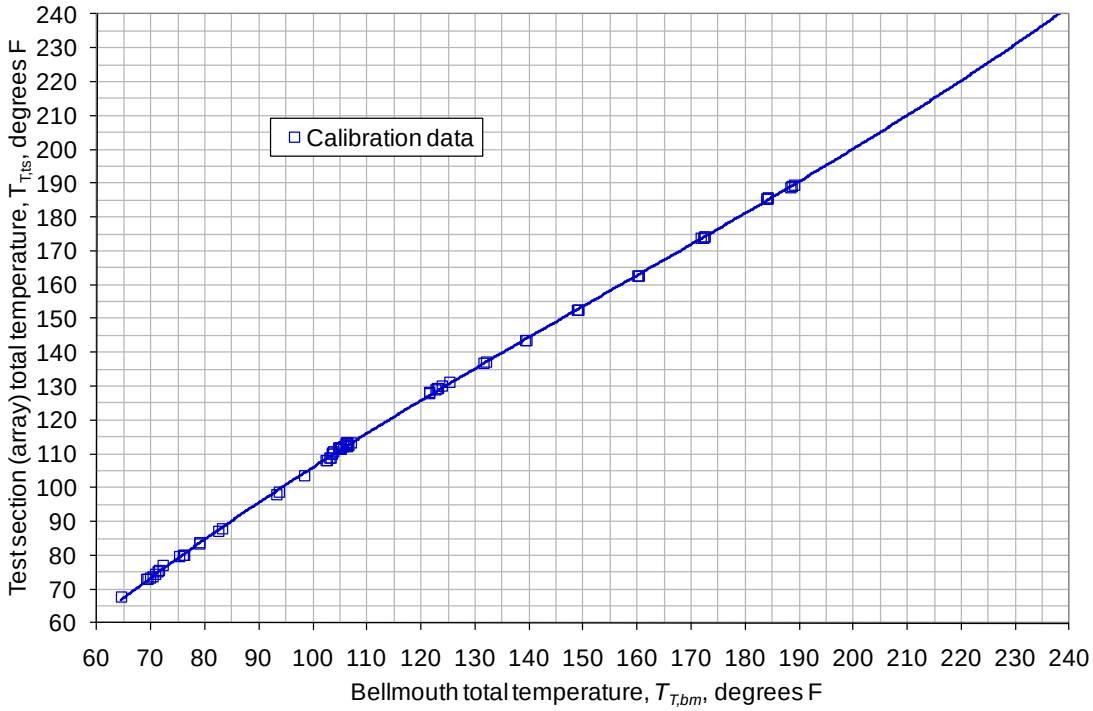

Figure 23.—Total temperature calibration for the 8x6 SWT test section over the entire operating range of the facility. Data collected from the array thermocouples were used to represent the test section total temperature. The curve shown is for the 14-ft, 5.8 percent porosity configuration.

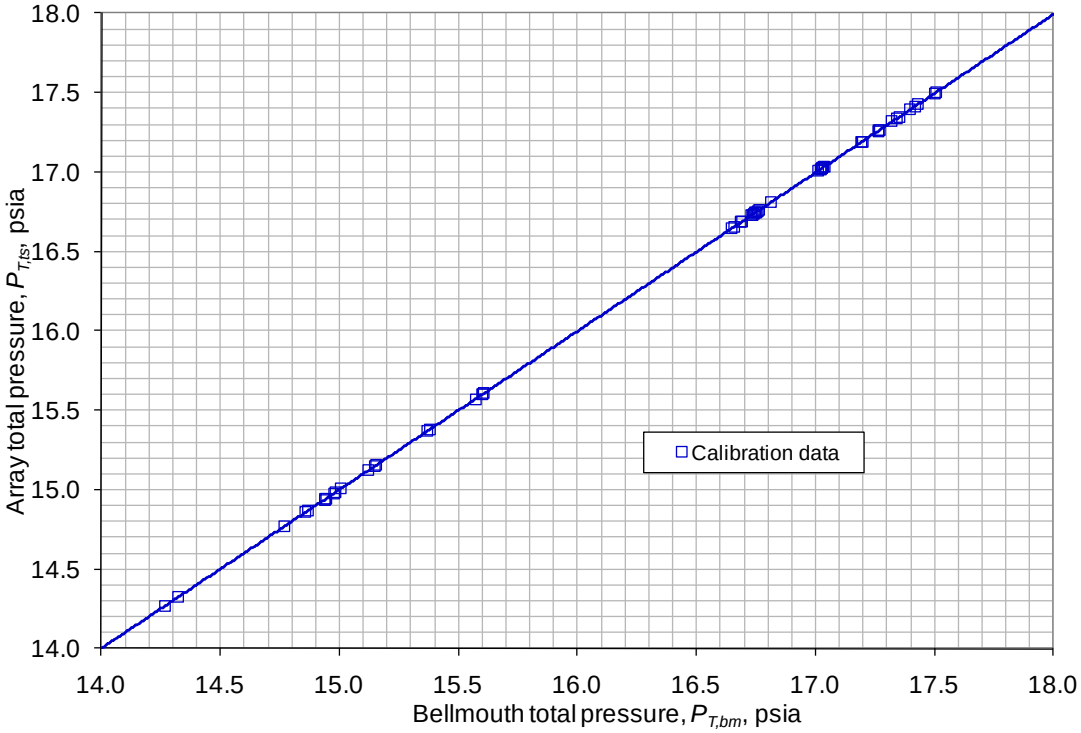

Figure 24.—Total pressure calibration for the 8x6 SWT test section over the subsonic operating range of the facility. Data collected from the array pressure probes were used to represent the test section total pressure. The curve shown is for the 14-ft, 5.8 percent porosity configuration.

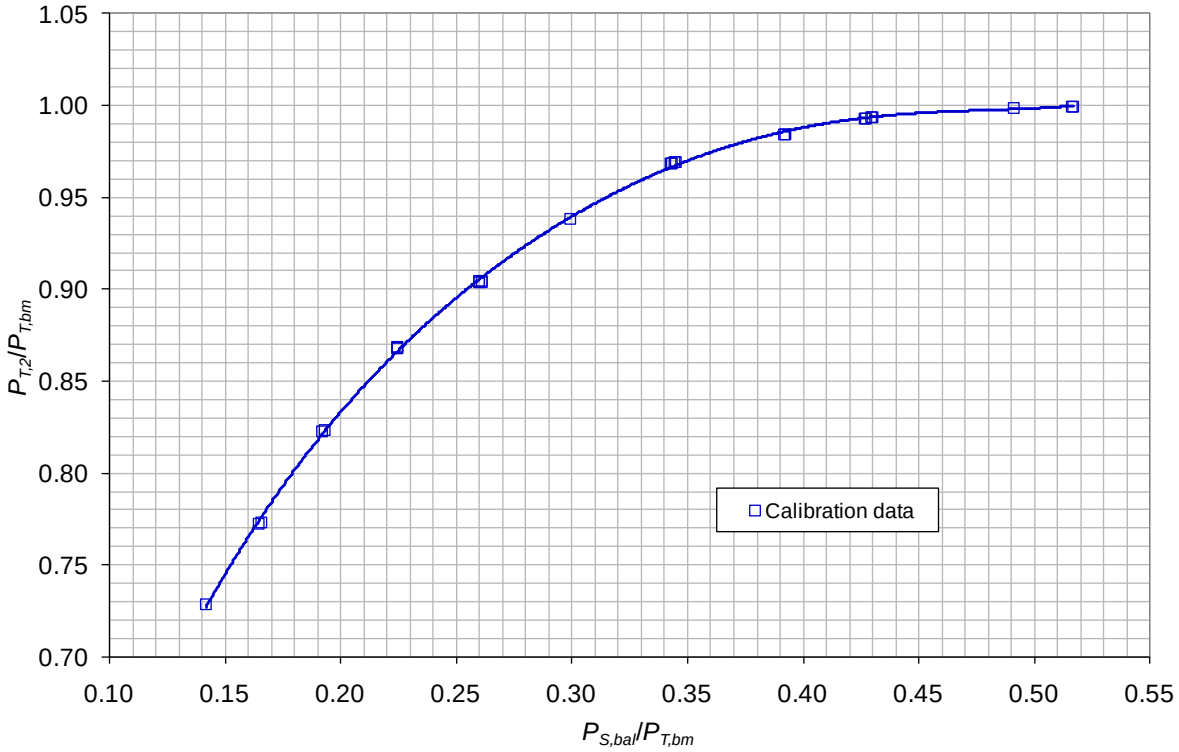

Figure 25.—Total pressure calibration for the 8x6 SWT test section over the supersonic operating range of the facility. Data collected from the array pressure probes is the pressure behind a normal shock and is related to the test section total pressure. The curve shown is for the 14-ft, 5.8 percent porosity configuration.

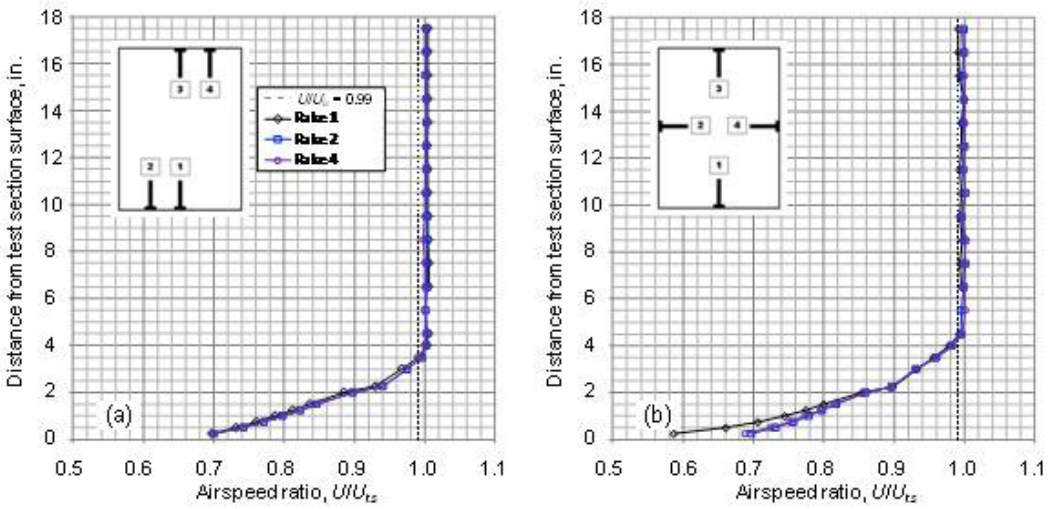

Figure 26.—Typical boundary layer profiles measured in the 8x6 SWT test section. Figure 9 provides additional information on the rake positions. (a) Inlet of the 14-ft test section, M_{nom} = 2.0. (b) Inlet of the 8-ft test section, centerline configuration, M_{nom} = 2.0.

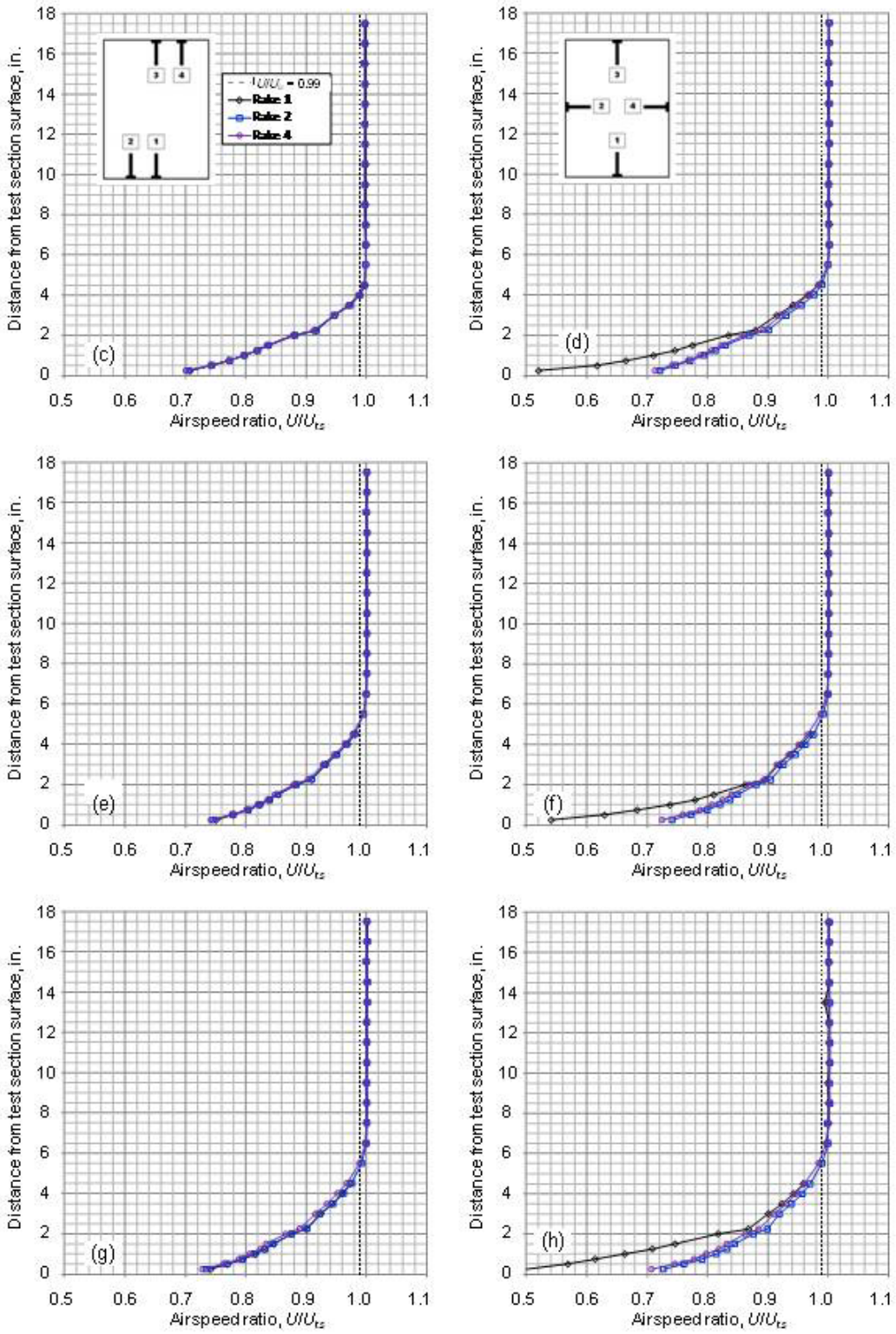

Figure 26.—Concluded. (c) Inlet of the 14-ft test section, M_{nom} = 1.2. (d) Inlet of the 8-ft test section, centerline configuration, M_{nom} = 1.2. (e) Inlet of the 14-ft test section, M_{nom} = 0.8. (f) Inlet of the 8-ft test section, centerline configuration, M_{nom} = 0.8. (g) Inlet of the 14-ft test section, M_{nom} = 0.5. (h) Inlet of the 8-ft test section, centerline configuration, M_{nom} = 0.5.

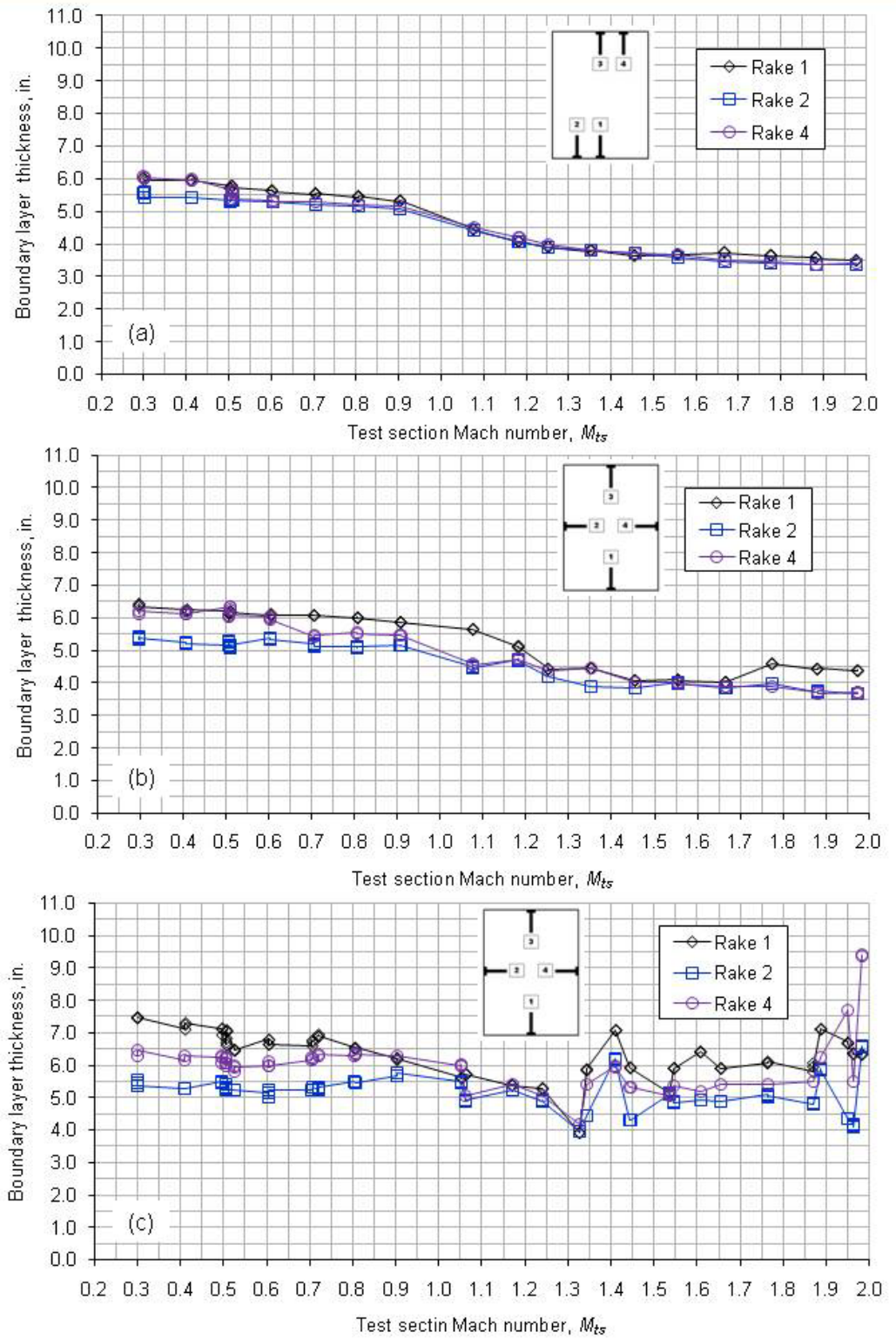

Figure 27.—Summary of the boundary layer thickness measurements for each test configuration over the Mach number range of the facility. The rake configuration is shown with each data chart. (a) 14-ft, 5.8 percent porosity test section, forward station. (b) 14-ft, 5.8 percent porosity test section, mid station (inlet of the 8-ft test section). (c) 14-ft, 5.8 percent porosity test section, aft station.

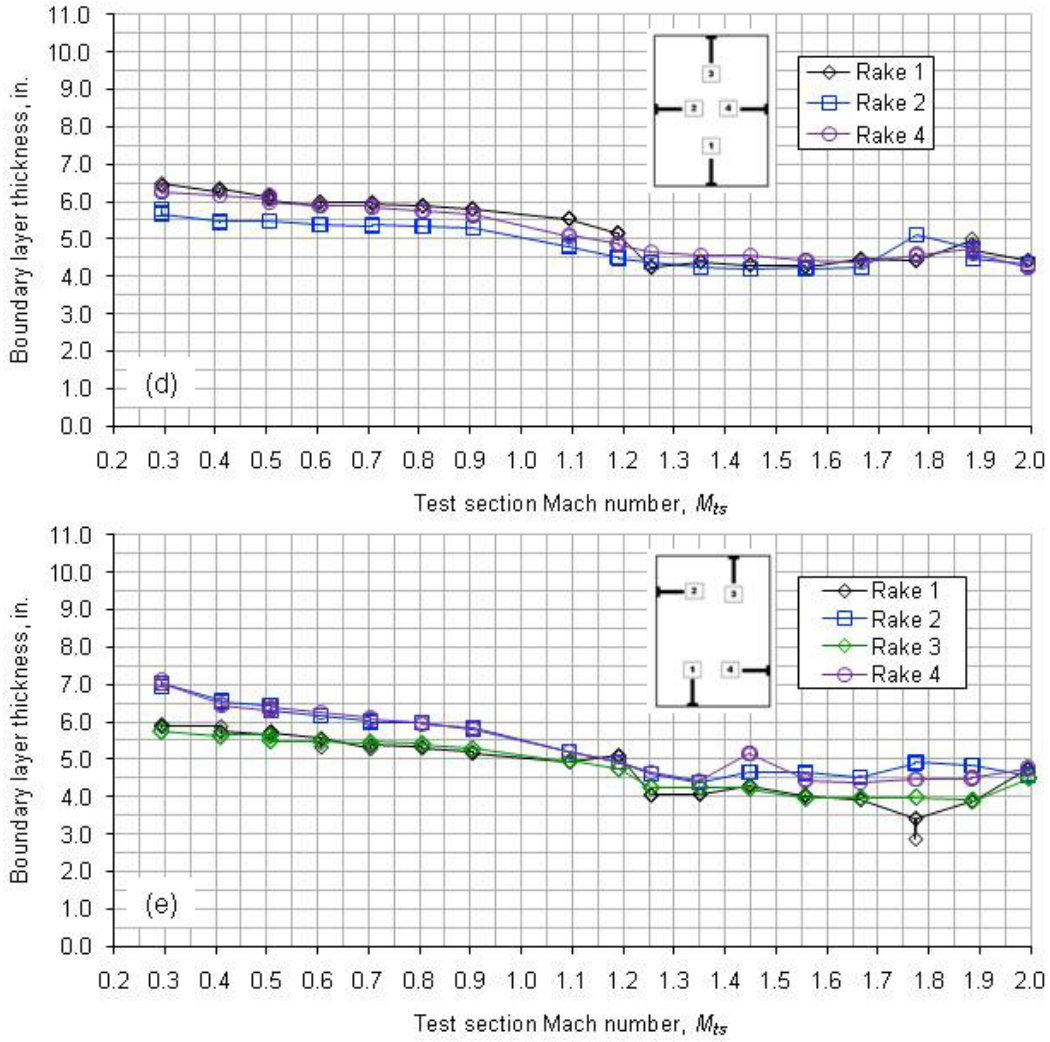

Figure 27.—Continued. (d) 8-ft, 6.2 percent modified porosity test section, mid station. (e) 8-ft, 6.2 percent modified porosity test section, mid station.

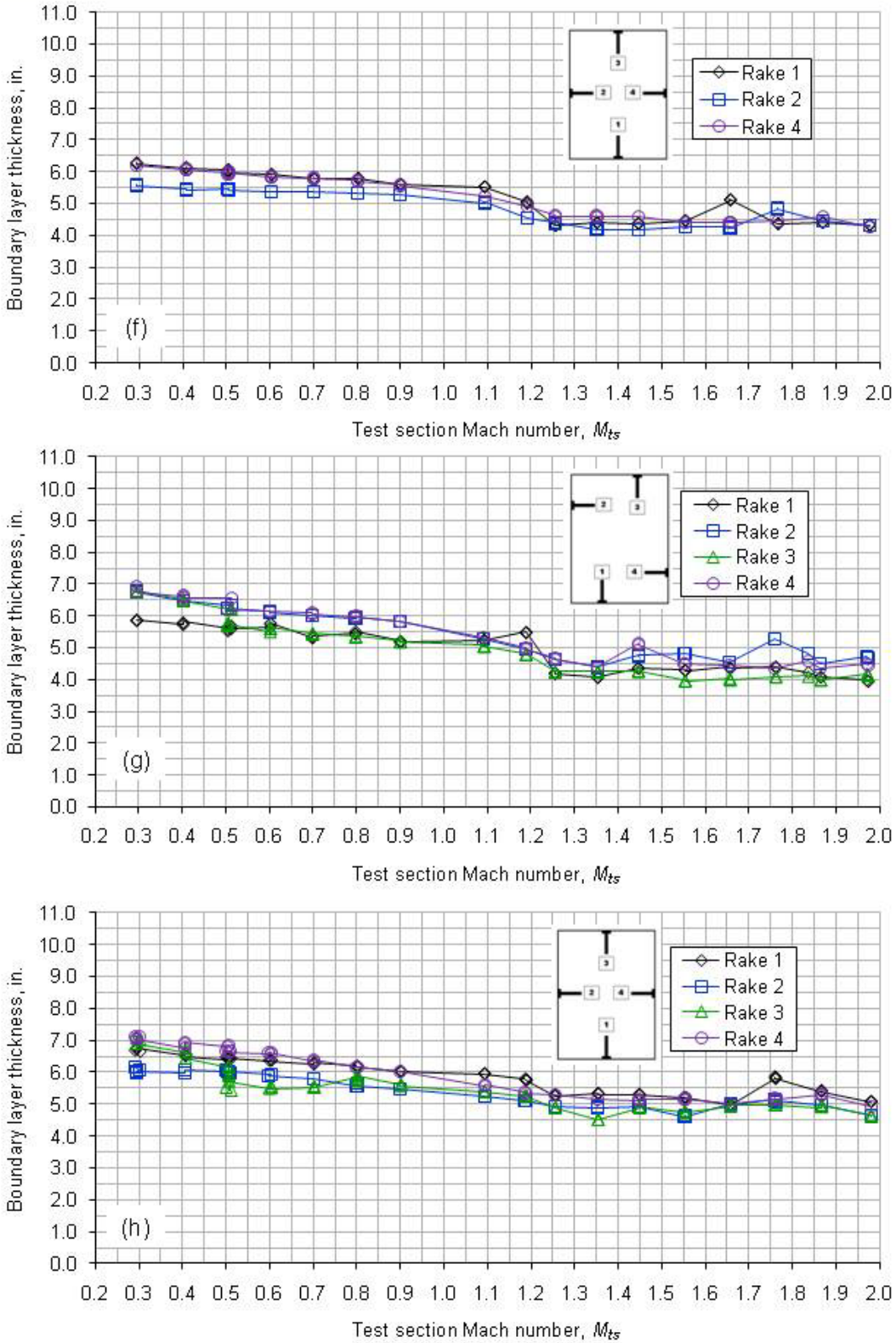

Figure 27.—Concluded. (f) 8-ft, 3.1 percent modified porosity, mid station. (g) 8-ft, 3.1 percent modified porosity, mid station. (h) 8-ft, 3.1 percent modified porosity, aft station.

Appendix A.—Symbols

a	speed of sound, ft/sec
i	boundary layer rake probe index (probes 1 through 25, where 1 is nearest the base)
j	boundary layer rake index (rakes 1 through 4)
l	unit length
q	dynamic pressure, psia
x	shorthand substitution for $PR_{bal/bm}$
A_0 to A_2	tunnel calibration coefficients for total pressure (subsonic conditions)
A_1, B_1	flow angle calibration coefficient (slope) for pitch and yaw angles, respectively
AS_0 to AS_2	tunnel calibration coefficients for total pressure (supersonic conditions)
B_0 to B_6	tunnel calibration coefficients for static pressure
C_0 and C_1	tunnel calibration coefficients for total temperature
L/D	length to diameter ratio
M	Mach number
P_1 to P_4	flow angle pressure, psia
P_5	total pressure measurement from the flow angularity probes
P_{av}	average of P_1 to P_4, psia
PR	pressure ratio
$PR_{bal/bm}$	ratio of balance chamber static pressure to bellmouth total pressure
P_T	total pressure, psia
P_S	static pressure, psia
P_α	pitch flow angle pressure ratio
P_β	yaw flow angle pressure ratio
R	gas constant = 1718 lb-ft/slug/ °R
Re	Reynolds number
T_T	total temperature, °R
T_S	static temperature, °R
U	velocity or resultant velocity, ft/sec
UR	velocity ratio
X	axial position from tunnel station 0, inches (positive downstream)
Y	lateral position from a test section surface, inches
Y_1 to Y_4	location of boundary layer rake within a measurement plane, inches
Z	distance from test section surface, in.
α	pitch flow angle, degrees
α_p, β_p	flow angle probe calibration parameters for pitch and yaw, respectively
β	yaw flow angle, degrees
γ	ratio of specific heats, constant = 1.4
ΔP_T	difference in measured total pressures
δ	boundary layer thickness, in.
μ	viscosity, slugs/(ft·sec)
ρ	density, slugs/ft^3

Subscripts

1	flow region upstream of a normal shock
2	flow region downstream of a normal shock
8-ft	measurement made using the 8-ft survey rake
array	measurement made using the transonic array instrumentation
avg	average value

bal	balance chamber value
bl	related to boundary layer measurements
bm	bellmouth tunnel rake parameter
cone	related to measurements from the cone portion of the cone cylinder model
cyl	related to measurements from the cylinder portion of the cone cylinder model
fs	freestream value or measurement
m	measured
model	measurement on the surface of the cone cylinder the model
nom	nominal value, usually the nominal Mach number setting
north, south	relating to the north or south bellmouth pressure rakes
ts	test section conditions

Appendix B.—Addition Data Figures

Most of the data in the main portion of this report focused on the 14-ft, 5.8 percent porosity test section configuration. The figures in this appendix provide flow field details for three of the remaining configurations:

- 8-ft, 6.2 percent modified porosity (Figs. 28 through 33)
- 8-ft, 3.1 percent modified porosity (Figs. 34 through 38)
- 14-ft schlieren window configuration (Figs. 39 and 40)

Notes:

1. The Mach number distribution data over the 4-in. diameter cone cylinder in the 8-ft, 3.1 percent modified porosity test section are not included in the appendix as that information was presented in Figure 17.
2. Only the cone cylinder data at supersonic conditions are presented for the 14-ft schlieren window configuration. The subsonic data and all of the data collected with the array match very closely to the data collected for the 14-ft, 5.8 percent porosity test section, so there was no need to repeat those charts.

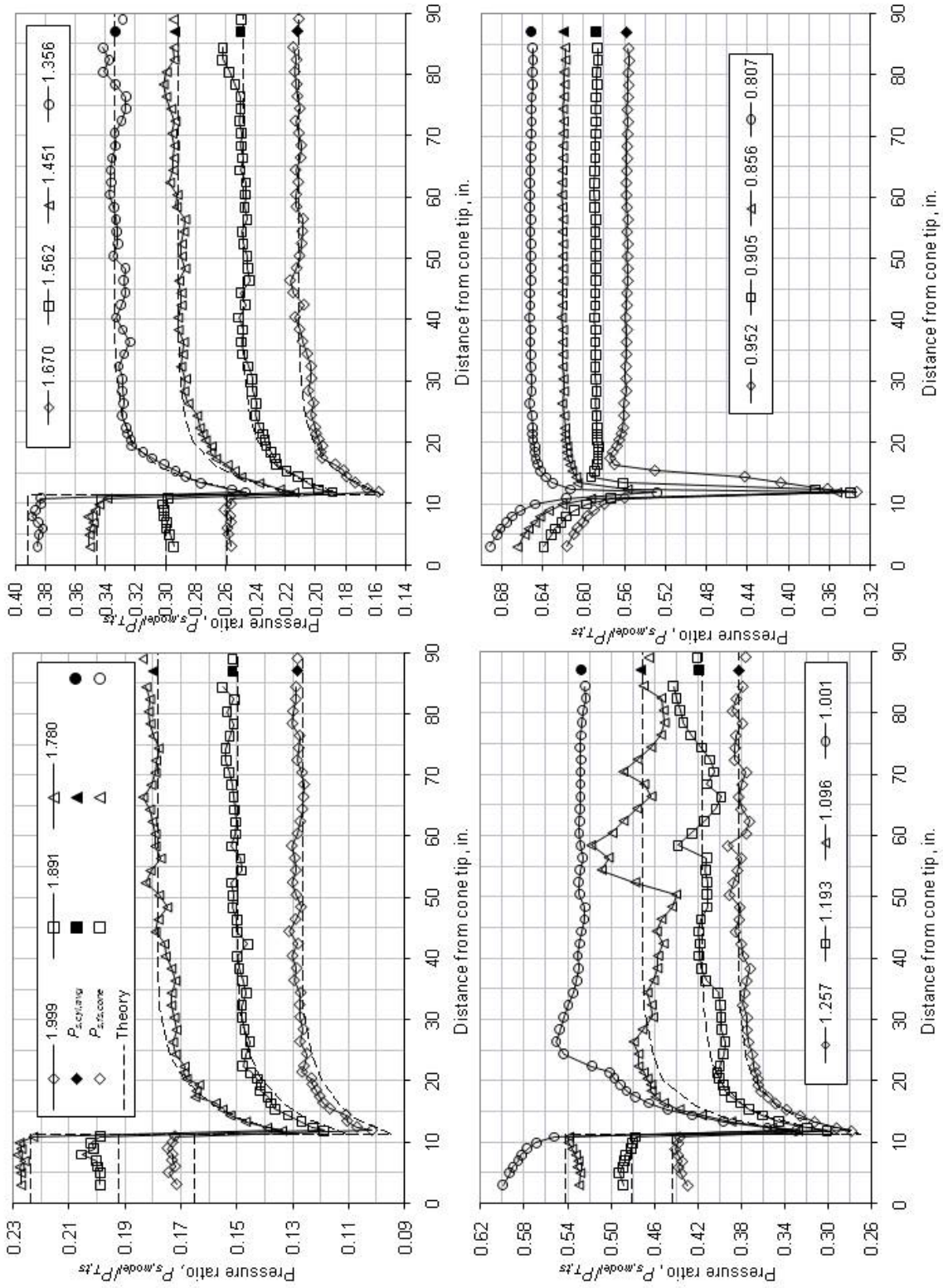

Figure 28.—Axial pressure profiles along the 4-in. diameter cone cylinder. Test section is set to the 8-ft, 6.2 percent modified porosity configuration. The tip of the cone is positioned at the inlet of the 8-ft test section (test section station 178).

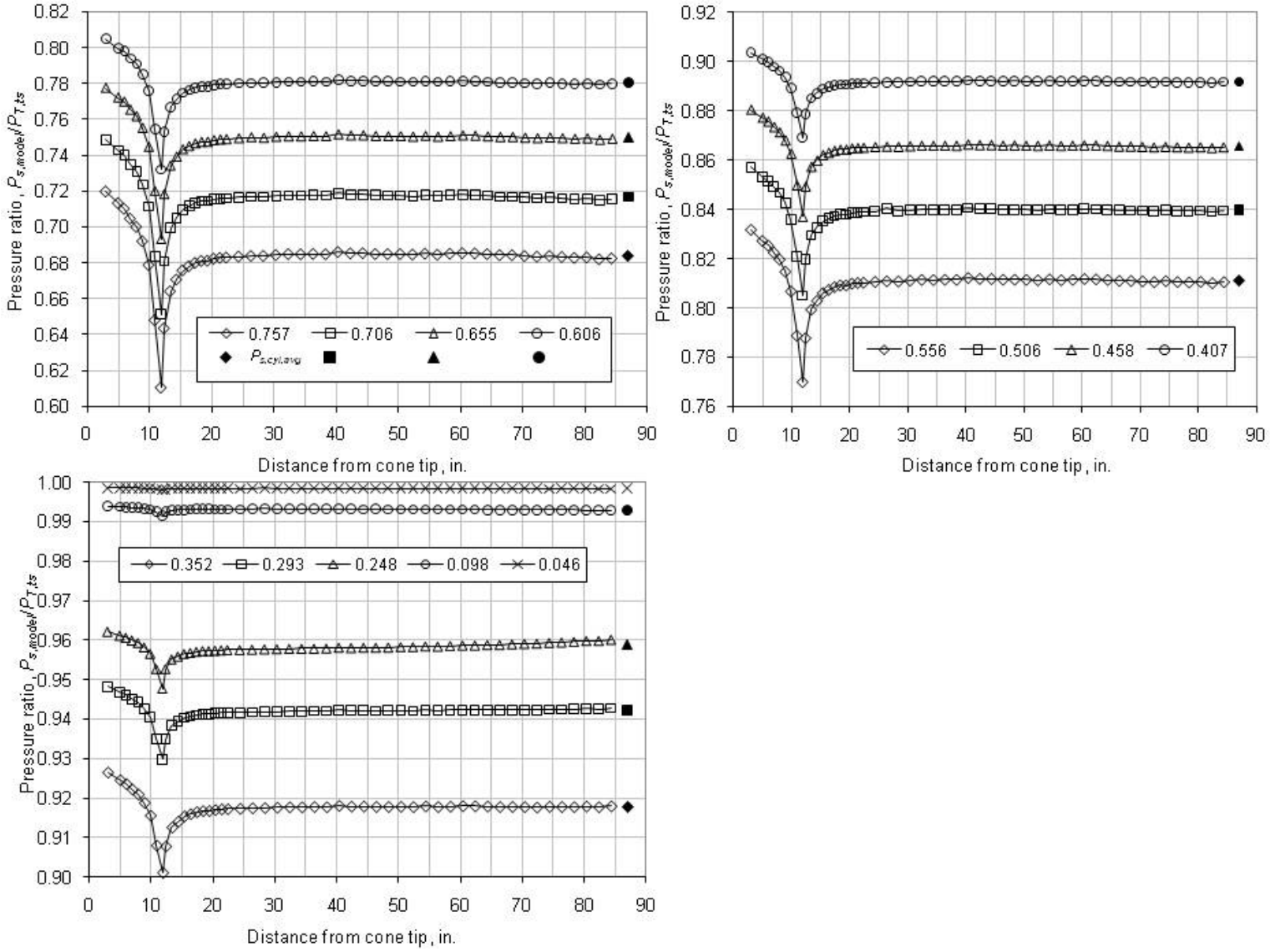

Figure 28.—Concluded.

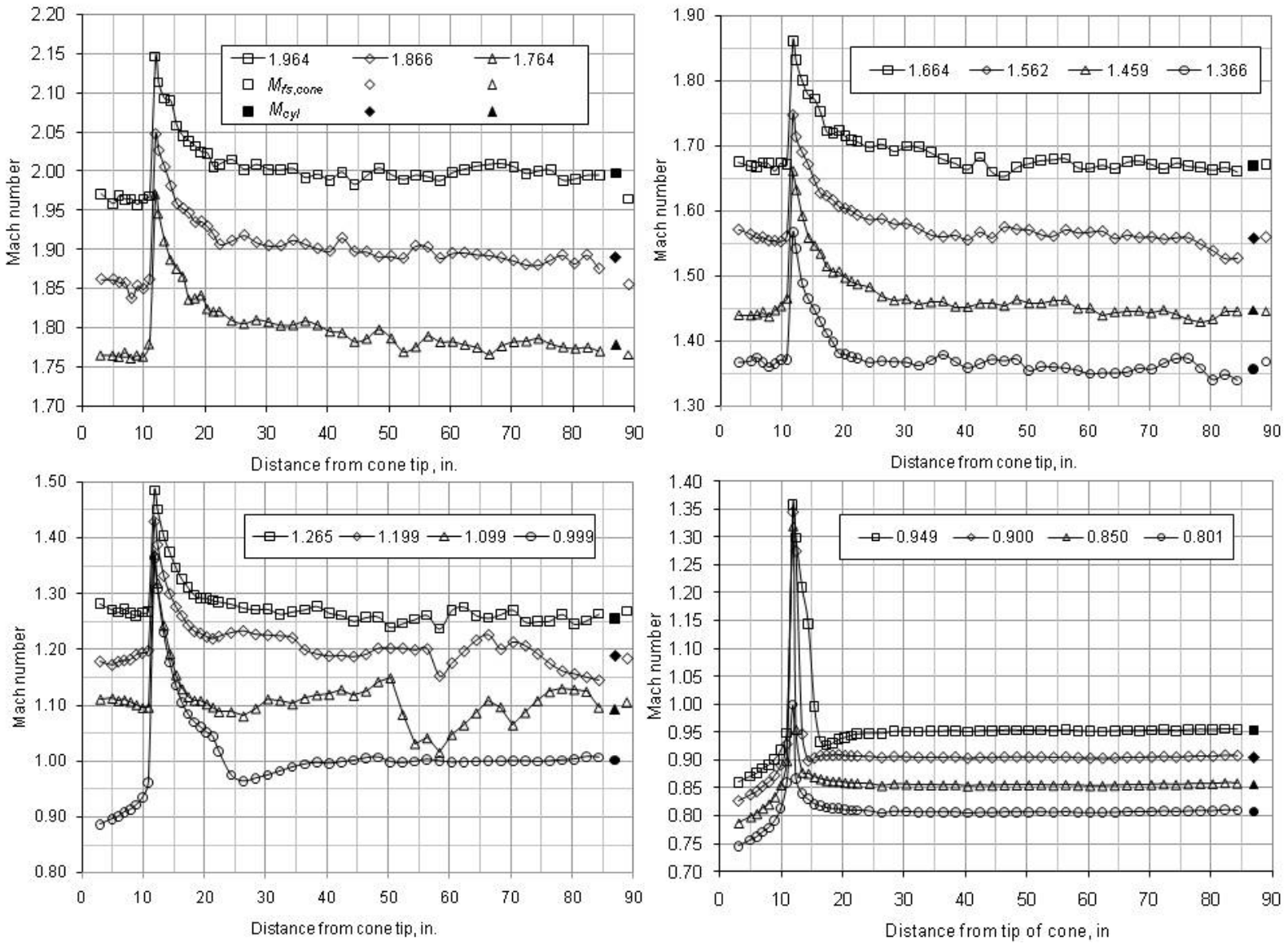

Figure 29.—Axial Mach number profiles along the 4-in. diameter cone cylinder. Test section is set to the 8-ft, 6.2 percent modified porosity configuration. The tip of the cone is positioned at the inlet of the 8-ft test section (test section station 178).

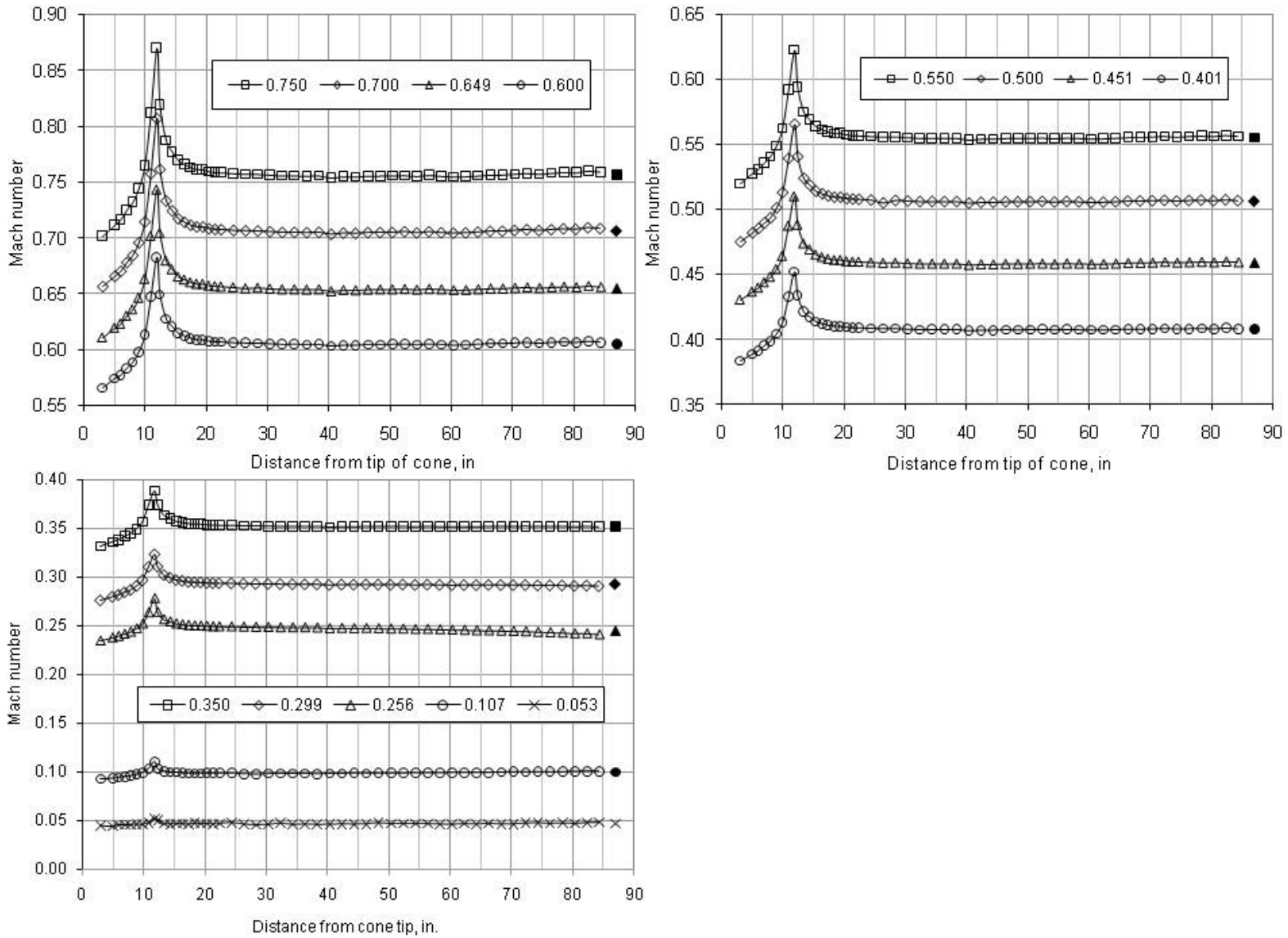

Figure 29.—Concluded.

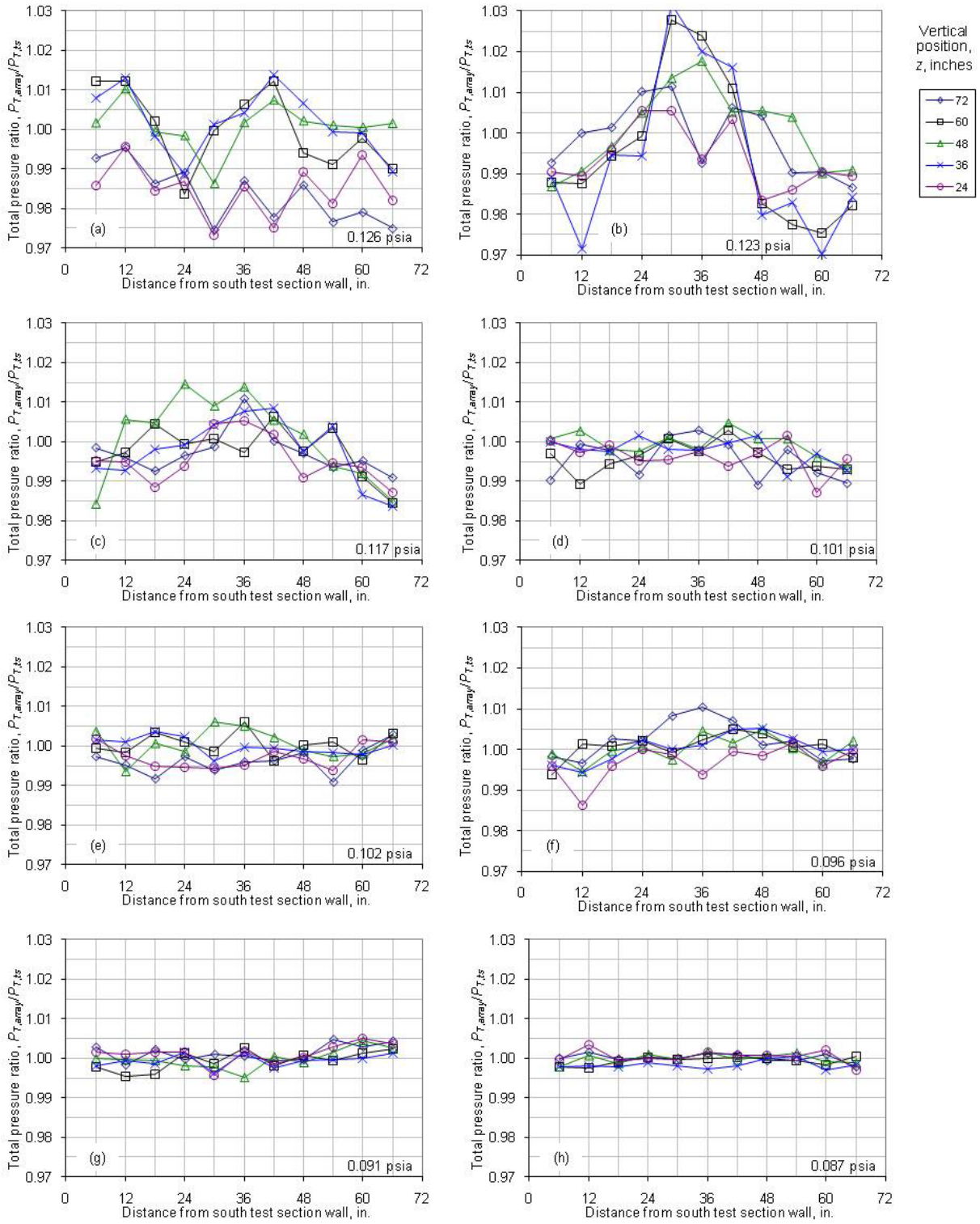

Figure 30.—Total pressure ratio distributions at each array position (5 positions) for each Mach number setting for the 8-ft, 3.1 percent modified porosity test section. Survey plane is at the inlet of the 8-ft test section (station 178). (a) M_{ts}=1.998; $P_{T,ts}$=25.148 psia. (b) M_{ts}=1.889; $P_{T,ts}$=24.543 psia. (c) M_{ts}=1.779; $P_{T,ts}$=23.431 psia. (d) M_{ts}=1.669; $P_{T,ts}$=21.794 psia (e) M_{ts} =1.560; $P_{T,ts}$ =20.353 psia. (f) M_{ts} =1.453 $P_{T,ts}$ =19.150 psia. (g) M_{ts} =1.355 $P_{T,ts}$ =18.156 psia. (h) M_{ts} =1.257; $P_{T,ts}$ =17.368 psia.

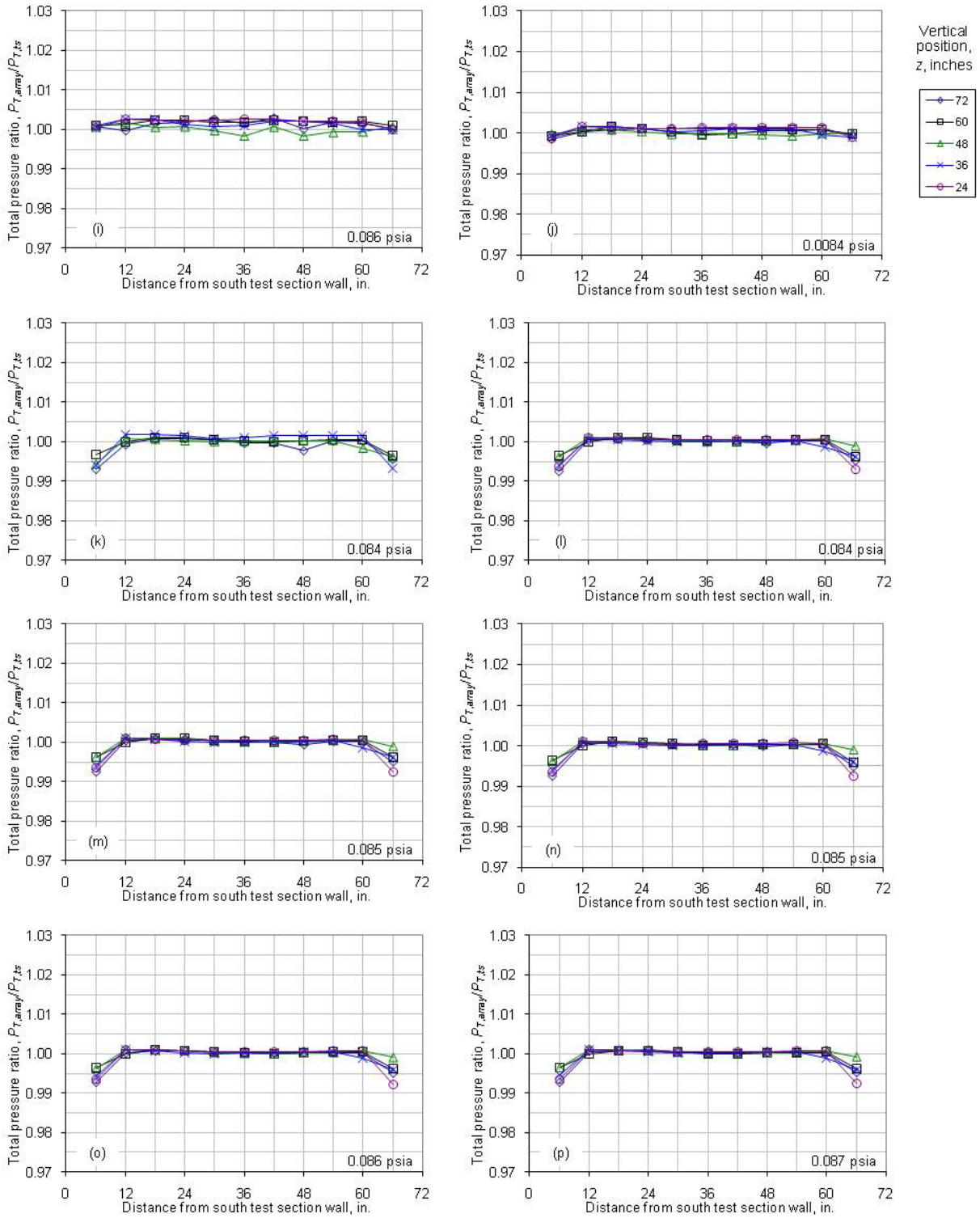

Figure 30.—Continued. (i) M_{ts} =1.191; $P_{T,ts}$ =17.144 psia. (j) M_{ts} =1.096 $P_{T,ts}$ =16.788 psia. (k) M_{ts} =0.996 $P_{T,ts}$ =16.786 psia. (l) M_{ts} =0.995; $P_{T,ts}$ =16.792 psia. (m) M_{ts} =0.905; $P_{T,ts}$ =16.915 psia. (n) M_{ts} =0.856 $P_{T,ts}$ =16.957 psia. (o) M_{ts} =0.807 $P_{T,ts}$ =17.245 psia. (p) M_{ts} =0.757; $P_{T,ts}$ =17.390 psia.

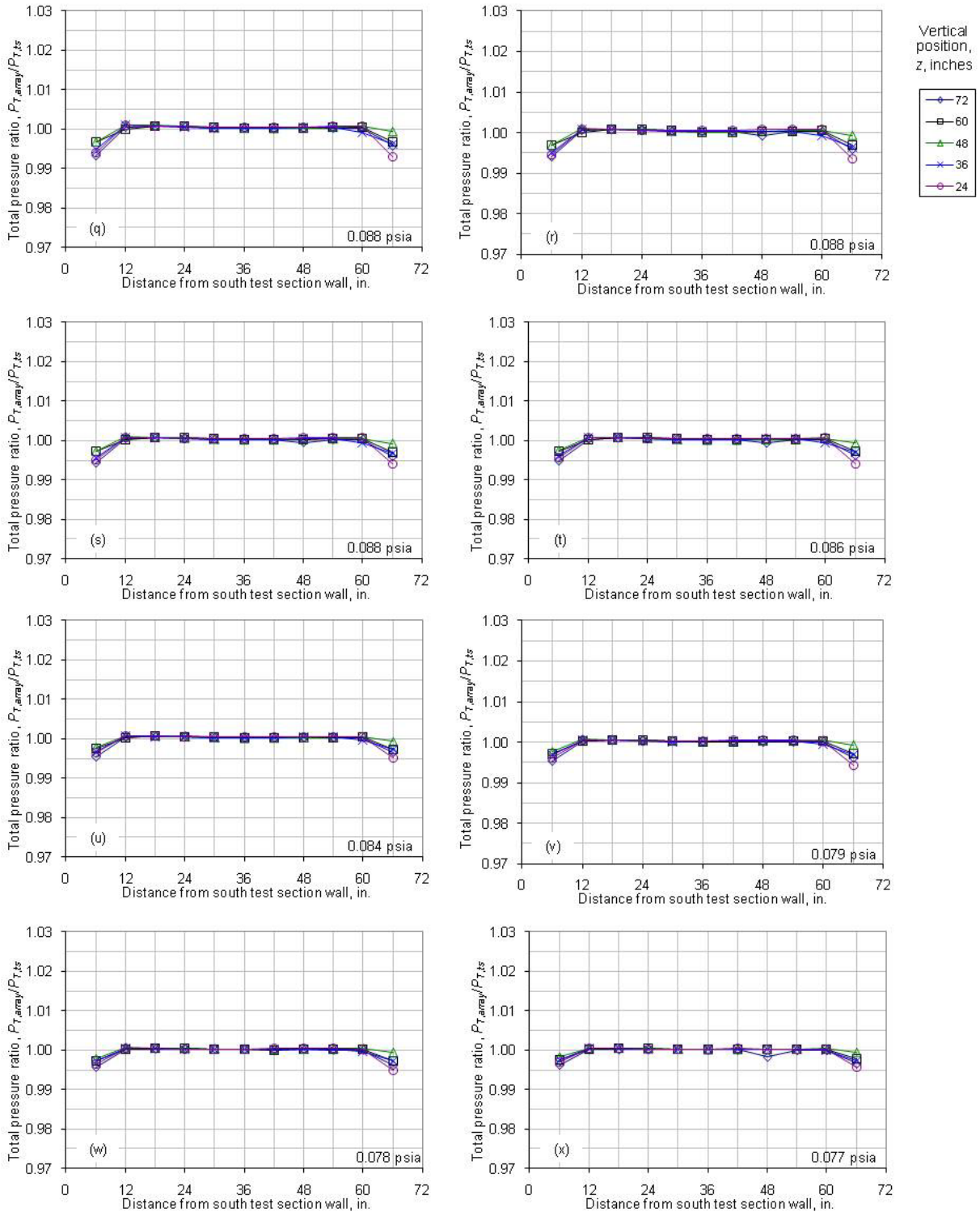

Figure 30.—Continued. (q) M_{ts} =0.706; $P_{T,ts}$ =17.591 psia. (r) M_{ts} =0.655 $P_{T,ts}$ =17.695 psia. (s) M_{ts} =0.606 $P_{T,ts}$ =17.516 psia. (t) M_{ts} =0.555; $P_{T,ts}$ =17.198 psia. (u) M_{ts} =0.507; $P_{T,ts}$ =16.872 psia. (v) M_{ts} =0.507 $P_{T,ts}$ =15.835 psia (1-motor operation). (w) M_{ts} =0.458 $P_{T,ts}$ =15.597 psia. (x) M_{ts} =0.408; $P_{T,ts}$ =15.377 psia.

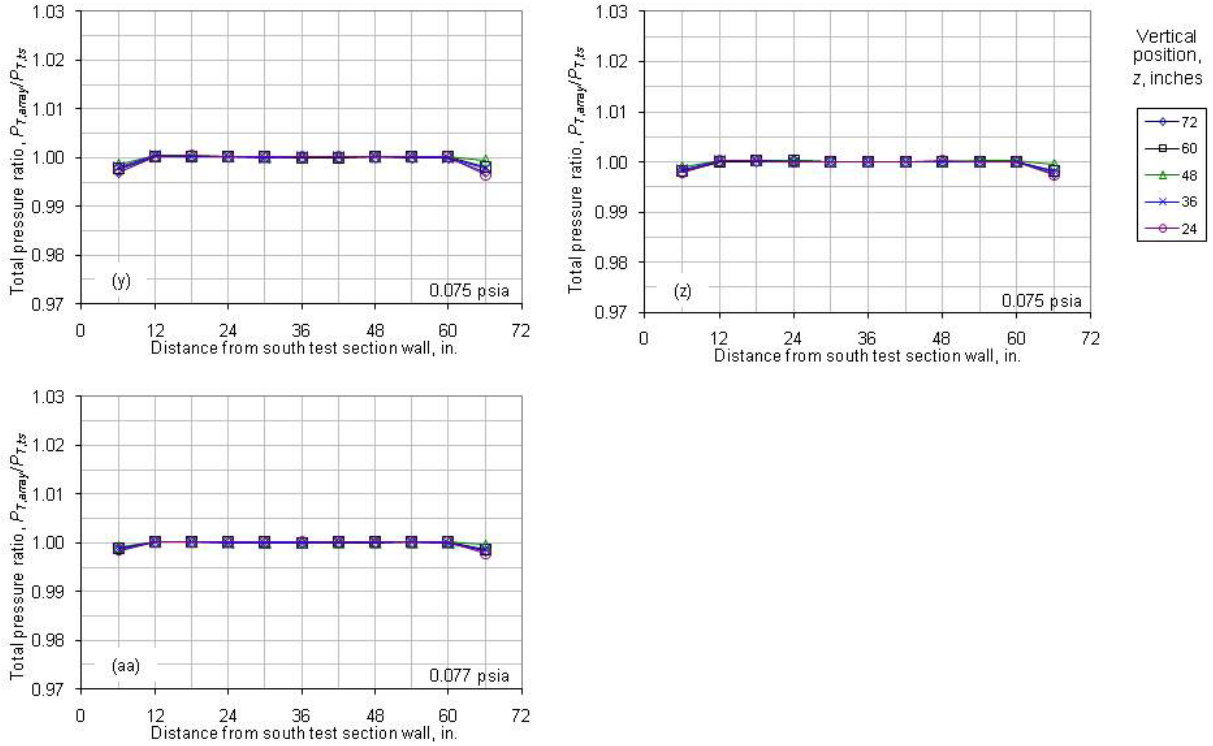

Figure 30.—Concluded. (y) M_{ts} =0.353; $P_{T,ts}$ =15.088 psia. (z) M_{ts} =0.297 $P_{T,ts}$ =14.999 psia. (aa) M_{ts} =0.247 $P_{T,ts}$ =15.320 psia.

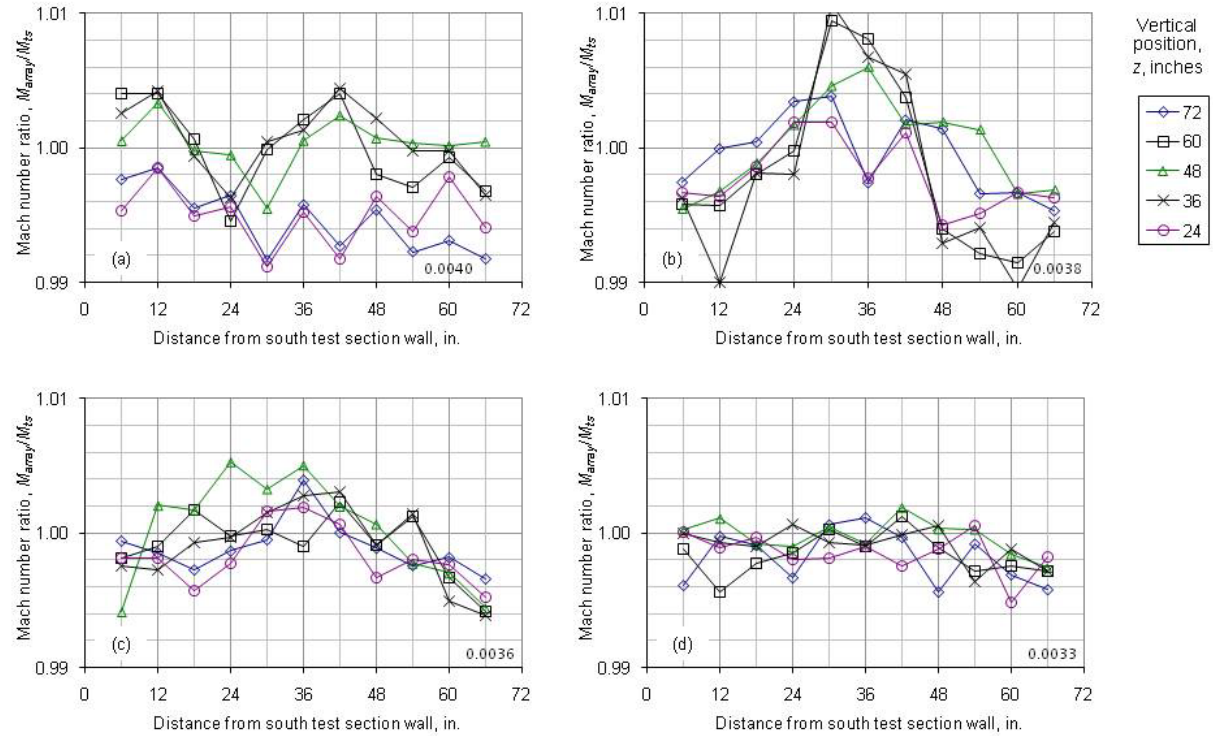

Figure 31.—Mach number ratio distributions at each array position (5 positions) for each Mach number setting for the 8-ft, 3.1 percent modified porosity test section. Survey plane is at the inlet of the 8-ft test section (station 178). The number in the lower right-hand corner is the approximate delta Mach number represented by the minor y-axis division. (a) M_{ts} = 1.998. (b) M_{ts} = 1.889. (c) M_{ts} = 1.779. (d) M_{ts} = 1.669.

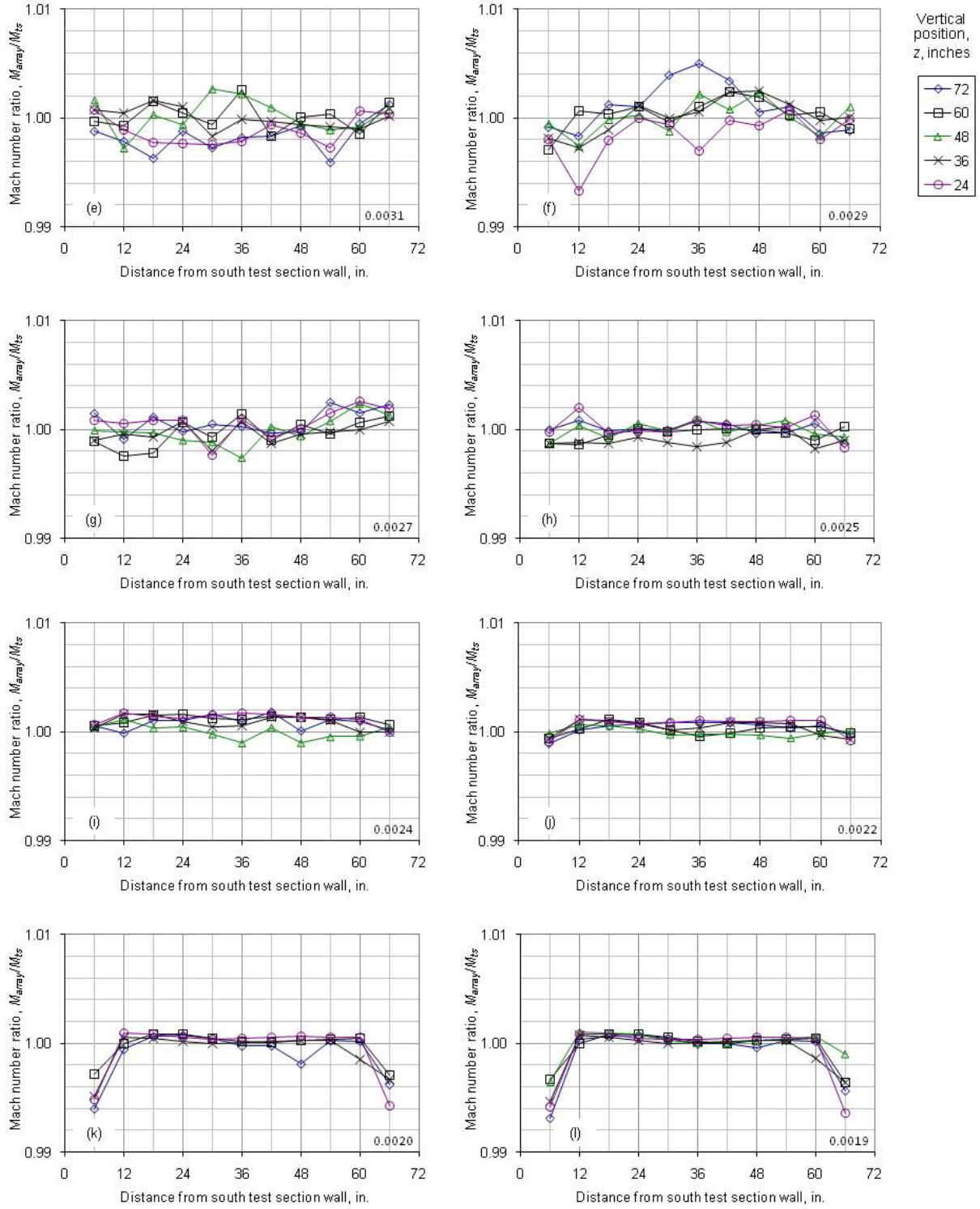

Figure 31.—Continued. (e) M_{ts} = 1.560. (f) M_{ts} = 1.453. (g) M_{ts} = 1.355. (h) M_{ts} = 1.257. (i) M_{ts} = 1.191. (j) M_{ts} = 1.096. (k) M_{ts} = 0.996. (l) M_{ts} = 0.955.

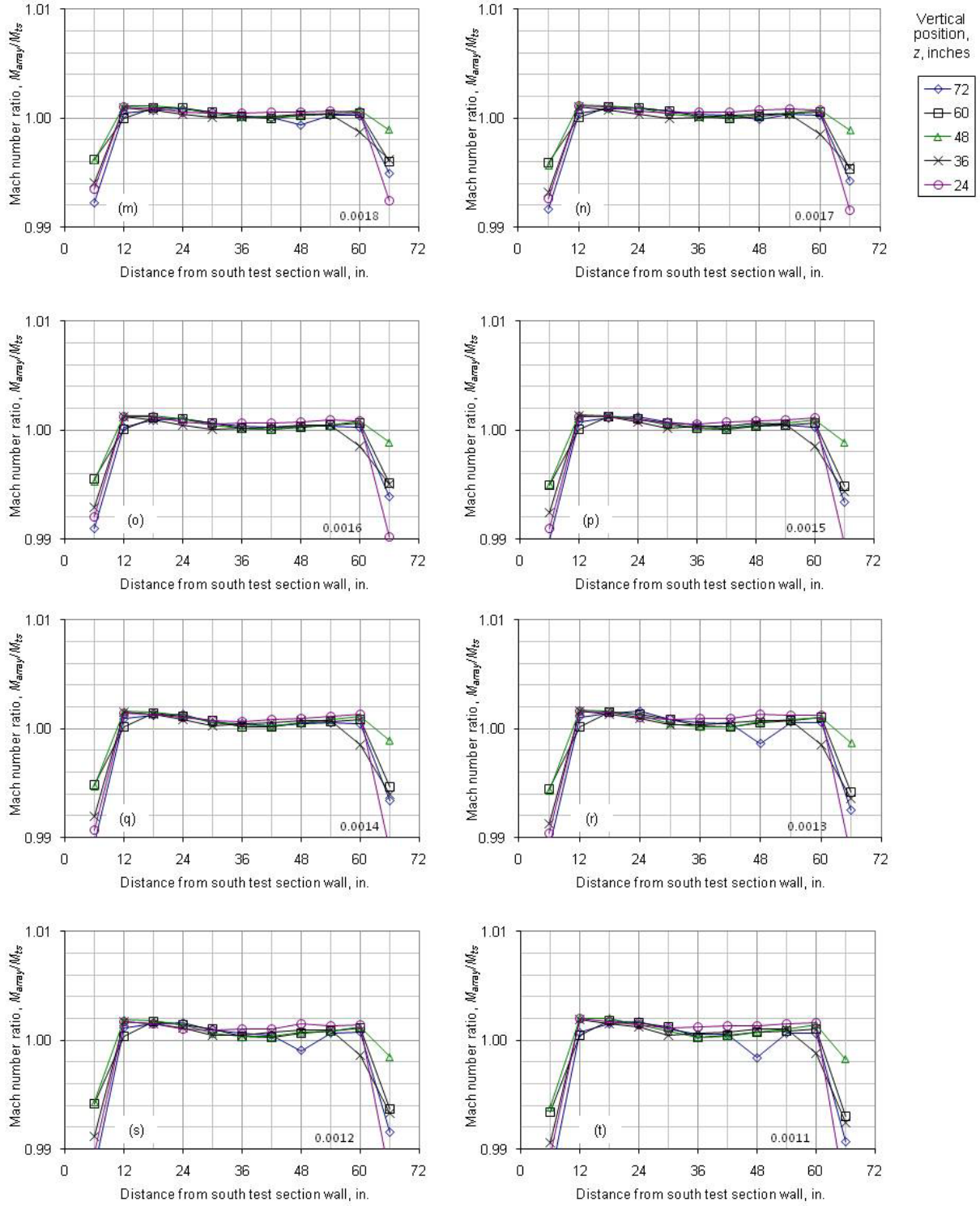

Figure 31.—Continued. (m) M_{ts} = 0.905. (n) M_{ts} = 0.856. (o) M_{ts} = 0.807. (p) M_{ts} = 0.757. (q) M_{ts} = 0.706. (r) M_{ts} = 0.655. (s) M_{ts} = 0.606. (t) M_{ts} = 0.555

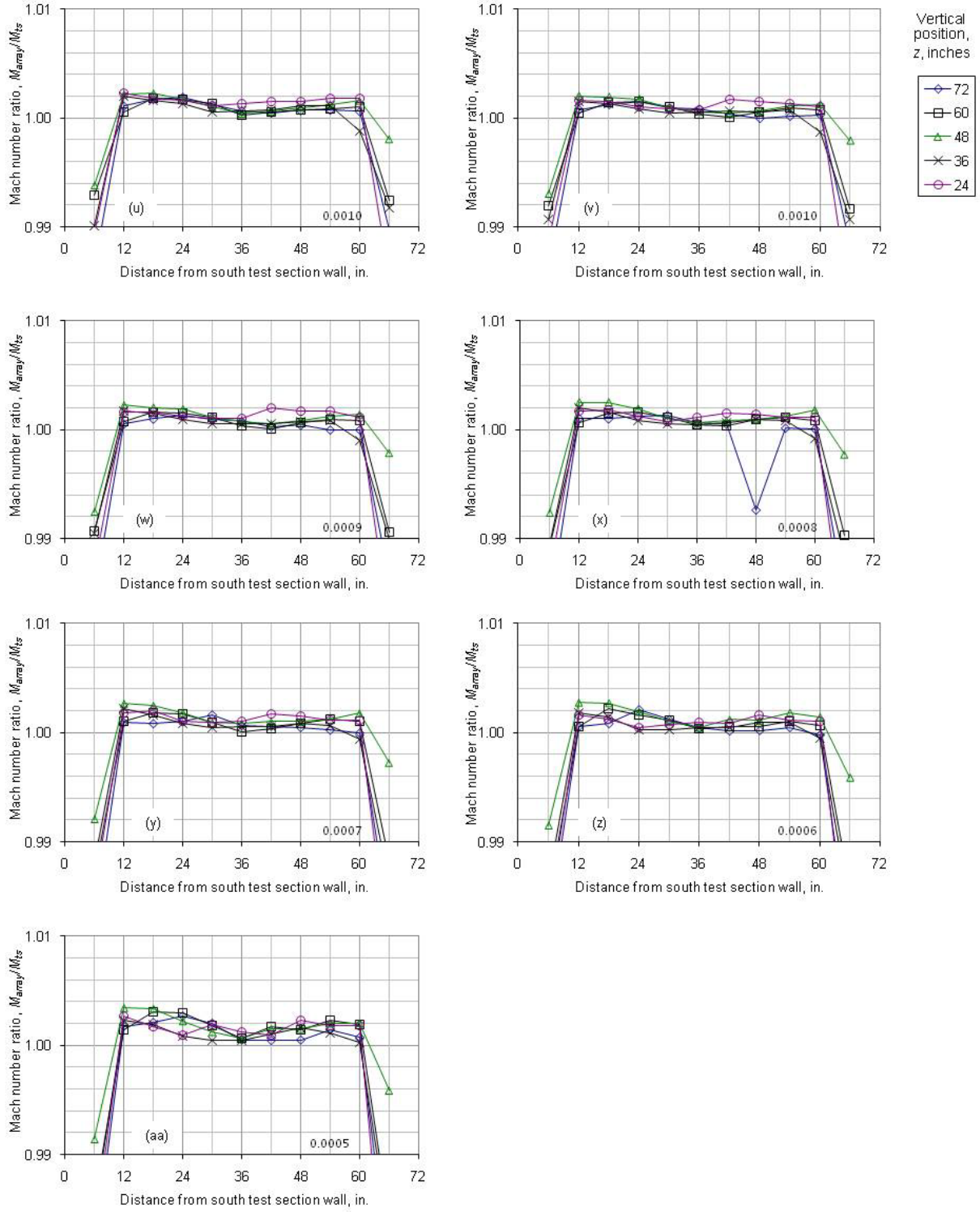

Figure 31.—Concluded. (u) M_{ts} = 0.507. (v) M_{ts} = 0.507 (1-motor). (w) M_{ts} = 0.458. (x) M_{ts} = 0.408. (y) M_{ts} = 0.353. (z) M_{ts} = 0.297. (aa) M_{ts} = 0.247

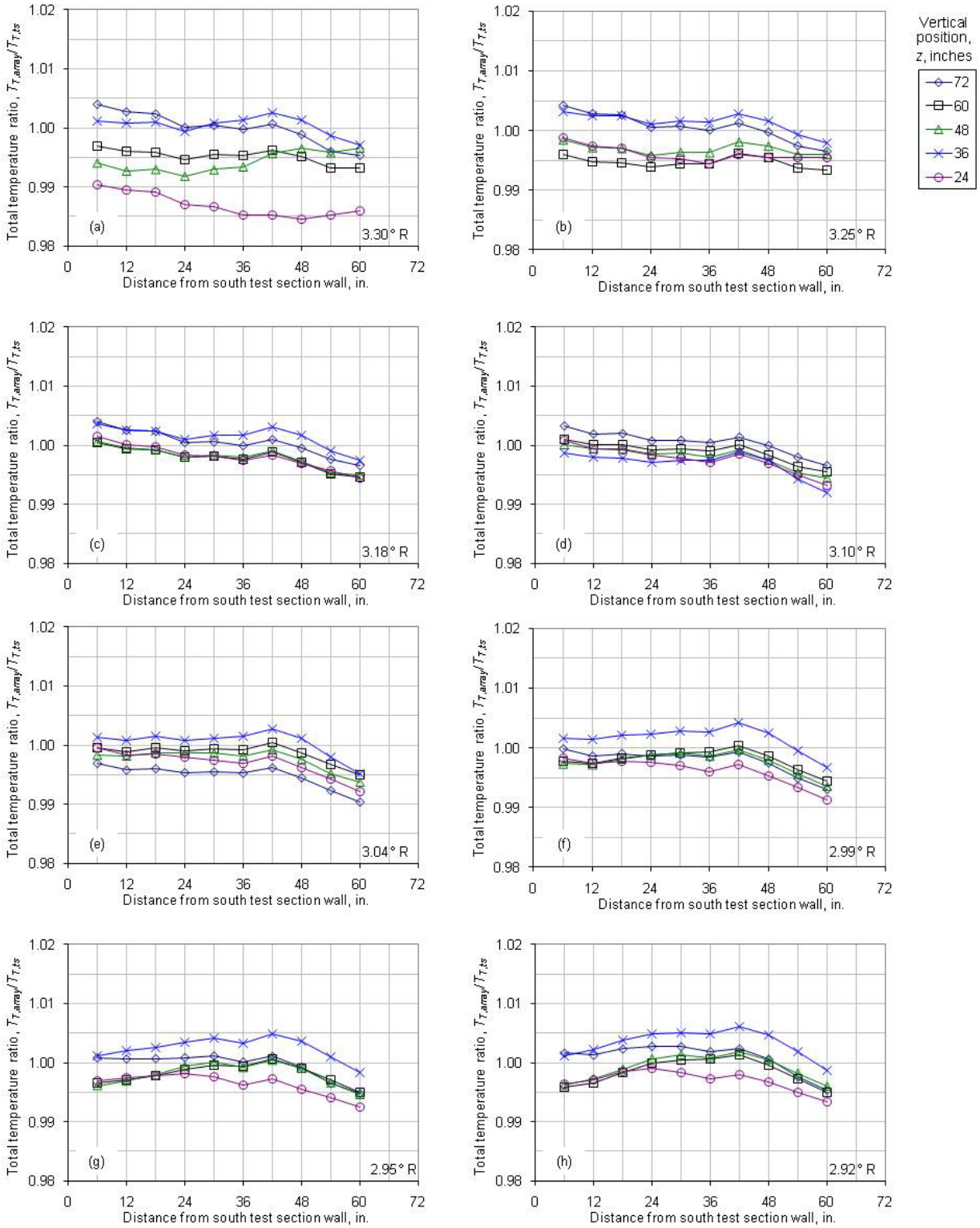

Figure 32.—Total temperature ratio distributions at each array position (5 positions) for each Mach number setting in the 8-ft, 6.2 percent modified porosity test section; survey plane is at the inlet of the 8-ft test section (station 178). The number in the lower right-hand corner is the approximate delta Mach number represented by the minor y-axis division. (a) M_{ts}=1.998; $T_{T,ts}$=659.4 R. (b) M_{ts}=1.889; $T_{T,ts}$=649.5 R. (c) M_{ts}=1.779; $T_{T,ts}$=635.0 R. (d) M_{ts}=1.669; $T_{T,ts}$=620.1 R.

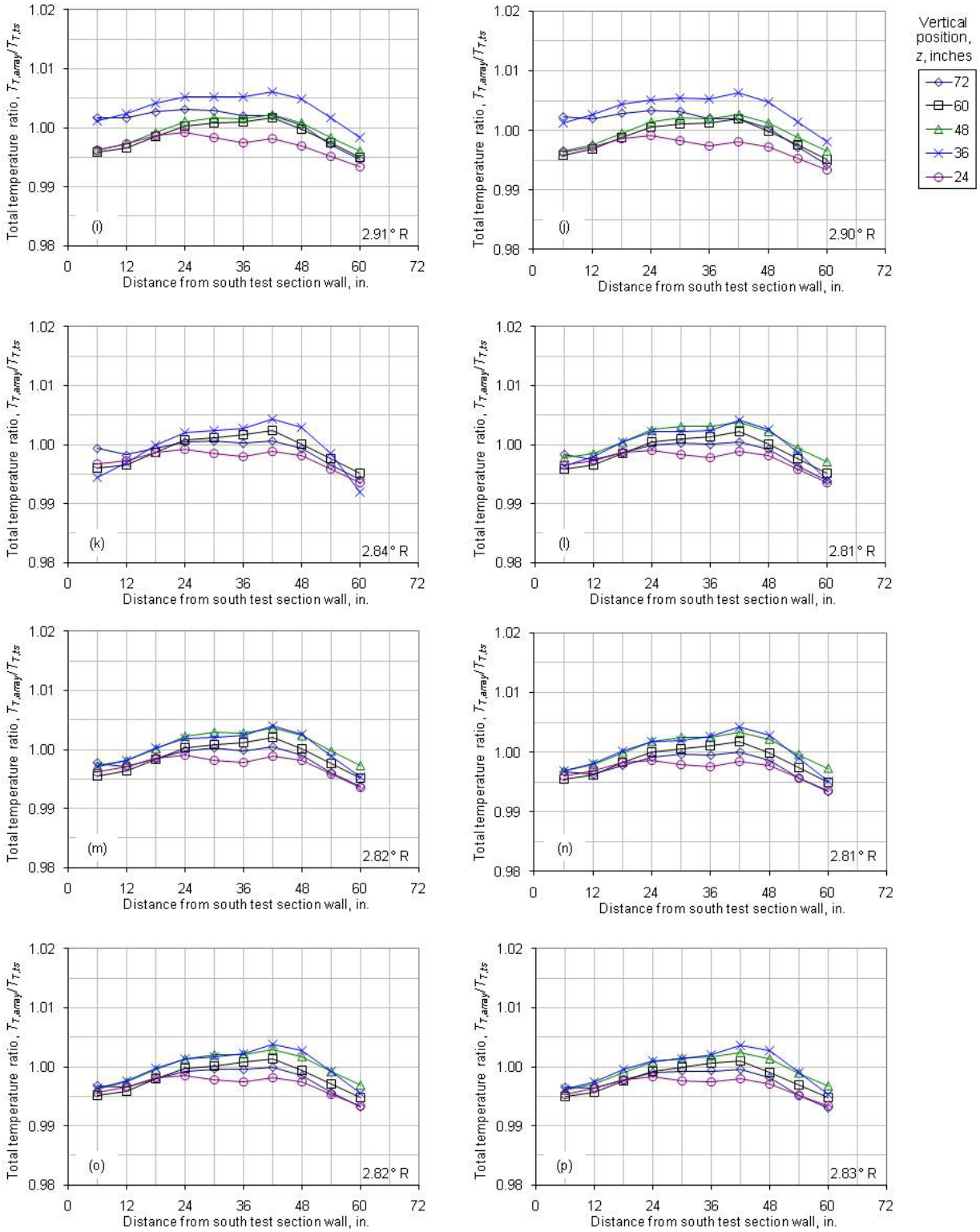

Figure 32.—Continued. (i) M_{ts}=1.191; $T_{T,ts}$=582.4 R. (f) M_{ts}=1.096; $T_{T,ts}$=579.5 R. (g) M_{ts}=0.996; $T_{T,ts}$=567.4 R. (h) M_{ts}=0.995; $T_{T,ts}$=562.7 R. (m) M_{ts}=0.905; $T_{T,ts}$=563.1 R. (n) M_{ts}=0.856; $T_{T,ts}$=562.8 R. (o) M_{ts}=0.807; $T_{T,ts}$=564.7 R. (p) M_{ts}=0.757; $T_{T,ts}$=565.1 R.

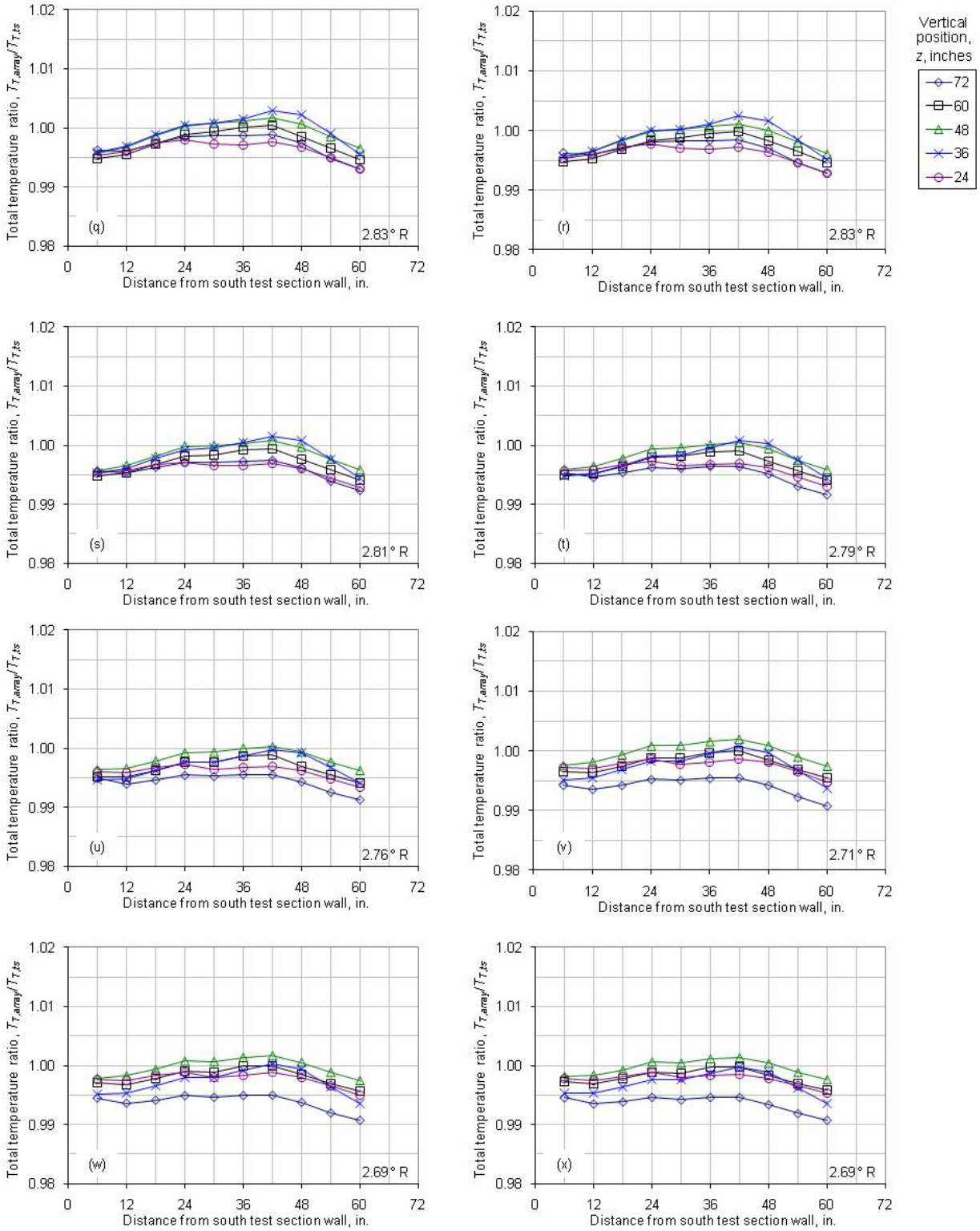

Figure 32.—Continued. (q) M_{ts}=0.706; $T_{T,ts}$=565.7 R. (r) M_{ts}=0.655; $T_{T,ts}$=565.3 R. (s) M_{ts}=0.606; $T_{T,ts}$=562.1 R. (t) M_{ts}=0.555; $T_{T,ts}$=557.3 R. (u) M_{ts}=0.507; $T_{T,ts}$=552.5 R. (v) M_{ts}=0.507; $T_{T,ts}$=541.5 R (1-motor). (w) M_{ts}=0.458; $T_{T,ts}$=537.5 R (1-motor). (x) M_{ts}=0.408; $T_{T,ts}$=533.6 R (1-motor).

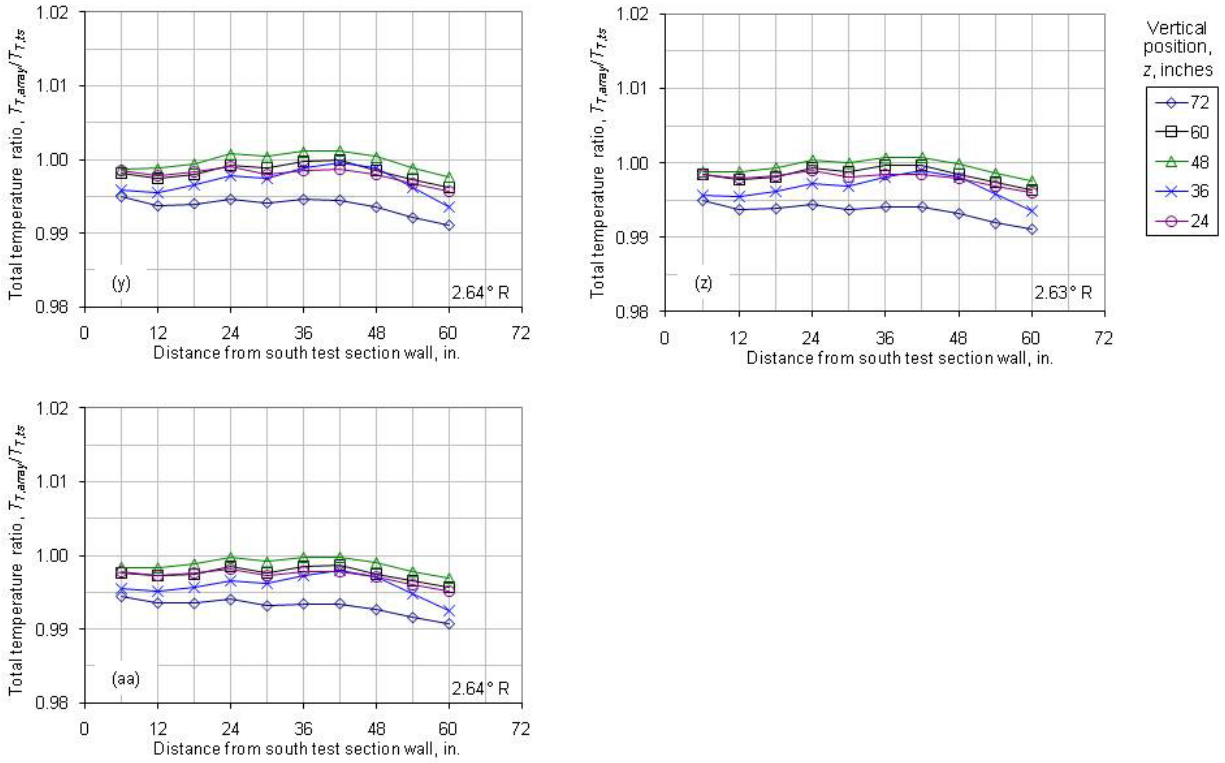

Figure 32.—Concluded - (y) M_{ts}=0.353; $T_{T,ts}$=529.0 R (1-motor). (z) M_{ts}=0.297; $T_{T,ts}$=526.3 R (1-motor). (aa) M_{ts}=0.247; $T_{T,ts}$=528.5 R (1-motor).

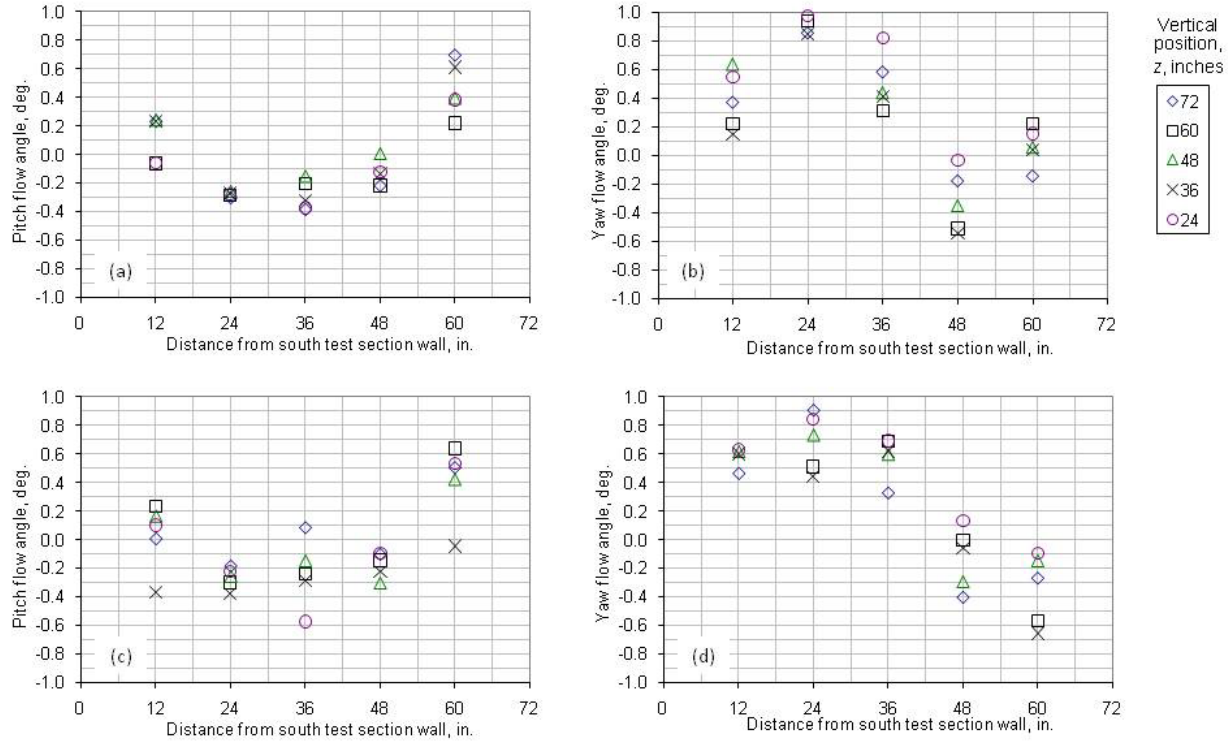

Figure 33.—Pitch and Yaw flow angle data at each array position (5 positions) for each Mach number setting for the 8-ft, 6.2 percent modified test section configuration. The survey plane was the inlet of the 8-ft test section (station 178). (a) M_{ts}=1.998. (b) M_{ts}=1.998. (c) M_{ts}=1.889. (d) M_{ts}=1.889.

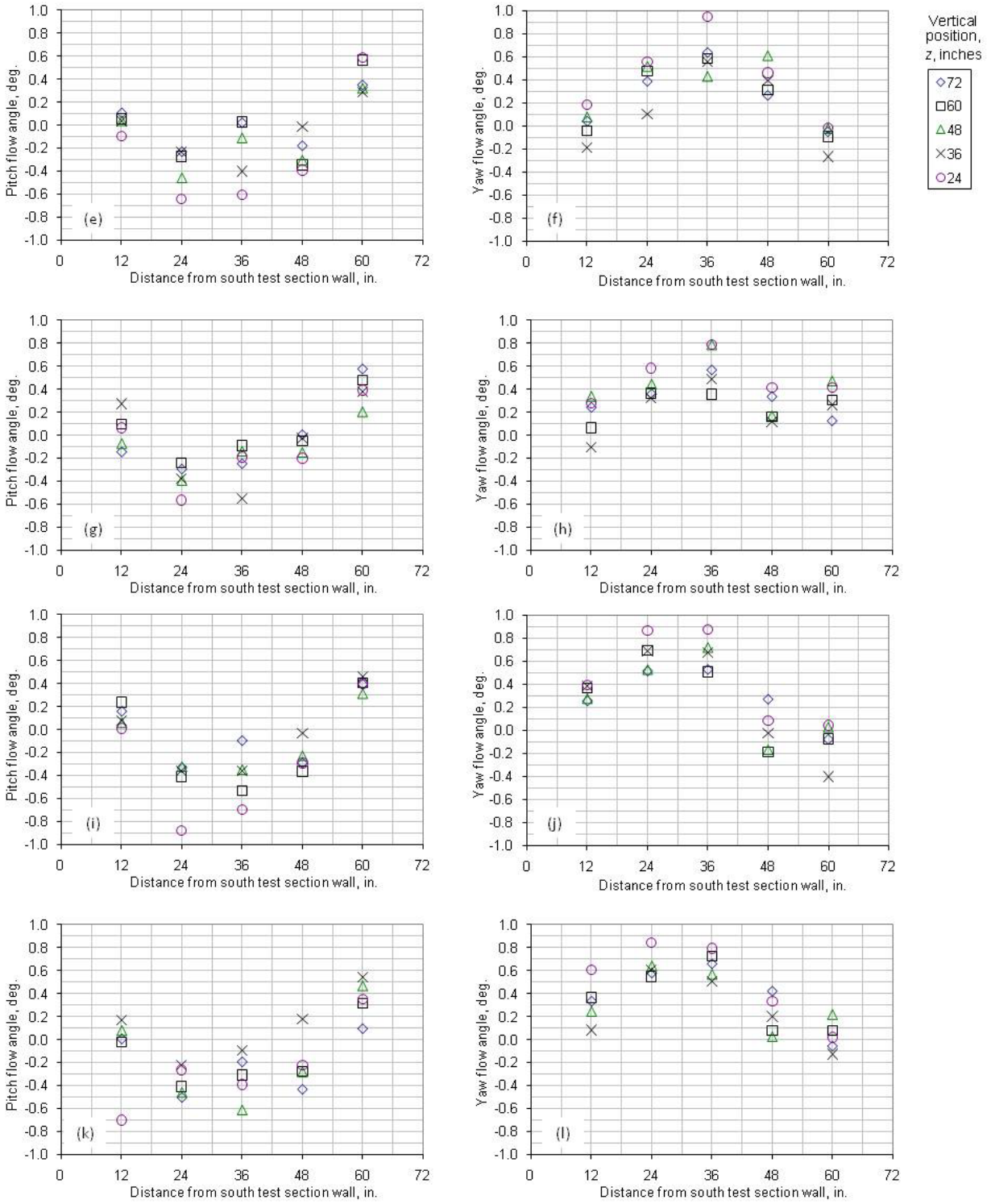

Figure 33.—Continued. (e) M_{ts}=1.779. (f) M_{ts}=1.779. (g) M_{ts}=1.669. (h) M_{ts}=1.669. (i) M_{ts}=1.560. (j) M_{ts}=1.560. (k) M_{ts}=1.453. (l) M_{ts}=1.453.

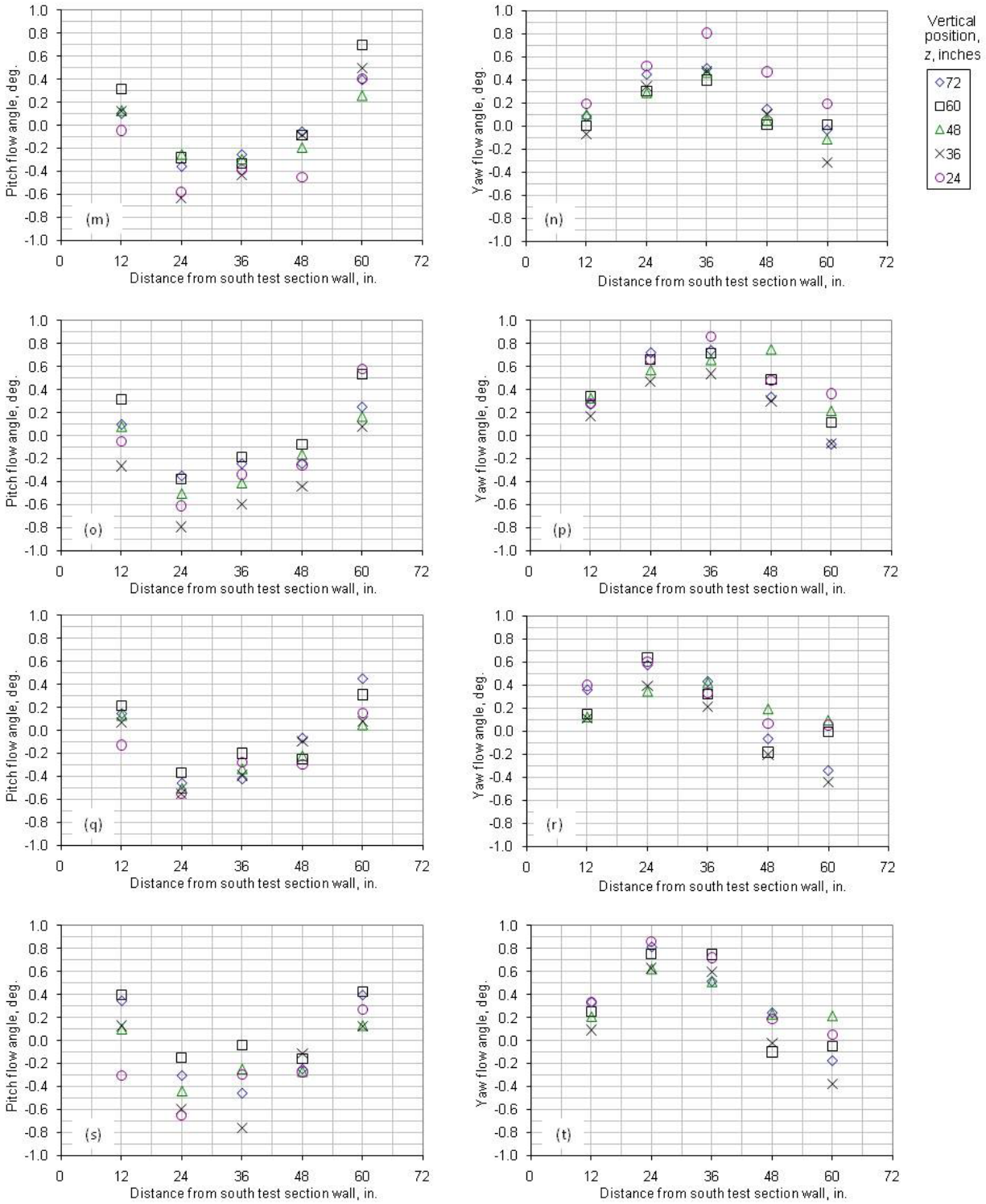

Figure 33.—Continued. (m) M_{ts}=1.355. (n) M_{ts}=1.355. (o) M_{ts}=1.257. (p) M_{ts}=1.257 (q) M_{ts}=1.191. (r) M_{ts}=1.191. (s) M_{ts}=1.096. (t) M_{ts}=1.096.

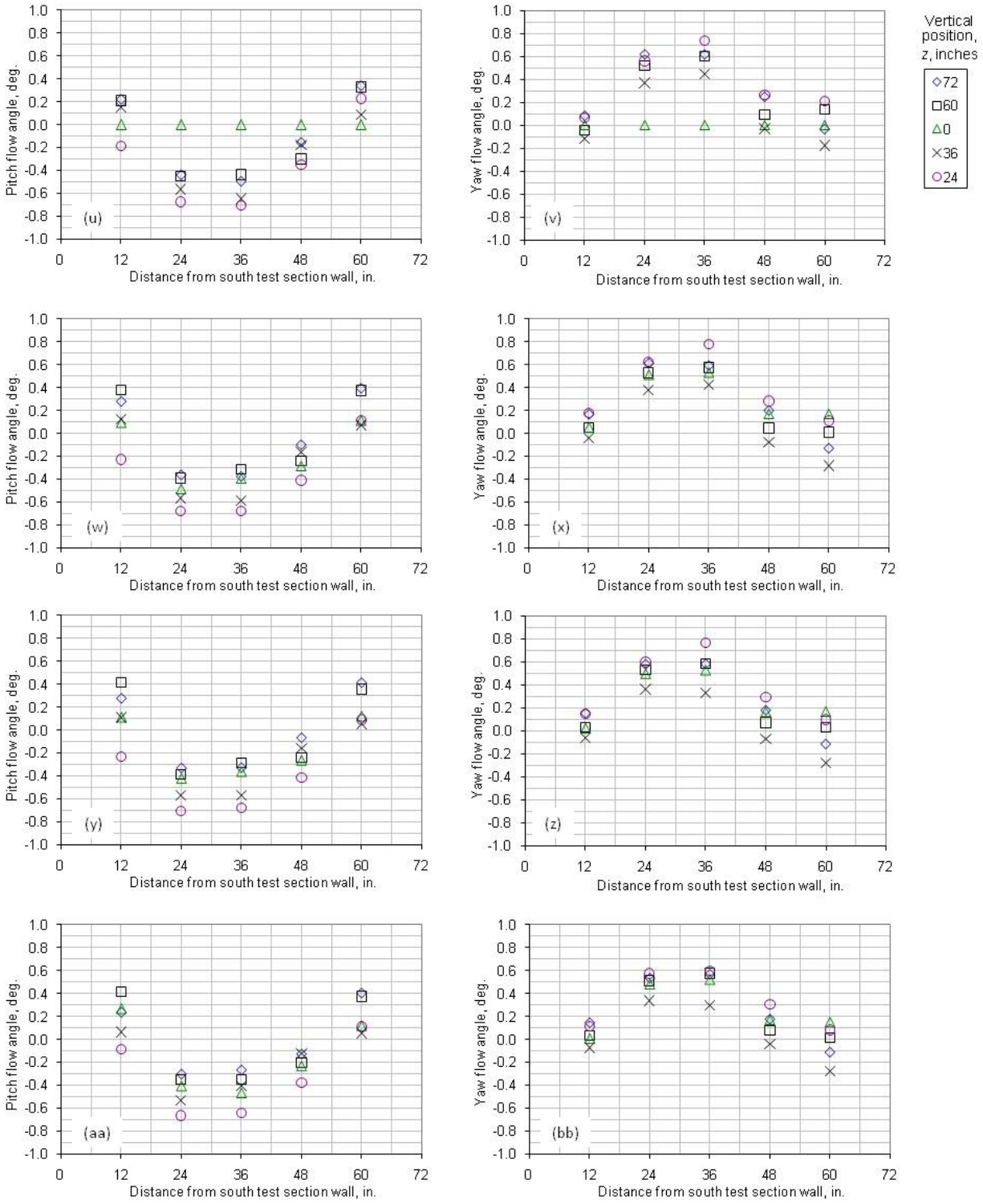

Figure 33.—Continued. (u) M_{ts}=0.996. (v) M_{ts}=0.996. (w) M_{ts}=0.955. (x) M_{ts}=0.955. (y) M_{ts}=0.905. (z) M_{ts}=0.905. (aa) M_{ts}=0.856. (bb) M_{ts}=0.856.

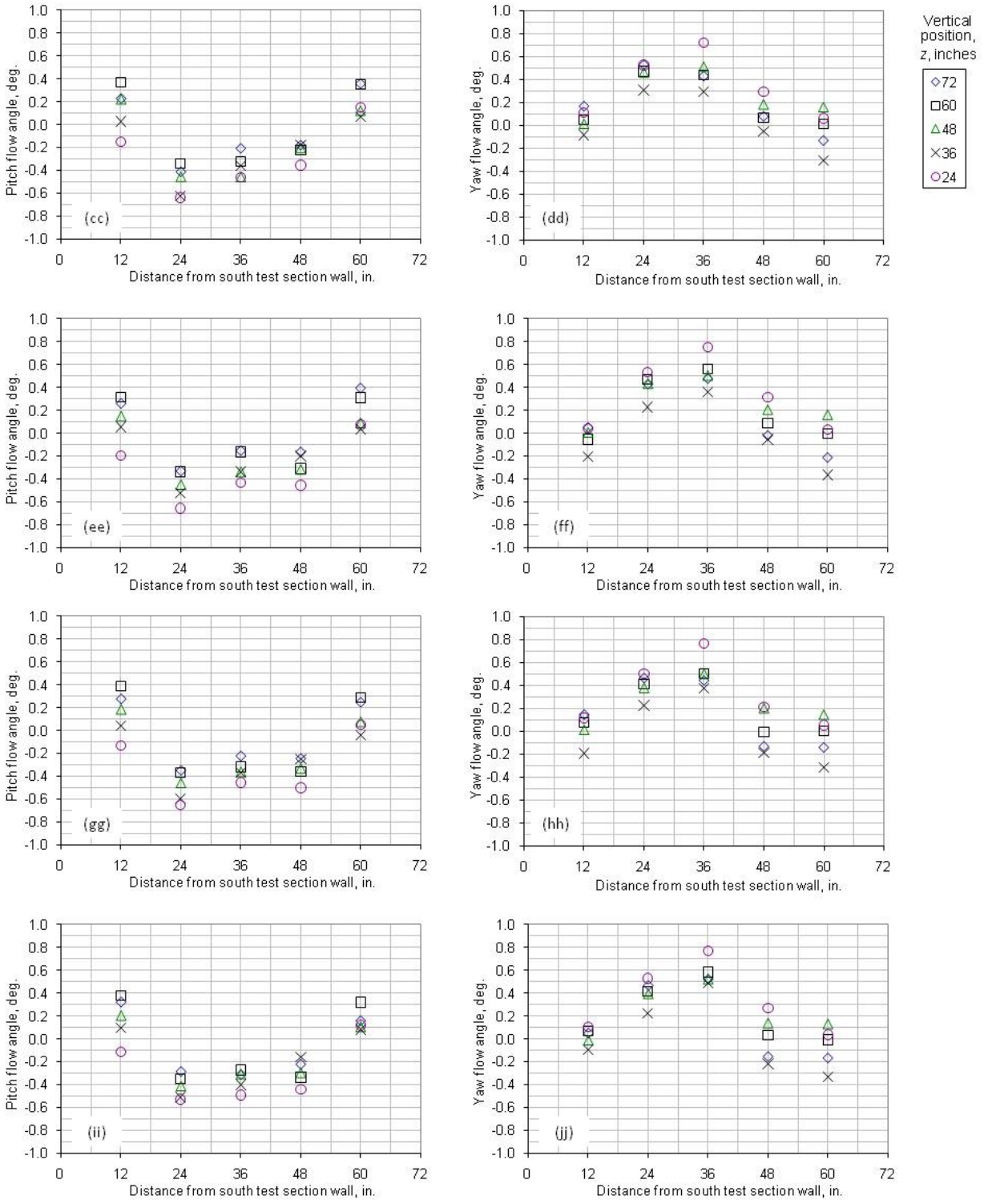

Figure 33.—Continued. (cc) M_{ts}=0.807. (dd) M_{ts}=0.807. (ee) M_{ts}=0.757. (ff) M_{ts}=0.757. (gg) M_{ts}=0.706. (hh) M_{ts}=0.706. (ii) M_{ts}=0.655. (jj) M_{ts}=0.655.

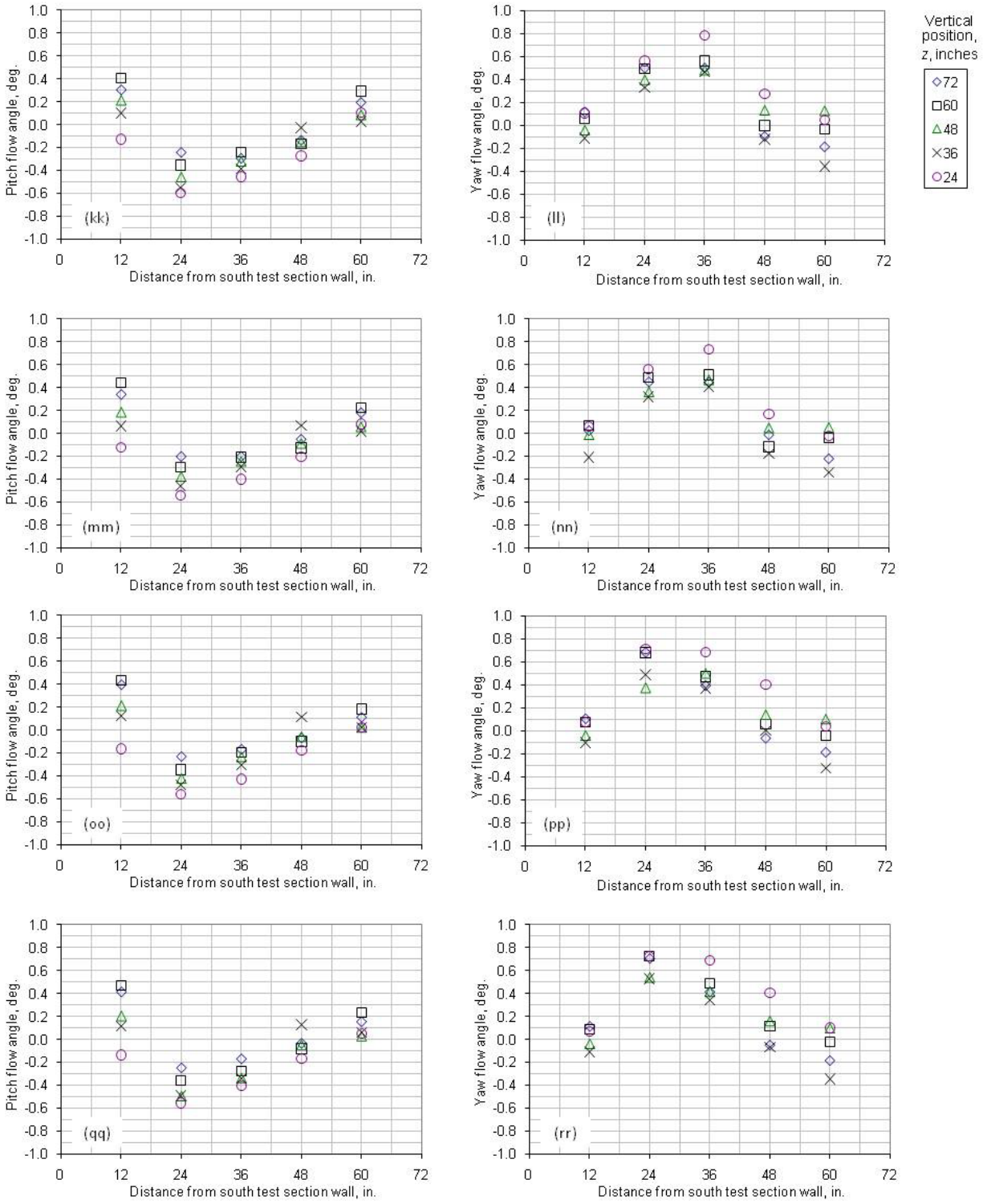

Figure 33.—Continued. (kk) M_{ts}=0.606. (ll) M_{ts}=0.606. (mm) M_{ts}=0.555. (nn) M_{ts}=0.555. (oo) M_{ts}=0.507. (pp) M_{ts}=0.507. (qq) M_{ts}=0.507 (1-motor). (rr) M_{ts}=0.507 (1-motor).

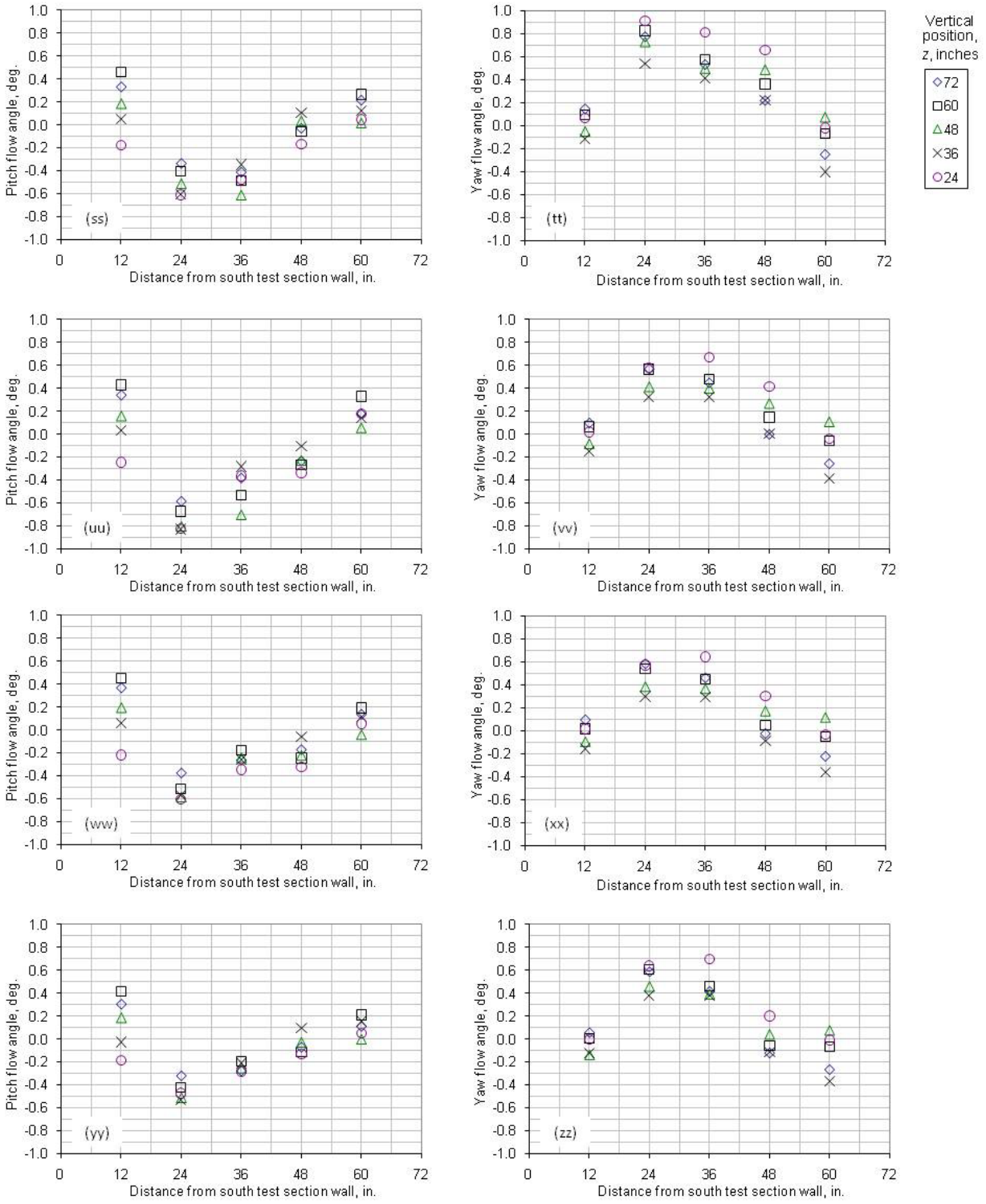

Figure 33.—Continued. (ss) M_{ts}=0.458 (1-motor). (tt) M_{ts}=0.458 (1-motor). (uu) M_{ts}=0.408 (1-motor). (rr) M_{ts}=0.408 (1-motor). (ww) M_{ts}=0.353 (1-motor). (xx) M_{ts}=0.353 (1-motor). (yy) M_{ts}=0.297 (1-motor). (zz) M_{ts}=0.297 (1-motor).

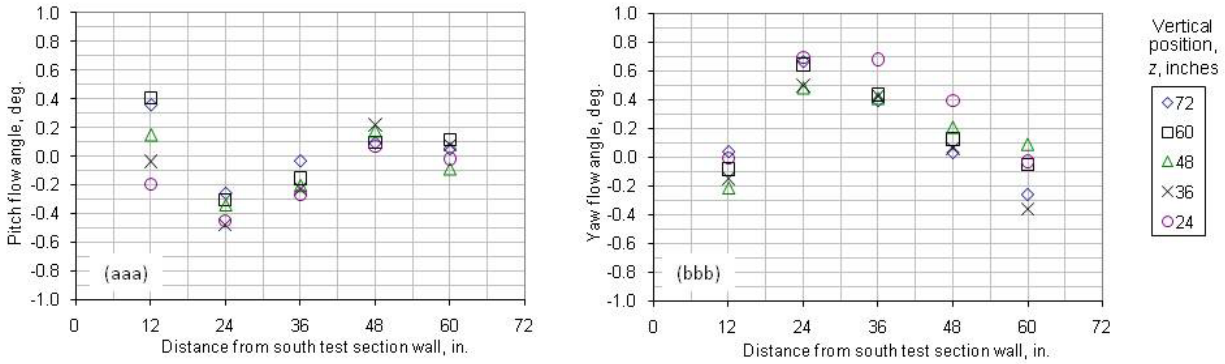

Figure 33.—Concluded. (aaa) M_{ts}=0.247 (1-motor). (bbb) M_{ts}=0.247 (1-motor).

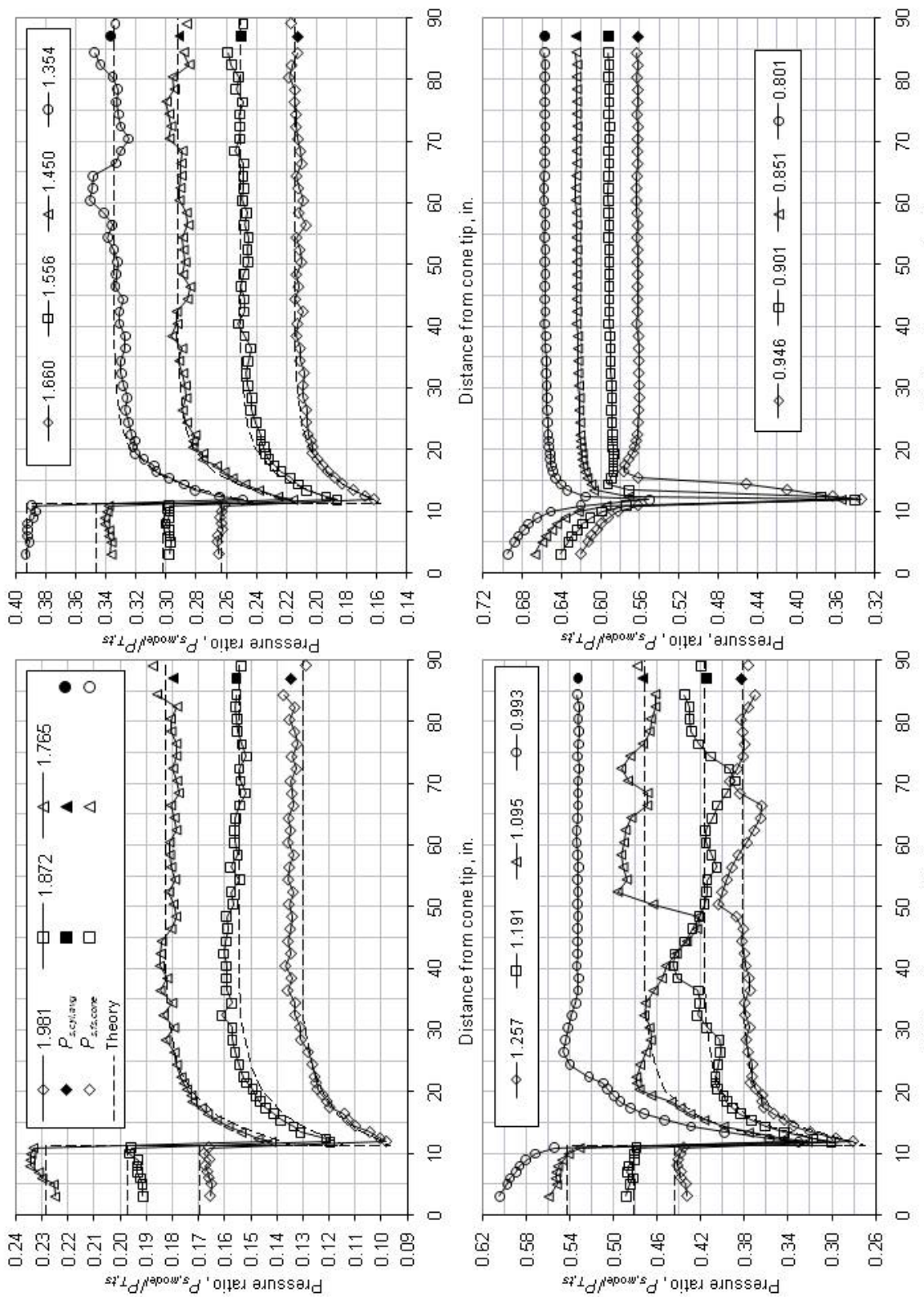

Figure 34.—Axial pressure profiles along the 4-in. diameter cone cylinder. Test section is set to the 8-ft, 3.1 percent modified porosity configuration. The tip of the cone is positioned at the inlet of the 8-ft test section (test section station 178).

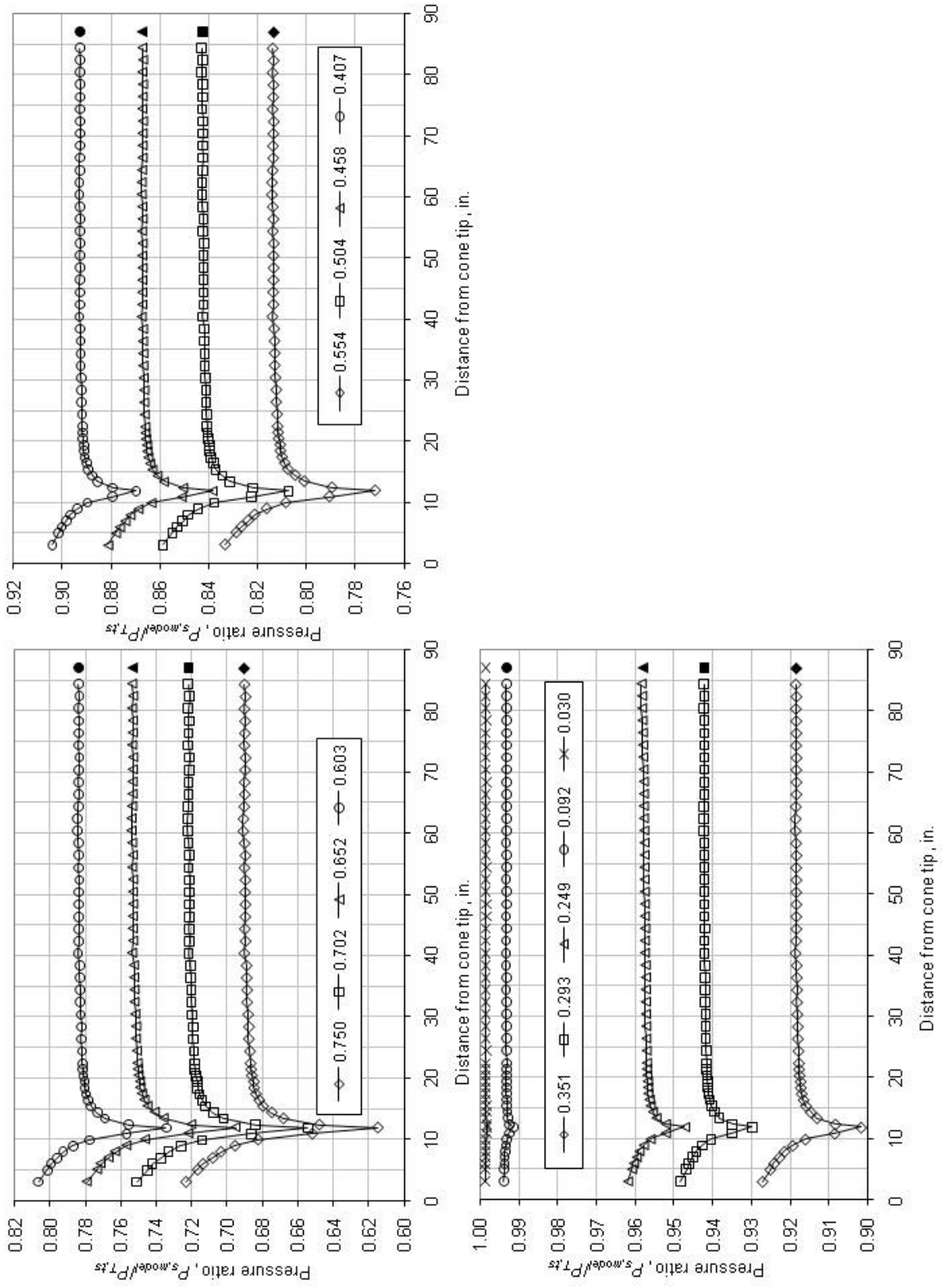

Figure 34.—Concluded.

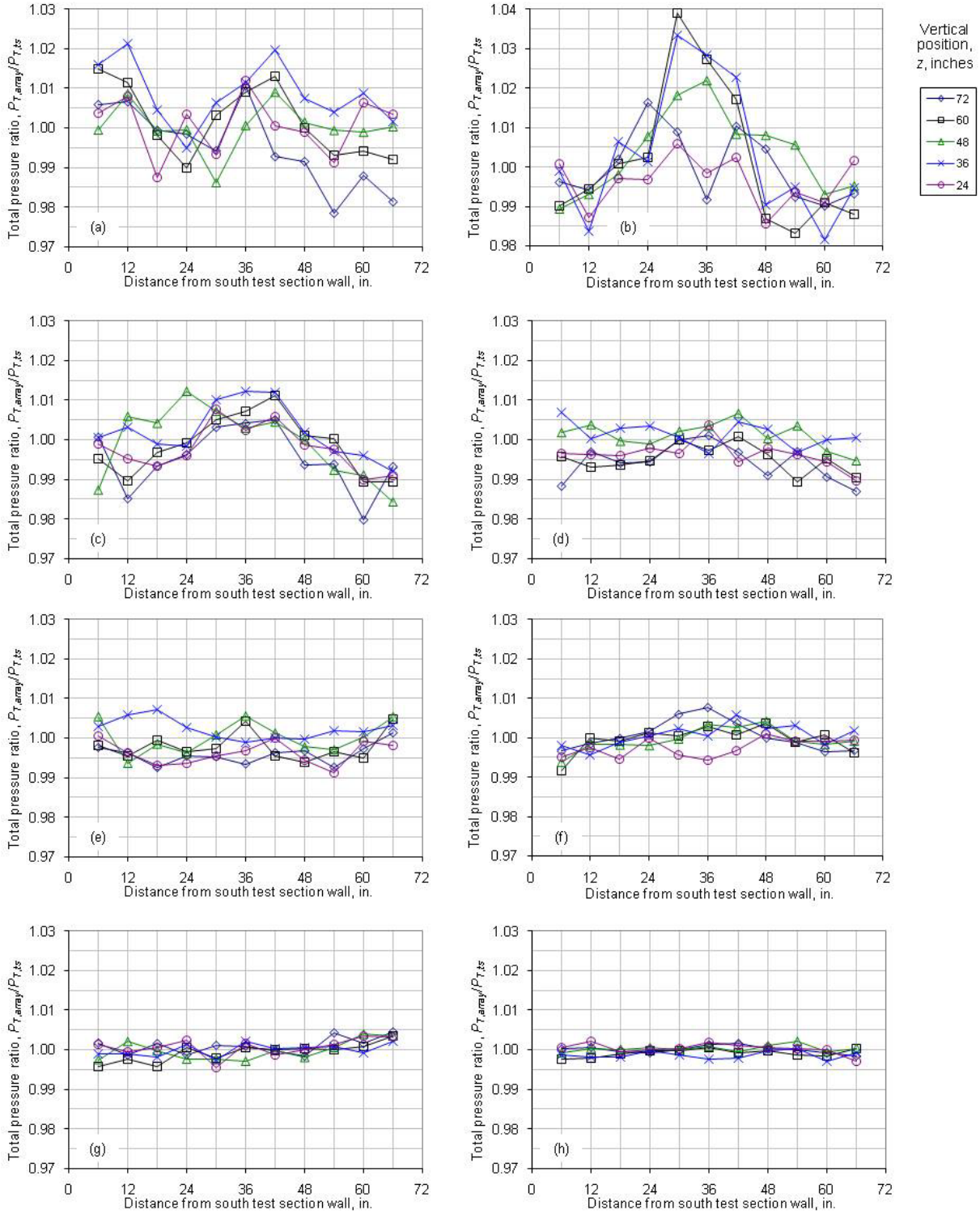

Figure 35.—Total pressure ratio distributions at each array position (5 positions) for each Mach number setting for the 8-ft, 3.1 percent modified porosity test section. Survey plane is at the inlet of the 8-ft test section (station 178). (a) M_{ts}=1.982; $P_{T,ts}$=24.783 psia. (b) M_{ts}=1.873; $P_{T,ts}$=24.121 psia. (c) M_{ts}=1.765; $P_{T,ts}$=23.181 psia. (d) M_{ts}=1.663; $P_{T,ts}$=21.692 psia. (e) M_{ts}=1.557; $P_{T,ts}$=20.320 psia. (f) M_{ts}=1.452; $P_{T,ts}$=19.135 psia. (g) M_{ts}=1.355; $P_{T,ts}$=18.158 psia. (h) M_{ts}=1.255; $P_{T,ts}$=17.377 psia.

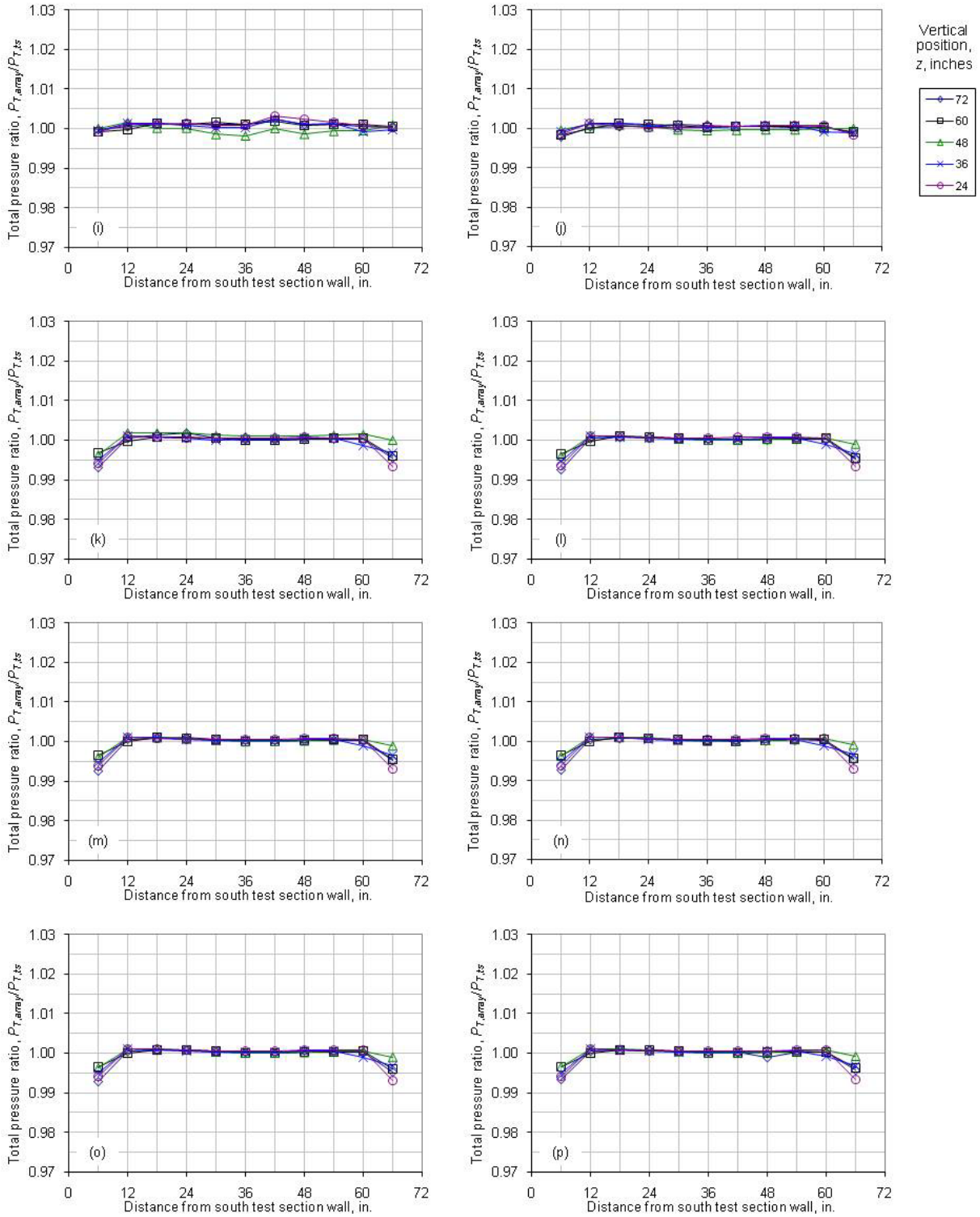

Figure 35.—Continued. (i) M_{ts}=1.191; $P_{T,ts}$=17.150 psia. (j) M_{ts}=1.094; $P_{T,ts}$=16.806 psia. (k) M_{ts}=0.996; $P_{T,ts}$=16.921 psia. (h) M_{ts}=0.957; $P_{T,ts}$=16.892 psia. (m) M_{ts}=0.908; $P_{T,ts}$=16.972 psia. (n) M_{ts}=0.850; $P_{T,ts}$=17.078 psia. (o) M_{ts}=0.811; $P_{T,ts}$=17.246 psia. (p) M_{ts}=0.761; $P_{T,ts}$=17.387 psia.

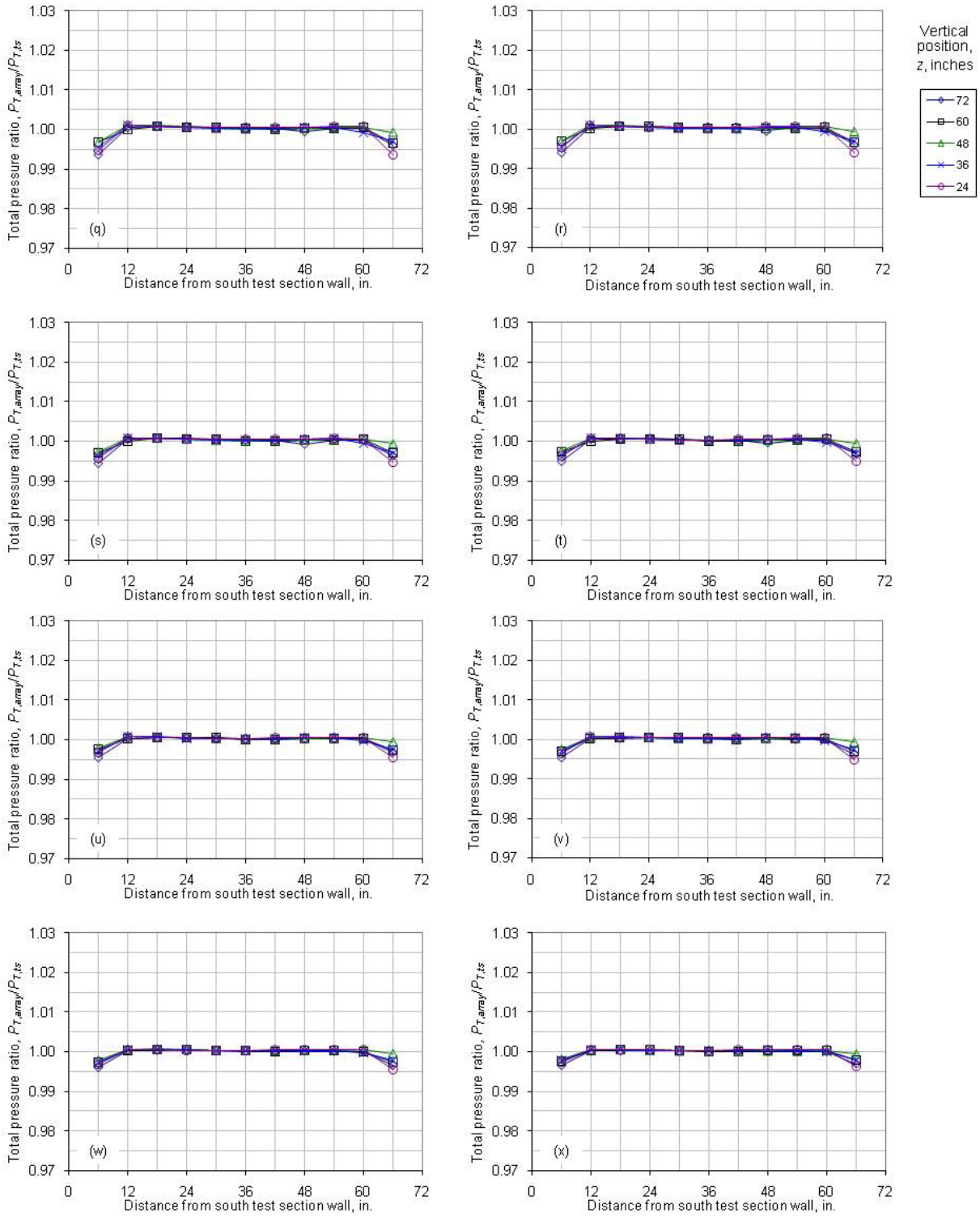

Figure 35.—Continued. (q) M_{ts}=0.713 $P_{T,ts}$=17.573 psia. (r) M_{ts}=0.662; $P_{T,ts}$=17.708 psia. (s) M_{ts}=0.613; $P_{T,ts}$=17.592 psia. (t) M_{ts}=0.564; $P_{T,ts}$=17.302 psia. (u) M_{ts}=0.513 $P_{T,ts}$=16.138 psia. (v) M_{ts}=0.506; $P_{T,ts}$=16.912 psia (1-motor). (w) M_{ts}=0.468; $P_{T,ts}$=15.649 psia. (x) M_{ts}=0.417; $P_{T,ts}$=15.470 psia.

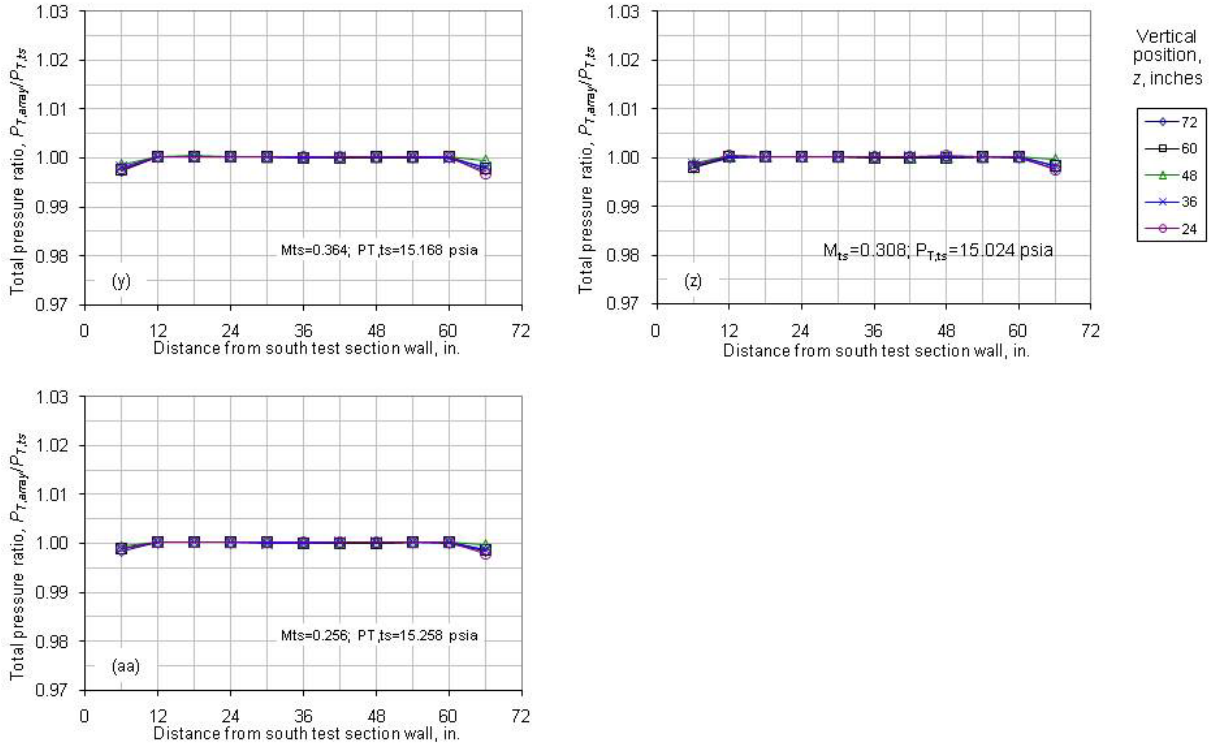

Figure 35.—Concluded. (y) M_{ts}=0.364 $P_{T,ts}$=15.168 psia. (z) M_{ts}=0.308; $P_{T,ts}$=15.024 psia. (aa) M_{ts}=0.256; $P_{T,ts}$=15.258 psia.

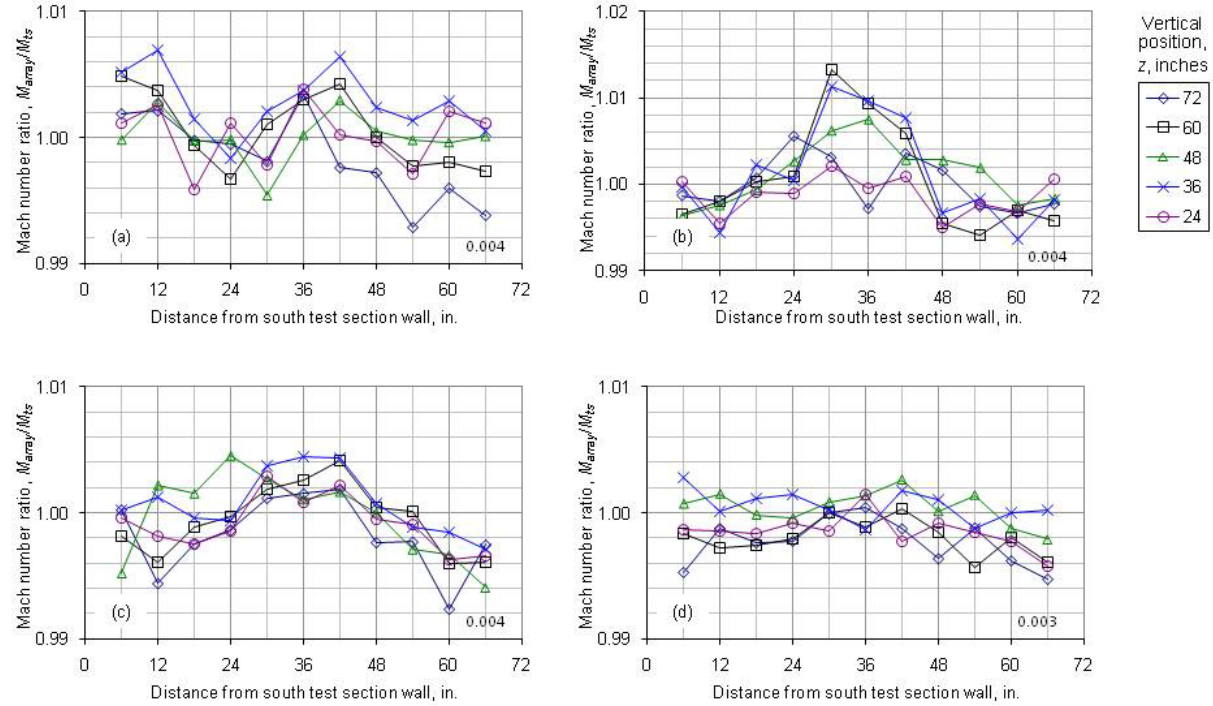

Figure 36.—Mach number ratio distributions at each array position (5 positions) for each Mach number setting for the 8-ft, 3.1 percent modified porosity test section. Survey plane is at the inlet of the 8-ft test section (station 178). The number in the lower right-hand corner is the approximate delta Mach number represented by the minor y-axis division. (a) M_{ts} = 1.982. (b) M_{ts} = 1.873. (c) M_{ts} = 1.765. (d) M_{ts} = 1.663.

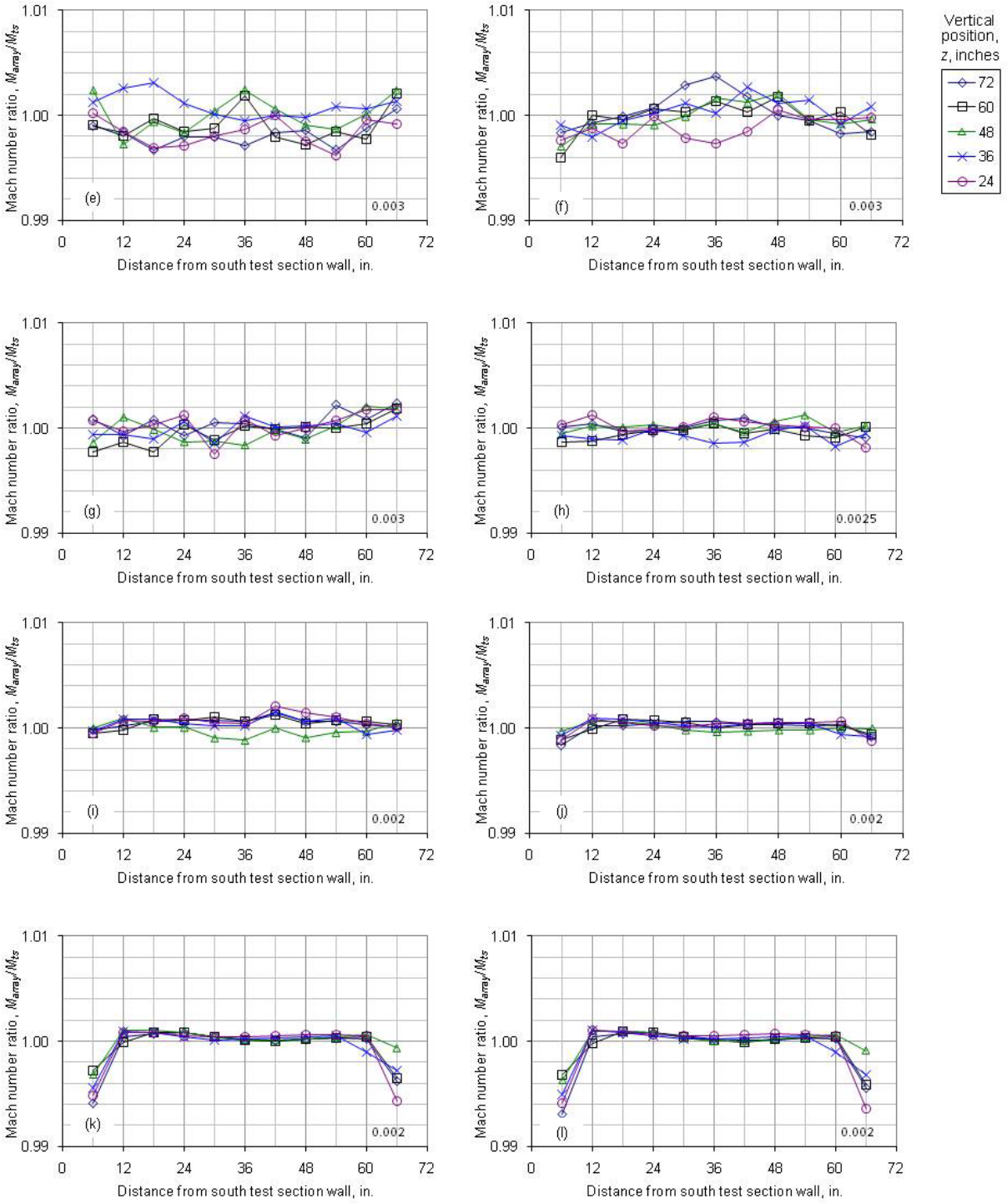

Figure 36.—Continued. (e) M_{ts} = 1.557. (f) M_{ts} = 1.452. (g) M_{ts} = 1.355. (h) M_{ts} = 1.255. (i) M_{ts} = 1.191. (j) M_{ts} = 1.094. (k) M_{ts} = 0.996. (l) M_{ts} = 0.957.

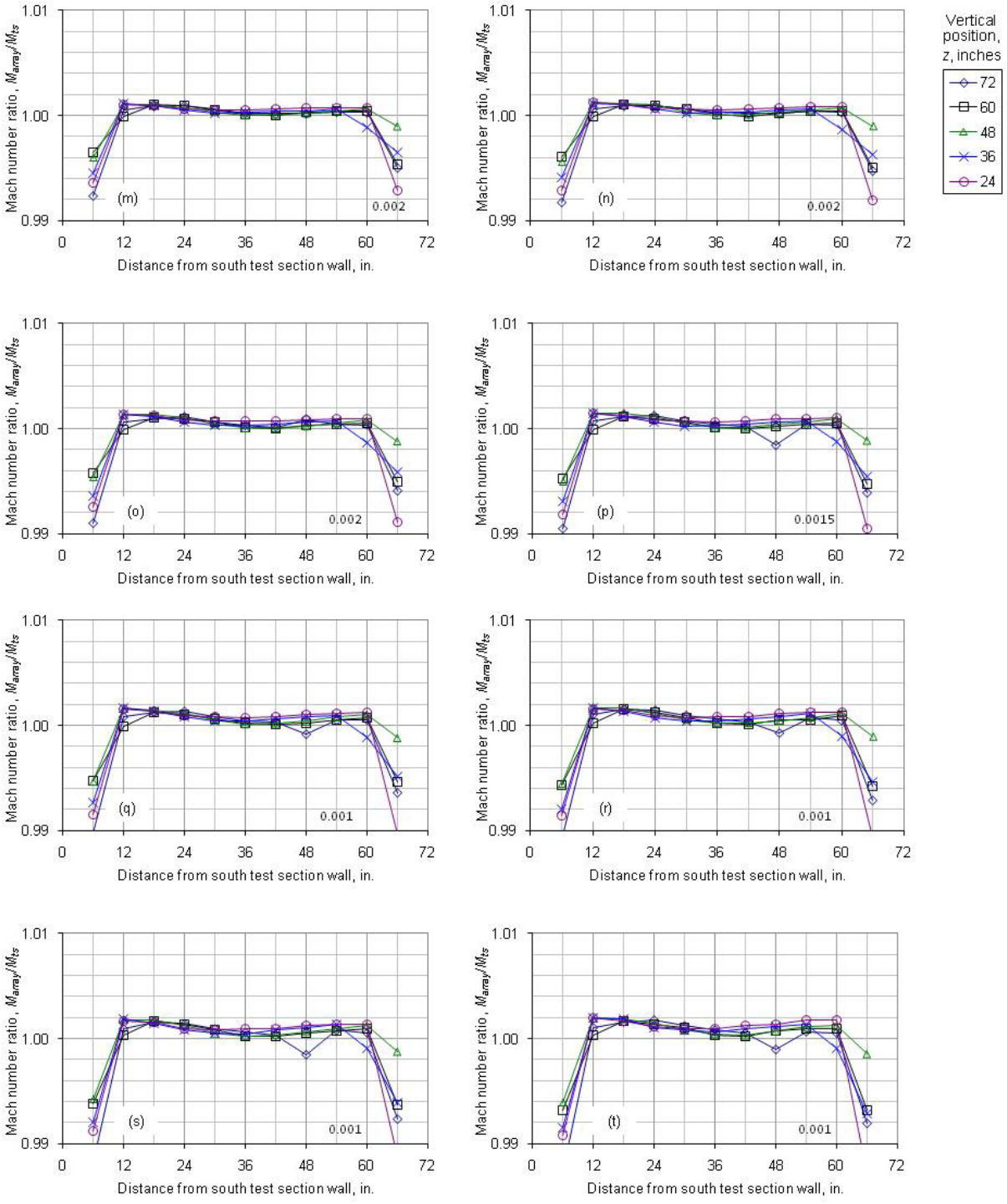

Figure 36.—Continued. (m) M_{ts} = 0.908. (n) M_{ts} = 0.860. (o) M_{ts} = 0.811. (p) M_{ts} = 0.761. (q) M_{ts} = 0.713. (r) M_{ts} = 0.662. (s) M_{ts} = 0.613. (t) M_{ts} = 0.564.

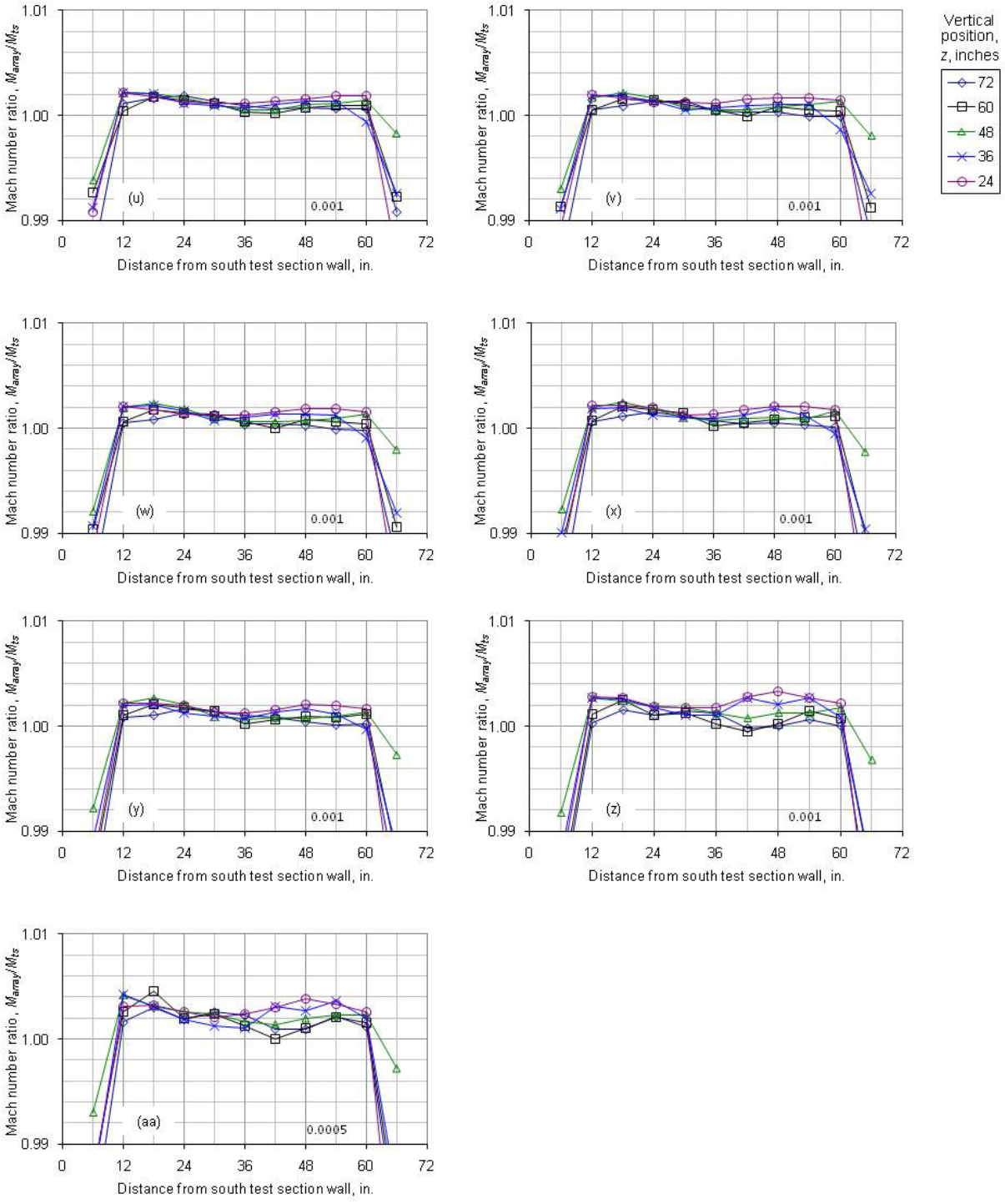

Figure 36.—Continued. (u) M_{ts} = 0.513. (v) M_{ts} = 0.506 (1-motor). (w) M_{ts} = 0.468. (x) M_{ts} = 0.417. (y) M_{ts} = 0.364. (z) M_{ts} = 0.308. (aa) M_{ts} = 0.256.

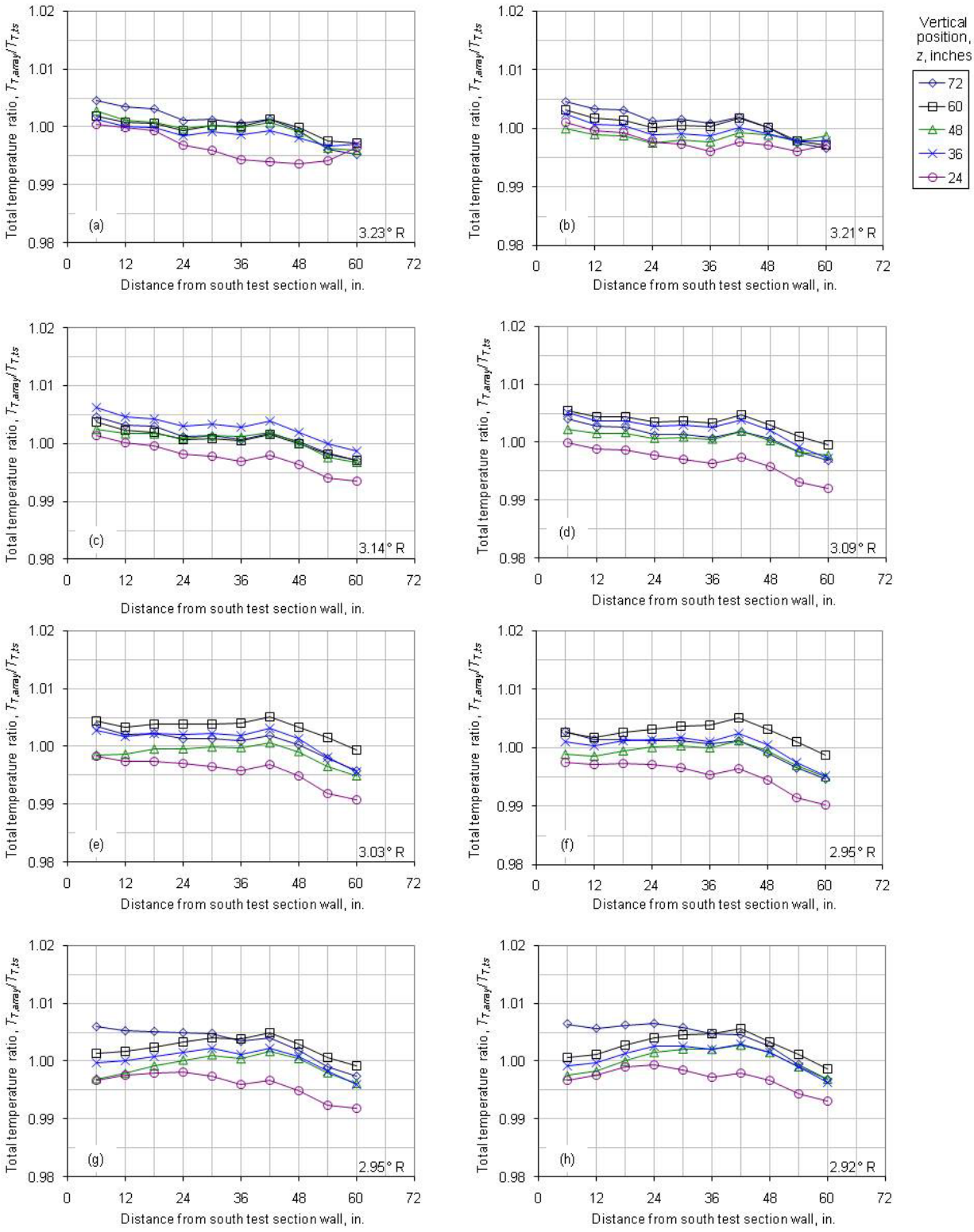

Figure 37.—Total temperature ratio distributions at each array position and Mach number setting in the 8-ft, 3.1 percent modified porosity test section; survey plane is at the inlet of the 8-ft test section (station 178). (a) M_{ts}=1.982; $T_{T,ts}$=645.2 R. (b) M_{ts}=1.873; $T_{T,ts}$=642.0 R. (c) M_{ts}=1.765; $T_{T,ts}$=628.6 R. (d) M_{ts}=1.663; $T_{T,ts}$=618.7 R. (e) M_{ts}=1.557; $T_{T,ts}$=606.7 R. (f) M_{ts}=1.452; $T_{T,ts}$=589.4 R. (g) M_{ts}=1.355; $T_{T,ts}$=589.4 R. (h) M_{ts}=1.255; $T_{T,ts}$=583.5 R.

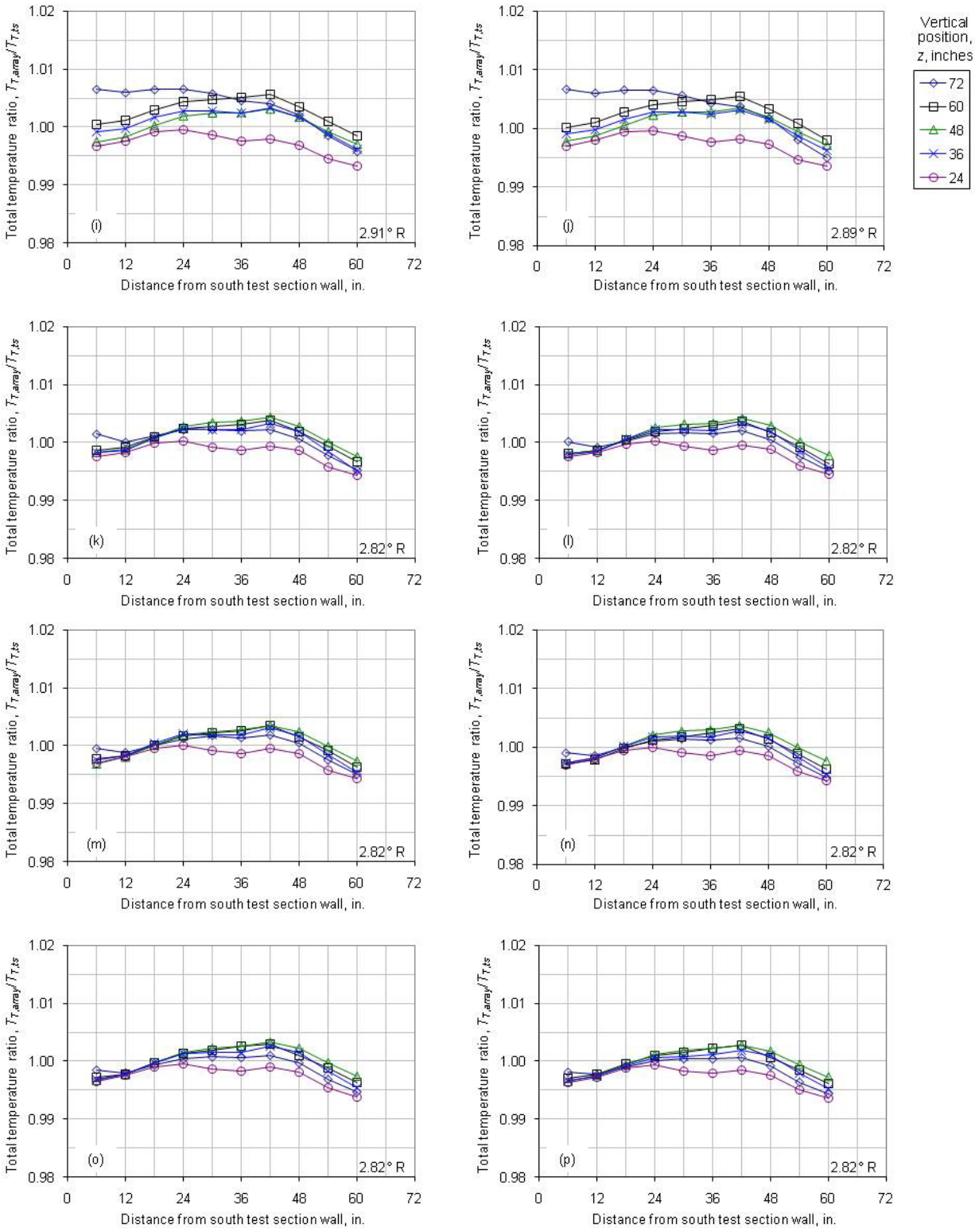

Figure 37.—Continued. (i) M_{ts}=1.191; $T_{T,ts}$=581.1 R. (j) M_{ts}=1.094; $T_{T,ts}$=578.0 R. (k) M_{ts}=0.996; $T_{T,ts}$=564.1 R. (l) M_{ts}=0.975; $T_{T,ts}$=563.1 R. m) M_{ts}=0.908; $T_{T,ts}$=563.1 R. (n) M_{ts}=0.860; $T_{T,ts}$=563.4 R. (o) M_{ts}=0.811; $T_{T,ts}$=564.0 R. (p) M_{ts}=0.761; $T_{T,ts}$=564.1 R.

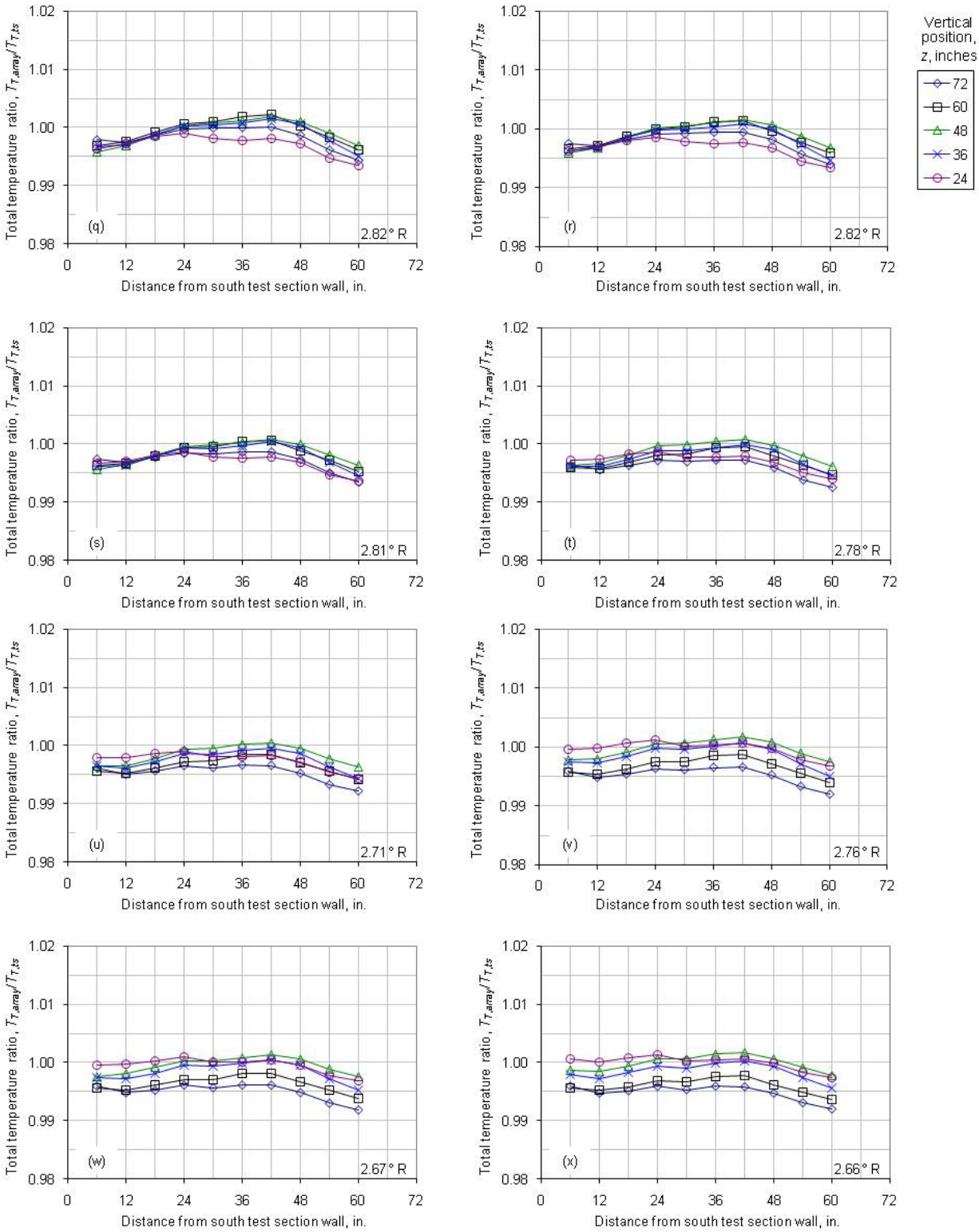

Figure 37.—Continued. (m) M_{ts}=0.908; $T_{T,ts}$=563.1 R. (n) M_{ts}=0.860; $T_{T,ts}$=563.4 R. (o) M_{ts}=0.811; $T_{T,ts}$=564.0 R. (p) M_{ts}=0.761; $T_{T,ts}$=564.1 R. (u) M_{ts}=0.513; $T_{T,ts}$=542.7 R. (v) M_{ts}=0.506; $T_{T,ts}$=551.0 R (1-motor). (w) M_{ts}=0.468; $T_{T,ts}$=533.8 R (1-motor). (x) M_{ts}=0.417; $T_{T,ts}$=532.2 R (1-motor).

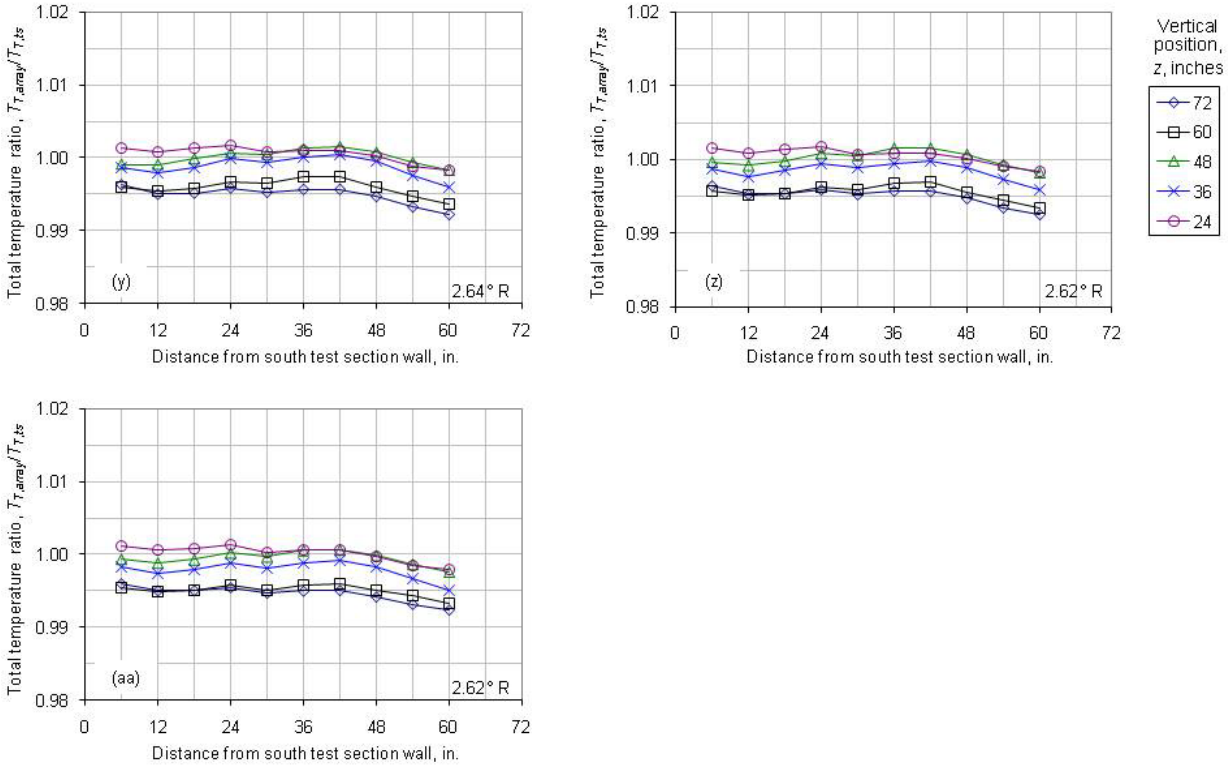

Figure 37.—Concluded. (y) M_{ts}=0.364; $T_{T,ts}$=527.3 R (1-motor). (z) M_{ts}=0.308; $T_{T,ts}$=523.9 R (1-motor). (aa) M_{ts}=0.256; $T_{T,ts}$=524.9 R (1-motor).

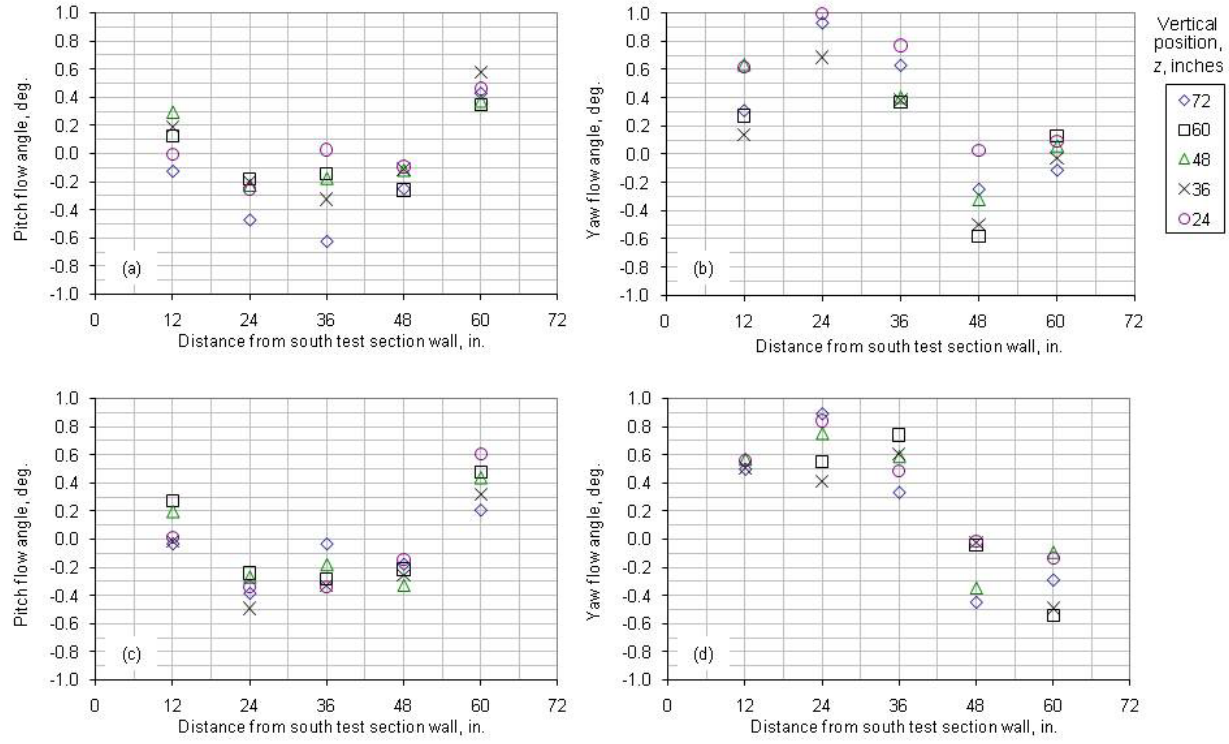

Figure 38.—Pitch and Yaw flow angle data at each array position (5 positions) and Mach number setting for the 8-ft, 3.1 percent modified porosity test section (measurement plane at station 178). (a) M_{ts}=1.982. (b) M_{ts}=1.982. (c) M_{ts}=1.873. (d) M_{ts}=1.873.

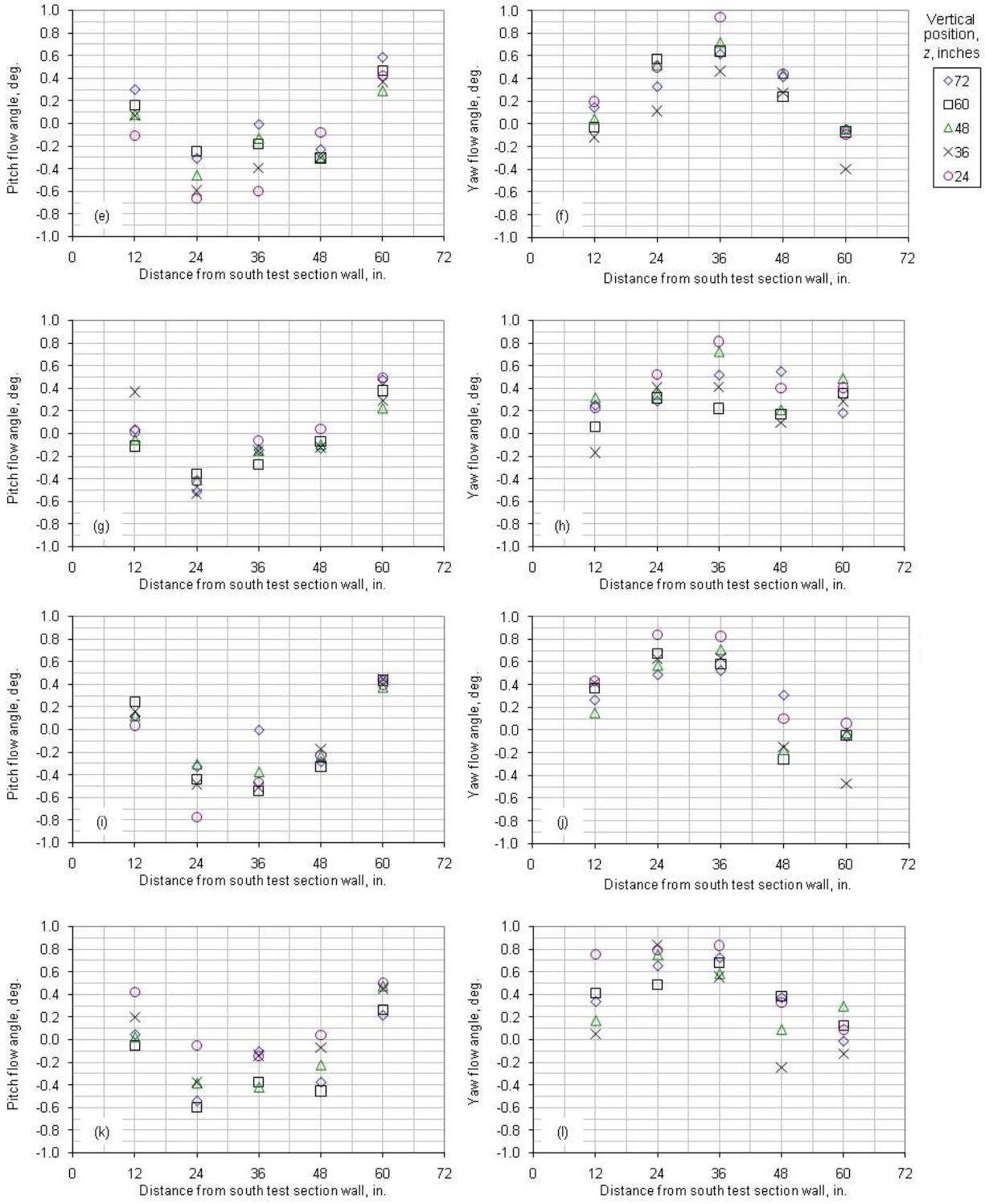

Figure 38.—Continued. (e) M_{ts}=1.765. (f) M_{ts}=1.765. (g) M_{ts}=1.663. (d) M_{ts}=1.663. (i) M_{ts}=1.557. (j) M_{ts}=1.557. (k) M_{ts}=1.452. (l) M_{ts}=1.452.

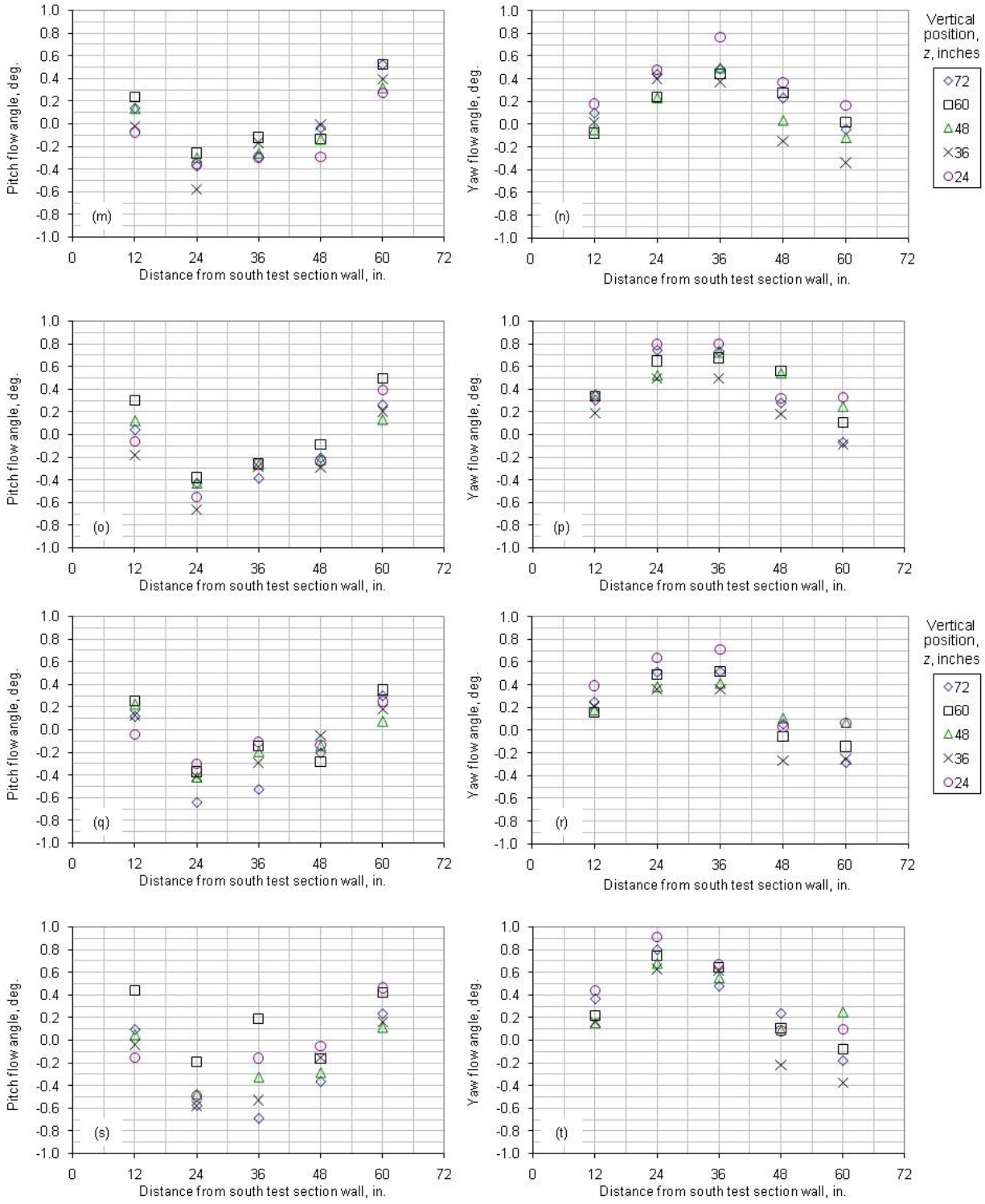

Figure 38.—Continued. (m) M_{ts}=1.355. (n) M_{ts}=1.355. (o) M_{ts}=1.255. (p) M_{ts}=1.255. (q) M_{ts}=1.191. (r) M_{ts}=1.191. (s) M_{ts}=1.094. (t) M_{ts}=1.094.

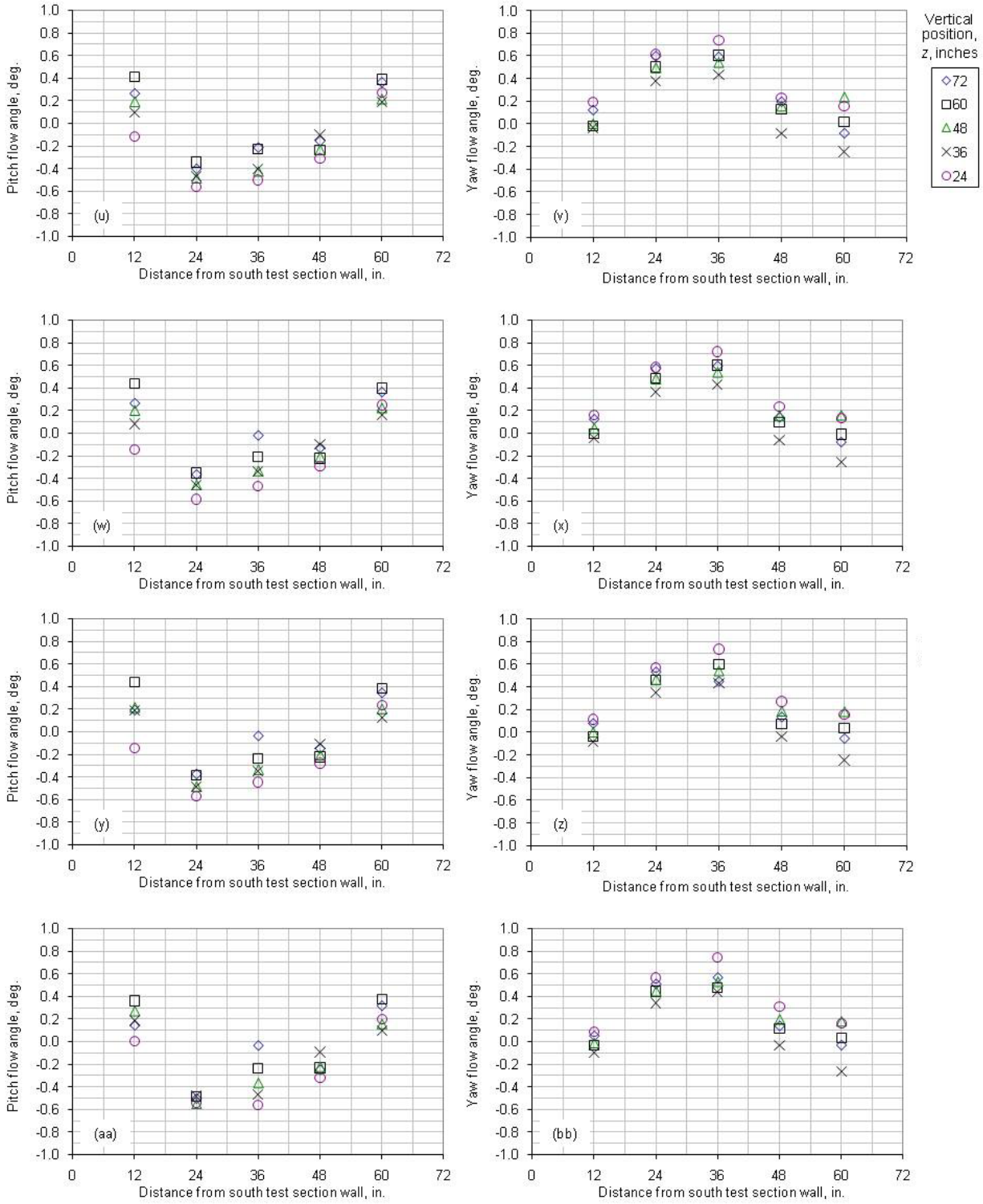

Figure 38.—Continued. (u) M_{ts}=0.996. (v) M_{ts}=0.996. (w) M_{ts}=0.957. (x) M_{ts}=0.957. (y) M_{ts}=0.908. (z) M_{ts}=0.908. (aa) M_{ts}=0.860. (bb) M_{ts}=0.860.

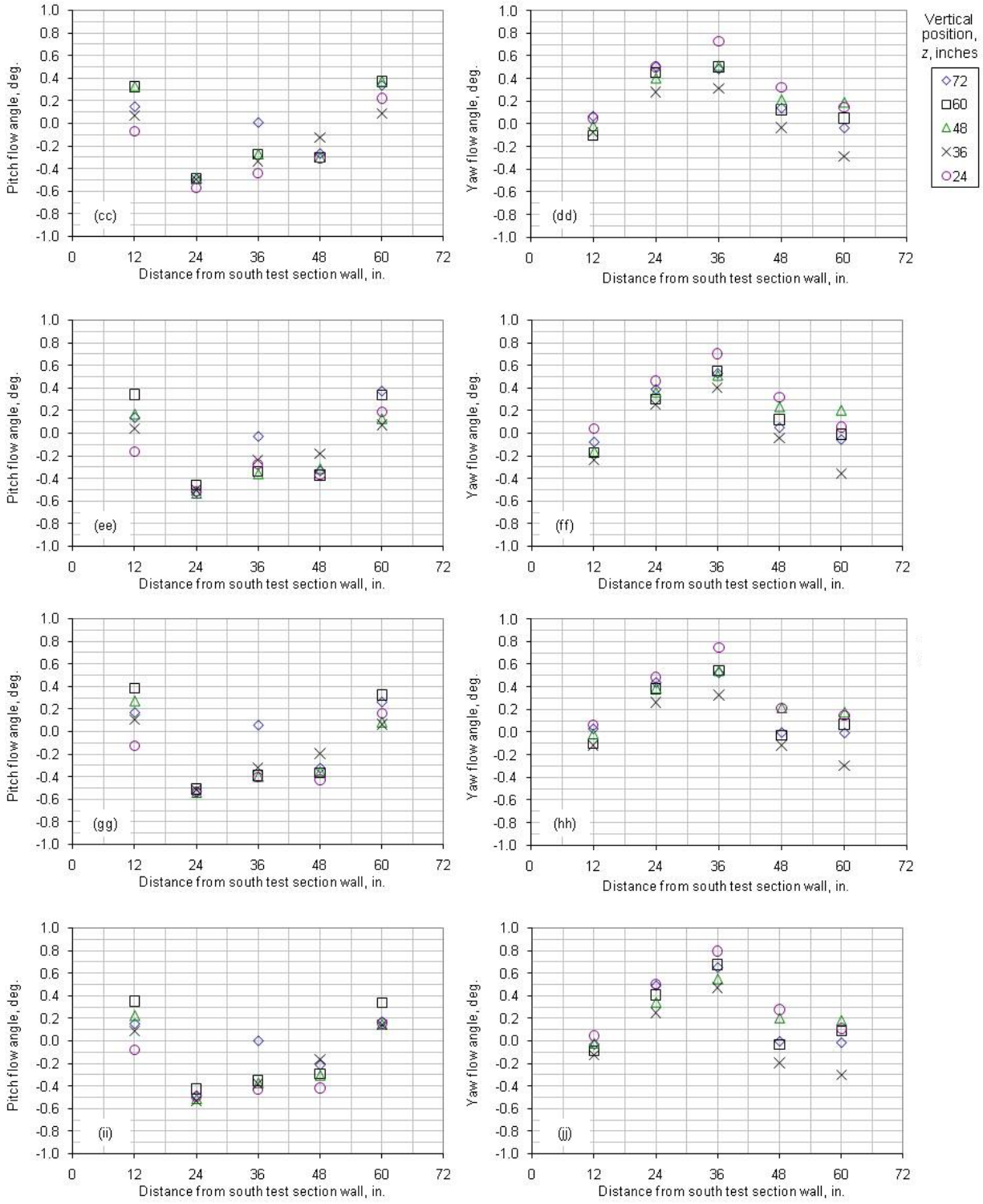

Figure 38.—Continued (cc) M_{ts}=0.811. (dd) M_{ts}=0.811. (ee) M_{ts}=0.761. (ff) M_{ts}=0.761. (gg) M_{ts}=0.713. (hh) M_{ts}=0.713. (ii) M_{ts}=0.654. (jj) M_{ts}=0.654.

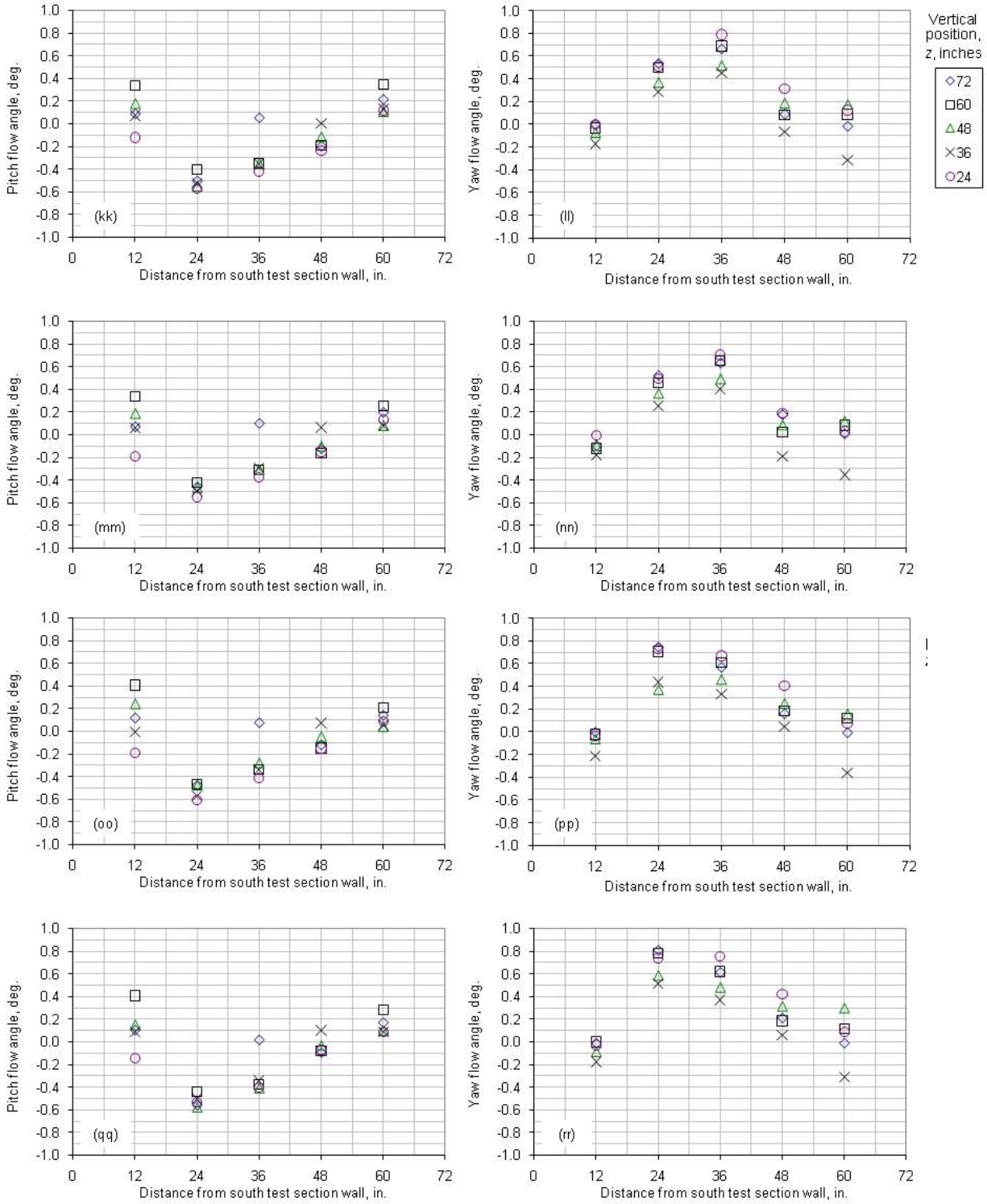

Figure 38.—Continued. (kk) M_{ts}=0.613. (ll) M_{ts}=0.613. (mm) M_{ts}=0.564. (nn) M_{ts}=0.564. (oo) M_{ts}=0.513. (pp) M_{ts}=0.513. (qq) M_{ts}=0.506 (1-motor). (rr) M_{ts}=0.506 (1-motor).

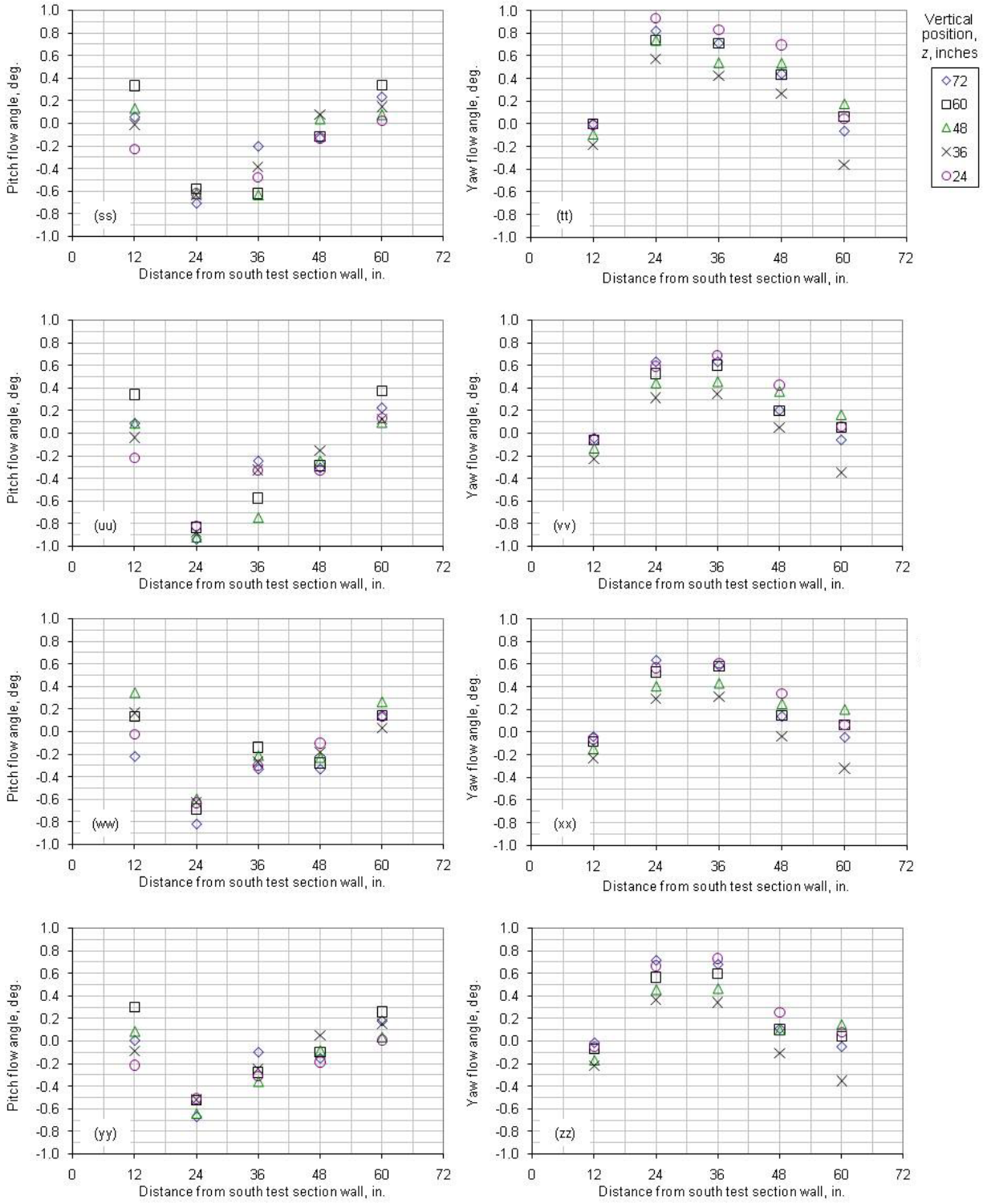

Figure 38.—Continued. (ss) M_{ts}=0.468 (1-motor). (tt) M_{ts}=0.468 (1-motor). (uu) M_{ts}=0.417 (1-motor). (vv) M_{ts}=0.417 (1-motor). (ww) M_{ts}=0.364 (1-motor). (xx) M_{ts}=0.364 (1-motor). (yy) M_{ts}=0.308 (1-motor). (zz) M_{ts}=0.308 (1-motor).

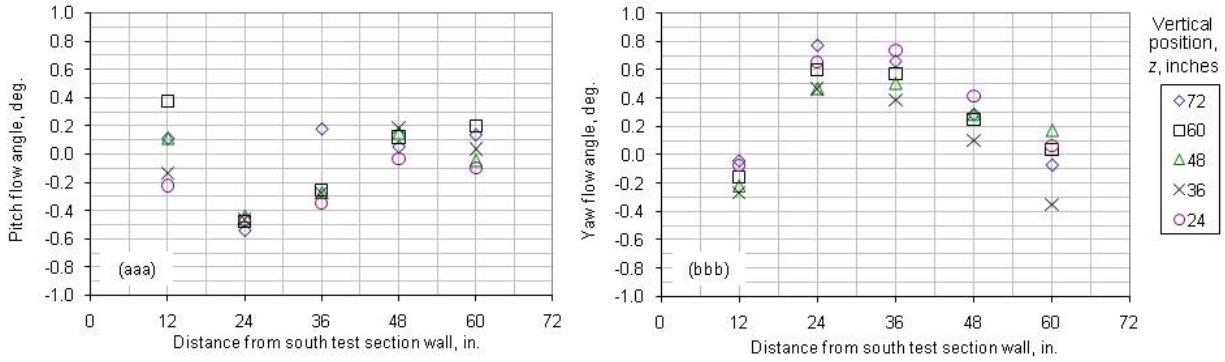

Figure 38.—Concluded. (aaa) M_{ts}=0.256 (1-motor). (bbb) M_{ts}=0.256 (1-motor).

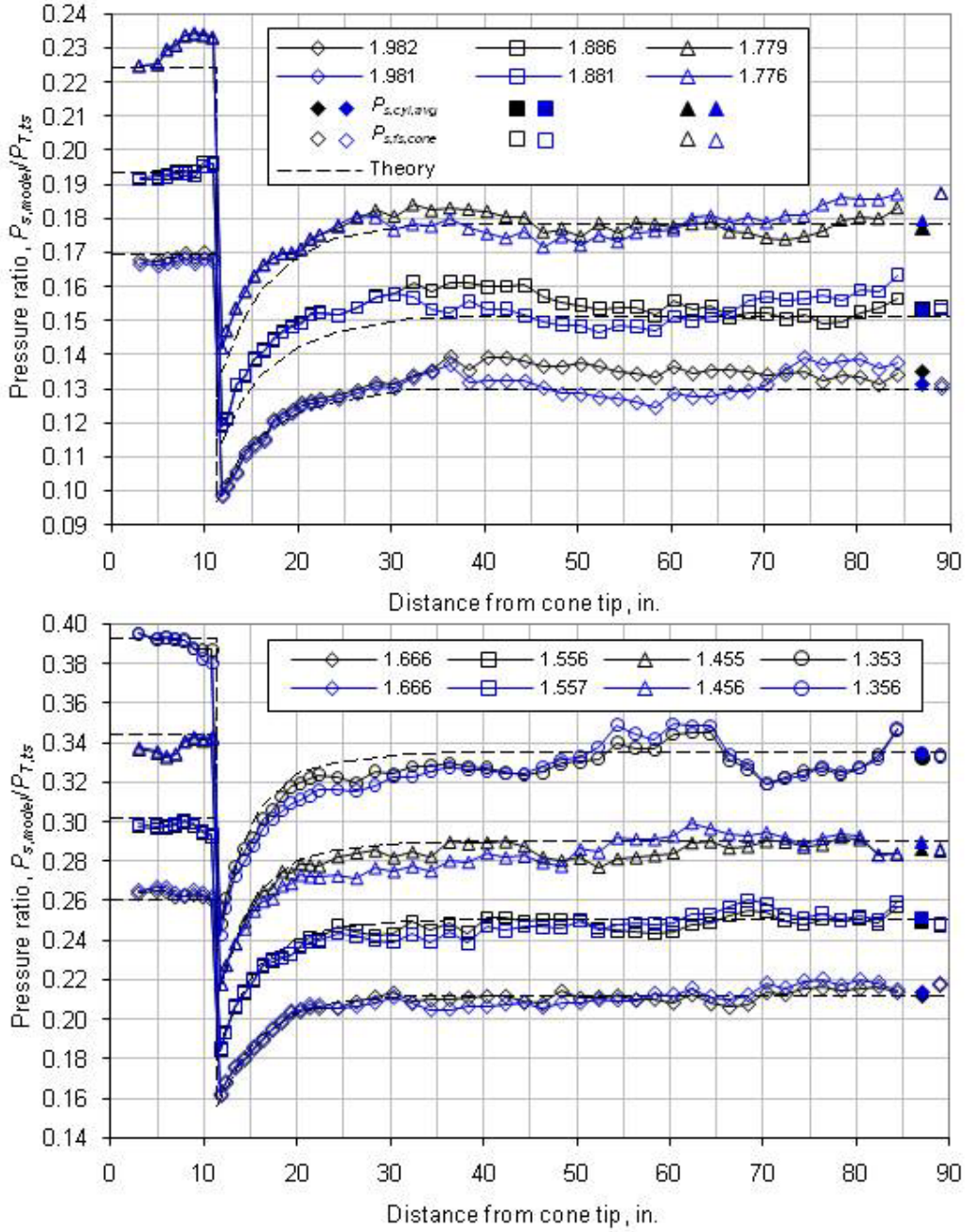

Figure 39.—Comparison of the axial station pressure distribution over the 4-in. diameter cone cylinder for the 14-ft, 5.8 percent porosity test section (blue symbols) and the 14-ft, schlieren window configuration (black symbols).

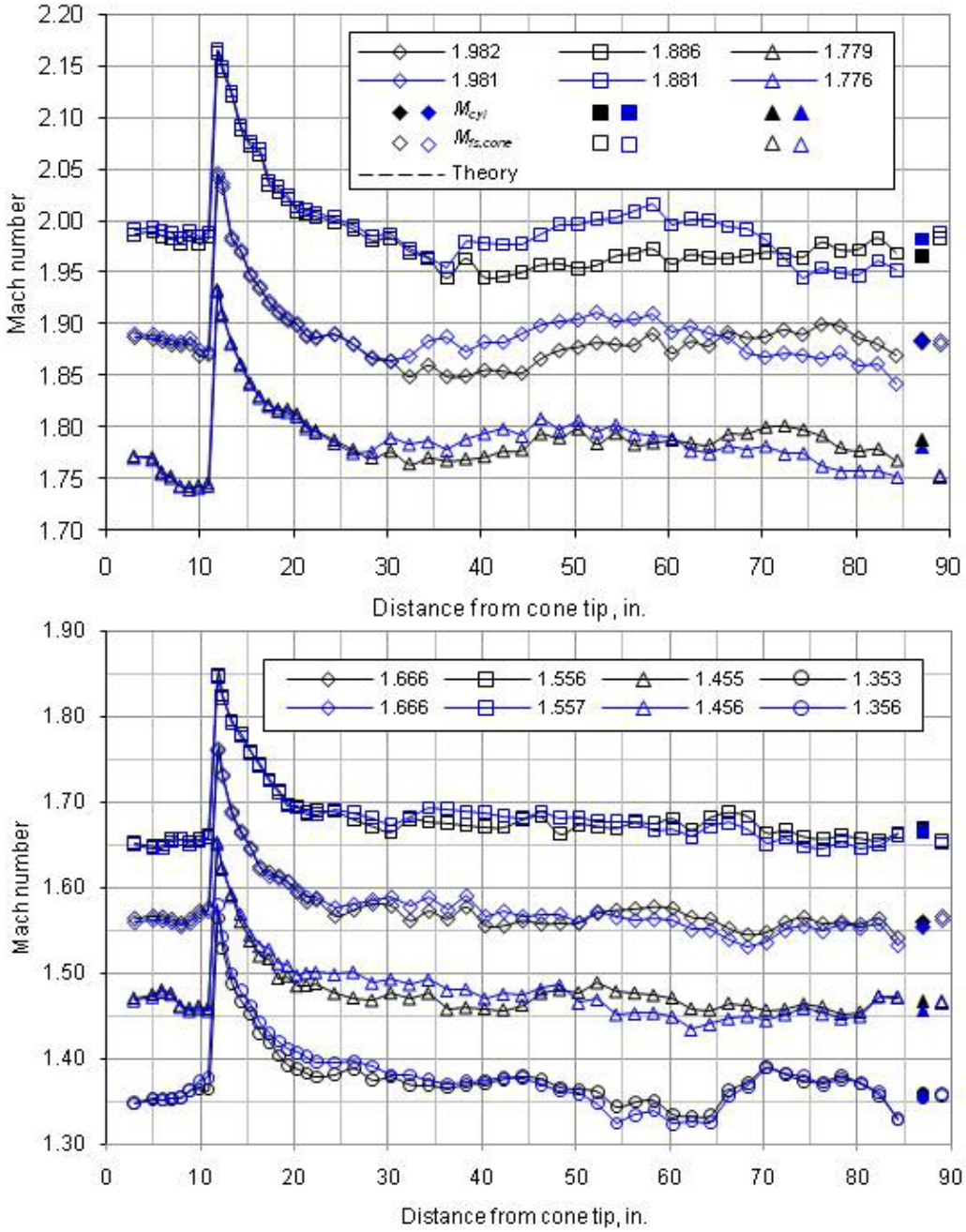

Figure 39.—Comparison of the axial Mach number distribution over the 4-in. diameter cone cylinder for the 14-ft, 5.8 percent porosity test section (blue symbols) and the 14-ft, schlieren window configuration (black symbols).

References

1. Arrington, E. A. and Pickett, M. T.: Baseline Calibration of the NASA Glenn research Center 8- By 6-Foot Supersonic Wind Tunnel (1991 and 1992 Tests). NASA TM-97-107431, 1997.
2. Arrington, E. A. and Pickett, M. T.: Flow Quality Studies of the NASA Glenn Research Center 8-by 6- Foot Supersonic/ 9-by 15-Foot Low Speed Wind Tunnel. NASA TM 105417, 1992.
3. Arrington, E. A.: Flow Field Surveys of the NASA Glenn Research Center 8- By 6-Foot Supersonic Wind Tunnel (1993 Test). NASA CR-1998-206610, 1998.
4. Arrington, E. A.; Gonsalez, J. C.; and Becks, E. A.: Flow Quality and Operational Enhancements in the NASA Lewis 8- by 6-Foot Supersonic Wind Tunnel. NASA/CR-1998-207930, AIAA-98-2706, 1998.
5. Arrington, E. A. and Gonsalez, J. C.: Low Speed Calibration of the NASA Glenn Research Center 8- By 6-Foot Supersonic Wind Tunnel (1995 Test). NASA CR 198527, 1997.
6. Soeder, R.H.: NASA Glenn 8- By 6-Foot Supersonic Wind Tunnel User Manual. NASA TM 105771, 1993.
7. Ames Research Staff: Equations, Tables and Charts for Compressible Flow. NACA TR-1135, 1953.
8. Clark, E. L.; Henfling, J. F.; and Aeschliman, D. P.: Calibration of Flow angularity Probes for NASA Glenn Research Center. Sandia National Laboratories, NASA Contract Number C-22995-P, 1991.
9. Clark, E.L.; Henfling, J. F.; and Aeschliman, D. P.: Calibration of Hemispherical-Head Flow Angularity Probes. AIAA 92-4005, 1992.
10. Henderson, A. Jr.; and McKinney, L. W.: Overview of the 1989 Wind Tunnel Calibration Workshop. NASA TP-3393, August, 1993.
11. Mitchell, G. A.: Blockage Effects on Cone-Cylinder Bodies on Perforated Wind Tunnel Wall Interference. NASA TM X-1655, 1968.

REPORT DOCUMENTATION PAGE	Form Approved OMB No. 0704-0188

1. REPORT DATE *(DD-MM-YYYY)*	2. REPORT TYPE	3. DATES COVERED *(From - To)*
01-01-2012	Final Contractor Report	

4. TITLE AND SUBTITLE
Calibration of the NASA Glenn 8- by 6-Foot Supersonic Wind Tunnel (1996 and 1997 Tests)

5a. CONTRACT NUMBER
NNC05CA95C

5b. GRANT NUMBER

5c. PROGRAM ELEMENT NUMBER

6. AUTHOR(S)
Arrington, E., Allen

5d. PROJECT NUMBER

5e. TASK NUMBER

5f. WORK UNIT NUMBER
Y0E5408

7. PERFORMING ORGANIZATION NAME(S) AND ADDRESS(ES)
Sierra Lobo, Inc.
102 Pinnacle Drive
Fremont, Ohio 43420

8. PERFORMING ORGANIZATION REPORT NUMBER
E-18026

9. SPONSORING/MONITORING AGENCY NAME(S) AND ADDRESS(ES)
National Aeronautics and Space Administration
Washington, DC 20546-0001

10. SPONSORING/MONITOR'S ACRONYM(S)
NASA

11. SPONSORING/MONITORING REPORT NUMBER
NASA/CR-2012-217270

12. DISTRIBUTION/AVAILABILITY STATEMENT
Unclassified-Unlimited
Subject Category: 09
Available electronically at http://www.sti.nasa.gov
This publication is available from the NASA Center for AeroSpace Information, 443-757-5802

13. SUPPLEMENTARY NOTES

14. ABSTRACT

There were several physical and operational changes made to the NASA Glenn Research Center 8- by 6-Foot Supersonic Wind Tunnel during the period of 1992 through 1996. Following each of these changes, a facility calibration was conducted to provide the required information to support the research test programs. Due to several factors (facility research test schedule, facility downtime and continued facility upgrades), a full test section calibration was not conducted until 1996. This calibration test incorporated all test section configurations and covered the existing operating range of the facility. However, near the end of that test entry, two of the vortex generators mounted on the compressor exit tailcone failed causing minor damage to the honeycomb flow straightener. The vortex generators were removed from the facility and calibration testing was terminated. A follow-up test entry was conducted in 1997 in order to fully calibrate the facility without the effects of the vortex generators and to provide a complete calibration of the newly expanded low speed operating range. During the 1997 tunnel entry, all planned test points required for a complete test section calibration were obtained. This data set included detailed in-plane and axial flow field distributions for use in quantifying the test section flow quality.

15. SUBJECT TERMS
Wind tunnel calibration

16. SECURITY CLASSIFICATION OF:			17. LIMITATION OF ABSTRACT	18. NUMBER OF PAGES	19a. NAME OF RESPONSIBLE PERSON
a. REPORT	b. ABSTRACT	c. THIS PAGE			STI Help Desk (email:help@sti.nasa.gov)
U	U	U	UU	120	19b. TELEPHONE NUMBER *(include area code)* 443-757-5802